THE UNIVERSITY
of EDINBURGH

Borane Transfer Reactions

THE UNIVERSITY
of EDINBURGH

Nicholas Taylor

Doctor of Philosophy

University of Edinburgh

2016

Declaration

I declare that the work in this dissertation was carried out in accordance with the requirements of the University of Edinburgh. This work is original, except where indicated by special reference in the text, and no part of the dissertation has been submitted for any other academic award. Any views expressed in the dissertation are those of the author.

Signed …….

Date ……..

Publications

The work presented in Chapter 2 has been communicated:

G. C. Lloyd-Jones, N. P. Taylor, *Chem. Eur. J.* **2015**, *21*, 5423–5428.

Abstract

Lewis base borane adducts ($LB{\cdot}BH_3$) constitute a well-known class of molecules with a number of diverse applications, including use as protected phosphines. The kinetics and thermodynamics of borane transfer reactions from a wide range of Lewis base borane complexes have been studied. The data generated has been used both as a quantitative tool to describe the nucleofugality (leaving group ability) of Lewis bases and as a means to improve the efficiency of phosphine borane deprotection reactions.

The kinetics of borane transfer from a range of tertiary phosphine borane complexes to a wide range of amines have been determined. All kinetic data obtained, in addition to computational evidence, are consistent with a direct (S_N2-like) mechanism, rather than a dissociative (S_N1-like) process. The identities of the amine, phosphine and to a lesser extent solvent, impact substantially on the rate and equilibrium of the transfer, which can span several orders of magnitude. In depth structure activity relationships have been explored both for a wide variety of amine nucleophiles and phosphine nucleofuges. Taken as a whole, the data allow informed optimisation of the "deprotection" of a phosphine borane complex from the standpoint of rate or synthetic convenience. Additionally, the kinetics of ethanolysis of tri(*o*-tolyl)phosphine borane complex have also been studied.

Using bridgehead amine quinuclidine as a benchmark, the kinetics of borane transfer from a wide range amine borane adducts have also been determined. Parameterisation of these data, in addition to that obtained for the analogous phosphine borane complexes, has allowed development of a novel nucleofugality scale (N^F_B) that quantifies the leaving group ability of a wide range of Lewis bases. Additivity in the kinetics across a series $R_{3-n}R'_nX{\cdot}BH_3$ (X = P, N; R/R' = aryl, alkyl) has led to the formulation of related substituent parameters (n^f_{PB}, n^f_{AB}) that quantify the nucleofugal influence of a substituent. Using the substituent nucleofugality parameter in concert with additivity provides a mean of calculating ligand nucleofugality (N^F_B) values for a wide range of Lewis bases that extends far beyond those experimentally derived. Good agreement was found between predicted (using N^F_B and n^F_B values) and experimental rates of borane transfer for ligands outside the training set, thus providing a means to predict the relative rate of phosphine borane deprotections. The utility of both parameters was demonstrated through correlations to rates of redox transformations at iridium (bearing phosphine spectator ligands) and MIDA boronate hydrolysis, (MIDA = *N*-methyliminodiacetic acid). Through these correlations, interesting subtleties in the mechanism of MIDA boronate hydrolysis have been identified.

Lay Summary

Developing an understanding of chemical reactivity plays an increasingly important role in modern society, enabling chemists to more efficiently design new process and improve existing ones. The definition of ‘improve’ in this context is deliberately vague, and with a good understanding of reaction mechanism (how a reaction happens) and how a reaction is influenced by a range of controllable variables (e.g. temperature), chemists are able to design a reaction to give optimal output, which could be defined in terms of yield, cost, rate, selectivity, and amount and toxicity of both reagents and waste. This study concerns the development of a greater understanding of both the mechanism and the influence of a number of variables on one particular ‘deprotection’ reaction.

Specific chemical or physical properties are often the desired goal of academic and industrial chemists alike, but constructing a desired molecule can often be very challenging. One trick employed by chemists is to chemically modify (reduce) the reactivity of a specific part of a synthetic intermediate, thus ‘protecting’ it from undergoing unwanted side reactions in subsequent reactions. This comes with a drawback however, as to obtain the desired final product a suitable ‘deprotection’ is required. This protection/deprotection strategy has been utilised widely, across many areas of chemistry. A class of molecules called phosphines (organic molecules containing a phosphorus atom) are commonly synthesised using a protection strategy as intermediates, and often the desired compounds themselves, can be so reactive as to degrade in air, spontaneously catching fire in the most extreme examples. Thus, a suitable ‘deprotection’ step is required and, whilst a number of techniques are known to do this, choosing the right conditions for a given substrate is not intuitive. This study seeks to shed light on this step allowing chemists to make an informed choice of conditions to give the most efficient reaction.

Kinetic data (how fast a reaction proceeds) obtained in this study also allowed the development of a new scale to quantify chemical reactivity. The reasons for doing this are much the same as above, although the scope of the reactions that can be understood is dramatically increased. Information about a different reaction can be compared to that of the novel scale, and this comparison not only aids understanding, but also allows quantitative predictions to be made about the reaction. This is a powerful tool that if utilised correctly has the ability to inform reaction design without consuming both the resources and the time necessary to carry out experiments.

Acknowledgements

Firstly, I would like to thank Professor Guy Lloyd-Jones, his advice and support over the past four years has been invaluable. Under his guidance my PhD has been both challenging and rewarding, in this respect, I am especially grateful for his insight and patience.

I have been fortunate enough to work with some wonderful people in the Lloyd-Jones group, they have been both supportive and have provided plenty of entertainment along the way. I'd like to thank Dr Louise Evans, Dr Ali Lennox, Dr Bertram Ong, Dr Liam Ball, Dr Tomas Racys, Dr Carl Poree, Dr Ruth Dooley, Dr Rob Cox, Joe Tate, Paul Cox, Jorge Augusto Gonzalez Gonzalez, Tom Corrie, Dr Alex Cresswell, Katherine Geogheghan, Matt Robinson, Dr Marc Reid, Dr Eric Keske, Dr Alba Collado, Eduardo Nieto, and Magdalene Teh. Thanks in particular go to the members of Team Boron, whom in addition to providing a great deal of advice and encouragement, it has been my great pleasure to work with. I would also like to thank Aurimas Nausedas for his both his enthusiasm and willingness to share ideas throughout the duration of his project.

Outside of the Lloyd-Jones group, I have worked with a number of people who deserve mention. Foremost among these are Drs Mairi Haddow and Gary Nichol who have both demonstrated great patience during my foray into crystallography. I am also indebted to Professor Jeremy Harvey whose advice and guidance on running calculations has been invaluable. Working with Professor Paul Pringle and Louise Hazeland has been particularly enjoyable and I am grateful for both their enthusiasm and patience in dealing with all things collaborative. Additionally, I would like to thank a number of technical and support staff at the universities of both Bristol and Edinburgh, who have ensured the smooth running of a number of facilities, often going above and beyond when times were difficult!

On a personal note, I'd like to thank my friends both in Bristol and Edinburgh for their support, thanks in particular go to Emma for helping me through the unpredictability of my PhD. Finally, I'd like to thank my family, to whom I am greatly indebted, their encouragement, support and patience have been unrelenting, I could not have made it this far without them.

Contents

Abbreviations

Ar	aryl
Bn	benzyl
b.p.	boiling point
^{n}Bu	normal butyl
^{t}Bu	tertiary butyl
Cy	cyclohexyl
DABCO	1,4-diazabicyclo[2.2.2]octane
DCM	dichloromethane
DFT	density functional theory
DMAP	4-dimethylaminopyridine
DMSO	dimethylsulfoxide
E_T^N	normalised Dimroth-Reichardt parameter
Et	ethyl
EtOH	ethanol
HSAB	Hard soft acid base theory
LB	Lewis base
LFER	linear free energy relationship
Me	methyl
MeOH	methanol
MIDA	*N*-methylimidodiacetic acid
m.p.	melting point
MS	mass spectrometry
NMR	nuclear magnetic resonance
Nu	nucleophile
PAMP	phenylmethyl(*o*-methoxyphenyl)phosphine
^{i}Pr	isopropyl
^{n}Pr	normal propyl
TEP	Tolman electronic parameter
THF	tetrahydrofuran

1 General introduction

1.1 Lewis base displacement reactions

1.1.1 Lewis adducts

Since its popularisation by Thomas Kuhn in 1962 the phrase "paradigm shift" is one that is often considered to be overused.[1] However, the phrase is probably rarely as aptly applied as when considering the progression in chemical understanding that took place in 1923, a year that saw the publication of Brönsted,[2] Lowry,[3] and Lewis'[4] theories on acid-base interactions. These pioneering theories are of such significance that they remain deeply rooted in the foundations of chemistry almost a century later. A testament to these concepts is that they remain remarkably unchanged today, with the IUPAC definition of a Lewis base as "*A molecular entity (and the corresponding chemical species) able to provide a pair of electrons and thus capable of coordination to a Lewis acid, thereby producing a Lewis adduct.*"[5] being almost identical to that of Lewis. The Lewis adducts referred to in the definition have a long and rich history, with a wide variety of such compounds now characterised and host of applications discovered.

With a vacant p-orbital, tri-coordinate boron centres can be considered archetypal Lewis acids, whose chemistry has been well studied. Lewis adducts containing boron-centred Lewis acids have been known for centuries, with publications reporting $H_3N{\cdot}BF_3$ by Gay-Lussac[6] and $H_3P{\cdot}BCl_3$ by Besson[7] dating as far back as 1809 and 1890, respectively. An interesting subset of these structures with a BH_3 Lewis acid fragment have been described, the first of which being $Me_3N{\cdot}BH_3$ synthesised by Burg and Schlesinger in 1937.[8] The reactivity of such Lewis adducts, in particular the displacement of the Lewis base from the corresponding adduct, has been of great interest, and research in this area has had a significant part to play in many of the subsequent developments in this area. Early synthetic routes to Lewis base borane complexes ($LB{\cdot}BH_3$) tended to rely on direct reaction between Lewis base and diborane (B_2H_6). However, since the discovery of $BH_3{\cdot}THF$ and $BH_3{\cdot}SMe_2$, displacement reactions using these weakly coordinating Lewis base complexes have gained popularity, largely replacing the diborane synthetic route.[9,10] Aside from their utility as synthetic precursors, the diverse and ever-expanding range of applications of Lewis base borane adducts has led to a surge in interest in these compounds. To date, amine and phosphine borane adducts have found use as hydroboration[11–13] or reducing[14–16] reagents in synthetic transformations, active pharmaceutical agents,[17] and even potential hydrogen storage materials.[18,19] In addition, amine and phosphine borane adducts are precursors to a

host of new materials (*via* dehydrocoupling)[20–22] and, when afforded suitable steric protection, have been used in frustrated Lewis pair chemistry[23–25]. Furthermore, borane complexation has found a great deal of use as a protecting group strategy for the synthesis of both phosphines[26–27] and amines, [28] typically conferring stability towards aerobic oxidation in the case of phosphines, and used to mask nucleophilic reactivity of amines.

1.1.2 Mechanisms of Lewis base displacements

Displacement of a Lewis base from its corresponding borane adduct is a reaction that has attracted a great deal of attention, both mechanistically and also for its ability to rank or quantify Lewis basicity. Hawthorne and co-workers have carried out an in-depth mechanistic analysis on a number of related displacement reactions of amine borane adducts, see Scheme 1.1.[29–31] The evidence collected suggests a continuum of mechanisms exist, with S_N2 and S_N1-type mechanisms occupying the extremities of this scale.

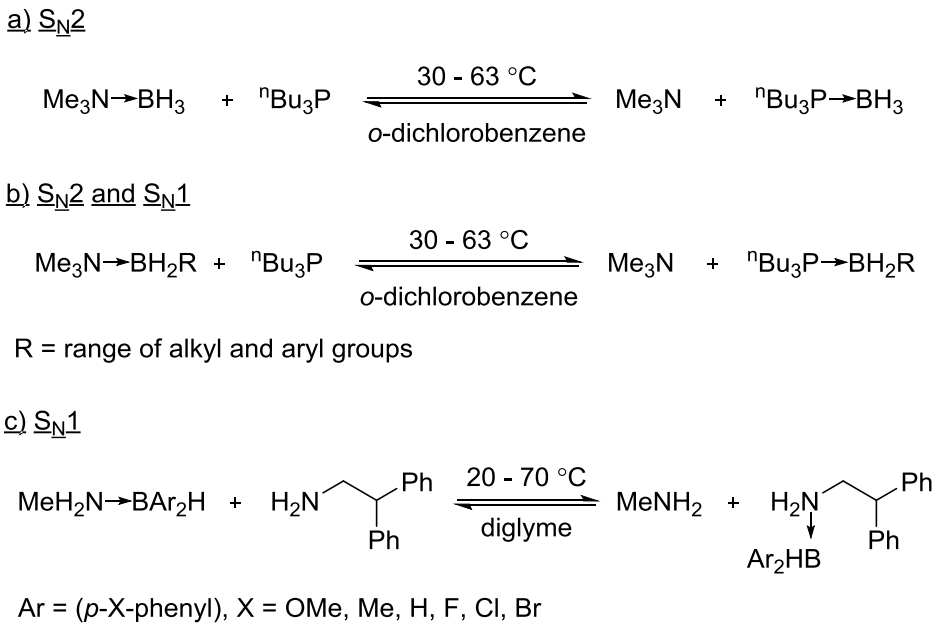

Scheme 1.1 Lewis base borane displacements carried out by Hawthorne and co-workers demonstrating that the mechanisms present range between S_N2 and S_N1, with substitution at boron playing a significant role in the determining the dominant mechanism.[29–31]

Displacements occurring between Et/$Me_3N{\cdot}BH_3$ adducts and a $^nBu_3P$ nucleophile were shown to follow a second order rate law, and have a negative entropy of activation (−5 cal K^{-1} mol^{-1} for $Me_3N{\cdot}BH_3$). This provides some compelling evidence of S_N2 type process occurring when using BH_3 Lewis acids. Conversely, when diaryl borane species were used

as the Lewis acid fragment, the rate was reported to be insensitive to both the identity and concentration of the nucleophile, see Scheme 1.1c, providing evidence for an S_N1-type mechanism. The reactions were also reported to obey a first order rate law, have positive entropies of activation and display a negative ρ value (Hammett plot), supporting an S_N1-type process. Hawthorne found that when using borane Lewis acids containing a single alkyl/aryl substituent (BH_2R), displacement reactions from the corresponding Me_3N complexes with $^nBu_3P$ displayed characteristics both of the proposed S_N1 and S_N2 type mechanisms, see Scheme 1.1b. Further evidence that both S_N1 and S_N2 type mechanisms can operate comes from a study by Mioskowki demonstrating an inversion of configuration at a chiral boron, upon undergoing a Lewis base displacement of a phosphine borane adduct.[32]

Whilst this mechanistic data, in addition to that collected by others,[33] suggests that phosphine and amine borane adducts ($R_3N/P{\cdot}BH_3$) are likely to react with Lewis bases in an associative S_N2-like manner, caution should be used when extrapolating to other systems. The factors known to affect the reaction mechanism include both solvation, and substitution at boron, with other variables such as the identities of the nucleophile and Lewis base fragment being less well understood.

1.1.3 Displacement reactions as a scale of Lewis basicity

Aside from the applications described above, one of the most interesting aspects of borane transfer reactions is their ability to provide scales of relative Lewis basicity and acidity. Traditionally, attempts to determine the relative affinity of Lewis bases with a given reference Lewis acid were largely dependent on comparisons of enthalpies of formation. Whilst useful, these studies could be complicated by additional enthalpy changes present (such as changes in solvation) and are somewhat restricted as they do not include entropic factors. Thus, the use of Lewis base displacement reactions proved a useful alternative to allow the ranking of Lewis bases/acids. Displacement reactions, however, do have their drawbacks: the equilibrium constants obtained from direct displacement reactions are not always easy to measure accurately, and can also be highly dependent on the conditions used. Moreover, these limitations, which arise from the large span in reactivity across Lewis bases/acids, prevent a universal scale[a] of Lewis basicity from being established.[34] The development of Lewis acidity/basicity scales however, remains a useful undertaking as,

[a] The development of a universal scale requires both accurate and reliable determination of equilibrium constants across a range of Lewis adduct formation or displacement reactions, using one reference Lewis acid and identical experimental conditions.

provided the scales are applied both prudently and within a limited domain, they can aid in both the development and understanding of reactions. With advances in suitable computational methods, attempts to quantify Lewis acidity/basicity, free of the limitations of experiment, have been made; whether these can provide a consistent and experimentally useful universal scale of Lewis acidity/basicity is yet to be determined.[35–38]

Many of the limitations of experimentally derived Lewis acidity/basicity scales arise from the desire to quantify reactivity (obtain accurate equilibrium constants). These problems can, to a certain extent, be circumvented through a qualitative analysis, and a great deal of work has been carried out in this regard. Stone made substantial contributions to this area, both in carrying out Lewis base displacement reactions, and collating the work performed by others, in an attempt to rationalise trends in group III/V Lewis acid/base adducts.[39] Typical conditions for these displacements tended to involve mixing a Lewis adduct with a competing Lewis base at elevated temperatures, with the aim of ensuring thermodynamic equilibrium was reached.[b] Data obtained by Graham and Stone,[40] Brown,[41] and Coates[42] provide qualitative information on the Lewis adduct stability, when using a range of group III Lewis acids such as BMe_3, $AlMe_3$ and $GaMe_3$ and a range of methylated group V/VII Lewis bases, see Scheme 1.2a. As might be expected based on Bent's rule, the thermodynamic stability of the Lewis adducts (seemingly independent of the nature of the Lewis acid) decreased when using the heavier congener Lewis bases.

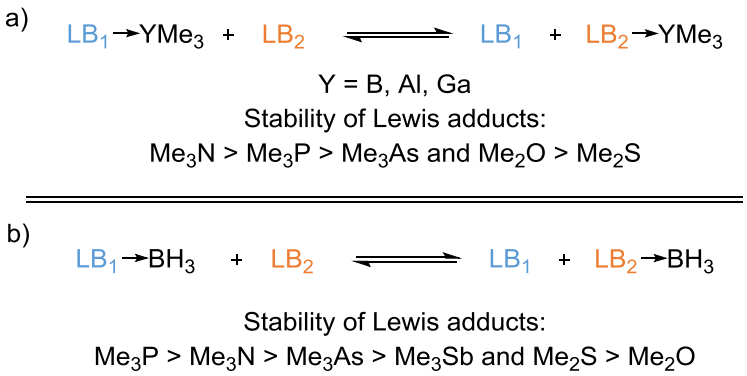

Scheme 1.2 Displacement reactions to determine the relative thermodynamic stability of a range of Lewis adducts. Using this information, the relative scales of Lewis basicity were established.[39]

The situation is more complicated however, as in the same report, Graham and Stone observed a partial reversal in the Lewis basicity trend when using BH_3 as a reference Lewis acid, Me_3N being displaced from its borane (BH_3) adduct by Me_3P, see Scheme 1.2b.

[b] This is important as Lewis basicity is defined by IUPAC as an equilibrium effect.[5]

Similarly, Me_2S was found to provide a more thermodynamically stable adduct with BH_3 than its lighter congener Me_2O, the inverse of the trend with a BMe_3 Lewis acid.[43] The relatively small difference in structure between BMe_3 and BH_3 suggests that relative Lewis basicity is a property that can be both finely poised and very sensitive to subtle changes in steric and electronic effects. Further support for the sensitivity of trends in Lewis basicity to the identity of the Lewis acid comes from a 1978 report detailing displacement reactions from Lewis adducts of the formula $Me_3N{\cdot}BF_nH_{3-n}$ (n = 0 - 3), see Scheme 1.3.[44] Consistent with previous studies, the Lewis adduct $Me_3P{\cdot}BH_3$ was found to be more thermodynamically stable than $Me_3N{\cdot}BH_3$, however, this trend was reversed when introducing one or more fluorine substituents on the boron. As before, even small changes to the structure of the Lewis acid show the propensity to change relative trends, reinforcing that idea that an experimentally derived absolute scale of Lewis basicity is an impossibility. Despite this, Maria and Gal have used BF_3 as a reference Lewis acid to describe a Lewis base affinity scale based on enthalpies of complexation in dichloromethane.[45] Whilst in the strictest sense not a Lewis basicity scale, the data collected are useful and have been shown to correlate with the solvation of alkali metal cations (the enthalpy parameter used to describe the Lewis basicity of the solvent).

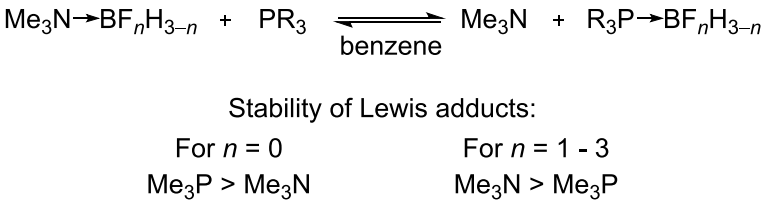

Scheme 1.3 Displacement reactions carried out by Genangel to determine the relative thermodynamic stability of a series of Lewis base/acid adducts.[44]

Lewis base displacements have had a significant part to play in rationalising trends in Lewis basicity/acidity, with the data concisely summarised in the following quote by Mulliken: "*However, it must be kept in mind that the strength of a (Lewis) acid is not quite a unique absolute quantity, but depends appreciably on specific features of its interaction with the base with which it is paired.*"[46] Aside from describing the complexity in this area, such statements provide an indication of the significance of direct displacement reactions in the evolution of theories concerning the nature of bonding, potentially laying the groundwork for theories such as Pearson's Hard soft acid base theory (HASB).[47] The determination and analysis of quantitative kinetic and thermodynamic information pertaining to Lewis base displacements from a wide variety of borane adducts forms the subject of this thesis.

1.2 References

[1] T. S. Kuhn, *The Structure of Scientific Revolutions*, University Of Chicago Press, **1962**.
[2] J. N. Brönsted, *Recl. Trav. Chim. Pays-Bas* **1923**, *42*, 718–728.
[3] T. M. Lowry, *J. Soc. Chem. Ind.* **1923**, *42*, 43–47.
[4] G. N. Lewis, *Valence and the Structure of Atoms and Molecules*, Chemical Catalogue Company Inc., New York, **1923**.
[5] P. Muller, *Pure Appl. Chem.* **1994**, *66*, 1077–1184.
[6] J. L. Gay-Lussac, *Mem. Phys. Chim. Soc. D'Arcueil* **1809**, *2*, 211.
[7] A. Besson, *Comptes Rendus l'Académie des Sci.* **1890**, *110*, 516–518.
[8] A. B. Burg, H. I. Schlesinger, *J. Am. Chem. Soc.* **1937**, *59*, 780–787.
[9] R. M. Adams, J. Beres, A. Dodds, A. J. Morabito, *Inorg. Chem.* **1971**, *10*, 2072–2074.
[10] P. V. Ramachandran, A. S. Kulkarni, *RSC Adv.* **2014**, *4*, 26207–26210.
[11] J. M. Clay, E. Vedejs, *J. Am. Chem. Soc.* **2005**, *127*, 5766–7.
[12] H. C. Johnson, R. Torry-Harris, L. Ortega, R. Theron, J. S. McIndoe, A. S. Weller, *Catal. Sci. Technol.* **2014**, *4*, 3486–3494.
[13] P. Shapland, E. Vedejs, *J. Org. Chem.* **2004**, *69*, 4094–4100.
[14] H. C. Brown, J. V. B. Kanth, M. Zaidlewicz, *J. Org. Chem.* **1998**, *63*, 5154–5163.
[15] P. V. Ramachandran, P. D. Gagare, K. Sakavuyi, P. Clark, *Tetrahedron Lett.* **2010**, *51*, 3167–3169.
[16] A. Pelter, R. M. Rosser, S. Mills, *J. Chem. Soc., Perkin Trans. 1* **1984**, 717–720.
[17] B. Burnham, *Curr. Med. Chem.* **2005**, *12*, 1995–2010.
[18] D. J. Heldebrant, A. Karkamkar, J. C. Linehan, T. Autrey, *Energy Environ. Sci.* **2008**, *1*, 156–160.
[19] M. Diwan, H. T. Hwang, A. Al-Kukhun, A. Varma, *AIChE J.* **2011**, *57*, 259–264.
[20] E. M. Leitao, N. E. Stubbs, A. P. M. Robertson, H. Helten, R. J. Cox, G. C. Lloyd-Jones, I. Manners, *J. Am. Chem. Soc.* **2012**, *134*, 16805–16816.
[21] T. N. Hooper, M. A. Huertos, T. Jurca, S. D. Pike, A. S. Weller, I. Manners, *Inorg. Chem.* **2014**, *53*, 3716–3729.
[22] D. J. Liptrot, M. S. Hill, M. F. Mahon, A. S. S. Wilson, *Angew. Chem. Int. Ed.* **2015**, *54*, 13362–13365.
[23] D. W. Stephan, G. Erker, *Angew. Chem. Int. Ed.* **2015**, *54*, 6400–6441.
[24] S. J. Geier, D. W. Stephan, *J. Am. Chem. Soc.* **2009**, *131*, 3476–3477.
[25] C. Jiang, O. Blacque, T. Fox, H. Berke, *Organometallics* **2011**, *30*, 2117–2124.
[26] M. Ohff, J. Holz, M. Quirmbach, A. Börner, *Synthesis* **1998**, *10*, 1391–1415.
[27] D. Hérault, D. H. Nguyen, D. Nuel, G. Buono, *Chem. Soc. Rev.* **2015**, *44*, 2508–2528.
[28] M. A. Zajac, *J. Org. Chem.* **2008**, *73*, 6899–6901.
[29] W. L. Budde, M. F. Hawthorne, *J. Am. Chem. Soc.* **1971**, *93*, 3147–3150.
[30] D. E. Walmsley, W. L. Budde, M. F. Hawthorne, *J. Am. Chem. Soc.* **1971**, *93*, 3150–3155.
[31] F. J. Lalor, T. Paxson, M. F. Hawthorne, *J. Am. Chem. Soc.* **1971**, *93*, 3156–3160.
[32] P. Vedrenne, V. Le Guen, L. Toupet, T. Le Gall, C. Mioskowski, *J. Am. Chem. Soc.* **1999**, *121*, 1090–1091.
[33] R. G. Potter, D. M. Camaioni, M. Vasiliu, D. A. Dixon, *Inorg. Chem.* **2010**, *49*, 10512–10521.
[34] C. Laurence, J. Graton, J.-F. Gal, *J. Chem. Educ.* **2011**, *88*, 1651–1657.
[35] H. Anane, S. El Houssame, A. El Guerraze, A. Jarid, A. Boutalib, I. Nebot-Gil, F. Tomás, *J. Mol. Struct. Thermochem.* **2004**, *709*, 103–107.
[36] H. Anane, A. Boutalib, I. Nebot-Gil, Francisco Tomàs, *Chem. Phys. Lett.* **1998**, *287*, 575–578.

[37] H. Umeyama, K. Morokuma, *J. Am. Chem. Soc.* **1976**, *98*, 7208–7220.
[38] V. Jonas, G. Frenking, M. T. Reetz, *J. Am. Chem. Soc.* **1994**, *116*, 8741–8753.
[39] F. G. A. Stone, *Chem. Rev.* **1958**, *58*, 101–129.
[40] W. A. G. Graham, F. G. A. Stone, *J. Inorg. Nucl. Chem.* **1956**, *3*, 164–177.
[41] N. Davidson, H. C. Brown, *J. Am. Chem. Soc.* **1942**, *64*, 316–324.
[42] G. E. Coates, *J. Chem. Soc.* **1951**, 2003–2013.
[43] W. J. Atkins, E. R. Burkhardt, K. Matos, *Org. Process Res. Dev.* **2006**, *10*, 1292–1295.
[44] J. M. VanPaasschen, R. A. Geanangel, *Inorg. Chem.* **1978**, *17*, 3302–3304.
[45] P. C. Maria, J.-F. Gal, *J. Phys. Chem.* **1985**, *89*, 1296–1304.
[46] R. S. Mulliken, *J. Am. Chem. Soc.* **1952**, *74*, 811–824.
[47] R. G. Pearson, *J. Am. Chem. Soc.* **1963**, *85*, 3533–3539.

2 Phosphine Borane Deprotection

2.1 Introduction

2.1.1 Phosphine borane adducts as protecting groups

The application of phosphines in fields as diverse as catalysis, materials and coordination chemistry is ever growing, and as such, the development of novel phosphines remains an increasingly important challenge. Thus, the elaboration and development of synthetic routes to phosphines, especially chiral phosphines, remains essential for academic and industrial laboratories alike. Whilst the reactivity and tuneable nature of phosphines allows for a wide range of applications, it can also provide problems with the synthesis, for example some phosphines react readily with atmospheric dioxygen.[1] Aside from reducing yields this autoxidation process can be very exothermic, (even causing spontaneous ignition in air) and this adds additional risk to the handling and storage of such compounds.[2] Therefore the use of rigorously anaerobic conditions is often necessary to obtain safe and high yielding reactions.

To counteract these drawbacks, several protection strategies exist that provide a means to handle a phosphine surrogate in aerobic conditions. One such strategy that has been widely utilised involves sequestering the phosphorus lone pair through coordination to borane (BH_3). This borane protecting strategy affords air and moisture stable phosphine borane complexes ($R_3P{\cdot}BH_3$) that have even been shown to survive aerobic column chromatography.[3–5] Reports on phosphine borane complexes demonstrate that the P-B linkage is stable to both the Jones and Corey-Kim oxidative conditions, see Scheme 2.1.[6] In addition, experiments by Metille and Burton have shown $Ph_3P{\cdot}BH_3$, **1**, can be quantitatively recovered after being heated to 150 °C for 3 hours in a 3 M aqueous HCl solution.[7,8] This may be misleading however, as hydrolysis products are observed when an organic solvent (diglyme) is included to homogenise the reaction mixture, see Scheme 2.1.[9]

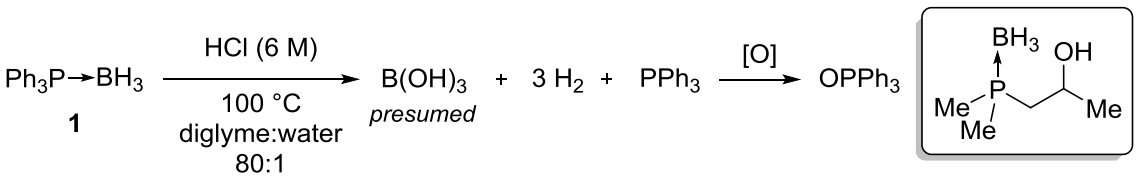

Scheme 2.1 Hydrolysis of $Ph_3P{\cdot}BH_3$, **1**, observed by Metille and Burton, oxidation to triphenylphosphine oxide occurred under the conditions above.[9] Insert: phosphine borane complex demonstrated by Pellon to resist P-B cleavage when subjected to either Jones or Corey-Kim oxidative conditions.[6]

The stability of the protected functional group is not the only pre-requisite for an effective protection strategy; the protection and deprotection reactions need to be robust and, ideally, high yielding. The borane protection of phosphines can be achieved in a number of ways, most commonly through reaction with a source of BH_3. Original reports used gaseous diborane, B_2H_6,[10,11] but this has been surpassed by commercially available reagents such as $Me_2S{\cdot}BH_3$ and $THF{\cdot}BH_3$.[12] These two weakly coordinating Lewis base borane adducts have a privileged status amongst borane protecting reagents, and have been shown to protect phosphines without eroding any isomeric enrichment at *P*-stereogenic centres.[13] Whilst not as commonplace, other Lewis base borane complexes have been used to protect phosphines including $Et_3N{\cdot}BH_3$,[14,15] $H_3N{\cdot}BH_3$[16] and $^{i}Pr_2NEt{\cdot}BH_3$.[17] Alternate syntheses using $NaBH_4$ as a source of the borane moiety have also been used to access protected phosphines, albeit requiring addition of a suitable hydride acceptor.[18–22] Phosphine borane complexes have also been synthesised from phosphine oxides and sulphides, with many one-pot reduction/protection protocols now reported.[19,23–27]

Aside from the air, moisture and configurational stability afforded by borane protection, differences in reactivity between the parent phosphine and the borane adduct can also be exploited. Notably, the protons in the alpha and beta position (relative to phosphorus) become more acidic after complexation of borane (calculated in the gas phase).[28,29] This has been widely exploited in the synthesis of chiral phosphines, with an alkyllithium/(−)-sparteine combination used by Evans capable of desymmetrising a prochiral phosphine borane, see Scheme 2.2.[30] Based on this, a range of similar systems have since been reported.[31–34] In addition to the desymmetrisation of phosphine borane complexes, several methods exist to synthesise *P*-stereogenic phosphines that use a borane protecting strategy, for example the ephedrine methodology of Jugé and Genêt[35–37] and menthol methodology of Gilheany and co-workers.[38]

In addition to protecting phosphines, phosphine borane adducts have a host of other applications. Through deployment of transition metal catalysis, primary and secondary phosphine borane adducts can be selectively transformed into a range of oligomeric and polymeric species; the polymers are of particular interest due to being valence isoelectronic with polyolefins.[39–45] Phosphine borane adducts have also found limited application as reagents for hydroboration,[46–48] hydrophosphination[49–52] and additionally are used as a shelf stable precursor to the Raines reagent for use in Staudinger reactions.[53–55] Also, upon "injection into the vitreous chamber of the injured eye", a phosphine borane complex has

been shown to exhibit neuroprotective properties in rats with severed ganglion cells, see Scheme 2.2.[56,57]

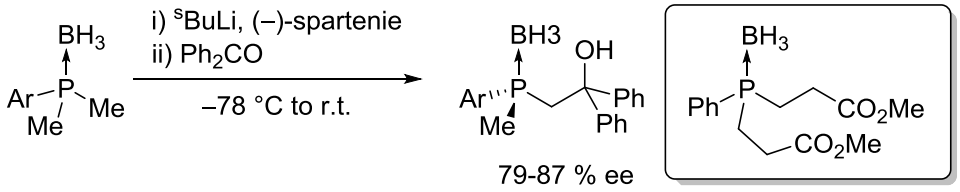

Scheme 2.2 Evans' enantioselective deprotonation desymmetrisation strategy to synthesise phosphines with P-stereogenic centres.[30] Insert: The phosphine borane complex found to exhibit neuroprotective properties when injected into eyes of rats.[56,57]

2.1.2 Deprotection methods

The concept of the borane protection strategy was pioneered by Imamoto, who reported the first example of the "deprotection"; using excess diethylamine, (*S*)-PAMP·BH_3 (PAMP = phenyl(*o*-anisyl)(methyl)phosphine) was decomplexed to give (*S*)-PAMP with retention of configuration.[24] Since Imamoto's publication, several deprotection methods have been reported, and these can be grouped into three categories: alcoholysis, acidolysis and displacement with a competing Lewis base (almost exclusively an amine). The first of these, alcoholysis, has received relatively little attention, despite the promising studies in the 1960's demonstrating the analogous hydrolysis of $Ph_3P{\cdot}BH_3$, **1**. The first example of a "deprotection" using an alcohol (ethanol) was reported by Jugé in 2000,[58] however, ethanolysis only received widespread attention after reports by Nozaki and Hiyama[59] and Van der Eycken[60] demonstrated its scope and limitations, see Scheme 2.3.

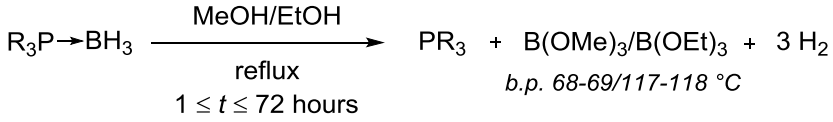

Scheme 2.3 Van der Eycken's reported conditions for alcoholysis of phosphine borane adducts.[60] The reported yields (between 0 and 100%) and time taken vary dramatically depending on the substituents at phosphorus.

Despite the attraction of the simple conditions and ease of work up (*in vacuo* removal of alcohol, and the borate), obtaining high conversions often requires very long reaction times and elevated temperatures. Additionally the evolution of three molar equivalents of dihydrogen throughout the reaction may lead to safety-related complications. Nevertheless,

the advantages of this procedure have allowed for development of a one-pot deprotection/hydrogenation protocol, through *in situ* generation of a rhodium phosphine complex.[61] The mechanism of alcoholysis of phosphine borane complexes has not been examined directly, but comparisons with the corresponding processes for amine borane adducts may provide some information on mechanisms likely to be operative.[62,63]

The acid mediated deprotection was first reported in 1994 by Livinghouse, who reported high yielding (89-99%) deprotections of diphosphine borane adducts using commercially available $HBF_4{\cdot}OMe_2$ followed by a basic hydrolytic work up, see Scheme 2.4.[64] Following this, other acids have successfully been applied in the deprotection, including trifluoroacetic acid[53,65] and trifluoromethylsulfonic acid.[66,67] One significant advantage of the acid mediated deprotection over both the alcoholyisis and the more conventional amine deprotection is the reduced timescale required for reactions containing electron rich phosphines. Given this advantage, McKinstry and Toto have reported on the mechanism of the $HBF_4{\cdot}OMe_2$ deprotection and, through comparison between experimental and calculated ^1H and ^{13}C NMR chemical shifts, have suggested an $R_3P{\cdot}BH_2F$ intermediate is formed through hydride/fluoride exchange at boron.[68]

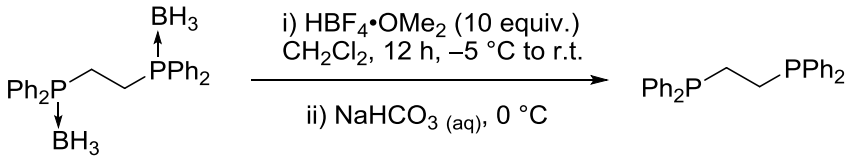

Scheme 2.4 Original acid mediated deprotection conditions reported by Livinghouse.[64]

Of all the deprotection techniques, Lewis base displacement of borane is by far the most well established, with Imamoto's pioneering report on the borane protecting strategy using an excess of diethylamine to enact the deprotection.[24] Since the initial report, a large number of phosphines have been synthesised using a borane protection strategy in combination with a diethylamine deprotection.[30,35,69–77] However, following a limited solvent and amine screen in 1993 by Pellon and Le Corre,[78] DABCO has risen to prominence as the reagent of choice for phosphine borane deprotections.[49,55,79–89] Although less common, a number of alternative amines have also found use in the deprotection including morpholine,[90–96] pyrrolidine,[32,97] triethylamine[98] and Hünig's base,[53] as well as a range of hydroxyl functionalised amines[99] (to make a water soluble amine borane adduct). Whilst the vast majority of deprotections use amines, they are not the only Lewis bases used in the displacement reaction, high pressures of carbon monoxide can also be effective allowing the development of *in situ* deprotection/hydroformylation protocols.[100] Despite the amine deprotections typically being

high-yielding there are drawbacks, with some reactions reported to take up to 5 days[101–103] and use a huge excess of amine (over 100 equiv. of DABCO).[104]

As can be seen from the variety of amines used, the choice of conditions is vast, with many variables such as the identity and equivalents of amine, solvent, temperature and reaction time not well understood. A further complicating factor is the relationship between these variables and the identity of the phosphine borane complex. With this in mind, we sought to establish a greater understanding of the mechanism of amine deprotection, and the impact of the variables discussed above on both the rate and efficiency of deprotection. Using this information we hoped to provide guidelines allowing for an informed choice of deprotection conditions.

2.2 Amine deprotection

2.2.1 Mechanism of amine deprotection

There is precedent for both S_N1 and S_N2-like mechanisms (see Scheme 2.5) in similar Lewis base displacement reactions. Hawthorne's reports on the mechanism of displacements from substituted amine borane adducts ($Me_3N{\cdot}BR_2H$) have demonstrated that the mechanism is dependent on the substitution at boron; with bulky or aromatic substituents tipping the balance in favour of S_N1.[105–107]

a) S_N1 dissociative

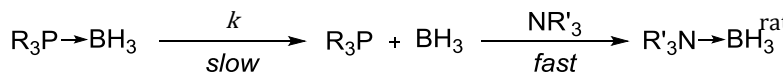

$$\text{rate} = k[\mathrm{R_3P \cdot BH_3}]$$

b) S_N1 associative

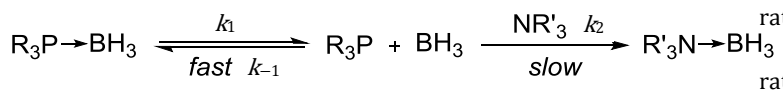

$$\text{rate} = k_2[\mathrm{R'_3N}][\mathrm{BH_3}]$$

$$\text{rate} = \frac{k_1 k_2[\mathrm{R'_3N}][\mathrm{R_3P \cdot BH_3}]}{k_{-1}[\mathrm{R_3P}] + k_2[\mathrm{R'_3N}]}$$

c) S_N2

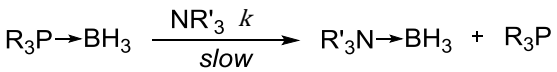

$$\text{rate} = k[\mathrm{R_3P \cdot BH_3}][\mathrm{R'_3N}]$$

Scheme 2.5 Mechanisms and corresponding rate laws that could be operating in the amine deprotection of phosphine borane complexes, steady state inferred in S_N1 associative rate law.

Furthermore, a report from Le Gall and Mioskowski, observing inversion of configuration at stereogenic boron centre $Ph_3P{\cdot}BH(CN)(R)$ (when reacted with a Me_2PhP nucleophile) provides excellent evidence for an S_N2-like mechanism with nucleophilic attack at boron.[103] Despite this body of work, mechanistic details on the amine deprotection of phosphine borane complexes are sparse, allowing room for speculation, with a number of reports suggesting the process is operating *via* a dissociative mechanism, i.e. Scheme 2.5a.[108–110]

In situ $^{11}B\{^1H\}$ NMR analysis of borane transfer from $Ph_3P{\cdot}BH_3$ **1**, (0.02 M in toluene), to quinuclidine, **2**, provided a suitable homogenous system for monitoring the conversion to quinuclidine borane, **3**, and Ph_3P, see Scheme 2.6. During the reaction no intermediate species were detected by $^{11}B\{^1H\}$ NMR.[c]

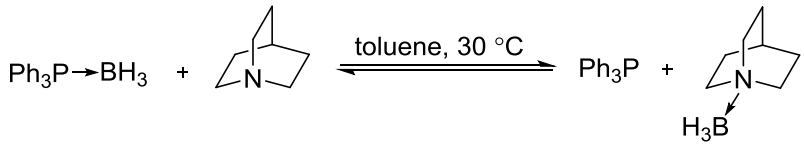

1 **2** **3**

$$\text{rate} = k([R_3P \cdot BH_3][R'_3N] - [R'_3N \cdot BH_3][R_3P]/K)$$

Scheme 2.6 Reaction conditions used to obtain the rate law, rate and equilibrium constants and activation parameters (reactions also performed at 40, 50, 60 and 70 °C), typically $[\mathbf{1}]_0$ = 0.02 M and $[\mathbf{2}]_0$ = 0.01-0.73 M.

The temporal concentration data obtained displayed a second order decay in the concentration of **1** at low quinuclidine loadings, rapidly progressing to pseudo-first order with greater than 4 equivalents of quinuclidine. Simulation of this data according to a standard bimolecular equilibrium model $-d[\mathbf{1}]/dt = k([\mathbf{1}][\mathbf{2}] - [Ph_3P][\mathbf{3}]/K)$ provided good fits across a wide range of $[\mathbf{2}]_0$ (0.01 - 0.73 M), see Figure 2.1. As can be seen by the magnitude of *K*, the equilibrium position is greatly in favour of the products, and consequently, the reactions displayed irreversible character under most of the conditions studied. Indeed, the value of *K* was obtained *via* examination of the rate of the back reaction ($[Ph_3P]_0$ = 0.04 M, $[\mathbf{3}]_0$ = 0.10 M). An additional experiment carried out at a different $[\mathbf{1}]_0$ (0.04 M) confirmed the first order dependence of the forward reaction on [**1**]. Furthermore, the temporal concentration data from this experiment showed excellent agreement with the simulation according to the same bimolecular equilibrium model as above. The dependence of the reaction rate on quinuclidine concentration excludes a S_N1 dissociative mechanism (with rate limiting P-B scission) being dominant. For an S_N1 associative pathway to be active, the rate

[c] Minimum threshold of detection defined by a signal-to-noise ratio of 1.5.

of consumption of **1** would deviate from a second order kinetic profile, as a consequence of build-up of the Ph_3P, see steady state rate law in Scheme 2.5b. Experimental evidence collected demonstrates that the temporal concentration profiles remain second order (or pseudo-first order) to high conversion (< 99%), suggesting that the S_N1 associative pathway is not operative. The key test however, comes from monitoring the rate of the model reaction in the presence of deuterated phosphine, d_{15}-Ph_3P. Not only would this be expected to retard the rate of formation of amine borane complex **3**, but also, BH_3 crossover between the two phosphines should occur on a timescale much faster than the deprotection reaction (as $k_{-1}[Ph_3P] >> k_2[R'_3N]$: what distinguishes associative from dissociative). When d_{15}-Ph_3P was added to a reaction, not only was no such crossover observed over the course of the reaction, but also the rate of formation of **3** was not inhibited, see Figure 2.2. Direct BH_3 exchange does occur between **1** and d_{15}-Ph_3P, but this occurs approximately 100-fold slower than reaction between **1** and quinuclidine ($k_{exchange}$ = 3.3 × 10^{-5} M^{-1} s^{-1} see Appendix, Figure 6.13 for details).

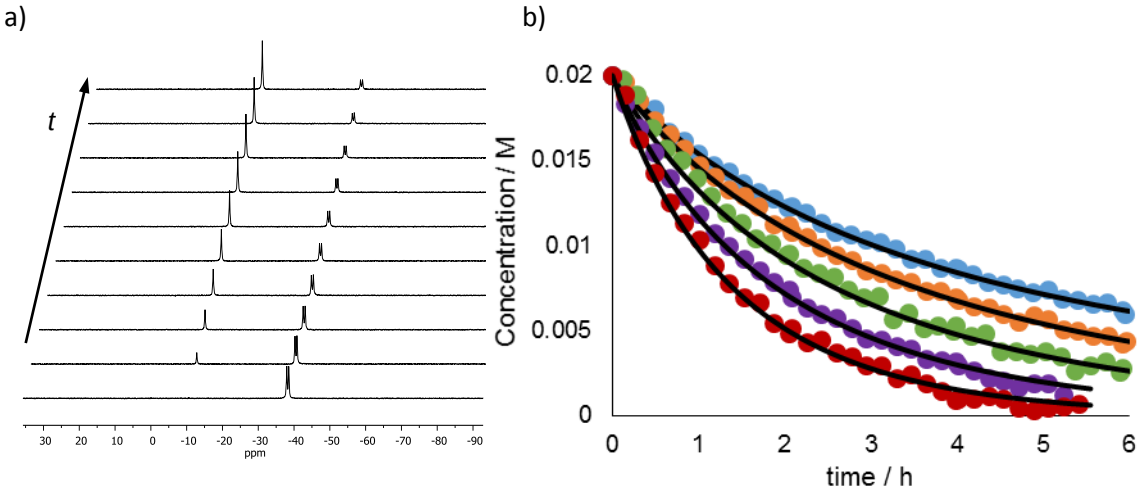

Figure 2.1 a) Set of stacked $^{11}B\{^1H\}$ NMR spectra displaying the conversion of $Ph_3P{\cdot}BH_3$ **1** to quinuclidine borane, **3**. b) Temporal concentration data for reaction of **1** ($[\mathbf{1}]_0$ = 0.02 M) with various initial concentrations of quinuclidine, **2**. Circles are experimental data (blue: $[\mathbf{2}]_0$ = 0.03 M, orange: $[\mathbf{2}]_0$ = 0.04 M, green: $[\mathbf{2}]_0$ = 0.05 M, purple: $[\mathbf{2}]_0$ = 0.06 M and red: $[\mathbf{2}]_0$ = 0.08 M. Lines are simulation according to $-d[\mathbf{1}]/dt = k([\mathbf{1}][\mathbf{2}]-[\mathbf{3}][Ph_3P]/K)$; k = 2.6 × 10^{-3} M^{-1} s^{-1}, K = 7.4 × 10^3.

Analysis of the model deprotection at a variety of temperatures furnishes rate constants which, when manipulated according to the Eyring equation, provide activation parameters.[d] Reactions were performed at temperatures between 30 and 70 °C inclusive, the corresponding Eyring plot is shown in Figure 2.2. For reaction between **1** and quinuclidine,

[d] For discussion on the errors and residuals associated with the experiments and models used to determine *k* values see Experimental, Section 5.1 and Appendix, Section 6.2.

the activation parameters ($\Delta H^{\ddagger}$ = +16.6 kcal mol^{-1}, $\Delta S^{\ddagger}$ = −16.0 cal K^{-1} mol^{-1}), in particular the negative entropy of activation, suggest an associative transition state. These data, in addition to the kinetic modelling and crossover studies rule out S_N1-like processes and are consistent with an S_N2-like mechanism.

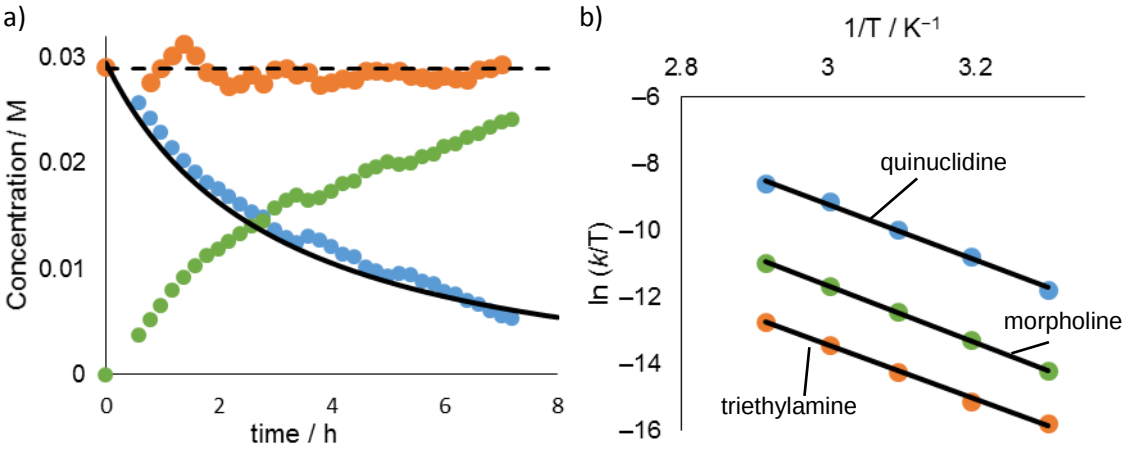

Figure 2.2 a) Deprotection of $Ph_3P{\cdot}BH_3$ ([**1**]$_0$ = 0.03 M) with quinuclidine ([**2**]$_0$ = 0.04 M) in the presence of d_{15}-Ph_3P ([d_{15}-Ph_3P]$_0$ = 0.03 M). Reaction monitored by $^{31}P\{^1H\}$ NMR, solid line is a simulation to the rate law $-d[\mathbf{1}]/dt = k([\mathbf{1}][\mathbf{2}]-[\mathbf{3}][Ph_3P]/K)$; k = 2.6 × 10^{-3} M^{-1} s^{-1}, K = 7.4 × 10^3, i.e. reaction in the absence of any added phosphine. Blue circles correspond to **1** orange to d_{15}-Ph_3P and green to Ph_3P, dotted line set to [d_{15}-Ph_3P]$_0$ to guide the eye. b) Eyring plot for reaction of $Ph_3P{\cdot}BH_3$ ([**1**]$_0$ = 0.02 M) with various amines in toluene at 30, 40, 50, 60, and 70 °C, [quinuclidine]$_0$ = 0.04 M, [morpholine]$_0$ = 0.12 M, [triethylamine]$_0$ = 0.40 M, straight lines are least squares minimisation to the data, all with Pearson R^2 values greater than 0.996. For discussion of resulting activation parameters for amines other than quinuclidine see below, Section 2.2.2.

2.2.2 Effect of amine

Using the deprotection of $Ph_3P{\cdot}BH_3$ in toluene 30 °C as a benchmark, we sought to determine the effect of the amine identity on the rate (k) and favourability (K) of the deprotection. *In situ* $^{11}B\{^1H\}$ NMR reaction monitoring provided access to temporal concentration profiles (Figure 2.3) which when fitted to a bimolecular equilibrium process, gave access to second order rate and equilibrium constants. This was achieved for a wide range of amines, including those commonly used in deprotection reactions, results are displayed in Table 2.1. A wide range of reactivity was observed, with second order rate constants spanning more than three orders of magnitude. A loose relationship appears to exist between the kinetics and thermodynamics of the borane transfer, with amines enacting fast deprotections (high k) tending to be capable of driving reactions to high conversion

(high *K*). Unsurprisingly, no simple correlation exists between second order rate constant (*k*) and the Brønsted acidity (as measured by aqueous pK_{aH}), but promising trends do exist with Mayr's nucleophilicity parameter (*N*),[111,112] albeit with a limited sample size, see Experimental, Section 5.3 for details.

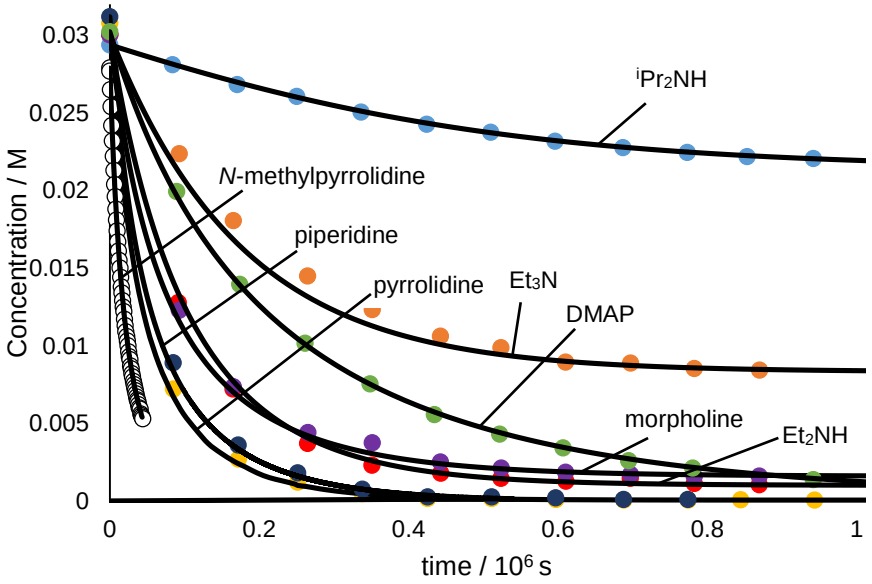

Figure 2.3 Temporal concentration data for the conversion of $Ph_3P{\cdot}BH_3$, **1**, to Ph_3P with a series of amines. Solid lines are simulation according to the rate equation $-d[\mathbf{1}]/dt = k([\mathbf{1}][amine]-[amine{\cdot}BH_3][Ph_3P]/K)$, with values of *k* and *K* listed in Table 2.1. Initial concentrations: $[^iPr_2NH]_0$ = 0.049 M, $[Et_3N]_0$ = 0.082 M, $[DMAP]_0$ = 0.06 M; DMAP = 4-dimethylaminopyridine, $[morpholine]_0$ = 0.045 M, $[Et_2NH]_0$ = 0.095 M, $[piperidine]_0$ = 0.049 M, $[pyrrolidine]_0$ = 0.045 and [*N*-methylpiperidine]$_0$ = 0.074 M + $[Ph_3P]_0$ = 0.098 M.

Despite the lack of a quantitative descriptor, some trends can be seen from this structure-activity relationship. Cyclic amines tend to react faster (*k*) and more efficiently (*K*) than their acyclic counterparts. Comparison of the activation parameters for the deprotection of **1** by triethylamine, morpholine and quinuclidine suggests that these differences arise predominately as a result of entropic differences, see Table 2.2. Acyclic amines suffer a larger entropic penalty on approach to the transition state (more negative $\Delta S^{\ddagger}$), but the degree of bond forming/breaking remains similar for all amines (similar $\Delta H^{\ddagger}$). Aside from affecting the kinetics this effect might also play a role in the thermodynamics of the system, going some way to explain the much greater *K* values observed for cyclic amines. Analogous factors may account for more subtle structural differences, for example between the rate and equilibrium constants obtained for diethylamine and triethylamine (Table 2.1, entries 2 and 4).

Table 2.1 Relative rate and equilibrium constants for the deprotection of $Ph_3P{\cdot}BH_3$, **1** by a variety of amines in toluene at 30 °C. For the absolute values and errors see Appendix, Table 6.2.

Entry	Amine	k_{rel}	K_{rel}	Equiv. R_3N for > 99% Ph_3P[a]
1	diisopropylamine	1	1	~4000
2	triethylamine	13	41	~100
3	DMAP	24	~4700	~2.0
4	diethylamine	28	560	8.5
5	morpholine	84	1400	4.2
6	piperidine	121	~29000	~1.2
7	pyrrolidine	152	~43000	~1.1
8	*N*-methylpyrrolidine	186	~2100	~3.0
9	quinuclidine	691	322000	~1.01
10	DABCO	1250[b]	17400[b]	~1.2

[a] Equivalents of amine relative of $Ph_3P{\cdot}BH_3$. [b] Data shown are for the first borane transfer to DABCO, see Figure 2.4.

$^{11}B\{^1H\}$ NMR analysis of reaction between **1** and substoichiometric DABCO provided evidence that DABCO was able to enact two decomplexations, 0.5 equiv. DABCO, giving greater than 78% conversion of $Ph_3P{\cdot}BH_3$. Unfortunately, $DABCO{\cdot}(BH_3)_2$ could not be quantifiably distinguished from $DABCO{\cdot}BH_3$ in the $^{11}B\{^1H\}$ NMR, however, through use of $^{13}C\{^1H\}$ NMR the rates of formation of both species were identified and fitted to a kinetic model, see Figure 2.4.

Table 2.2 Activation parameters for the deprotection of $Ph_3P{\cdot}BH_3$, **1**, by amines in toluene.

Entry	Amine	$\Delta H^{\ddagger}$ / kcal mol^{-1}	$\Delta S^{\ddagger}$ / cal K^{-1} mol^{-1}
1	quinuclidine	16.5	−16.0
2	morpholine	16.8	−20.1
3	triethylamine	16.2	−25.5

Whilst overall DABCO provides the fastest rates of deprotection, when statistically normalised to provide rate per nitrogen, quinuclidine **2** displays the fastest rate, consistent with a negative inductive effect of the second nitrogen in DABCO. However, despite the kinetic and thermodynamic advantages, DABCO is substantially cheaper than quinuclidine (£0.37 vs £118.50 per gram),[113] and thus remains the amine of choice for rapid deprotections. However, whilst not as fast as DABCO, a range of other amines (pyrrolidine, piperidine and *N*-methylpyrrolidine) still give faster and more favourable deprotections than

diethylamine, and offer the same advantage of volatility that can be used to simplify the work up.

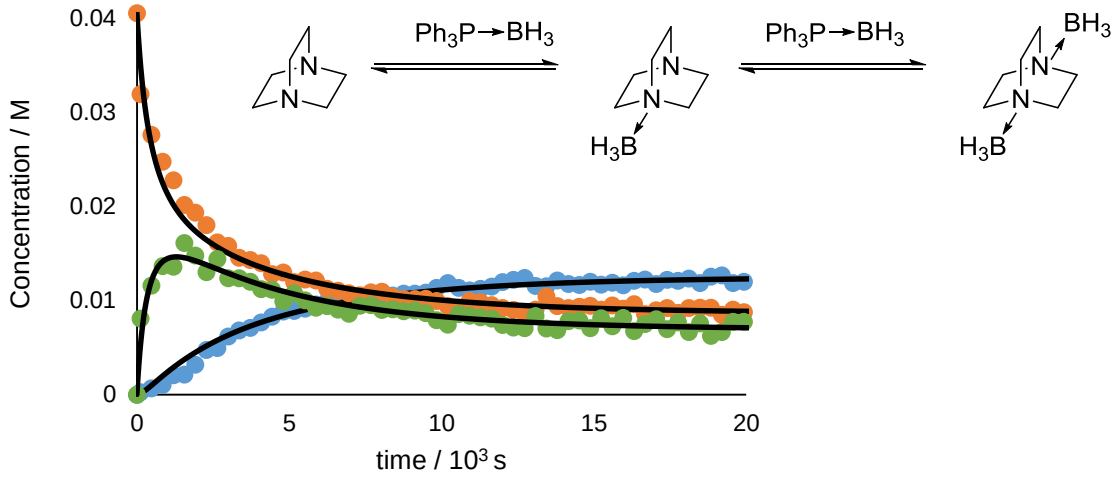

Figure 2.4 Temporal concentration data for sequential transfer of BH_3 from **1** (orange circles $[\mathbf{1}]_0$ = 0.04 M) to DABCO ($[DABCO]_0$ = 0.02 M). Green circles correspond to DABCO·BH_3, blue circles correspond to DABCO·$(BH_3)_2$. Solid lines are simulation according to two bimolecular equilibria with k_1 = 4.6 × 10^{-3} M^{-1} s^{-1}, K_1 ≥ 400, k_2 = 8.6 × 10^{-4} M^{-1} s^{-1}, K_2 = 7, full details and errors in Appendix, Table 6.2.

2.2.3 Effect of solvent

We sought to expand our studies to establish the impact of the solvent medium of the rate of deprotection. Due to limited solubility in a number of solvents at 30 °C, $Ph_3P{\cdot}BH_3$ could not be used as a model substrate. Switching to chlorinated derivative (*p*-chlorophenyl)$_3$P·BH_3, **4** gave a homogenous system for a wide range of solvents and allowed for kinetics of borane deprotection to be analysed. **4** reacted faster than **1**, as might be expected based on an increase in the inductive effect (k_{rel} = 6.4). For a more detailed discussion on the electronic influence of phosphine substituents see Section 2.3.1. Second order rate constants obtained from fitting to temporal concentration data obtained *via* $^{11}B\{^1H\}$ NMR monitoring were correlated to the normalised Dimroth-Reichardt parameter E_T^N (based on the solvatochromism of a betaine dye), see Figure 2.5.[114] Whilst overall a reasonably good correlation exists, it is clear that chloroform is an outlier, reacting 6 times slower than would be predicted based on the model. This can be explained through H-bonding between quinuclidine and chloroform, as reported by Kowalewski,[115] effectively reducing the net concentration of quinuclidine available to enact the deprotection. Use of dichloromethane as solvent provides a more extreme example of solvent inhibition, by reacting directly with the

amine nucleophile. This is of particular significance for quinuclidine, which has a half-life of 1.8 hours dichloromethane at 25.0 °C.[116]

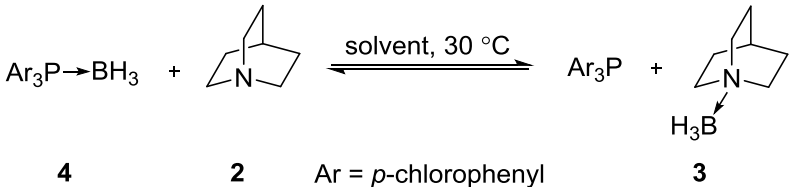

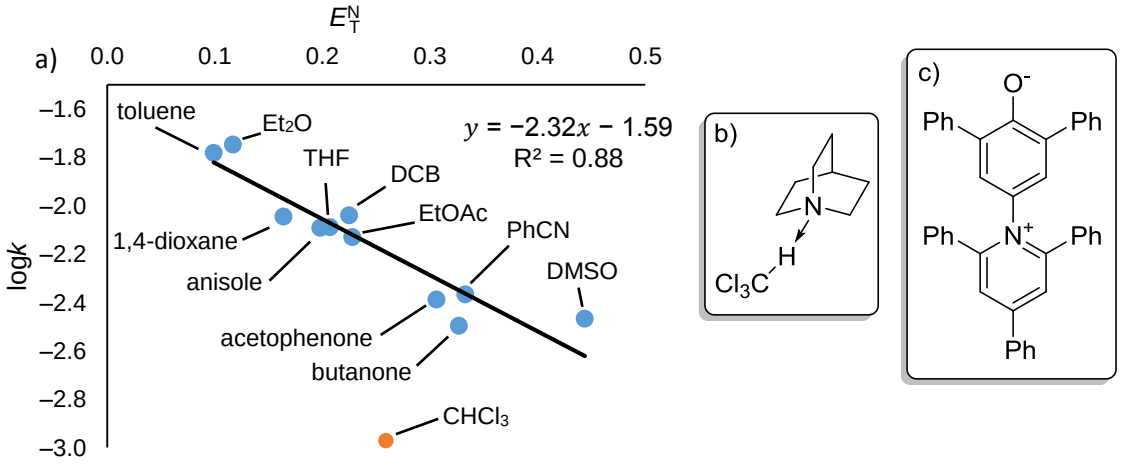

Figure 2.5 a) Correlation between log*k* (second order rate constant for reaction above) and the normalised Dimroth-Reichardt parameter, E_T^N. Line is a least squares linear regression of the data. b) Schematic of the deactivation of quinuclidine *via* hydrogen bonding with $CHCl_3$. c) Betaine dye used in the formulation of the Dimroth-Reichardt parameter.

The solvent effect on the deprotection kinetics is notably smaller than that of the identities of the amine and phosphine borane complex (*vide infra*), but nonetheless, judicious choice of solvent (Et_2O, toluene) can still afford rate advantages over more ion-stabilising solvents (DMSO), around a 5 fold difference in *k* in this instance. Although this effect is too small to be investigated quantitatively by a polarisable continuum model (PCM) in DFT studies, it can however be qualitatively rationalised by considering the charge dispersion in the ground state *vs* transition state, see Figure 2.6. Considering the reduction in the formal dipole present in phosphine borane complex **1** upon going from the ground to transition state, more ion-stabilising solvents (high E_T^N) would be expected to greater stabilise the ground state (relative to transition state) than solvents such as toluene (low E_T^N). This results in lower activation barriers, and faster deprotections, for poor ion-stabilising solvents. Pleasingly, DFT calculations for a S_N2-like deprotection of $Ph_3P{\cdot}BH_3$ by quinuclidine (toluene, 30 °C) were found to be in excellent agreement with those produced experimentally.

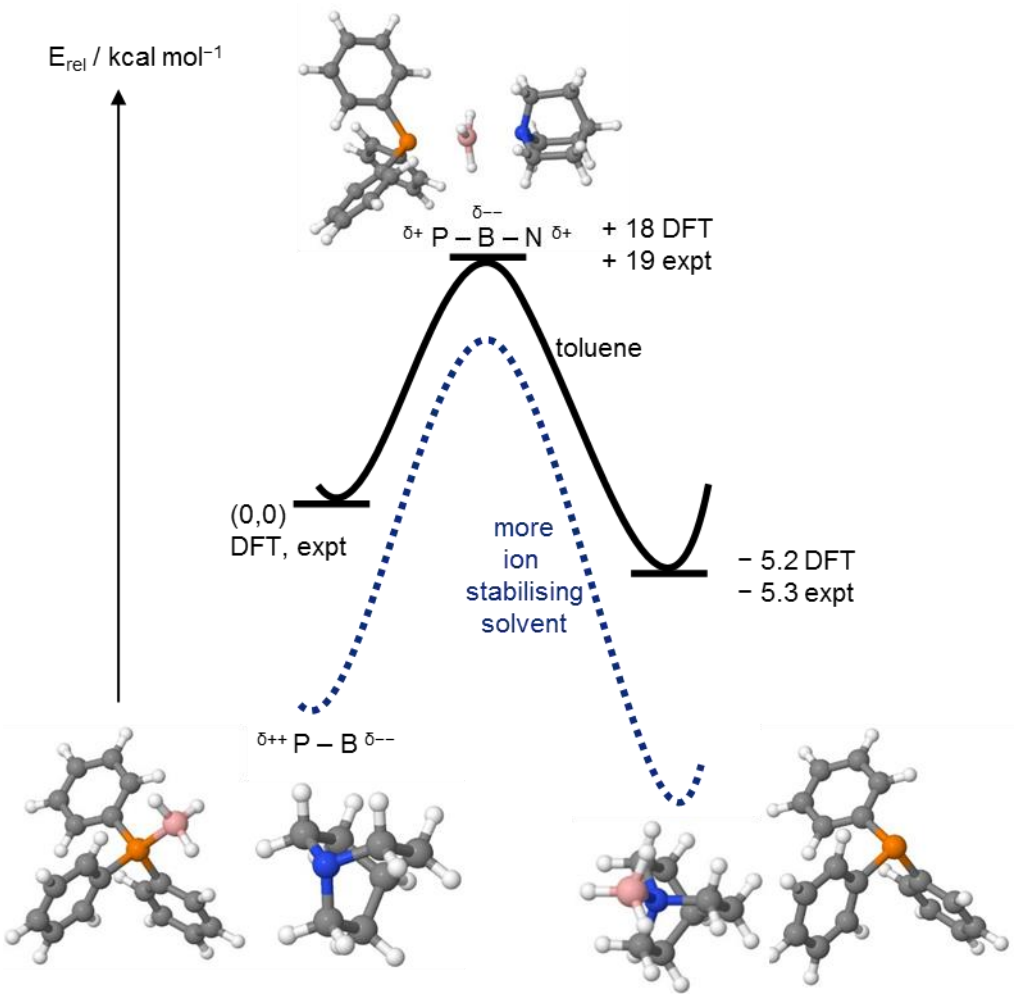

Figure 2.6 Upper (solid) curve: comparison of DFT and experimentally determined kinetic and thermodynamic parameters. Lower (dashed) curve: schematic for the reaction profile in a solvent with greater ion-stabilising ability. DFT energies calculated using B3LYP, 6-31G(d) in toluene PCM at 298.15 K with Grimme's dispersion correction, see experimental for details.

Notably, a number of amines have a low ion-stabilising ability (as measured by Dimroth-Reichardt E_T^N) including diethylamine, $E_T^N = 0.145$. Consequently, the use of amine as a reactant and solvent can provide benefit in terms of the effect of low polarity reaction medium and high concentration of the amine.

2.3 Effect of the phosphine

2.3.1 Electronic aryl effects

Independent rate measurements of the deprotection of a range of *para/meta*-substituted triarylphosphine borane complexes (with quinuclidine, toluene, 30 C°) were carried out to determine the electronic impact of the phosphine on the deprotection rate, see Figure 2.7. Consistent with an S_N2-like mechanism, phosphine borane complexes appended with electron withdrawing substituents (e.g. (*p*-trifluoromethylphenyl)$_3$P·BH$_3$, **5**) demonstrated enhanced rates of deprotection compared to their electron rich counterparts (e.g. (*p*-methoxyphenyl)$_3$P·BH$_3$, **6**), greater than 500 fold in this case. Excellent correlation was obtained between the Hammett σ values[117] and the logarithm of the relative rate constants for deprotection, giving a ρ value of 3.3. Normalising by a factor of 3 (for each substituent affixed to P) gives a corrected ρ value of 1.1. Evidence for the substituent effects being additive (as assumed in this correction) is presented in Section 3.2.1.

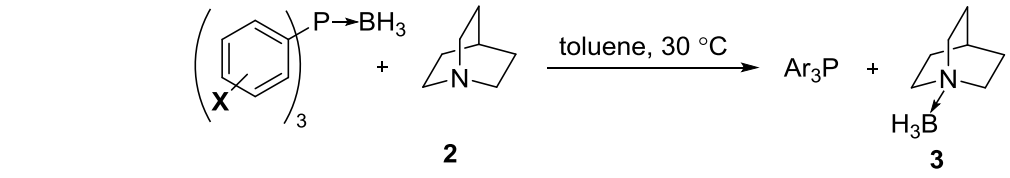

X = *p*-OMe **6**, *p*-Me **7**, *m*-Me **8**, *p*-H **1**, *p*-F **9**, *p*-Cl **4**, *p*-CF_3 **5**, *o*-Me **10**, *o*-OMe **11**, *o*-F **12**

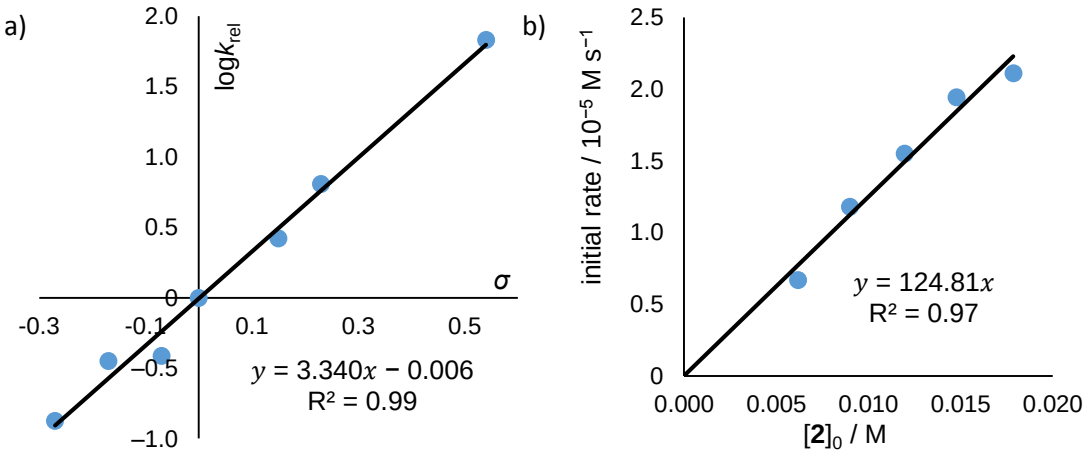

Figure 2.7 a) Correlation between logk_{rel} (k_{rel} = second order rate constant for deprotection of phosphine borane complexes relative to Ph$_3$P·BH$_3$) and Hammett's σ value. b) Relationship between initial rate of **3** formation and [**2**]$_0$, when reacting (*o*-tolyl)$_3$P·BH$_3$, **10**, with **2** in toluene at 30 °C.

2.3.2 Steric aryl effects

To probe the effect of increased steric bulk of the phosphine component, the deprotection kinetics were measured for a range of ortho-substituted triarylphosphine borane complexes (**10**-**12)** under analogous conditions, see Figure 2.8. Considerable rate enhancement was observed when steric bulk was present, with (*o*-tolyl)$_3$P·BH$_3$, **10**, undergoing deprotection close to 200 times faster than Ph$_3$P·BH$_3$, and almost 500 times faster than the perhaps more electronically similar (*p*-tolyl)$_3$P·BH$_3$, **7**. Given the significant rate increase, further studies were carried out on the deprotection of **10** to rule out a change in mechanism. As was the case with the deprotection of **1**, the rate of deprotection of **10** displayed a first order dependence on **2** (see Figure 2.7b), and no BH$_3$ crossover was observed between **10** and d_{12}-(*o*-tolyl)$_3$P over the course of a deprotection.[e] Confident of no change in mechanism, the origin of this substantial rate enhancement was probed crystallographically, see Figure 2.8.

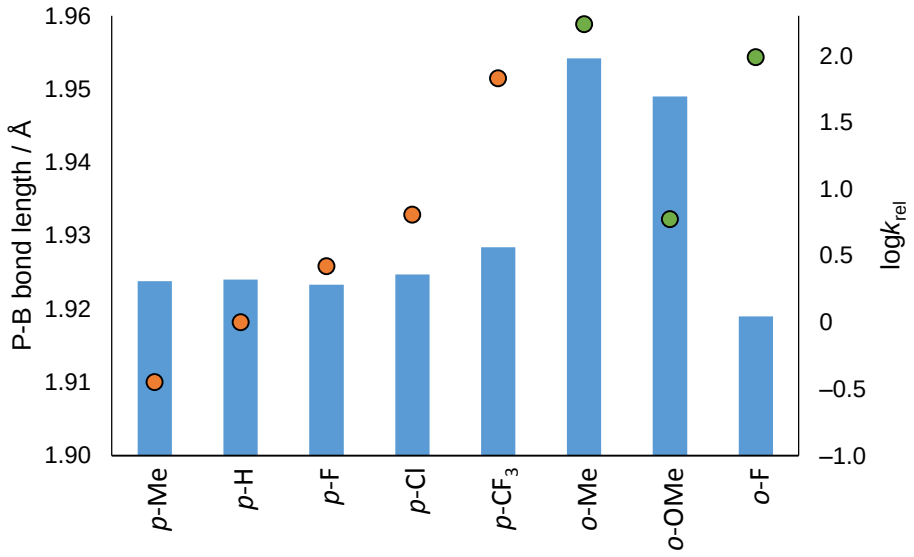

Figure 2.8 P-B bond lengths for a range of triarylphosphine borane complexes, for full details of crystal structures see Experimental, Figures 5.2-5.5. Relative rate data (to Ph$_3$P·BH$_3$) shown on secondary axis, orange circles correspond to *p*-substituted systems, whereas green correspond to *o*-substituted systems. Bond length data for Ph$_3$P·BH$_3$ taken from report by Muralidharan.[118]

Interestingly, across a range of *p*-substituted triarylphosphine borane complexes, very little difference in bond length was observed.[f] This suggests that the wide span of deprotection

[e] BH$_3$ crossover does occur between d_{12}-(*o*-tolyl)$_3$P and **10** in the absence of quinuclidine, but is a much slower process, $k = 1.2 \times 10^{-3}$ M^{-1} s^{-1}, see Appendix, Figure 6.13 for details.

[f] P-B bond lengths obtained for *p*-substituted triarylphosphine borane complexes are not significantly different, significant defined in this case as $\pm 3\sigma_{s.d}$, $\sigma_{s.d}$ = standard deviation.

rates observed in this series (Hammett plot Figure 2.7) does not result from a ground state effect that is manifest in an elongation/contraction of the P-B bond length. Instead, the differences in rate might be better rationalised by a transition state effect, i.e. differential nucleofugality (leaving group ability) of the phosphine component. A significant P-B bond length increase is observed for (*o*-tolyl)$_3$P·BH$_3$ **10** compared to the *p*-substituted series. Consequently, it can be inferred that the dominant role of the methyl groups is a primarily steric weakening of the P-B interaction, destabilising the phosphine borane ground state towards attack by quinuclidine. This argument however, cannot apply in all cases, for example, the P-B bond length of (*o*-fluorophenyl)$_3$P·BH$_3$, **12**, is not significantly different to its *p*-substituted counterpart, and as such, a steric effect is unlikely to explain the 37 fold difference in *k*. The enhanced rate of the *o*-substituted analogue is probably better explained by an electronic effect, consistent with greater inductive withdrawal through a reduced number of bonds. The (*o*-methoxyphenyl)$_3$P·BH$_3$, **11**, displays a significantly longer P-B bond length than the *p*-substituted series, but as with **12**, one might expect a significant electronic contribution to the deprotection rate. Consequently, it is assumed that both steric and electronic factors play a role in the rate enhancement (44 fold relative to (*p*-methoxyphenyl)$_3$P·BH$_3$).

Complicating this analysis is the potential for a disparity between the structures measured crystallographically, and the active species in the deprotection (in toluene solution). One potential difference could be the conformation adopted by the phosphine substituents in the borane complex, with many reports identifying an effect of phosphine conformation on reactivity.[119–121] Highlighting this are the structures obtained for (*o*-methoxyphenyl)$_3$P·BH$_3$, **11** and (*o*-tolyl)$_3$P·BH$_3$, **10**, Figure 2.9, which display different solid state conformations with respect to rotation about the P-C bonds.

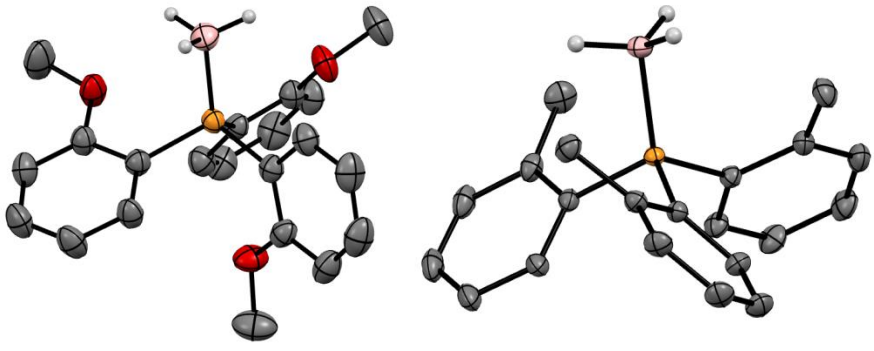

Figure 2.9 Thermal ellipsoids calculated at 50% probability, showing crystal structures of (*o*-methoxyphenyl)$_3$P·BH$_3$, **11** (*exo*$_2$ conformation) and (*o*-tolyl)$_3$P·BH$_3$, **10** (*exo*$_3$ conformation). Non-BH$_3$ hydrogens removed for clarity. For full details, see Experimental, Table 5.1.

2.3.3 Alkyl substituents

Deprotection kinetics under the standard conditions (quinuclidine, toluene, 30 °C), of the series $Ph_{3-n}Cy_nP{\cdot}BH_3$ (**1**, **13**, **14**, **15**; n = 0, 1, 2, 3 respectively) were used to analyse the effect of alkyl substitution. Consistent with increased induction, progressive attenuation of the rate was observed with increasing alkyl substitution (n), see Table 2.3. The regular change in k, approximately 10 fold, with increase in n provides evidence for independent and additive substituent effects, and this is discussed in depth later (see Section 3.2.1). Additionally, through measurement of the rate of the reverse process, (quinuclidine borane complex, **3**, and phosphine) the equilibrium constants could be determined. As with the rate, the favourability of the forward reaction (deprotection of phosphine borane complexes) decreases with increasing alkyl substitution (n). The large variation in k and K can be seen in the temporal concentration data shown in Figure 2.10, especially as starting concentrations were manipulated in an attempt to get reaction profiles within a timescale amenable to measurement.

Table 2.3 Rate and equilibrium constants for BH_3 transfer to quinuclidine from $Ph_{3-n}Cy_nP{\cdot}BH_3$ complexes in toluene at 30 °C. For associated errors see Appendix, Table 6.5.

Entry	$R_3P{\cdot}BH_3$	k / M^{-1} s^{-1}	K	Equiv. R_3N for > 99% Ph_3P[a]
1	$Ph_3P{\cdot}BH_3$	2.6×10^{-3}	7.4×10^{3}	1.003
2	$CyPh_2P{\cdot}BH_3$	2.1×10^{-4}	5.2×10^{2}	1.19
3	$Cy_2PhP{\cdot}BH_3$	1.9×10^{-5}	2.4×10^{1}	5.1
4	$Cy_3P{\cdot}BH_3$	2.5×10^{-6}	1.4×10^{0}	71

[a] Equivalents of amine relative to $R_3P{\cdot}BH_3$.

The absolute magnitudes of K and k are of particular significance for the deprotections of alkyl-rich phosphine borane complexes. Low K values require the use of a large excess of quinuclidine to obtain high levels of conversion; even when considering the rate advantage that this brings (exploiting the biomolecularity of the process) the low k values mean the reactions take a long time. A further disadvantage in the design of synthetic deprotection procedures comes from the kinetic and thermodynamic competency of expensive amine quinuclidine, relative to other amines tested, see Tables 2.1 (reaction with $Ph_3P{\cdot}BH_3$) and 2.5 (reaction with $^tBu_3P{\cdot}BH_3$). One factor that could well be exploited in an effort to reduce reaction times is increasing temperature. However, high temperature studies can be limited by the volatility or stereochemical integrity of the desired product. For $Cy_3P{\cdot}BH_3$, where these problems are not encountered, an increase in temperature (to 70 °C) gives a

substantially greater rate constant (k = 1.3 × 10^{-4} M^{-1} s^{-1}),[g] and additionally through manipulation of starting concentrations this can manifest itself in considerably reduced reaction times.

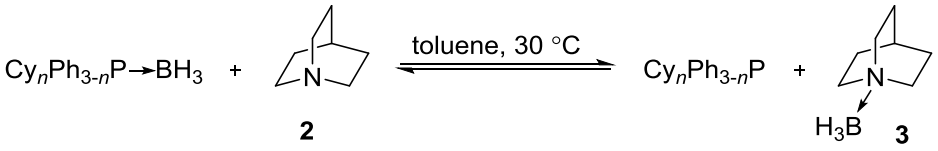

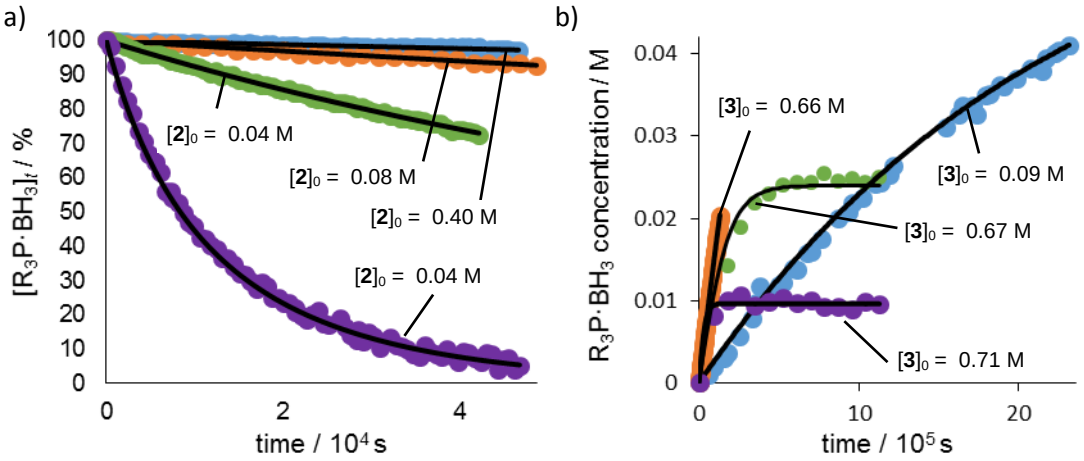

Figure 2.10 Temporal conversion/concentration profiles for a) forward (blue circles: $[Cy_3P{\cdot}BH_3]_0$ = 0.05 M, orange circles: $[Cy_2PhP{\cdot}BH_3]_0$ = 0.02 M, green circles: $[CyPh_2P{\cdot}BH_3]_0$ = 0.02 M, and purple circles $[Ph_3P{\cdot}BH_3]_0$ = 0.02 M) and b) backward reactions (blue circles: $[Cy_3P]_0$ = 0.30 M, orange circles: $[Cy_2PhP]_0$ = 0.48 M, green circles: $[CyPh_2P]_0$ = 0.70 M, and purple circles $[Ph_3P]_0$ = 1.00 M) in toluene at 30 °C. Circles are experimentally measured by $^{11}B\{^1H\}$ NMR, lines are simulation to a biomolecular equilibrium with values of k and K listed in Table 2.3.

In an effort to expand the range of alkyl/phenyl phosphine borane complexes studied, deprotection kinetics using the standard system (toluene, 30 °C, quinuclidine) were measured for a range of complexes described by the formula $Ph_{3-n}R_nP{\cdot}BH_3$; R = Me (**16**, **17**, **18**), ^{t}Bu (**19**, **20**, **21**), n = 1-3 respectively; ^{n}Bu (**22**), n = 3; ^{i}Pr (**23**, **24**), n = 1, 3. Interestingly, for a given value of n, the second order rate constant obtained in all cases displayed little variation, i.e. the deprotection rates of $PhR_2P{\cdot}BH_3$ appear to be relatively insensitive to the identity of R, see Table 2.4. This observation is somewhat surprising given the wide variation in size of the phosphines (as measured by the Tolman cone angle; ^{t}Bu$_3$P = 182°, Me$_3$P = 118°)[122] and the sensitivity to steric bulk observed in aryl systems.

[g] This value of k should only be taken as approximate as during the fitting process, equilibrium constant (K_{70}) was fixed to equal that at 30 °C, K_{30}.

One possible rationale for this apparent similarity in deprotection kinetics is an electronic compensation for increase in steric bulk. For example, ^{t}Bu is expected to exhibit greater electronic stabilisation *via* the inductive effect than Me (see Hammett σ values).[117] Given this similarity and the additivity observed for R = Cy, it is unsurprising that an almost constant rate suppression is observed when progressing (increasing *n*) across a series $Ph_{3-n}R_nP{\cdot}BH_3$ for R = ^{t}Bu, Me and ^{i}Pr. As alluded to earlier, the effect of a particular phosphine substituent (on the deprotection kinetics) appears to be independent of the identity of the other substituents. A wide range of alkyl and aryl substituents appear to follow this trend, suggesting a general phenomenon. This concept is developed further in chapter 3, which describes the formulation of a nucleofugality parameter.

Table 2.4 Rate constants for BH_3 transfer to quinuclidine from $Ph_{3-n}R_nP{\cdot}BH_3$ complexes in toluene at 30 °C, for n = 0, $k = 2.6 \times 10^{-3}$ M^{-1} s^{-1}. For associated errors see Appendix, Table 6.5.

Entry	$R_3P{\cdot}BH_3$	k / M^{-1} s^{-1}			
		R = Me	R = ^{t}Bu	R = ^{n}Bu	R = ^{i}Pr
1	$RPh_2P{\cdot}BH_3$	3.5×10^{-4}	4.9×10^{-4}	-	1.8×10^{-4}
2	$R_2PhP{\cdot}BH_3$	3.5×10^{-5}	2.9×10^{-5}	-	-
3	$R_3P{\cdot}BH_3$	3.6×10^{-6}	2.0×10^{-6}	2.6×10^{-6}	1.4×10^{-6}

In addition to the similar *k* values, trialkylphosphine borane complexes also have similar and relatively low equilibrium constants (calculated *via* $^{11}B\{^{1}H\}$ NMR analysis of the reverse reaction), K = 1.8 for $Me_3P{\cdot}BH_3$, K = 1.5 for $^{t}Bu_3P{\cdot}BH_3$ and K = 2.6 for $^{n}Bu_3P{\cdot}BH_3$. These similar values (given the range seen in Table 2.3) can be rationalised by considering the same steric/electronic compensation effect used to explain the similarity in the kinetics of deprotection.

A subset of the amines previously examined (in the deprotection of $Ph_3P{\cdot}BH_3$) were tested using $^{t}Bu_3P{\cdot}BH_3$ **21** as an example of a phosphine borane complex which is "difficult to deprotect" (both kinetically and thermodynamically). Rate and equilibrium constants obtained by fitting temporal concentration data (*in situ* $^{11}B\{^{1}H\}$ NMR, toluene at 30 °C) to a bimolecular equilibrium model $-d[\mathbf{21}]/dt = k([\mathbf{21}][\text{amine}]-[\text{amine}{\cdot}BH_3][\ ^{t}Bu_3P]/K)$ are displayed in Table 2.5. All amines examined displayed a large decrease in both the rate (k) and favourability (K) of the deprotection of $^{t}Bu_3P{\cdot}BH_3$, **21** (relative to $Ph_3P{\cdot}BH_3$, **1**). Moreover, analogous trends between amine identity and both *k* and *K* appear to be present in

both cases, i.e. the relative deprotecting ability of an amine is independent of the phosphine borane complex.

Table 2.5 Relative rate and equilibrium constants for BH_3 transfer to a variety of amines from $^tBu_3P{\cdot}BH_3$ complexes in toluene at 30 °C. For absolute values and errors see Appendix, Table 6.6. Constants are reported relative to Et_2NH (k = 7.1 × 10^{-8} M^{-1} s^{-1}, K = 6.1 × 10^{-3}).

Entry	Amine	k_{rel}	K_{rel}	Equiv. R_3N for > 99% $^tBu_3P$[a]
1	diethylamine	1	1	16,000
2	morpholine	2.7	2.6	6,200
3	piperidine	4.8	44	370
4	pyrrolidine	2.9	~105	150
5	quinuclidine	28	240	67
6	DABCO[b]	54	167	96

[a] Equivalents of amine relative of $^tBu_3P{\cdot}BH_3$. [b] Data are assumed to be for one transfer of BH_3 per DABCO.

The data in Table 2.5 highlights the same increased kinetic and thermodynamic competency of cyclic amines relative to their acyclic counterparts. This difference in proficiency is very dramatic, with some amines needing thousands or even tens of thousands of equivalents in order to obtain 99% conversion to the free phosphine (morpholine and diethylamine). The number of equivalents is substantially lower for the bridgehead amines DABCO and quinuclidine, demonstrating the need for informed choice of conditions in instances like this.

2.4 Alcoholysis deprotection

2.4.1 Mechanistic studies

Unlike the amine deprotection, the mechanism of the alcoholysis of phosphine boranes has attracted less speculation, with far fewer reports mentioning the subject. A system comprised of (o-tolyl)$_3$P·BH_3, **10**, in ethanol/toluene mixtures provided reactions on a timescale amenable to measurement by *in situ* NMR analysis, see Scheme 2.7. In agreement with studies by Van der Eycken[60] high conversions of the phosphine product could be obtained in the absence of molecular sieves (4Å), in direct contradiction of the report by Nozaki and Hiyama.[59]

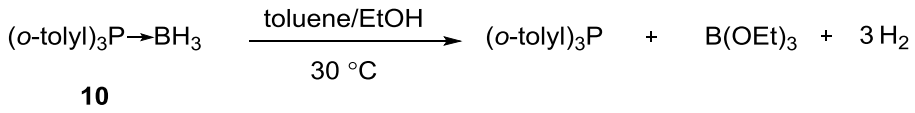

10

Scheme 2.7 Reaction conditions used to investigate the mechanism of alcoholysis; typically [**10**]$_0$ = 0.03 M and [EtOH]$_0$ = 4.11-5.14 M.

$^{11}B\{^1H\}$ NMR temporal concentration profiles displayed pseudo-first order consumption of phosphine borane complex, **10**, generation of an intermediate, and subsequent conversion to $B(OEt)_3$ (confirmed by spiking $B(OEt)_3$ in), see Figure 2.11. Monitoring the same process using ^{11}B NMR gives a clue to the nature of the intermediate, with a doublet observed (J = 160 Hz), suggesting a B-H bond. Similarly, reaction monitoring using $^{31}P\{^1H\}$NMR shows two peaks, with conversion to the phosphine shown to occur at the same rate as consumption of **10**, indicating that the intermediate (and product) observed by $^{11}B\{^1H\}$ NMR contain no phosphorus, see Figure 2.11.

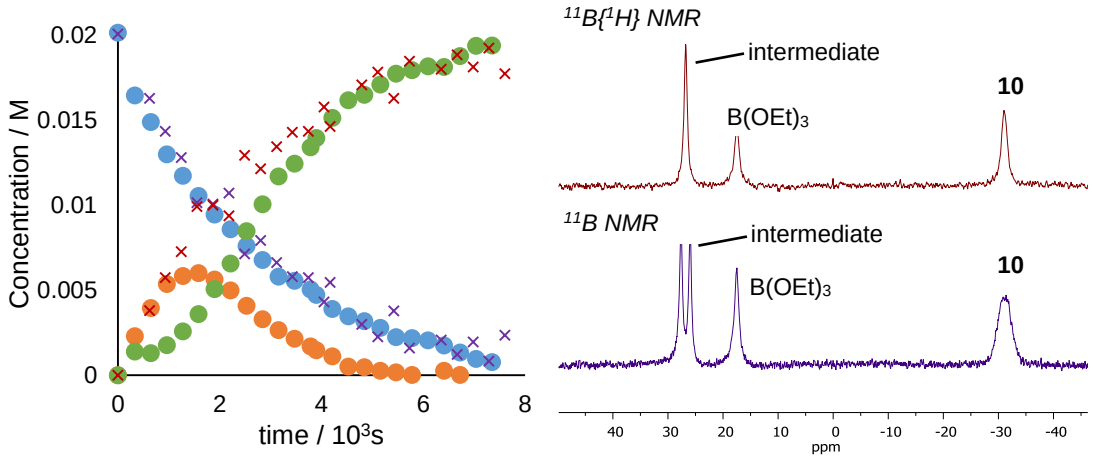

Figure 2.11 Temporal concentration profiles for two different ethanolyses of **10**, monitored by $^{11}B\{^1H\}$ (filled blue circles: **10**, filled orange circles: intermediate, filled green circles: $B(OEt)_3$) and $^{31}P\{^1H\}$ (purple crosses: **10**, red crosses: $(o\text{-tolyl})_3P$). Conditions: [**10**]$_0$ = 0.02 M, [EtOH]$_0$ = 5.14 M. $^{11}B\{^1H\}$ and ^{11}B NMR spectra recorded during the ethanolysis of **10**.

Repetition of experiments using *in situ* $^{11}B\{^1H\}$ NMR analysis demonstrated a high degree of variability in the reaction profiles, with the maximum concentration of intermediate (as high as 65% of [**10**]$_0$), and rate of intermediate consumption varying substantially between experiments. Despite this, the pseudo-first order consumption of **10**, as seen in Figure 2.11, was found to be reproducible. Variation in [EtOH]$_0$ was found to influence the rate of consumption of **10**, with greater [EtOH]$_0$ giving faster rates. This relationship was non-linear, as might be expected given the ability of ethanol to aggregate in hydrocarbon solvents.[123] Simulation of a rapid dimerisation equilibrium in concert with monomeric

EtOH reaction with **10** was found to fit experimental data, over an almost 40 fold change in $[EtOH]_0$, see Figure 2.12.

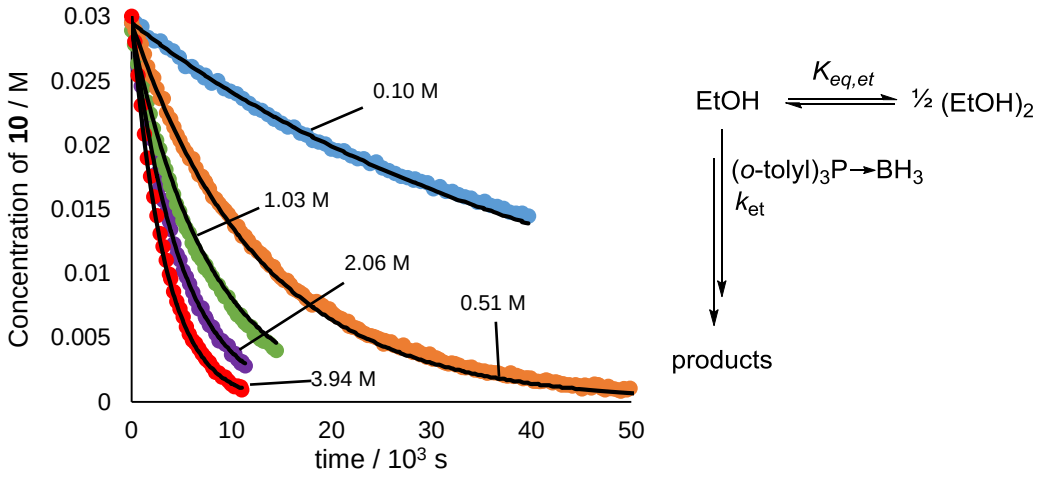

Figure 2.12 Temporal concentration profiles for consumption of **10** by EtOH, in toluene, initial ethanol concentrations displayed on graph. Circles are experimental data (*in situ* $^{11}B\{^1H\}$ NMR), lines are simulation according to the model displayed (k_{et} = 2.3 ± 0.04 × 10^{-4} $M^{-1}s^{-1}$, $K_{eq,et}$ = 0.72 ± 0.04 M^{-1}, equilibrium is set to be fast, relative to reaction). For discussion of the associated errors see Appendix.

An additional experiment using 2,2,2-tifluoroethanol in place of ethanol gave an approximate 15 fold reduction in the rate constant (k_{et}), rate = k_{obs}[**10**], k_{obs} = k_{et}[ROH], $[ROH]_0$ = 1.0 M. This suggests the alcohol is acting as a nucleophile, rather than a Brønsted acid, as trifluoroethanol is substantially less nucleophilic (*N* = 2.93 vs 7.03, values obtained in v/v 90% alcohol, 10% water mixtures)[124] and more acidic (pK_a = 23.5 vs 29.8 in DMSO)[125] than ethanol. The good fits between experimental and simulated data, in combination with *in situ* $^{31}P\{^1H\}$ NMR data and the relative decreased reactivity of trifluoroethanol are consistent with an initial nucleophilic displacement of borane from **10** by ethanol, see Scheme 2.8.

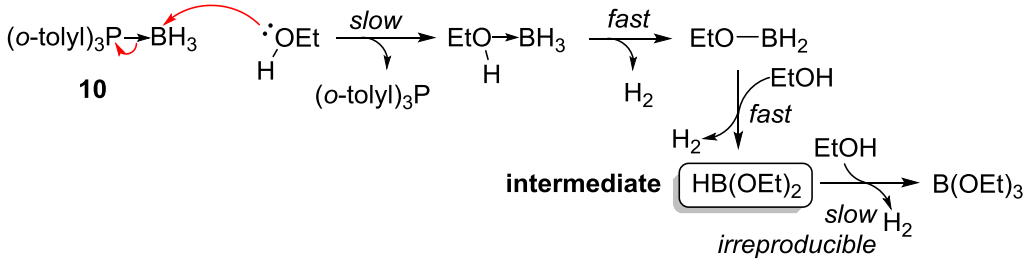

Scheme 2.8 Proposed mechanism for the ethanolysis of $(o\text{-tolyl})_3P{\cdot}BH_3$, **10**, in ethanol toluene mixtures at 30 °C.

Unfortunately, no definitive cause of the irreproducibility in the kinetic stability of the intermediate was established. Initial intermediate production matched the (reliable) pseudo-first order consumption of **10**, suggesting that the reproducibly issues arise in the consumption of the intermediate. Limited evidence was obtained to suggest that reaction vessel surface effects (promoting dihydrogen evolution) play an influential role in this process, however studies carried out under a pressure of dihydrogen (3 bar) were inconclusive.

2.5 Summary

The mechanism of quinuclidine deprotection of $Ph_3P{\cdot}BH_3$ has been examined, with kinetic and computational evidence precluding S_N1-type mechanisms and consistent with an S_N2-like mechanism. Structure activity relationships have been explored regarding the identity of the amine partner, with cyclic amines demonstrating relative proficiency in both the rate and favourability of borane transfer. The effect of solvent on the rate of a model deprotection has been examined, with results consistent with increased charge dispersion at the transition state, relative to ground state.

In-depth structure activity studies of the phosphine component have been carried out, determining the influence of electronic and steric effects for aryl substituents and additionally examining a range of alkyl groups. Interestingly, additive substituent effects have been identified for alkyl substituted phosphines, and this effect is explored in-depth in the following chapter. Taken as a whole, the data collected allow guidelines for optimal deprotections based on either rate or synthetic convenience.

2.6 References

[1] S. A. Buckler, *J. Organomet. Chem.* **1962**, *84*, 3093–3097.

[2] M. J. Pitt, *Bretherick's Handbook of Reactive Chemical Hazards*, Butterworth-Heinmann, Oxford, UK, **1999**.

[3] D. H. Nguyen, J. Bayardon, C. Salomon-Bertrand, S. Jugé, P. Kalck, J.-C. Daran, M. Urrutigoity, M. Gouygou, *Organometallics* **2012**, *31*, 857–869.

[4] S. E. Denmark, N. S. Werner, *Org. Lett.* **2011**, *13*, 4596–4599.

[5] A. Grabulosa, *P-Stereogenic Ligands in Enantioselective Catalysis*, Royal Society Of Chemistry, **2010**.

[6] P. Pellon, *Tetrahedron Lett.* **1992**, *33*, 4451–4452.

[7] M. A. Frisch, H. G. Heal, H. Mackle, I. O. Madden, *J. Chem. Soc.* **1965**, 899–907.

[8] H. G. Heal, I. O. Madden, *Nature* **1962**, *195*, 280.

[9] F. J. Mettille, D. J. Burton, *J. Inorg. Nucl. Chem.* **1968**, *30*, 333–335.

[10] E. L. Gamble, P. Gilmont, *J. Am. Chem. Soc.* **1940**, *62*, 717–721.

[11] A. B. Burg, R. I. Wagner, *J. Am. Chem. Soc.* **1953**, *75*, 3872–3877.

[12] R. M. Adams, J. Beres, A. Dodds, A. J. Morabito, *Inorg. Chem.* **1971**, *10*, 2072–2074.

[13] E. A. Colby, T. F. Jamison, *J. Org. Chem.* **2003**, *68*, 156–166.

[14] R. A. Baldwin, R. M. Washburn, *J. Org. Chem.* **1961**, *26*, 3549–3550.

[15] R. A. Baldwin, K. A. Smitheman, R. M. Washburn, *J. Org. Chem.* **1961**, *29*, 3547–3549.

[16] P. V. Ramachandran, A. S. Kulkarni, *RSC Adv.* **2014**, *4*, 26207–26210.

[17] J. Tomasz, B. R. Shaw, K. Porter, B. F. Spielvogel, A. Sood, *Angew. Chem. Int. Ed.* **1992**, *31*, 1373–1375.

[18] J. McNulty, Y. Zhou, *Tetrahedron Lett.* **2004**, *45*, 407–409.

[19] T. Reetz, *J. Am. Chem. Soc.* **1960**, *82*, 5039–5042.

[20] T. Reetz, B. Katlafsky, *J. Am. Chem. Soc.* **1960**, *82*, 5036–5039.

[21] K. C. Nainan, G. E. Ryschkewitsch, *Inorg. Chem.* **1969**, *8*, 2671–2674.

[22] N. P. Kenny, K. V. Rajendran, D. G. Gilheany, *Chem. Commun.* **2015**, *51*, 16561–16564.

[23] E. J. Corey, Z. Chen, G. J. Tanoury, *J. Am. Chem. Soc.* **1993**, *115*, 11000–11001.

[24] T. Imamoto, T. Kusumoto, N. Suzuki, K. Sato, *J. Am. Chem. Soc.* **1985**, *107*, 5301–5303.

[25] K. V. Rajendran, D. G. Gilheany, *Chem. Commun.* **2012**, *48*, 10040–10042.

[26] L. Pehlivan, E. Métay, D. Delbrayelle, G. Mignani, M. Lemaire, *Tetrahedron* **2012**, *68*, 3151–3155.

[27] S. Sowa, M. Stankevič, A. Szmigielska, H. Małuszyńska, A. E. Kozioł, K. M. Pietrusiewicz, *J. Org. Chem.* **2015**, *80*, 1672–1688.

[28] J. Ren, D. B. Workman, R. R. Squires, *J. Am. Chem. Soc.* **1998**, *120*, 10511–10522.

[29] M. Hurtado, M. Yánez, R. Herrero, A. Guerrero, J. Z. Dávalos, J.-L. M. Abboud, B. Khater, J.-C. Guillemin, *Chem. Eur. J.* **2009**, *15*, 4622–4629.

[30] A. R. Muci, K. R. Campos, D. A. Evans, *J. Am. Chem. Soc.* **1995**, *117*, 9075–9076.

[31] B. Wolfe, T. Livinghouse, *J. Org. Chem.* **2001**, *66*, 1514–1516.

[32] B. Wolfe, T. Livinghouse, *J. Am. Chem. Soc.* **1998**, *120*, 5116–5117.

[33] M. J. Johansson, L. Schwartz, M. Amedjkouh, N. Kann, *Tetrahedron: Asymmetry* **2004**, *15*, 3531–3538.

[34] M. J. Johansson, L. O. Schwartz, M. Amedjkouh, N. C. Kann, *Eur. J. Org. Chem.* **2004**, *2004*, 1894–1896.

[35] S. Juge, M. Stephan, J. A. Laffitte, J. P. Genet, *Tetrahedron Lett.* **1990**, *31*, 6357–6360.

[36] S. Jugé, M. Stephan, R. Merdès, J. P. Genet, S. Halut-Desportes, *J. Chem. Soc., Chem. Commun.* **1993**, 531–533.

[37] S. Jugé, M. Stephan, J. P. Genet, S. Halut-Desportes, S. Jeannin, *Acta Crystallogr. Sect. C Cryst. Struct. Commun.* **1990**, *46*, 1869–1872.
[38] K. V. Rajendran, K. V. Nikitin, D. G. Gilheany, *J. Am. Chem. Soc.* **2015**, *137*, 9375–9381.
[39] T. N. Hooper, M. A. Huertos, T. Jurca, S. D. Pike, A. S. Weller, I. Manners, *Inorg. Chem.* **2014**, *53*, 3716–3729.
[40] M. A. Huertos, A. S. Weller, *Chem. Sci.* **2013**, *4*, 1881–1888.
[41] M. A. Huertos, A. S. Weller, *Chem. Commun.* **2012**, *48*, 7185–7187.
[42] T. J. Clark, J. M. Rodezno, S. B. Clendenning, S. Aouba, P. M. Brodersen, A. J. Lough, H. E. Ruda, I. Manners, *Chem. Eur. J.* **2005**, *11*, 4526–4534.
[43] H. Dorn, E. Vejzovic, A. J. Lough, I. Manners, *Inorg. Chem.* **2001**, *40*, 4327–4331.
[44] H. Dorn, R. A. Singh, J. A. Massey, J. M. Nelson, C. A. Jaska, A. J. Lough, I. Manners, *J. Am. Chem. Soc.* **2000**, *122*, 6669–6678.
[45] H. Dorn, R. A. Singh, J. A. Massey, A. J. Lough, I. Manners, *Angew. Chem. Int. Ed.* **1999**, *38*, 3321–3323.
[46] P. Shapland, E. Vedejs, *J. Org. Chem.* **2004**, *69*, 4094–4100.
[47] M. Scheideman, P. Shapland, E. Vedejs, *J. Am. Chem. Soc.* **2003**, *125*, 10502–10503.
[48] A. Pelter, R. Rosser, S. Mills, *J. Chem. Soc., Chem. Commun.* **1981**, 1014–1015.
[49] C. A. Busacca, J. A. Milligan, E. Rattanangkool, C. Ramavarapu, A. Chen, A. K. Saha, Z. Li, H. Lee, S. J. Geib, G. Wang, C. H. Senanayake, P. Wipf, *J. Org. Chem.* **2014**, *79*, 9879–9887.
[50] C. A. Busacca, E. Farber, J. DeYoung, S. Campbell, N. C. Gonnella, N. Grinberg, N. Haddad, H. Lee, S. Ma, D. Reeves, S. Shen, C. H. Senanayake, *Org. Lett.* **2009**, *11*, 5594–5597.
[51] B. Join, D. Mimeau, O. Delacroix, A.-C. Gaumont, *Chem. Commun.* **2006**, 3249–3251.
[52] D. Mimeau, O. Delacroix, A.-C. Gaumont, *Chem. Commun.* **2003**, 2928–2929.
[53] M. Mühlberg, D. M. M. Jaradat, R. Kleineweischede, I. Papp, D. Dechtrirat, S. Muth, M. Broncel, C. P. R. Hackenberger, *Bioorganic Med. Chem.* **2010**, *18*, 3679–3686.
[54] C. Grandjean, A. Boutonnier, C. Guerreiro, J. M. Fournier, L. A. Mulard, *J. Org. Chem.* **2005**, *70*, 7123–7132.
[55] M. B. Soellner, B. L. Nilsson, R. T. Raines, *J. Org. Chem.* **2002**, *67*, 4993–4996.
[56] M. Almasieh, C. J. Lieven, L. A. Levin, A. Di Polo, *J. Neurochem.* **2011**, *118*, 1075–1086.
[57] C. R. Schlieve, A. Tam, B. L. Nilsson, C. J. Lieven, R. T. Raines, L. A. Levin, *Exp. Eye Res.* **2006**, *83*, 1252–1259.
[58] D. Moulin, S. Bago, C. Bauduin, C. Darcel, S. Jugé, *Tetrahedron: Asymmetry* **2000**, *11*, 3939–3956.
[59] M. Schröder, K. Nozaki, T. Hiyama, *Bull. Chem. Soc. Jpn.* **2004**, *77*, 1931–1932.
[60] M. Van Overschelde, E. Vervecken, S. G. Modha, S. Cogen, E. Van der Eycken, J. Van der Eycken, *Tetrahedron* **2009**, *65*, 6410–6415.
[61] C. Darcel, E. B. Kaloun, R. Merdès, D. Moulin, N. Riegel, S. Thorimbert, J. P. Genêt, S. Jugé, *J. Organomet. Chem.* **2001**, *624*, 333–343.
[62] M. Couturier, J. L. Tucker, B. M. Andresen, P. Dubé, J. T. Negri, *Org. Lett.* **2001**, *3*, 465–467.
[63] S. Basu, A. Brockman, P. Gagare, Y. Zheng, P. V. Ramachandran, W. N. Delgass, J. P. Gore, *J. Power Sources* **2009**, *188*, 238–243.
[64] L. McKinstry, T. Livinghouse, *Tetrahedron Lett.* **1994**, *35*, 9319–9322.
[65] G. Knühl, P. Sennhenn, G. Helmchen, *J. Chem. Soc., Chem. Commun.* **1995**, *5*, 1845–1846.

[66] T. Imamoto, J. Watanabe, Y. Wada, H. Masuda, H. Yamada, H. Tsuruta, S. Matsukawa, K. Yamaguchi, *J. Am. Chem. Soc.* **1998**, *120*, 1635–1636.
[67] Z. Yang, D. Liu, Y. Liu, M. Sugiya, T. Imamoto, W. Zhang, *Organometallics* **2015**, *34*, 1228–1237.
[68] L. Mckinstry, J. J. Overberg, C. Soubra-Ghaoui, D. S. Walsh, K. A. Robins, T. T. Toto, J. L. Toto, *J. Org. Chem.* **2000**, *65*, 2261–2263.
[69] J. A. Ramsden, J. M. Brown, M. B. Hursthouse, A. I. Karalulov, *Tetrahedron: Asymmetry* **1994**, *5*, 2033–2044.
[70] E. B. Kaloun, R. Merdès, J.-P. Genêt, J. Uziel, S. Jugé, *J. Organomet. Chem.* **1997**, *529*, 455–463.
[71] N. Riegel, C. Darcel, O. Stéphan, S. Jugé, *J. Organomet. Chem.* **1998**, *567*, 219–233.
[72] O. Desponds, C. Huynh, M. Schlosser, *Synthesis* **1998**, 983–985.
[73] L. J. Higham, A. J. Middleton, K. Heslop, P. G. Pringle, A. Barber, A. G. Orpen, *J. Organomet. Chem.* **2004**, *689*, 2963–2968.
[74] D. L. Dodds, M. F. Haddow, A. G. Orpen, P. G. Pringle, *Organometallics* **2006**, *25*, 5937–5945.
[75] J. H. Downing, J. Floure, K. Heslop, M. F. Haddow, J. Hopewell, M. Lusi, H. Phetmung, A. G. Orpen, P. G. Pringle, R. I. Pugh, D. Zambrano-Williams, *Organometallics* **2008**, *27*, 3216–3224.
[76] E. F. Clarke, E. Rafter, H. Müller-Bunz, L. J. Higham, D. G. Gilheany, *J. Organomet. Chem.* **2011**, *696*, 3608–3615.
[77] D. L. Dodds, J. Floure, M. Garland, M. F. Haddow, T. R. Leonard, C. L. McMullin, A. G. Orpen, P. G. Pringle, *Dalt. Trans.* **2011**, *40*, 7137–7146.
[78] H. Brisset, Y. Gourdel, P. Pellon, M. Le Corre, *Tetrahedron Lett.* **1993**, *34*, 4523–4526.
[79] P. Pellon, C. Le Goaster, L. Toupet, *Tetrahedron Lett.* **1996**, *37*, 4713–4716.
[80] D. Moulin, C. Darcel, S. Jugé, *Tetrahedron: Asymmetry* **1999**, *10*, 4729–4743.
[81] P. Pellon, E. Brulé, N. Bellec, K. Chamountin, D. Lorcy, *J. Chem. Soc. Perkin Trans. 1* **2000**, 4409–4412.
[82] T. Imamoto, Y. Saitoh, A. Koide, T. Ogura, K. Yoshida, *Angew. Chem. Int. Ed.* **2007**, *46*, 8636–2639.
[83] C. A. Busacca, J. C. Lorenz, N. Grinberg, N. Haddad, H. Lee, Z. Li, M. Liang, D. Reeves, A. Saha, R. Varsolona, C. H. Senanayake, *Org. Lett.* **2008**, *10*, 341–344.
[84] F. Chaux, S. Frynas, H. Laureano, C. Salomon, G. Morata, M.-L. Auclair, M. Stephan, R. Merdès, P. Richard, M.-J. Ondel-Eymin, J.-C. Henry, J. Bayardon, C. Darcul, S. Jugé, *Comptes Rendus Chim.* **2010**, *13*, 1213–1226.
[85] Q. T. Tran, J.-F. Bergamini, C. Mangeney, C. Lagrost, P. Pellon, *Electrochem. commun.* **2011**, *13*, 844–847.
[86] A. Lapprand, N. Khiri, D. Fortin, S. Jugé, P. D. Harvey, *Inorg. Chem.* **2013**, *52*, 2361–2371.
[87] K. Jouvin, R. Veillard, C. Theunissen, C. Alayrac, A.-C. Gaumont, G. Evano, *Org. Lett.* **2013**, *15*, 4592–4595.
[88] R. Veillard, E. Bernoud, I. Abdellah, J.-F. Lohier, C. Alayrac, A.-C. Gaumont, *Org. Biomol. Chem.* **2014**, *12*, 3635–3640.
[89] A. Flores-Gaspar, S. Orgué, A. Grabulosa, A. Riera, X. Verdaguer, *Chem. Commun.* **2015**, *51*, 1941–1944.
[90] T. Imamoto, T. Oshiki, T. Onozawa, T. Kusumoto, K. Sato, *J. Am. Chem. Soc.* **1990**, *112*, 5244–5252.
[91] T. R. Ward, L. M. Venanzi, A. Albinati, F. Lianza, T. Gerfin, V. Gramlich, G. M. R. Tombo, *Helv. Chim. Acta* **1991**, *74*, 983–988.

[92] T. Imamoto, M. Matsuo, T. Nonomura, K. Kishikawa, M. Yanagawa, *Heteroat. Chem.* **1993**, *4*, 475–486.
[93] G. Brenchley, E. Merifield, M. Wills, M. Fedouloff, *Tetrahedron Lett.* **1994**, *35*, 2791–2794.
[94] T. Seitz, A. Muth, G. Huttner, *Chem. Ber.* **1994**, *127*, 1837–1842.
[95] B. Mohr, D. M. Lynn, R. H. Grubbs, *Organometallics* **1996**, *15*, 4317–4325.
[96] H. Yang, N. Lugan, R. Mathieu, *Organometallics* **1997**, *16*, 2089–2095.
[97] S. Orgué, A. Flores-Gaspar, M. Biosca, O. Pàmies, M. Diéguez, A. Riera, X. Verdaguer, *Chem. Commun.* **2015**, *51*, 17548–17550.
[98] E. Juaristi, M. A. Aguilar, *J. Org. Chem.* **1991**, *56*, 5919–5924.
[99] D. B. G. Williams, H. Lombard, M. van Niekerk, P. P. Coetzee, C. W. Holzapfel, *Phosphorus. Sulfur. Silicon Relat. Elem.* **2002**, *177*, 2799–2803.
[100] D. B. G. Williams, P. D. R. Kotze, A. C. Ferreira, C. W. Holzapfel, *J. Iran. Chem. Soc.* **2011**, *8*, 240–246.
[101] L. J. Higham, K. Heslop, P. G. Pringle, A. G. Orpen, *J. Organomet. Chem.* **2004**, *689*, 2975–2978.
[102] K. Bourumeau, A.-C. Gaumont, J.-M. Denis, *J. Organomet. Chem.* **1997**, *529*, 205–213.
[103] P. Vedrenne, V. Le Guen, L. Toupet, T. Le Gall, C. Mioskowski, *J. Am. Chem. Soc.* **1999**, *121*, 1090–1091.
[104] S. Yamago, M. Yanagawa, E. Nakamura, *J. Chem. Soc., Chem. Commun.* **1994**, 2093–2094.
[105] W. L. Budde, M. F. Hawthorne, *J. Am. Chem. Soc.* **1971**, *93*, 3147–3150.
[106] D. E. Walmsley, W. L. Budde, M. F. Hawthorne, *J. Am. Chem. Soc.* **1971**, *93*, 3150–3155.
[107] F. J. Lalor, T. Paxson, M. F. Hawthorne, *J. Am. Chem. Soc.* **1971**, *93*, 3156–3160.
[108] M. Ohff, J. Holz, M. Quirmbach, A. Börner, *Synthesis* **1998**, *10*, 1391–1415.
[109] N. Brodie, S. Jugé, *Inorg. Chem.* **1998**, *37*, 2438–2442.
[110] K. Izod, C. Wills, E. Anderson, R. W. Harrington, M. R. Probert, *Organometallics* **2014**, *33*, 5283–5294.
[111] F. Brotzel, B. Kempf, T. Singer, H. Zipse, H. Mayr, *Chem. Eur. J.* **2007**, *13*, 336–345.
[112] F. Brotzel, Y. C. Chu, H. Mayr, *J. Org. Chem.* **2007**, *72*, 3679–3688.
[113] from *www.sigmaaldrich.com*, accessed 18 October 2015.
[114] C. Reichardt, *Chem. Rev.* **1994**, *94*, 2319–2358.
[115] A. Maliniak, J. Kowalewski, *J. Phys. Chem.* **1986**, *90*, 6330–6334.
[116] G. O. Nevstad, J. Songstad, *Acta Chem. Scand. B* **1984**, *38*, 469–177.
[117] C. Hansch, A. Leo, W. Taft, *Chem. Rev.* **1991**, *91*, 165–195.
[118] S. R. Ghanta, M. H. Rao, K. Muralidharan, *Dalt. Trans.* **2013**, *42*, 8420–8425.
[119] J. A. S. Howell, M. G. Palin, P. McArdle, D. Cunningham, Z. Goldschmidt, H. E. Gottlieb, D. Hezroni-Langerman, *Inorg. Chem.* **1991**, *30*, 4683–4685.
[120] R. A. Widenhoefer, H. A. Zhong, S. L. Buchwald, *Organometallics* **1996**, *15*, 2745–2754.
[121] A. G. Sergeev, A. Spannenberg, M. Beller, *J. Am. Chem. Soc.* **2008**, *130*, 15549–15563.
[122] C. A. Tolman, *J. Am. Chem. Soc.* **1970**, *92*, 2953–2956.
[123] M. Costas, D. Pattterson, *J. Chem. Soc., Faraday Trans. 1* **1985**, *81*, 635–654.
[124] S. Minegishi, S. Kobayashi, H. Mayr, *J. Am. Chem. Soc.* **2004**, *126*, 5174–5181.
[125] W. N. Olmstead, Z. Margolin, F. G. Bordwell, *J. Org. Chem.* **1980**, *45*, 3295–3299.

3 Nucleofugality Parameters

3.1 Introduction

3.1.1 Linear free energy relationships

The gulf between microscopic (quantum) chemical theories and the ability to predict macroscopic properties, such as reaction yields, remains significant. Consequently, the use of empirical models to predict and explain chemical reactivity continues to be relevant. A desire to accurately quantify and understand chemical reactivity is not new, with a rich history of empirically derived linear free energy relationships[1] (LFERs) dating back to the pioneering work of Brönsted[h] and Hammett in 1924[2] and 1937,[3] respectively. Since then, a large number of parameters have been developed based on a variety of thermodynamic, kinetic, physical, and more recently computationally derived properties, with this area now occupying a significant branch of physical organic chemistry.[4] Whilst there remains some debate on the nature of LFERs, whether they are "fundamental chemical laws, or local empirical rules",[5] with judicious application, LFERs undoubtedly provide benefit across many areas including predicting biological activity, obtaining mechanistic insight and aiding the elaboration of new synthetic methodologies.[1]

Many LFERs are single term (e.g. the Hammett equation, Equation 3.1) allowing for intuitive interpretation. However, in part due to the increase in computing power,[6] many multi-term LFERs have been developed, and the scope of these models is impressive. Given that correlations with multi-term LFERs are better[i] than single-term LFERs, the uptake of this type of analysis has been substantial, with many chemists/statisticians involved in quantitative structure activity relationship (QSAR) analyses.[7] In the field of coordination chemistry many multi-term LFERs exist, including the 'ligand knowledge base' developed by Fey, Harvey and Orpen,[8] and Prock and Giering's quantitative analysis of ligand effects (QALE),[9,10] with alternative formulation by Poë.[11,12] Whilst these types of correlation analyses have been successful, care needs to be taken in the formulation and interpretation of the results, a subject that is not beyond controversy, with reported disagreements often concerning the statistical nature of the models.[13–15] Furthermore, multi-term LFER results are not as intuitive as those from a single-term LFER analysis, and often multi-term LFER input variables are derived from their single-term counterparts. For example, the QALE model consists of a linear combination of several parameters, including the seminal work of

[h] For discussion on the use of Brönsted vs Brønsted see reference 4, page 81.
[i] By definition, multi-term LFERs provide correlations equal to or better than the single-term LFERs of the same variables.

Tolman in the form of his electronic and cone angle parameters. Thus, providing they are significantly different from existing scales, there remains a need for the development of new single-term LFERs. To illustrate this point, since its publication, Hammett's original equation has been subjected to numerous extensions and revisions, including, the development of σ^{+}[16] and σ^{-}[17] parameters, and equations that combine such scales such as the Yukawa-Tsuno equation, $\log k_{rel} = \rho(\sigma + r(\sigma^{+} - \sigma))$.[18]

$$\log k_i = \rho\sigma_i + \log k_0 \tag{3.1}$$

The nature of precisely what a given LFER describes is a subject surrounded by much debate and many layers of theory. For example, Hammett's σ parameter is widely accepted to describe purely electronic effects, but the exact nature and relative magnitudes of the components involved in an electronic effect (inductive, mesomeric, field, etc.) is not obvious, and has been subject to much scrutiny.[19] Moreover, several LFERs have been formulated based on the idea of deconvoluting such effects, for example the Taft[20] and Swain-Lupton[21] equations. With this in mind, it is unsurprising that many LFERs now exist, and taken individually or collectively, are capable of accurately describing a wide range of chemical and physical properties. When considering the S_N2-like Lewis base displacement studied in chapter 2, existing parameters based on nucleophilicity and nucleofugality (leaving group ability) seem the most likely to provide meaningful correlations. Additionally, LFERs based on Brönsted basicity may also be valuable, although given the unique position the proton occupies on the hard/soft scale, poor correlations may result (*vide infra*).

3.1.2 Linear free energy relationships based on nucleophilicity

Unlike nucleofugality, the quantification of nucleophilicity has received much more attention, despite the two not necessarily being connected.[j] Pearson's 1963 report on 'hard soft acid base' (HSAB) theory demonstrates that both the nucleophilicity (kinetic) and Lewis basicity (thermodynamic) of a reactive centre are dependent on the corresponding electrophile/Lewis acid.[22] Additionally, relative nucleophilic capability can show a strong dependency on the reaction medium.[23] As such, any LFER describing nucleophilicity requires a constant electrophilic reaction partner and solvent. Even with this condition met, poor correlations are likely between the parameter and any reactions occurring in significantly different chemical systems. This reinforces the idea that LFERs are not

[j] For example, iodide is both a competent nucleophile and nucleofuge in S_N2 reactions.

fundamental laws, but only general similarity models as discussed above. Nonetheless, there are a range of LFERs describing nucleophilicity and many of these have found a number of applications, demonstrating the utility of such parameters. Of particular importance in this area is an understanding of mechanism, as it is vital to ensure the rate of the reference reactions is dictated by differences in nucleophilicity and does not include other factors.[k]

One of the most comprehensive nucleophilicity parameters to date is Mayr's system, denoted '*N*', and derived from a 1994 study examining the kinetics of reactions between benzhydrylium cations and nucleophiles, Scheme 3.1.[24,25] Mayr's system shrewdly circumvents the need for a constant electrophilic partner through simultaneous definition of an electrophilicity scale (*E*), thus allowing kinetic data to be collected for a wide span of reactivity, currently over 25 orders of magnitude.[26]

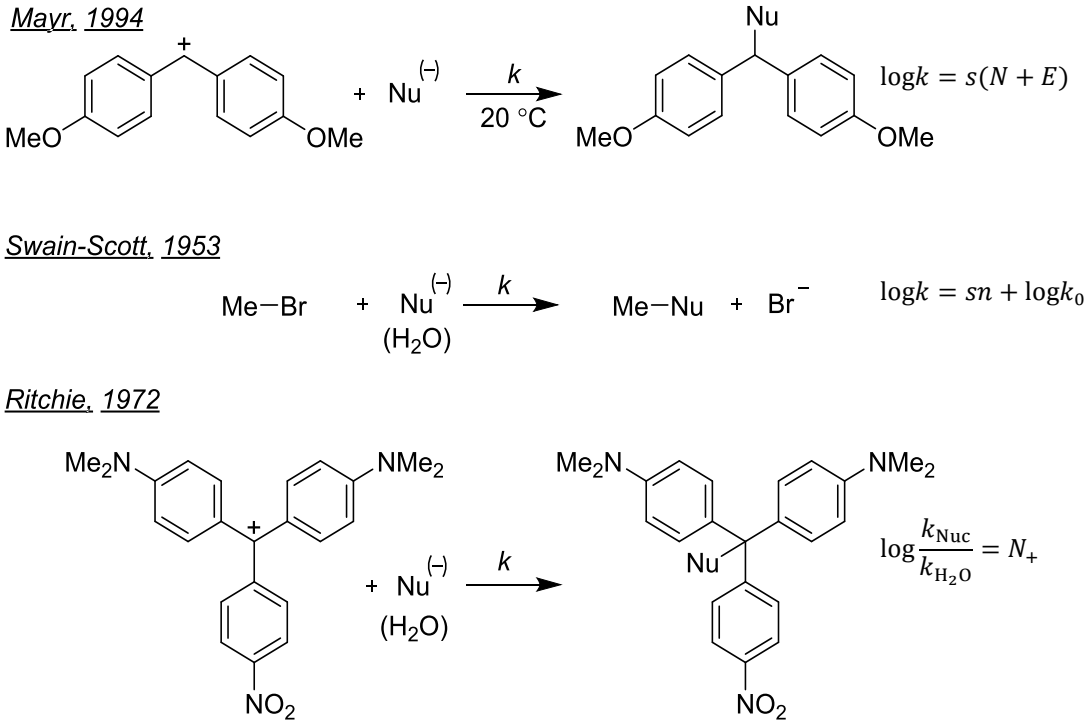

Scheme 3.1 Existing LFER equations and the nucleophilic reference systems they each employ.

An older example of a nucleophilic LFER is that published by Swain and Scott in 1953, using kinetics of nucleophilic displacement of methylbromide to define nucleophilicity (*n*) values.[27] The Swain-Scott equation is a single-term LFER of the form of Equation 3.1, referenced to water as a nucleophile ($n = 0$) with other effects (such as the electrophilic

[k] Measuring rates of 'typical' S_N1 reactions, for example, would not provide any information on relative ability of the nucleophiles tested.

partner) described by a sensitivity value (*s*), *s* being defined as 1 for the reaction with methylbromide in water at 25 °C. Based on this idea, a range of similar LFERs have been developed, primarily through a change in the reference system, broadening the scope to include transition metal displacements. Pearson and Songstad have reported systems referenced to the kinetics of nucleophilic displacements at both methyl iodide and *trans*-[Pt(pyridine)$_2$Cl$_2$] using methanol as reference nucleophile.[28] Interestingly, as might be predicted according to Peason's HSAB, there is a poor linear correlation ($R^2 = 0.43$) between the n_{MeI} and corresponding n_{Pt} values obtained. Whilst the number of *n* values determined in these LFERs is substantially smaller than the collection obtained by Mayr, these parameters have been shown to correlate with a range of reactions.[29,30]

A further nucleophilic LFER based on the rate of reaction of a bis(*p*-dimethylaminophenyl)-*p*-nitrophenylmethyl cation with nucleophiles in a given solvent, has been developed by Ritchie, see Scheme 3.1.[31] This N_+ scale is referenced to the rate of reaction between water and the cation, in water.[l] Interestingly, Ritchie's equation lacks a sensitivity parameter (such as Hammett's ρ) associated with the electrophile; the reason behind this is the apparent "constant selectivity" of different cations towards various nucleophiles. Evidence for this constant selectively relationship came from the kinetics of cation anion recombinations covering over six orders of magnitude. However, since Ritchie's report, work by Mayr on similar systems has shown that a constant selectivity model does not hold over larger sets of data and consequently, a sensitivity correction is included in Mayr's equation, see Scheme 3.1.[24] Given the large number of reactions involving a nucleophilic step, there remains a great deal of interest in the quantification on nucleophilicity, and it is unsurprising to find many additional reports on the subject. This is especially true when considering that LFERs based on thermodynamic data (as opposed to kinetic) may also provide correlations with nucleophilicity, one such example being Edwards' two-term nucleophilicity/basicity LFER.[32]

3.1.3 Linear free energy relationships based on nucleofugality

Relative to nucleophilicity, studies attempting to quantify nucleofugality[m] are scarce, and must be met with caution, as even relative (as opposed to absolute) leaving group abilities

[l] Unusually, for the reference reaction with water as solvent and nucleophile, the pseudo-first order rate constant (k_{obs}) is used, whereas for other nucleophiles the second order rate constant (k_{Nuc}) is used.
[m] A nucleofuge is defined by IUPAC as "a leaving group that carries away an electron pair". The term nucleofugacity is found throughout the literature, and is deemed to mean the same.

are dependent on a range of properties such as reaction medium and the corresponding electrofuge.[33,34] Despite these apparent drawbacks, investigations into quantification of nucleofugality have been carried out, with the most compressive scale again coming from Mayr in collaboration with Kronja.[35] As with nucleophilicity, Mayr uses the same "semi-quantitative" approach, adapting his equation (Scheme 3.1) in order to quantify both the electrofugality and nucleofugality of a range of benzhydryl based complexes, see Scheme 3.2.[36] Mechanistic considerations prove to be equally important in the formulation of suitable nucleofugality LFERs. This is particularly significant for the work of Mayr and Kronja, as the cations generated are suitably stable that their subsequent capture (by solvent for example) can be slower than their generation; this is in contrast to the "textbook" S_N1 type mechanism, with slow ionisation and fast capture of the cation (see S_N1 associative and S_N1 dissociate mechanism in Scheme 2.5). As such, monitoring the rate of product formation (e.g. the solvolysis product) in these reactions, will not give quantitative information on just the electrofugality/nucleofugality of the starting material, it will also depend on the relative nucleophilicity/electrophilicity of the solvent and intermediate. To circumvent these problems, the addition of nucleophilic amines to rapidly and quantitatively trap the intermediate allow the kinetics to be determined.

Mayr-Kronja, 2006

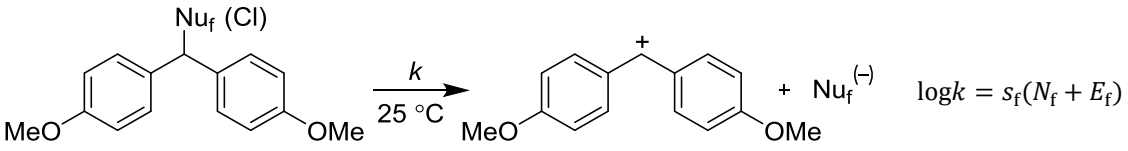

Stirling, 1979

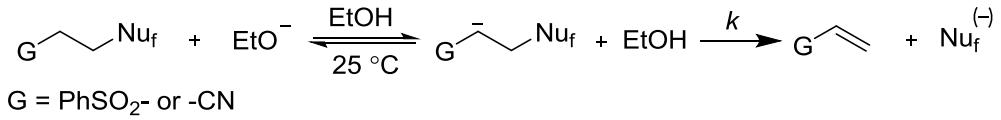

Scheme 3.2 Mayr-Kronja nucleofugality/electrofugality LFER and reference system. Stirling's E_1cB elimination reactions, *k* giving a measure of nucleofugality.

Whilst in the strictest sense not a LFER, Stirling has collected kinetic data that provides a quantitative description of the relative nucleofugality of a range of leaving groups.[37] This was achieved using the kinetics of E_1cB eliminations, in combination with a careful mechanistic analysis, see Scheme 3.2. It is well known that elimination mechanisms are very substrate dependent,[38] and through judicious choice of substrate class and deuterium labelling studies, Stirling was able to extract rate constants that provide information

exclusively related to the nucleofugal ability of the leaving group.[39] The use of adjacent anion stabilising substituents (G in Scheme 3.2) was vital to ensure a fast and reversible deprotonation, allowing the rate of product formation to be associated with the second step, the departure of the leaving group (and its effect on the deprotonation equilibrium).[n] Using this system Stirling was able to construct a collection of kinetic data that could be used to rank nucleofugality. As with the Mayr-Kronja nucleofugality/electrofugality LFER however, the collection of leaving groups studied is biased toward anionic (X-type) nucleofuges, with Stirling analysing a range of oxygen and sulphur centred leaving groups.

Whilst there are existing parameters able to describe nucleophilicity and nucleofugality, there is always scope for further quantification of alternative relevant systems. Herein, the development of a series of nucleofugality parameters based on displacements of borane adducts as reported in chapter 2 is described. These parameters are capable of quantifying both common Lewis base ligands (N^F_B) and the contribution of a given substituent to the nucleofugality of tri-coordinate phosphines and amines (n^f_{PB} and n^f_{AB}, respectively).

3.2 Formulation of nucleofugality parameters

3.2.1 Phosphine substituent additivity

As discussed in chapter 2, the kinetics of the deprotection of a range of phosphine borane complexes following the formula $Ph_{3-n}R_nP{\cdot}BH_3$ displayed a stepwise response to change in *n*. This can be seen in Figure 3.1 (and Table 2.3) where an increase in *n* resulted in an approximate 10 fold reduction in *k* across the series $Ph_{3-n}Cy_nP{\cdot}BH_3$. Furthermore, this additive effect was found to hold across a range of alkyl groups R = Cy, Me, ^{t}Bu (*n* = 0 - 3), and also for ^{i}Pr (*n* = 0, 1 and 3 only), suggesting that each substituent at phosphorus contributes to the nucleofugality of the phosphine independently of the other substituents. In an effort to determine whether this was a general phenomenon, rates of quinuclidine displacements were measured for a range of aryl phosphine borane complexes described by the formula $Ph_{3-n}Ar_nP{\cdot}BH_3$, Ar = *o*-tolyl (**25**, **26**, **10**); *o*-methoxyphenyl (**27**, **28**, **11**); *p*-methoxyphenyl (**29**, **30**, **6**); *n* = 1 - 3 respectively. Remarkably, this additivity was present

[n] This class of E_1cb is often written $(E_1cB)_R$, the R indicating that the first step is reversible, in contrast to $(E_1cB)_I$, see reference 38 for more details.

in all cases, see Figure 3.1, even for the case of Ar = *o*-tolyl, where steric effects are known to play a role in the relative rate, see Section 2.3.2.

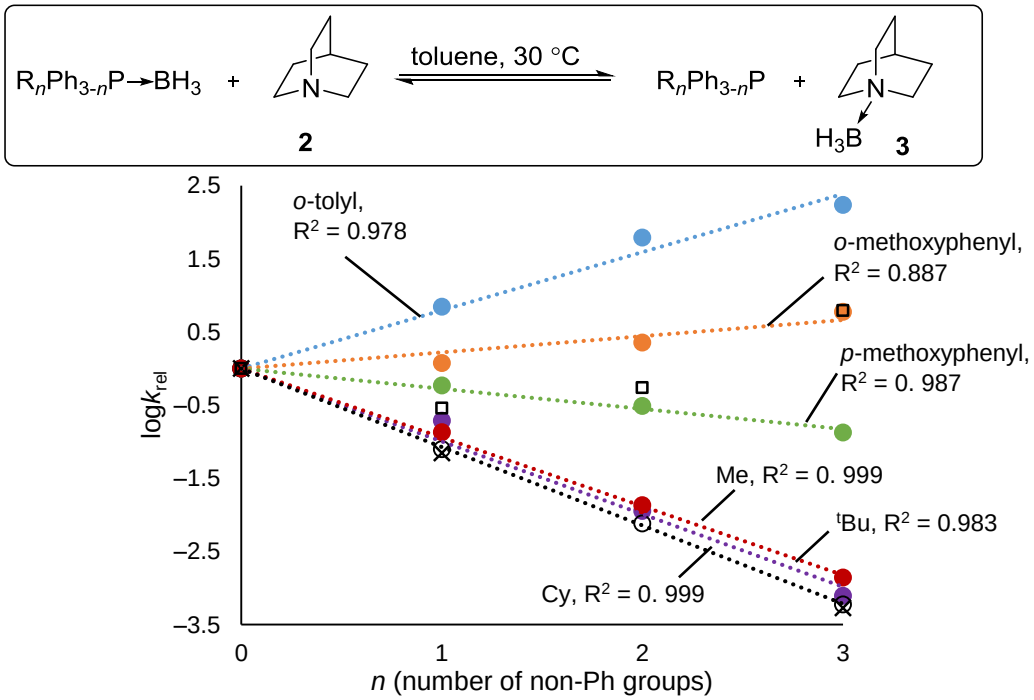

Figure 3.1 Correlations between logk_{rel} (relative to $Ph_3P{\cdot}BH_3$, **1**, i.e. n = 0) and n for a range of quinuclidine displacements from phosphine borane complexes in the series $Ph_{3-n}R_nP{\cdot}BH_3$, R = Cy, Me, ^{t}Bu, ^{i}Pr, *o*-tolyl, *o*-methoxyphenyl and *p*-methoxyphenyl, data points for ^{i}Pr are shown as crosses, with an R^2 = 0.999. Hollow squares correspond to R = OPh, no trendline is shown for this series. Pearson R^2 values are shown with the trendlines fixed to go through the origin.

3.2.2 Formulation of nucleofugality parameters

The collection of data in Figure 3.1 can be seen as a measure of the relative kinetic lability of phosphines from the borane adducts, with all species tested showing additive substituent effects. Thus, it is possible to quantify the nucleofugality of a phosphine by summing the nucleofugality 'conveyed' by each substituent. Formalising this mathematically gives Equation 3.2.

Given, ^{i}Pr$_3$P was the poorest nucleofuge, the substituent nucleofugality value, $n^f_{PB}(^i\text{Pr})$, was defined as zero, meaning that the ligand nucleofugality value $N^F_B(P^iPr_3)$ was also zero.[o]

[o] In principle, any value could be taken as the reference, taking the slowest reacting phosphine merely ensures the subsequent values will be positive.

Extrapolation of Equation 3.2 to quantify the relative nucleofugality of other phosphines was achieved through comparison to kinetic data in the form of single-term LFER Equation 3.3. Defining ρ = 1 for the reference conditions (quinuclidine, toluene, 30 °C) and k_0 as the second order rate constant for the displacement of $^{i}Pr_3P$, nucleofugality values were then calculated[p] for a range of phosphines (N^F_B) and substituents (n^f_{PB}), and these values are reported in Tables 3.1 and 3.2, respectively.

$$N^F_B(PR_1R_2R_3) = n^f_{PB}(R_1) + n^f_{PB}(R_2) + n^f_{PB}(R_3) \quad (3.2)$$

$$\log\frac{k_X}{k_0} = \rho\, N^F_B \quad (3.3)$$

The excellent correlation between N^F_B and logk_{rel} (i.e. LFER defining Equation 3.3) for borane transfer (quinuclidine, toluene, 30 °C) validates the treatment of the substituent effects as additive and independent, see Figure 3.2a. The absolute values of N^F_B provide a quantitative assessment of leaving group ability, low values indicating poor nucelofuges and high values indicating relatively competent nucleofuges. The same analysis is true of the substituent n^f_{PB} values, with sterically bulky or electronically activated aryl groups with high n^f_{PB} values able to impart significant nucleofugal character to the parent phosphine relative to their alkyl counterparts, see Table 3.2.

At first glance, the N^F_B values for phosphines show apparent similarity to the Tolman electronic parameter (TEP) which is based on the CO stretching frequencies in L·Ni(CO)$_3$ complexes.[40] In fact, in his seminal 1970 publication describing the formulation of the TEP, Tolman observed the same additive substituent effect as seen in the kinetics of borane transfer. Thus, as might be expected, with judicious choice of data (excising any *o*-substituted aryl phosphines) a moderate correlation does exist between logk_{rel} (or N^F_B) and TEP, (R^2 = 0.861), see Figure 3.2b. Whilst this correlation can be used as a rough gauge of the nucleofugality of phosphines, there is a dramatic failure for *o*-substituted aryl phosphines. In the most extreme cases, *deviations of greater than 3 orders of magnitude* exist between experimental *k* values and those predicted by the correlation.

[p] N^F_B and n^f_{PB} values for phosphines were calculated using a linear regression model in combination with the equation resulting from substitution of Equation 3.2 into 3.3.

Table 3.1 Ligand nucleofugality values (N^F_B) for phosphines, amines and pyridines defined according to Equations 3.2 and 3.3.

Entry	Ligand	N^F_B	Entry	Ligand	N^F_B
1	$^{i}Pr_3P$	0	34	Ph_2(2-pyridyl)P	3.24
2	Cy_3P	0.03	35	$^{t}Bu_2$(*o*-biphenyl)P	3.25
3	$^{n}Bu_3P$	0.27	36	$EtNMe_2$	3.25
4	$^{t}Bu_3P$	0.27	37	4-methylpyridine	3.28
5	Me_3P	0.43	38	Et_2NMe	3.31
6	Cy_2PhP	1.13	39	Ph_3P	3.32
7	$^{t}Bu_2PhP$	1.29	40	*N*-methylpyrrolidine	3.33
8	Me_2PhP	1.39	41	Et_3N	3.38
9	4-dimethylaminopyridine	1.77	42	Cy_2NH	3.43
10	pyrrolidine	1.78	43	3-methylpyridine	3.46
11	piperidine	2.03	44	(*o*-methoxyphenyl)Ph_2P	3.52
12	$^{i}PrNH_2$	2.03	45	pyridine	3.57
13	$^{i}PrPh_2P$	2.22	46	*N*-methylpiperidine	3.58
14	$CyPh_2P$	2.23	47	2-methylpyridine	3.60
15	$^{t}BuPh_2P$	2.30	48	*N*-ethylpiperidine	3.64
16	$MePh_2P$	2.36	49	$^{n}Pr_3N$	3.68
17	(*p*-methoxyphenyl)$_3$P	2.42	50	(*p*-fluorophenyl)$_3$P	3.69
18	Me_2NH	2.46	51	(*o*-methoxyphenyl)$_2$PhP	3.72
19	$^{t}BuNH_2$	2.51	52	$^{n}Bu_3N$	3.73
20	Et_2NH	2.59	53	(*o*-methoxyphenyl)$_3$P	3.92
21	morpholine	2.61	54	(*p*-chlorophenyl)$_3$P	4.08
22	^{n}BuMeNH	2.64	55	(*o*-tolyl)Ph_2P	4.10
23	(*p*-methoxyphenyl)$_2$PhP	2.72	56	2,6-dimethylpyridine	4.29
24	$BnPh_2P$	2.78	57	2-isopropylpyridine	4.31
25	^{n}PrNH	2.79	58	2-(PPh_2)pyridine	4.71
26	(*p*-tolyl)$_3$P	2.82	59	(2-thienyl)$_3$P	4.75
27	(*m*-tolyl)$_3$P	2.86	60	2-methoxypyridine	4.80
28	CyEtNH	3.01	61	4-trifluoromethylpyridine	4.86
29	(*p*-methoxyphenyl)Ph_2P	3.02	62	(*o*-tolyl)$_2$PhP	4.87
30	$^{i}Pr_2NH$	3.05	63	(*p*-trifluoromethylphenyl)$_3$P	5.11
31	4-methoxypyridine	3.13	64	(*o*-fluorophenyl)$_3$P	5.26
32	Me_3N	3.19	65	(2-furyl)$_3$P	5.63
33	^{t}BuMeNH	3.24	66	(*o*-tolyl)$_3$P	5.65

Table 3.2 Substituent nucleofugality values (n^f_{PB}) for phosphines defined according to Equations 3.2 and 3.3.

Entry	Substituent	n^f_{PB}	Entry	Substituent	n^f_{PB}
1	^{i}Pr[a]	0	11	H	1.11
2	Cy	0.01	12	*p*-fluorophenyl	1.23
3	^{n}Bu	0.09	13	*o*-methoxyphenyl	1.31
4	^{t}Bu	0.09	14	*p*-chlorophenyl	1.36
5	Me	0.14	15	2-thienyl	1.58
6	Bn	0.57	16	*p*-trifluoromethylphenyl	1.70
7	*p*-methoxyphenyl	0.81	17	*o*-fluorophenyl	1.75
8	*p*-tolyl	0.94	18	2-furyl	1.88
9	*m*-tolyl	0.95	19	*o*-tolyl	1.88
10	2-pyridyl	1.03	20	*o*-biphenyl	3.07

[a] By definition

Furthermore, the inclusion of kinetic data measured under reference conditions with a range of -O linked phosphine nucleofuges[q] in the series $Ph_{3-n}(OPh)_nP{\cdot}BH_3$ (**31**, **32**, **33**; n = 1, 2, 3, respectively) and $(p\text{-tolyl-O})_3P{\cdot}BH_3$, **34**, also highlights the failure of TEP to accurately predict the nucleofugality of phosphines from borane adducts (k_{pred}/k_{expt} > 6000 in the worst case).

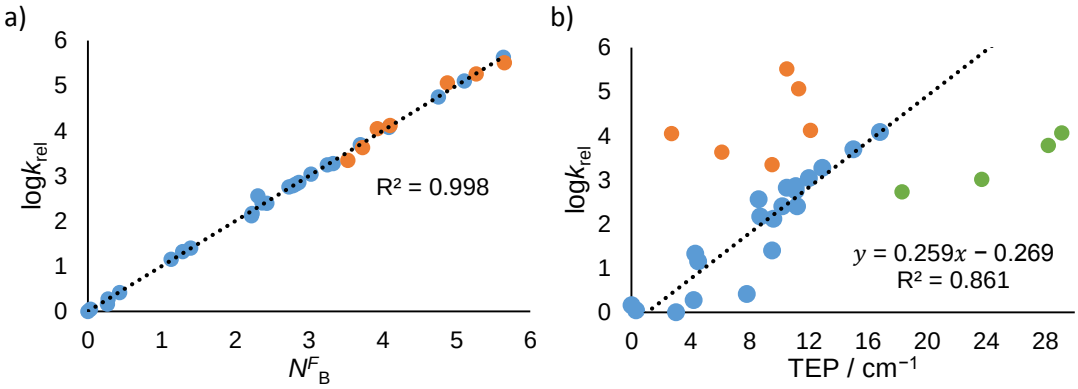

Figure 3.2 a) Correlation resulting from the application of Equations 3.3 (LFER) and 3.2 (additivity) to kinetic data obtained in the borane transfer from phosphine borane adducts to quinuclidine, in toluene at 30 °C. By definition, the gradient (ρ) is equal to 1. b) Correlation between logk_{rel} (relative to ^{i}Pr$_3$P·BH$_3$) and Tolman's electronic parameter (TEP) for phosphines, trendline is fit to only blue circles (alkyl and *p*/*m*-substituted aryl phosphines), orange circles are *o*-substituted aryl phosphines, and green circles are phosphines containing O-linked substituents.[q]

[q] The word phosphines in this context is used to include phosphinites, phosphonites and phosphites.

The ‘unexpected stability’ possessed by phosphite borane adducts has been noted before.[41] Indeed, further analysis of the relative rates across the series $Ph_{3-n}(OPh)_nP{\cdot}BH_3$ shows, unlike their -C linked counterparts, a non-linear correlation between n and $\log k_{rel}$, see Figure 3.1 (hollow squares). The failure of the substituent additivity for these substrates, perhaps originating from increased conformational freedom, means it is not possible to obtain a meaningful n^f_{PB}(OPh) value. Therefore, unlike -C linked substituents, knowledge of the number of O-linked groups is necessary for an *a priori* prediction of relative nucleofugality. Despite this, the relative nucleofugality of phosphines containing O-linked substituents can be directly compared with other phosphine ligands *via* N^F_B.

3.2.3 Testing the parameters

As can be seen by Equation 3.2, the additivity provides a means to predict N^F_B values for a range of Lewis bases that extends far beyond those experimentally derived. In the first instance, this was tested by comparing predicted and experimental rates of borane transfer from phosphine borane complexes outside of the training set (under reference reaction conditions). In this capacity, phosphine borane adducts **35**-**38** were subjected to the reference reaction conditions, and the predicted[r] and experimental k values are reported in Table 3.3. Excellent agreement is observed between predicted and observed rate constants, all values being within a factor of 2.5. Putting this in the context of the large variation in k (greater than 10^5) observed over the entire dataset gives an indication of relative and promising accuracy of the predictions.

Based on the agreement between experimental and predicted rate constants in the reference reaction, we sought to expand the scope of the predictions. Staying within the realm of borane transfer reactions, but using amines other than quinuclidine, predictions were made based on the additivity model in concert with factoring in the differences in relative nucleophilicity of the amines (based on $Ph_3P{\cdot}BH_3$). Again, there is excellent agreement between predicted and experimental rate constants, see Table 3.3, meaning that in theory, using Tables 2.1 and 3.2 together it is possible to provide quantitative estimations on the rate of over 10,000 borane deprotections.[s]

[r] For example, the N^F_B (pred) value for phosphine borane complex **37** is calculated according to: N^F_B (pred) = 0.09 (^{t}Bu) + 0.14 (Me) + 0.81 (*p*-methoxyphenyl) = 1.04. Using this value with Equation 3.3 (ρ = 1, for reference conditions) allows determination of predicted rate constants (k_{pred}).

[s] The relative accuracy of the predictions in Table 3.3 implies that a ‘constant selectivity’ relationship for the amine nucleophiles is a reasonable enough assumption to provide semi-quantitative analysis.

Table 3.3 Predicted and experimentally determined second order rate constants for amine displacement of phosphine borane adducts. For absolute values and errors in Appendix, Table 6.7.

Entry	Phosphine	N^F_B (pred)	Amine	k_{expt}/k_{pred}
1	$^tBu_2CyP$, **35**	0.19	quinuclidine	1.25
2	$^tBuCy_2P$, **36**	0.11	quinuclidine	1.08
3	^{t}BuMe(*p*-methoxyphenyl)P, **37**	1.04	quinuclidine	1.14
4	Cy_2(*o*-tolyl)P, **38**	1.90	quinuclidine	2.48
5	Cy_2(*o*-tolyl)P, **38**	1.90	morpholine	2.46
6	$^tBu_2PhP$, **20**	1.29	DABCO	0.90
7	(*p*-chlorophenyl)$_3$P, **4**	4.08	triethylamine	0.87
8	Ph(*o*-methoxyphenyl)$_2$P, **28**	3.72	morpholine	1.01
9	Ph_2MeP, **16**	2.36	diethylamine	1.16

3.2.4 Extension to pyridines

The LFER Equation 3.3, whilst derived using phosphine nucleofuges, can be applied to any species capable of undergoing the reference reaction (displacement from a borane adduct by quinuclidine, **2**, in toluene at 30 °C). In addition to their potential capacity as hydrogen storage materials,[42,43] amine borane adducts have been studied for similar reasons to their phosphine borane counterparts and, as such, are well-known and even commercially available species. Looking to provide a quantitative comparison to phosphines, the kinetics of a range of substituted-pyridine borane adducts were subjected to quinuclidine displacement, under pseudo-reference conditions (d_8-toluene was used to allow ^{1}H NMR analysis),[t] see Scheme 3.3. Reactions were typically carried out with a small excess of quinuclidine and, consistent with an associative S_N2-like mechanism, second order temporal concentration profiles were observed. As with phosphines, simulation and fitting of these profiles according to a bimolecular equilibrium rate law: $-\mathrm{d}[\text{pyridine}\cdot BH_3]/\mathrm{d}t = k([\text{pyridine}\cdot BH_3][\mathbf{2}]-[\text{pyridine}][\mathbf{3}]/K)$ provided access to a range of k

Differentiation between the R and S enantiomers for P-stereogenic phosphines is not considered in this analysis, both expected to deprotect at identical rates.

[t] The switch to d_8-toluene has a minimal effect on the kinetics, as tested through the reaction of **1** with **2** ($k_{toluene}/k_{d8\text{-toluene}} = 1.002$).

values.[u] These were then used with Equation 3.3 to calculate N^F_B values for pyridines, see Table 3.1.

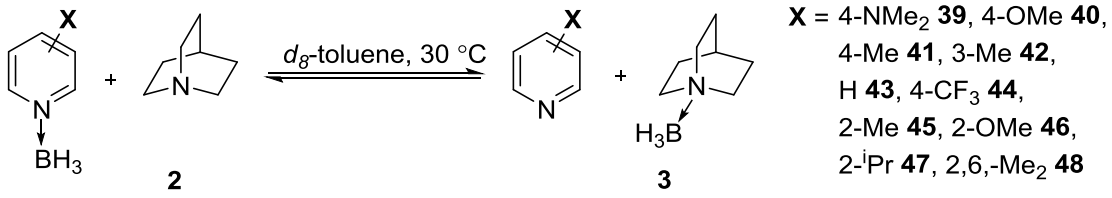

Scheme 3.3 Reaction conditions used to obtain the kinetics and subsequently N^F_B values of borane transfer from substituted-pyridines. Typically [X-pyridine·BH_3]$_0$ = 0.02 - 0.07 M and [**2**]$_0$ = 0.02 - 0.08 M.

As observed with phosphines, electron-deficient (pyridine) nucleofuges were more readily displaced from the borane adduct, leading to larger k and N^F_B values than electron-rich analogues. Correlation of the N^F_B values with Hammett's σ parameter not only allows analysis of the extent to which electronic effects influence the nucleofugality of pyridines,[v] it also provides a means to predict N^F_B values of 3/4-substituted pyridines not yet determined, see Figure 3.3. Unsurprisingly, the resulting ρ value for pyridines (2.2) is greater than the corrected ρ value for phosphines (1.1), as the substituent is closer to the reactive centre.

Kinetics measured for a range of 2-substituted pyridine borane adducts revealed large k values relative to unsubstituted derivatives. This suggests that the presence of steric bulk around the reactive centre acts to destabilise the ground state borane adduct, relative to the transition state. This steric rate enhancing effect varied substantially in magnitude, with 2-methylpyridine borane, **45**, reacting at a very similar rate to the unsubstituted pyridine borane adduct, **43**. The presence of bulkier groups, such as 2-isopropyl however, provided a substantial rate increase relative to pyridine, as did 2,6-di-methyl-substitution (k_{rel} = 5.4 and 5.1, respectively). As with the phosphine borane examples, it is difficult to completely separate any electronic contribution to the kinetic lability of 2-substiutited pyridines borane complexes; these electronic factors might be particularly relevant in the 47 fold increase in rate observed for 2-methoxypyridine borane, **46**, relative to its 4-substituted counterpart, **40**.

We sought to test the predictive power of the correlations between N^F_B and Hammett's σ value displayed in Figure 3.3. For the equations allowing prediction of substituent nucleofugality values for phosphines (n^f_{PB}), this was achieved through correlation to experimental kinetic data relating to the hydrolysis of aryl-MIDA boronates (MIDA = *N*-methyliminodiacetic acid), see Section 3.3. For N^F_B values corresponding to pyridines

[u] Values of K were often too large to be accurately determined under the conditions studied.
[v] For sterically similar pyridines, i.e. not bearing any substitution in the 2 or 6 positions.

however, the predictive power was tested through the quinuclidine displacement of 3-bromo-5-methylpyridine borane, **49**, in d_8-toluene at 30 °C. Pleasingly, good agreement was found between the predicted and experimental second order rate constant for this substrate (k_{expt}/k_{pred} = 2.44); again the large variation observed in *k* for substituted pyridine borane complexes (over 3 orders of magnitude) provides an encouraging indication of the accuracy of this prediction. Aside from testing the correlation between N^F_B and Hammett's σ, the good agreement found for di-substituted **49** also confirms that it is reasonable to consider Hammett σ values as additive for this system.

3.2.5 Extension to amines

As discussed previously, the ligand nucleofugality parameter (N^F_B) has the scope to quantify leaving group ability for any Lewis base capable of forming an adduct with BH_3. Further expansion of the parameter was achieved through measuring the relative rates of borane displacement from a range of aliphatic amine borane complexes under reference conditions (quinuclidine, toluene, 30 °C). To economise on both reagent and time costs an alternate approach involving determination of relative as opposed to absolute rate constants was used. In two separate experiments, both $Me_2NH{\cdot}BH_3$, **50**, and $Me_3N{\cdot}BH_3$, **51**, were formed *in situ* (*via* reaction of the parent amine with $Me_2S{\cdot}BH_3$) and subjected to a large excess of quinuclidine. The resulting displacement reactions were monitored using $^{13}C\{^1H\}$ NMR.[w] Using this system as a benchmark, the kinetics of borane transfer for up to four amine borane adducts (including always either **50** or **51**) were analysed simultaneously.[x] Kinetic modeling using a contemporaneous second order displacement (for all amines present) gave access to relative rate constants. Correcting by the absolute rate constant measured for either **50** or **51** then gave *k* values which were used to calculate N^F_B values for a wide range of amines, see Table 3.1.

Interestingly, aliphatic amines appeared to show the same independent and additive substituent effects as seen with phosphine nucleofuges. This was confirmed by observing a progressive change in *k* across a series $Me_{3-n}Et_nN{\cdot}BH_3$ (**51**, **52**, **53**, **54**; *n* = 0-3 respectively), see Figure 3.4a. With this information in hand, the N^F_B values for aliphatic amines were subjected to linear regression according to Equations 3.3 and 3.4 (analogous to 3.2) and thus

[w] In order to obtain good signal to noise within a suitable timeframe, the $^{13}C\{^1H\}$ NMR experiment used was not quantitative. As such, only the decay of signals corresponding to amine·BH_3 adducts were analysed.

[x] The switch to $^{13}C\{^1H\}$ NMR was essential to obtain resolved signals for each amine borane adduct present in the mixture.

a new amine substituent parameter n^f_{AB} was developed, values shown in Table 3.4. Using this model, excellent agreement was found between logk_{rel} and the calculated N^F_B values, see Figure 3.4b, providing validation the treatment of substituent effects as additive.

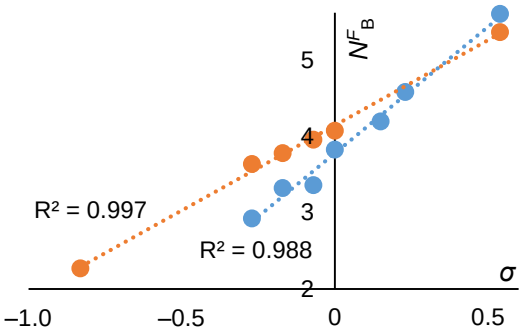

$$N^F_B(pred) = 3.32\sigma + 3.28 \qquad phosphines$$

$$n^F_{PB}(pred) = \frac{N^F_B(pred)}{3} \qquad phosphine\ substituents$$

$$N^F_B(pred) = 2.23\sigma + 3.64 \qquad pyridines$$

Figure 3.3 Correlation between N^F_B values and Hammett σ values for *m*/*p*-triarylphosphines (blue circles) and 3/4-substituted pyridines (orange circles). Given the substituent additivity and the above plot being constructed using symmetrical triply substituted phosphines i.e. (Ar_3P), n^f_{PB} values for individual phosphine substituents can be predicted by dividing the correlation with N^F_B above by a factor of 3.

$$N^F_B(NR_1R_2R_3) = n^f_{AB}(R_1) + n^f_{AB}(R_2) + n^f_{AB}(R_3) \qquad (3.4)$$

As found with phosphines, the substituent identities of an amine had a profound effect on the kinetic lability from the borane adduct, with *k* values spanning nearly two orders of magnitude. Broadly speaking, substituents considered as 'bulky' or sterically encumbered were found to increase the nucleofugality of the amine, with ^{t}Bu and ^{i}Pr having significantly larger n^f_{AB} values than their ^{n}Bu/^{n}Pr counterparts. Moreover, this effect is also manifested in the increased nucleofugality upon increasing alkyl chain length (Me < Et < ^{n}Pr < ^{n}Bu), although it is less marked than the effect of branching. This trend is not found with phosphine nucleofuges, with primary (Me), secondary (^{n}Bu), tertiary (^{i}Pr, Cy) and quaternary (^{t}Bu) alkyl groups displaying very similar n^f_{PB} values. Given the $n^f_{PB/AB}$ values for phosphines and amines display different trends (potentially arising from conformational or bond length effects), the two scales are suitably distinct and therefore can offer different and complementary descriptions of substituent effects.

As a consequence of Equation 3.4, cyclic groups on amines such as piperidine, pyrrolidine and morpholine were treated as two substituents, thus allowing the calculation of n^f_{AB} values corresponding to *half* of the ring system, see Table 3.4.

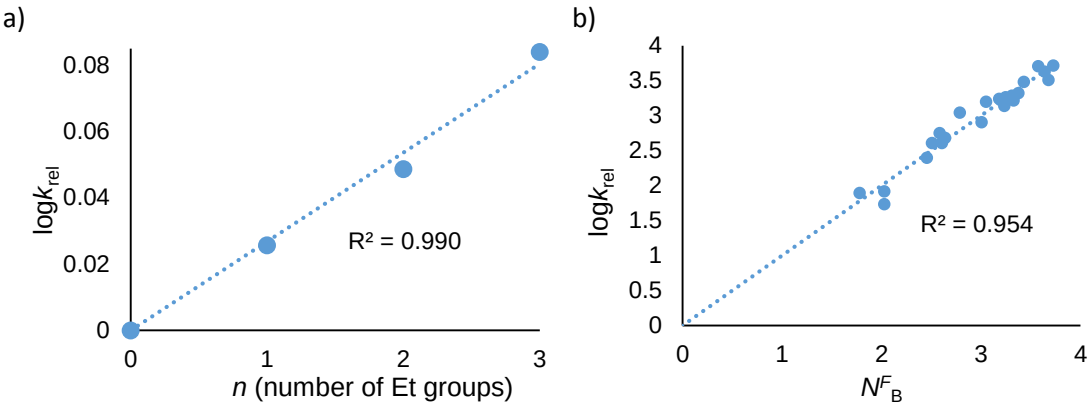

Figure 3.4 a) Correlation between logk_{rel} (relative to $Me_3N{\cdot}BH_3$, **51**, i.e. $n = 0$) and n for quinuclidine displacements from amine borane complexes in the series $Me_{3-n}Et_nN{\cdot}BH_3$. b) Correlation between logk_{rel} (relative to $^iPr_3P{\cdot}BH_3$, **24**) for reference quinuclidine displacements and N^F_B values for aliphatic amines, calculated according to Equations 3.3 and 3.4. Pearson R^2 values are shown with the trendlines fixed to go through the origin.

Interestingly, cyclic amines demonstrated substantially increased sensitivity to alkylation at *N* than their acyclic counterparts: $k_{rel} = 61$ (*N*-methylpiperdine/piperdine) *vs* $k_{rel} = 6.9$ (trimethylamine/dimethylamine).[y] To reflect the relative stability of a -H substituent present on cyclic amine borane complexes, a n^f_{AB}(cyclic-H) value was calculated (distinct from the n^f_{AB}(-H) value for acyclic amines), see Table 3.4. This use of two n^f_{AB} values to describe what is nominally the same substituent was important to allow all other substituents to be assigned one n^f_{AB} value, independent of whether present on a cyclic or acyclic amine. Having done this, a range of cyclic amine borane adducts were then successfully fitted to the model described by Equations 3.3 and 3.4, the good fit between model and experiment can be seen by the high R^2 value describing all amines (both cyclic and acyclic) in Figure 3.4b.

Table 3.4 Substituent nucleofugality values (n^f_{AB}) for amines, according to Equations 3.3 and 3.4.

Entry	Substituent	n^f_{AB}	Entry	Substituent	n^f_{AB}
1	cyclic-H	−0.49	7	^{n}Bu	1.24
2	H	0.34	8	½ piperidine	1.26
3	Me	1.06	9	^{i}Pr	1.36
4	Et	1.13	10	½ morpholine	1.55
5	½ pyrrolidine	1.13	11	Cy	1.55
6	^{n}Pr	1.23	12	^{t}Bu	1.84

[y] This could arise from a differences in the conformational freedom between cyclic and acyclic amines.

Having done this, a range of cyclic amine borane adducts were then successfully fitted to the model described by Equations 3.3 and 3.4, the good fit between model and experiment can be seen by the high R^2 value describing all amines (both cyclic and acyclic) in Figure 3.4b.

3.3 Applications of the nucleofugality parameters

3.3.1 MIDA boronate ester hydrolysis

MIDA boronate esters have shown great promise as latent sources of boronic acids for use in cross-coupling reactions, such as Suzuki-Miyaura cross-couplings.[44] In particular, the use of MIDA boronate esters in has allowed successful couplings of reagents whose corresponding boronic acids are typically considered unstable, such as 2-pyridyl boronic acid.[45] Controlled hydrolysis of MIDA boronate esters, under suitable reaction conditions, prevents the accumulation of the unstable boronic acid, and thus minimises any associated undesirable side reactions. The mechanisms of these hydrolyses under both "slow-release" (Scheme 3.4) and "fast-release" conditions have been studied by Burke and Lloyd-Jones.[46]

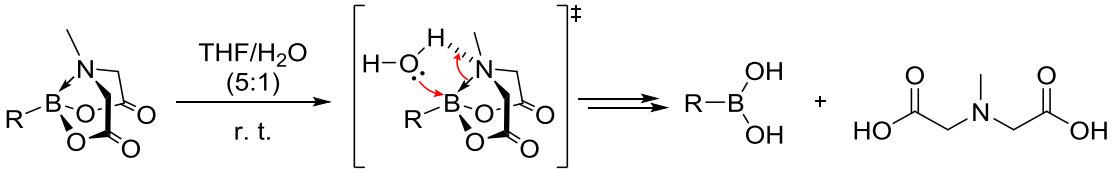

Scheme 3.4 Burke and Lloyd-Jones' "slow-release" conditions used to study the hydrolysis of MIDA boronate esters. The MIDA product may exist, at least to some extent, as a zwitterion.[46]

As part of this study, a good correlation between relative hydrolysis rate (more specifically logarithms of the pseudo-first order rate constants, logk_{obs}) and Hammett's σ parameter was found under slow-release conditions. In addition to providing mechanistic information on the hydrolysis, the correlation with Hammett's σ also allows prediction of reaction rates for a range of *m*/*p*-substituted aryl MIDA boronate esters. Quantifiable expansion beyond these substrates is not possible, although through rationalisation of the known influence of electronic effects, qualitative estimations are often made.

Pleasingly, a good correlation was found between slow-release hydrolysis rates (k_{obs}) and phosphine substituent nucleofugality parameter (n^f_{PB}), for a range of alkyl and aryl MIDA

boronate esters, see Figure 3.5. Special note should be made of the predictive capabilities of this model, not just encompassing alkyl and *m*/*p*-substituted aryl systems, but also an *o*-substituted aryl MIDA boronate (*o*-tolyl MIDA boronate, $k_{expt}/k_{pred} = 0.99$). Also, of interest is the calculation of n^f_{PB} values for *m*-nitrophenyl and *m*,*m*-bistrifluoromethylphenyl, based on the correlation between N^F_B and Hammett's σ values for triarylphosphines, i.e. Figure 3.3.

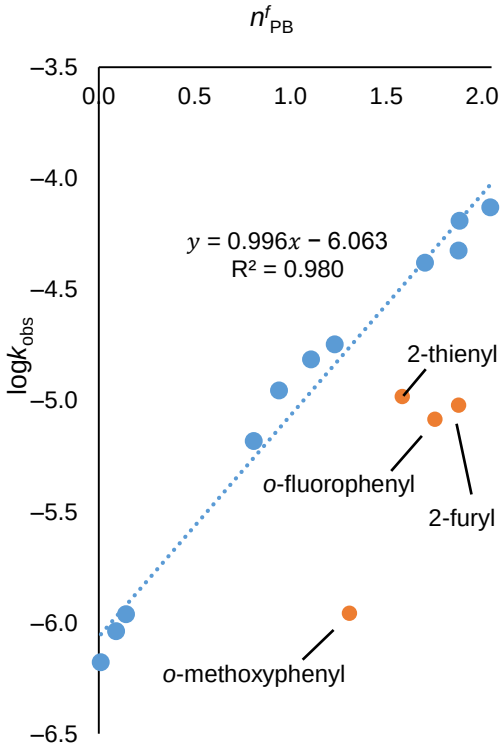

Entry	Substituent	k_{expt}/k_{pred}
1	Cy	0.66
2	^{n}Bu	0.81
3	Me	0.88
4	*p*-methoxyphenyl	1.21
5	*p*-tolyl	1.55
6	Ph	1.44
7	*p*-fluorophenyl	1.25
8	*p*-trifluoromethylphenyl	0.97
9	*m*-nitrophenyl	0.68
10	*o*-tolyl	0.99
11	*m*,*m*-bistrifluoromethylphenyl	0.72
12	*o*-methoxyphenyl	0.06
13	*o*-fluorophenyl	0.17
14	2-furyl	0.15
15	2-thienyl	0.31

Figure 3.5 Correlation between logk_{obs} for MIDA boronate hydrolysis under slow-release conditions, and phosphine substituent nucleofugality parameter, n^f_{PB}. Predicted rate constants for blue data points have been calculated by considering the correlation in the absence of the data corresponding to the substrate of interest. Kinetics of MIDA boronate ester hydrolyses for substrates not in the original publication[46] have been measured by Jorge A. Gonzalez.

Despite the good correlation for a wide range of aryl and alkyl MIDA boronate esters, some substituents fall away from the trend, see Figure 3.5. 2-Heterocyclic and *o*-heteroatom substituted aryl systems show a substantial decrease in reactivity compared to that predicted. One possible explanation for the unexpected kinetic stability of these substrates, could arise from a destabilisation of the transition state, see Scheme 3.4. Burke and Lloyd-Jones have proposed a transition state (under slow-release conditions) involving a concerted

nucleophilic attack of water at boron, and protonation of the MIDA ligand. Thus, suitably positioned lone pairs present on substituents could repulse the incoming water nucleophile, providing a higher energy transition state, and a slower hydrolysis. As such, the correlation in Figure 3.5 not only provides a means to quantitatively predict rates of hydrolysis, it has also allowed the identification of a class of substrates that display unexpected kinetic stability.

3.3.2 Redox reactions at iridium

In addition to testing a substituent nucleofugality parameter (n^f_{PB}), we sought a system that could be rationalised and potentially predicted through use of the ligand nucleofugality parameter (N^F_B). The ligand dependence of the rates of oxidative addition and reductive elimination at iridium(I) and (III) centres have been studied by Collman[47], Kubota[48] and Mays,[49] see Scheme 3.5.

Kubota

$$Ir(CO)XL_2 \xrightarrow[\text{benzene}]{\text{MeI, 25 °C}} Ir(CO)MeXIL_2 \qquad \text{rate} = k[\text{MeI}][\text{Ir(CO)L}_2]$$

L = Ph_3P, (*p*-tolyl)$_3$P, Ph_2MeP, $PhMe_2P$; X = Cl, Br, I

Mays

$$[IrH_2(CO)_2L_2]X + P(OMe)_3 \xrightarrow[CHCl_3]{25\ °C} [Ir(CO)_2L_2P(OMe)_3]X + H_2 \qquad \text{rate} = k_{obs}[IrH_2(CO)_2L_2X]$$

L = Ph_3P, Ph_2MeP, $^iPr_3P$, Cy_3P; X = BPh_4

Scheme 3.5 Conditions for Kubota's oxidative addition of methyl iodide to iridium(I) complexes and for Mays' reductive elimination of dihydrogen from iridium(III) complexes.

Good correlations ($R^2 \geq 0.975$) were found between N^F_B (of the spectator ligands) and the second order rate constants collected by Kubota for a range of iridium complexes (X = Cl, Br and I), see Figure 3.6a. All correlations have negative gradients meaning iridium complexes containing ligands that are poor nucleofuges undergo oxidative addition with methyl iodide faster than those with more nucleofugal ligands. This is as expected, considering the proposed mechanism involves nucleophilic attack at methyl iodide by iridium(I). Interestingly, the correlation also shows that the identity of the X ligands not only influence the absolute rate of oxidative addition, but also impact substantially on the L ligand dependency. For example, in the case of L = Ph_3P, the Cl species provides faster rates than the Br and I analogues, however, based on the gradients obtained, the Cl substituted complex

is predicted to give the slowest rates with L = $PhMe_2P$. Some of the factors that could explain these trends are the relative Ir-X bond lengths and the balance of electron withdrawing and donating capabilities of the X groups. Notably, independent of the nature of X, the N^F_B parameter comes out favourably when compared to the commonly used Tolman electronic parameter, which provides poorer correlations with Kubota's data ($0.610 \leq R^2 \leq 0.837$).

Studies by Mays on the reductive elimination of H_2 from iridium(III) suggest a ligand - $P(OMe)_3$ in this instance- capture of a four-coordinate iridium(I) species is preceded by rate limiting extrusion of H_2, see Scheme 3.5. The resulting first order rate constants show an excellent correlation with the N^F_B values for the spectator ligands, see Figure 3.6b. The positive gradient demonstrates that, when present as ligands on the iridium(III), nucleofugally competent phosphines impart faster rates of reductive elimination relative to their poor nucleofuge counterparts. This can be rationalised considering the ligand's ability to stabilise iridium(I) vs (III). For example, ligands that form kinetically stable adducts with BH_3 also form relatively more stable iridium(III) complexes[z] than ligands that form labile adducts with BH_3. The equations present in Figure 3.6 provide a means to quantitatively predict reaction rates for oxidation and reduction processes of iridum complexes, certainly a long way from the initial borane displacement framework.

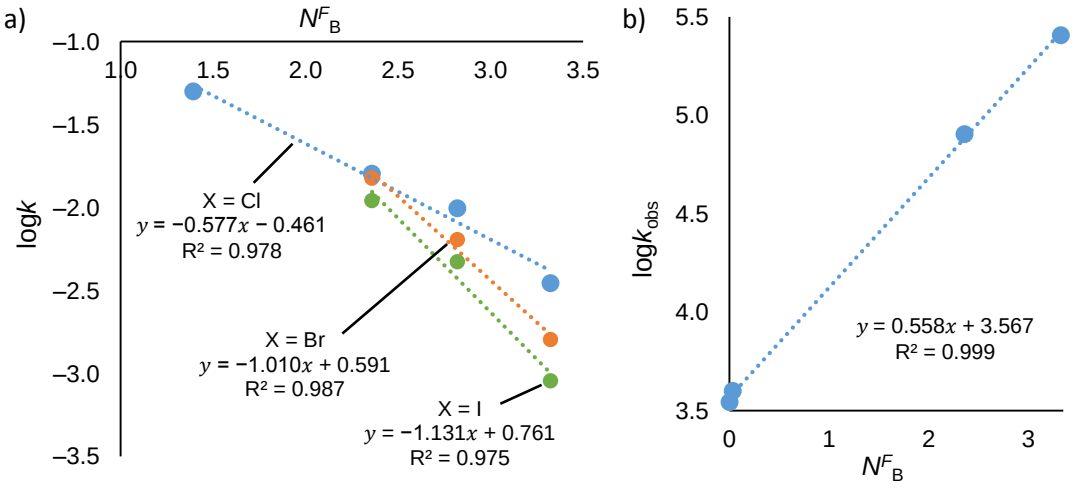

Figure 3.6 a) Correlation between N^F_B and Kubota's rates (log$k$) of oxidative addition of methyl iodide to a variety of iridium complexes. b) Correlation between N^F_B and Mays' rates (logk_{obs}) of reductive elimination of hydrogen from a variety of iridium complexes. For conditions see Scheme 3.5

[z] Relative to iridium(I)

3.4 Summary

A novel nucleofugality LFER (N^F_B) has been developed that is capable of describing a large range of Lewis bases such as phosphines, pyridines and amines. The parameter is referenced to a quinuclidine displacement of a Lewis base borane adduct, in toluene at 30 °C, where all the mechanistic evidence collected is consistent with an S_N2-like process (see Section 2.2.1). Substituent effects for phosphine nucleofuges were found be both independent and additive, allowing the formulation of a separate substituent nucleofugality parameter (n^f_{PB}) that not only quantifies the impact of a substituent on the nucleofugality of the ligand, but also allows prediction/expansion of a wide range of ligand parameter N^F_B values, well beyond those experimentally derived. This additivity model was validated through good agreement between prediction and experiment of a wide range of Lewis base borane displacements, within a factor of three in all cases. A similar additive model was found to work well for amines, thus allowing the development of an additional complementary substituent nucleofugality parameter (n^f_{AB}), which shares the same characteristics as its phosphine counterpart. Finally, the utility of the new parameters was explored through correlation with kinetic data obtained for redox transformations at iridium centres and slow-release hydrolysis of MIDA boronate esters. Through these correlations to the N^F_B or n^f_{PB} scales, quantitative predictions can be made over a striking range of reactivity, and furthermore these correlations have allowed identification of outlier substrates that display unusual kinetic stability and potentially different mechanistic pathways.

3.5 References

[1] P. R. Wells, *Linear Free Energy Relationships*, Academic Press Inc. Ltd., London, **1968**.
[2] J. N. Brönsted, K. Pedersen, *Z. Phys. Chem.* **1924**, *108*, 185–235.
[3] L. P. Hammett, *J. Am. Chem. Soc.* **1937**, *59*, 96–103.
[4] N. B. Chapman, J. Shorter, *Correlation Analysis in Chemistry*, Plenum Press, New York, **1978**.
[5] M. J. Kamlet, R. W. Taft, *Acta Chem. Scand. Ser. B* **1985**, *39*, 611–628.
[6] G. E. Moore, *Int. Electron. Devices Meet.* **1975**, *21*, 11–13.
[7] A. Cherkasov, E. N. Muratov, D. Fourches, A. Varnek, I. I. Baskin, M. Cronin, J. C. Dearden, P. Gramatica, Y. C. Martin, R. Todeschini, V. Consonni, V. E. Kuz'min, R. Cramer, R. Benigni, C. Yang, J. Rathman, L. Terfloth, J. Gasteiger, A. Richard, A. Tropsha, *J. Med. Chem.* **2014**, *57*, 4977–5010.
[8] N. Fey, A. C. Tsipis, S. E. Harris, J. N. Harvey, A. G. Orpen, R. A. Mansson, *Chem. Eur. J.* **2005**, *12*, 291–302.
[9] M. N. Golovin, M. M. Rahman, J. E. Belmonte, W. P. Giering, *Organometallics* **1985**, *4*, 1981–1991.
[10] M. M. Rahman, H. Y. Liu, A. Prock, W. P. Giering, *Organometallics* **1987**, *6*, 650–658.
[11] A. J. Poë, *New J. Chem.* **2013**, *37*, 2957–2964.
[12] C. Babij, A. J. Poë, *J. Phys. Org. Chem.* **2004**, *17*, 162–167.
[13] S. Wold, M. Sjöström, *Acta Chem. Scand. Ser. B* **1986**, *40*, 270–277.
[14] M. Sjöström, S. Wold, *Acta Chem. Scand. Ser. B* **1981**, *35*, 537–554.
[15] T. W. Bentley, *Angew. Chem. Int. Ed.* **2011**, *50*, 3608–3611.
[16] H. C. Brown, Y. Okamoto, *J. Am. Chem. Soc.* **1957**, *79*, 1913–1917.
[17] M. Yoshioka, K. Hamamoto, T. Kubota, *Bull. Chem. Soc. Jpn.* **1962**, *35*, 1723–1728.
[18] Y. Yukawa, Y. Tsuno, *Bull. Chem. Soc. Jpn.* **1959**, *32*, 971–981.
[19] A. R. Katritzky, R. D. Topsom, *J. Chem. Educ.* **1971**, *48*, 427–431.
[20] R. W. Taft Jr., *J. Am. Chem. Soc.* **1952**, *74*, 3120–3128.
[21] C. G. Swain, E. C. Lupton Jr., *J. Am. Chem. Soc.* **1968**, *90*, 4328–4337.
[22] R. G. Pearson, *J. Am. Chem. Soc.* **1963**, *85*, 3533–3539.
[23] J. Miller, A. J. Parker, *J. Am. Chem. Soc.* **1961**, *83*, 117–123.
[24] H. Mayr, M. Patz, *Angew. Chem. Int. Ed.* **1994**, *33*, 938–957.
[25] H. Mayr, *Tetrahedron* **2015**, *71*, 5095–5111.
[26] For an up to date collection of Mayr's *N* and *E* values see the database, available at: www.cup.lmu.de/oc/mayr/reaktionsdatenbank
[27] C. G. Swain, C. B. Scott, *J. Am. Chem. Soc.* **1953**, *75*, 141–147.
[28] R. G. Pearson, H. Sobel, J. Songstad, *J. Am. Chem. Soc.* **1968**, *90*, 319–326.
[29] C. P. Speans, S.-I. Kang, N. G. Kundu, T. Shammaa, G. A. Olaha, *Curr. Top. Med. Chem.* **1997**, *2*, 85–100.
[30] P. E. Dietze, W. P. Jencks, *J. Am. Chem. Soc.* **1986**, *108*, 4549–4555.
[31] C. D. Ritchie, P. O. I. Virtanen, *J. Am. Chem. Soc.* **1972**, *94*, 4966–4971.
[32] J. O. Edwards, *J. Am. Chem. Soc.* **1954**, *76*, 1540–1547.
[33] T. W. Bentley, I. Sun, *Arkivoc* **2012**, *2012*, 25–34.
[34] J. P. Richard, T. L. Amyes, D. J. Rice, *J. Am. Chem. Soc.* **1993**, *115*, 2523–2524.
[35] N. Streidl, B. Denegri, O. Kronja, H. Mayr, *Acc. Chem. Res.* **2010**, *43*, 1537–1549.
[36] B. Denegri, A. Streiter, S. Jurić, A. R. Ofial, O. Kronja, H. Mayr, *Chem. Eur. J.* **2006**, *12*, 1648–1656.
[37] C. J. M. Stirling, *Acc. Chem. Res.* **1979**, *12*, 198–203.

[38] M. B. Smith, J. March, *March's Advanced Organic Chemistry*, John Wiley & Sons, Inc., Hoboken, New Jersey, **2007**.
[39] D. R. Marshall, P. J. Thomas, C. J. M. Stirling, *J. Chem. Soc., Perkin Trans. 2* **1977**, 1898–1909.
[40] C. A. Tolman, *J. Am. Chem. Soc.* **1970**, *92*, 2953–2956.
[41] T. Reetz, *J. Am. Chem. Soc.* **1960**, *82*, 5039–5042
[42] F. Baitalow, J. Baumann, G. Wolf, K. Jaenicke-Rößler, G. Leitner, *Thermochim. Acta* **2002**, *391*, 159–168.
[43] C. W. Hamilton, R. T. Baker, A. Staubitz, I. Manners, *Chem. Soc. Rev.* **2009**, *38*, 279–93.
[44] A. J. J. Lennox, G. C. Lloyd-Jones, *Chem. Soc. Rev.* **2014**, *43*, 412–443.
[45] G. R. Dick, E. M. Woerly, M. D. Burke, *Angew. Chem. Int. Ed.* **2012**, *51*, 2667–2672.
[46] J. A. Gonzalez, O. M. Ogba, G. F. Morehouse, M. J. Schmidt, K. N. Houk, A. G. Leach, P. H.-Y. Cheong, M. D. Burke, G. C. Lloyd-Jones, *Nat. Chem.* **2016**, *accepted*.
[47] J. P. Collman, M. Kubota, F. D. Vastine, J. Y. Sun, J. W. Kang, *J. Am. Chem. Soc.* **1968**, *90*, 5430–5437.
[48] M. Kubota, G. W. Kiefer, R. M. Ishikawa, K. E. Bencala, *Inorg. Chim. Acta* **1973**, *7*, 195–202.
[49] M. J. Mays, R. N. F. Simpson, F. P. Stefanini, *J. Chem. Soc. A* **1970**, 3000–3002.

4 Conclusions and Future Work

4.1 Phosphine borane deprotection

Mechanistic studies into the amine deprotection of phosphine borane complexes have been performed. Both the kinetic data and crossover experiments carried out are consistent with an associative mechanism for the deprotection of $Ph_3P{\cdot}BH_3$, **1**, and $(o\text{-tolyl})_3P{\cdot}BH_3$, **10** (quinuclidine **2**, toluene, 30 °C). Eyring analysis using $Ph_3P{\cdot}BH_3$ provided further evidence for an associative process ($\Delta S^{\ddagger}$ = negative) when either quinuclidine, morpholine or triethylamine were used as the deprotecting agent. Computational studies showed that an S_N2 transition state was reasonable, with good agreement between experimental and computed activation energies, see Scheme 4.1. Notably, the evidence amassed precludes a dissociative mechanism from being dominant, disproving some existing speculation.[1,2]

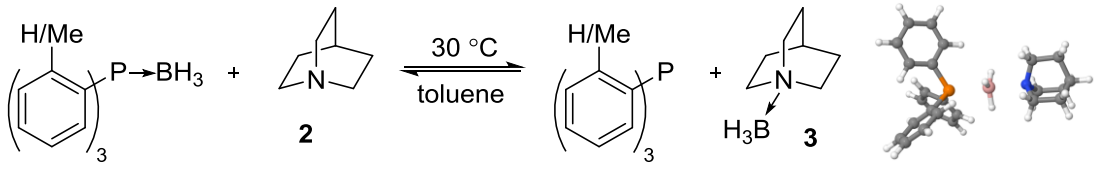

$$\text{rate} = k([R_3P \cdot BH_3][R'_3N] - [R'_3N \cdot BH_3][R_3P]/K)$$

$\Delta G^{\ddagger}_{calc}$ = 18 kcal mol^{-1}

$\Delta G^{\ddagger}_{expt}$ = 21 kcal mol^{-1}

Scheme 4.1 Model system used to study the mechanism of phosphine borane deprotection.

Structure-activity relationships have been carried out for several components of the reaction mixture, including the effect of the amine, solvent and phosphine on the kinetics and thermodynamics of the deprotection. Cyclic and bridgehead amines were found to provide advantages in terms of both rate and favourability compared to their acylic counterparts. DABCO remains[3] a competent and relatively cost effective reagent for deprotection, particularly for phosphine borane complexes difficult to deprotect. Volatile amines (such as Et_2NH), although typically lacking the efficacy of DABCO, provide a synthetic advantage in that they can readily be removed from the reaction mixture at reduced pressures, which is especially useful if the corresponding amine borane adduct is also volatile. Notably, pyrrolidine, which offers the same volatility advantage, was found to possess a substantial increase in kinetic and thermodynamic reactivity compared with Et_2NH. Through correlation with the Dimroth-Reichardt parameter, E_T^N, the solvent effect on the rate of deprotection was quantified. Poor ion-stabilising solvents, such as toluene, gave faster reaction rates than competent ion-stabilising solvents such as DMSO. Thus, for the fastest deprotections, and if the thermal integrity of the phosphine product is not a problem, bridgehead amines such as DABCO should be used in combination with high boiling poor ion-stabilising solvents, such as xylene. Solvents capable of acting as hydrogen-bond donors were found to retard the rate

of deprotection to a greater extent than was predicted based on the correlation with Dimroth-Reichardt's E_T^N. This was as a result of a hydrogen-bond interaction with the amine,[4] thus effectively reducing the concentration of the active species present.

An in-depth structure activity relationship analysing the effect of the phosphine identity on the kinetics of quinuclidine deprotection was carried out. A good correlation with Hammett's σ was found ($R^2 = 0.99$) with positive ρ value indicating that electron deficient phosphines undergo deprotection faster than their electron rich counterparts, consistent with the phosphine acting as a leaving group in an S_N2-like process. The presence of steric bulk in the *o*-position of aryl phosphine borane complexes was found to provide a rate enhancement relative to unsubstituted systems, likely arising from ground state destabilisation through weakening of the P-B interaction. When present in place of aryl groups, alkyl substituents on phosphines were found to retard the deprotection both kinetically and thermodynamically, consistent with greater induction. Across the series $Cy_nPh_{3-n}P{\cdot}BH_3$ a progressive attenuation in both *k* and *K* was found, approximately 10 fold for each increase in *n* (*n* = 0 - 3). That this factor remained constant suggested that each type of substituent contributed a fixed amount to the nucleofugality of the phosphine, and did so independently of the other substituents. This effect was found for a range of alkyl (^{t}Bu, Cy, Me, ^{i}Pr) and aryl (*p*-methoxyphenyl, *o*-methoxyphenyl, *o*-tolyl) substituents with each affording a regular change in *k* relative to Ph. Studies with $^tBu_3P{\cdot}BH_3$ suggested that the trends in amine reactivity discussed above (with $Ph_3P{\cdot}BH_3$) are replicated for phosphines that are both kinetically and thermodynamically more resistant to amine deprotection. As such, alkyl rich phosphines require deprotection conditions involving a large excess of cyclic amine (acyclic amines are neither kinetically nor thermodynamically competent) and high temperatures, in order to obtain reactions on a reasonable timescale. Given the wide span in reactivity (> 10^5), aryl rich phosphine borane complexes can be deprotected using far less forcing conditions allowing for the advantages afforded by volatile amines to be exploited.

In addition to amine deprotection, the mechanism of ethanolysis of $(o\text{-tolyl})_3P{\cdot}BH_3$, **10**, has been studied, with a range of kinetic evidence supporting an initial BH_3 transfer to ethanol. Whilst this process does liberate the free phosphine, and as such deprotects the phosphine borane complex, the fate of the borane group is not as straightforward. NMR evidence suggests that an $(EtO)_2BH$ intermediate is produced, but its consumption was found to be highly irreproducible. Further investigation into the cause of this is required as unreliable rates of hydrogen evolution can cause serious safety concerns, especially at the elevated temperatures required for these reactions.

Whilst the kinetic and thermodynamic data obtained in this study provide guidelines on conditions for amine deprotection, further work needs to be done in order to answer the question: "what are the best conditions for the deprotection of phosphine borane complex A?" Given that the proposed alocholysis and amine deprotection mechanisms both involve a phosphine acting as a nucleofuge, it might be expected that both processes follow the same trends in relative reactivity. Therefore, in order to answer the above question, and especially for the phosphine borane complexes that are difficult to deprotect with amines, an understanding of the acid-mediated deprotection is required alongside further investigation into the alcoholysis.

4.2 Nucleofugality parameters

A new parameter (N^F_B) was developed using single-term LFER Equation 4.1, which quantifies the nucleofugality of a range of Lewis bases. The reference system (defining $\rho = 1$) was based on the second order rate constants (k) for quinuclidine displacements of Lewis bases from their corresponding borane adduct in toluene at 30 °C, see Scheme 4.2.

$$\log\frac{k_X}{k_0} = \rho\, N^F_B \qquad (4.1)$$

The reference Lewis base (defining k_0) was taken as $^iPr_3P$, which was experimentally observed to have the smallest k of the Lewis bases studied. The independent and additive substituent effects for phosphines in these borane displacement reactions allowed the nucleofugal influence of each substituent to be quantified, see Equation 4.2. Using this in combination with Equation 4.1, a parallel substituent nucleofugality parameter (n^f_{PB}) has been described. Notably, the use of Equation 4.2 allows predictions of N^F_B to be made for a range of phosphines comprised of substituents whose n^f_{PB} values are known, thus substantially expanding the scope of phosphines described beyond those which were experimentally derived.

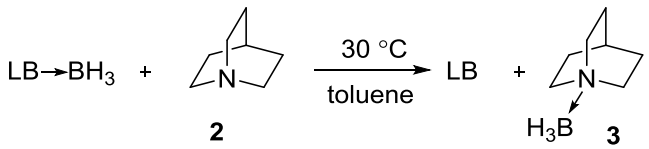

Scheme 4.2 System used to define $\rho = 1$ for nucleofugality parameter N^F_B as described by Equation 4.1. LB = Lewis Base.

The predictive power of Equation 4.2 has been tested through kinetic investigation of borane displacements for Lewis bases not present in the training set. Good agreement was found between the predicted and experimental *k* values, even when using different amines (i.e. not quinuclidine, **2**). In order to obtain predictions for values of *k* in non-reference conditions, a correction for the relative nucleophilicity of the different amines was applied. This was determined using relative rates of $Ph_3P{\cdot}BH_3$ deprotection as a benchmark, i.e. k_{rel} in Table 2.1, and thus collectively, data in Tables 2.1 and 3.2 provide a quantitative prediction of *k* for over ten thousand phosphine borane deprotections.

$$N_B^F(PR_1R_2R_3) = n_{PB}^f(R_1) + n_{PB}^f(R_2) + n_{PB}^f(R_3) \quad (4.2)$$

Expansion of the N^F_B parameter to incorporate a range of *N*-donor ligands was achieved through kinetic analysis of borane transfer reactions from a range of pyridine and aliphatic amine borane adducts. This extension means the N^F_B parameter provides direct and quantitative comparison of the nucleofugality of a range of phosphines and amines. Good correlations found between Hammett's σ and N^F_B for both triarylphosphines and substituted-pyridines have allowed a further means to predict N^F_B and n^f_{PB} values. The predictive power of this correlation was tested using the kinetics of a di-substituted pyridine borane adduct, not included in the original training set, under reference reaction conditions.

Additive and independent substituent effects, as found for phosphines, were also observed for aliphatic amines and confirmed through kinetic studies on the series $Me_{3-n}Et_nN{\cdot}BH_3$ (n = 0 - 3). Thus, Equation 4.3 was developed, defining a new substituent nucleofugality parameter for amines n^f_{AB}, analogous to that for phosphines (n^f_{PB}). Through *in situ* generation and reaction of a range of amine borane adducts, and using Equations 4.1 and 4.3, a wide range of ligand (N^F_B) and substituent nucleofugality parameter (n^f_{AB}) values were generated for amines. The resulting correlation between $\log(k_X/k_0)$ and N^F_B (i.e. Equation 4.1) is shown in Figure 4.1, the high R^2 values obtained validate the treatment of both phosphine and amine substituent effects as additive.

$$N_B^F(NR_1R_2R_3) = n_{AB}^f(R_1) + n_{AB}^f(R_2) + n_{AB}^f(R_3) \quad (4.3)$$

Correlation of n^f_{PB} to the rate of both alkyl and aryl MIDA boronate ester hydrolysis under slow-release conditions[5] has demonstrated the applicability of the parameter well outside of borane transfer reactions. Not only has this correlation (see Figure 3.5) allowed for quantitative predictions of hydrolysis rates for substrates not yet determined, it has also highlighted substrates that display unusual kinetic stability.

The utility of N^F_B has been demonstrated through correlations with experimental data collected by Kubota[6,7] and Mays[8] on the ligand dependence of the kinetics of oxidative addition and reductive elimination of iridium complexes. For both data sets, the correlations allows quantitative predictions to be made for ligands outside the set examined, providing a means to *a priori* tailored reaction rates. The correlation with Kubota's oxidative addition data also highlights an interesting X ligand effect (X = Cl^-, Br^-, I^-), which after extrapolation provides an N^F_B value (and thus a suitable ligand) that should render two iridium complexes with different X ligands isokinetic.

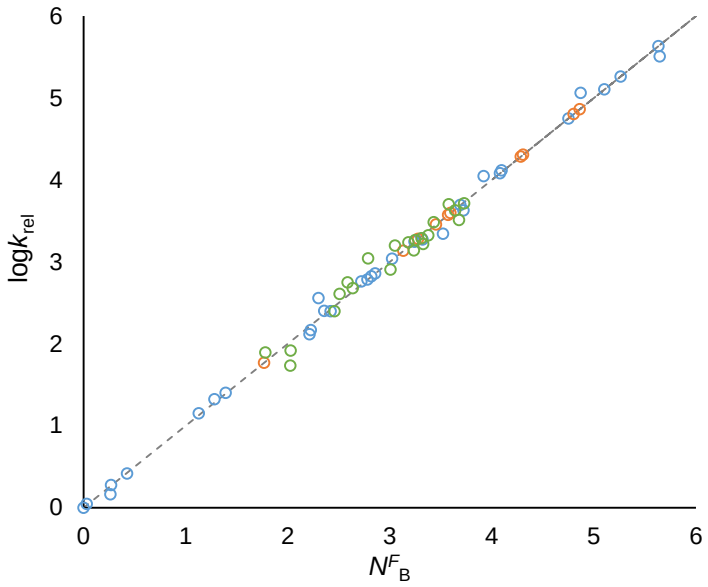

Figure 4.1 Correlation between logk_{rel} (relative to ^{i}Pr$_3$P) and N^F_B for phosphines (blue, R^2 = 0.998), pyridines (orange, R^2 = 1, by definition) and amines (green R^2 = 0.953). Dashed line corresponds to ρ = 1.

As with any parameter, the scope of N^F_B could be expanded through incorporation of more Lewis bases into the data set. Aside from providing a basis for discussion and *a priori* information about a given experiment, the inclusion of more Lewis bases would broaden the utility of the parameter, increasing the number of reactions that the parameter could be correlated with. The situation for n^f_{PB} and n^f_{AB} however, is somewhat more complicated. Due to the nature of the regression analysis used to determine these values, the incorporation of more phosphines and amines into the data set could ultimately provide a range of n^f_{PB} and n^f_{AB} values which are different to those obtained with the current training set. Whilst this could result in a potentially confusing scenario where multiple sets of the same parameter exist, with a discerning selection of the data allowed to affect these values, a more complete description of the nucleofugal influence of a substituent may be obtained. Obviously, there is

a balance to be struck between the completeness of the training set and the level of accuracy one can expect from predictive models. There is great deal of potential to test the utility of all of the parameters developed (N^F_B, n^f_{PB} and n^f_{AB}) through correlation and ultimately prediction of reactivity in a host of chemical systems.

Aside from testing and broadening the scope of the nucleofugality parameters with experimentally derived data, obtaining an understanding of the more fundamental factors that underpin 'leaving group ability' is also of interest. Using computational tools in concert with principle component analysis may provide not only a greater understanding of the nucleofugality of Lewis bases from borane adducts, but may also provide insight into the reactions that the nucleofugality parameters are shown to correlate with. Moreover, if computational studies can adequately describe the nucleofugality parameters, *in silico* predictions of N^F_B, n^f_{PB} or/and n^f_{AB} values can be made. As well as increasing the scope of the parameter dramatically, these *in silico* predictions might ultimately be able to quantitatively predict rate constants for a wide range of processes, leaving the nucleofugality parameters redundant. Until these calculations, if found to be feasible, are both accessible and inexpensive, there remains a need for such empirical derived parameters as described within.

4.3 References

[1] M. Ohff, J. Holz, M. Quirmbach, A. Börner, *Synthesis* **1998**, *10*, 1391–1415.

[2] N. Brodie, S. Jugé, *Inorg. Chem.* **1998**, *37*, 2438–2442.

[3] H. Brisset, Y. Gourdel, P. Pellon, M. Le Corre, *Tetrahedron Lett.* **1993**, *34*, 4523–4526.

[4] A. Maliniak, J. Kowalewski, *J. Phys. Chem.* **1986**, *90*, 6330–6334.

[5] J. A. Gonzalez, O. M. Ogba, G. F. Morehouse, M. J. Schmidt, K. N. Houk, A. G. Leach, P. H.-Y. Cheong, M. D. Burke, G. C. Lloyd-Jones, *Nat. Chem.***2016**, *accepted*.

[6] J. P. Collman, M. Kubota, F. D. Vastine, J. Y. Sun, J. W. Kang, *J. Am. Chem. Soc.* **1968**, *90*, 5430–5437.

[7] M. Kubota, G. W. Kiefer, R. M. Ishikawa, K. E. Bencala, *Inorg. Chim. Acta* **1973**, *7*, 195–202.

[8] M. J. Mays, R. N. F. Simpson, F. P. Stefanini, *J. Chem. Soc. A* **1970**, 3000–3002.

5 Experimental

5.1 General experimental details

All starting materials were obtained from commercial sources (*Sigma-Aldrich* or *Alfa Aesar*) and used without purification. ^{1}H, ^{11}B, ^{13}C and ^{31}P spectra were recorded on JEOL GX 300, Eclipse 300, Varian 400, Bruker Ascend 400 or 500 spectrometers. ^{1}H and ^{13}C spectra collected in deuterated solvent were referenced to residual protonated signal (e.g. $CHCl_3$ in $CDCl_3$). ^{11}B and ^{31}P spectra in $CDCl_3$ were externally referenced, whereas ^{11}B, ^{31}P and ^{13}C NMR spectra recorded in non-deuterated solvent (for kinetic analysis) were not referenced. Spectral processing and analysis was carried out using MestreNova versions 6 and 9. ^{1}H-^{1}H and ^{13}C-^{31}P coupling constants (*J*) are reported to the nearest 0.1 Hz. Where reported, the phosphorus boron coupling constants (measured to the nearest 1 Hz) were measured in the $^{11}B\{^{1}H\}$ spectra. The peak attributed to phosphine borane complexes in $^{31}P\{^{1}H\}$ NMR was found to be very broad, the quartet/sextet expected from coupling to $^{11}B/^{10}B$ nuclei was not well resolved. The following abbreviations are used to describe multiplicities: s (singlet), d (doublet), t (triplet), q (quartet), m (multiplet), app. (apparent) and b (broad). NMR tubes used to record spectra were made from either borosilicate glass or Natural Quartz (*GPE Scientific Limited*). Temperature precision and control on each NMR spectrometer used in this study is difficult to estimate, however, for relatively low temperatures (30 °C) an error of ±3 °C is seen as a maximum.

IR spectra were recorded in the range 4000-600 cm^{-1} using a *Bruker Platinum ATR Quicksnap™* attachment (diamond cell) on a *Bruker Alpha FT-IR Spectrometer*. Measuring points were measured *using Stuart Digital SMP10* apparatus in open capillaries. Mass spectra were recorded by the University of Edinburgh mass spectrometry service by electrospray ionisation (ESI) using a *Bruker micrOTOF II* spectrometer.

Kinetic simulations were performed using Dynochem 2011 v4.

X-ray measurements were made on crystals coated in high-vacuum grease and mounted on a glass pin using a Bruker Smart CCD area-detector diffractometer with either Mo or Cu anode X-ray source at 100.0 K. Details of data analysis are provided in the appendix.

Dry solvents were obtained by passing solvent through a column of anhydrous alumina using either an *Anhydrous Engineering* Grubbs-type system or a PPT/Glass Contour Grubbs-type system. Strauss flasks fitted with J. Youngs valves were used to collect and freeze-pump-thaw degas anhydrous solvent. Solvents that required degassing were subjected to three cycles of freeze-pump-thawing. Commercial grade solvents were used. Deuterated solvents for NMR analysis were purchased from *Sigma-Aldrich*.

All reactions involving the use of air and moisture sensitive materials were performed under an atmosphere of dry nitrogen using standard Schlenk techniques on a vacuum line attached to a double manifold equipped with an oil pump (0.4 torr). Glassware necessary for these manipulations were previously oven dried (200 °C) and allowed to cool under vacuum (0.4 torr, oil pump). Exceptions to this include NMR tubes and volumetric flasks (fitted with a J. Youngs valve) which were not oven dried, but dried under vacuum. The removal of solvents *in vacuo* was achieved using a rotary evaporator (with a water bath at temperatures up to 40 °C), or at 0.4 torr on a vacuum line at room temperature. Any manipulations involving use of borane dimethyl sulfide were always confined to a fumehood.

5.2 Lewis base borane adduct preparation

Triphenylphosphine borane complex, 1

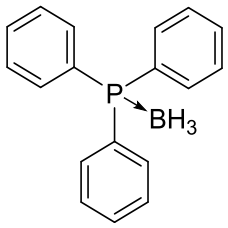

To a solution of triphenylphosphine (1.50 g, 5.72 mmol) in dry dichloromethane (10 mL), borane dimethylsulfide complex (5.5 mL, 57 mmol) was added under an atmosphere of nitrogen. After stirring for 22 hours at room temperature, a saturated aqueous NH_4Cl solution (10 mL) was added and the reaction was stirred for a further 2 hours. A significant amount of effervescence was observed during this period, and consequently the vessel was opened to prevent an accumulation of pressure. The reaction mixture was poured onto water (50 mL) and then extracted into dichloromethane (3 x 50 mL). The combined organics were washed with a saturated aqueous $NaHCO_3$ solution (50 mL), dried over $MgSO_4$, filtered, and the solvent was removed *in vacuo* to afford a white solid. This was redissolved in dichloromethane and filtered through silica, eluting with dichloromethane. Removal of solvent *in vacuo* gave phosphine borane complex **1** as a white solid (1.52 g, 96% yield). **^{1}H NMR** (300 MHz, $CDCl_3$) δ = 7.60-7.40 (m, 15H), 1.76-0.80 (br, q (*unresolved*), 3H); **^{13}C{^{1}H} NMR** (100 MHz, $CDCl_3$) δ = 133.4 (d, $J_{C\text{-}P}$ 9.8 Hz), 131.4 (d, $J_{C\text{-}P}$ 2.3 Hz), 129.3 (d, $J_{C\text{-}P}$ 57.9 Hz), 128.9 (d, $J_{C\text{-}P}$ 10.0 Hz); **^{11}B{^{1}H} NMR** (96 MHz, $CDCl_3$) δ = −39.2 (br d, $^{1}J_{B\text{-}P}$ 52 Hz); **^{31}P{^{1}H} NMR** (162 MHz, $CDCl_3$) δ = 20.7 (br, app. d).

Data are in accordance with that previously reported.[1]

Quinuclidine borane complex, 3

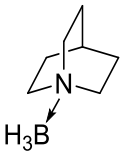

To a solution of quinuclidine (0.111 g, 0.994 mmol) in dry dichloromethane (2 mL), borane dimethylsulfide complex (0.95 mL, 10 mmol) was added under an atmosphere of nitrogen. After stirring for 3 hours at room temperature, a saturated NH_4Cl solution (10 mL) was added and the reaction was stirred for a further 1.5 hours. A significant amount of effervescence was observed during this period, and consequently the vessel was opened to prevent an accumulation of pressure. The reaction mixture was poured onto water (10 mL) and extracted into dichloromethane (3 x 15 mL). The combined organics were washed with a saturated aqueous $NaHCO_3$ solution (30 mL), dried over $MgSO_4$, filtered, and the solvent was removed *in vacuo* to afford a white solid. This was redissolved in dichloromethane and filtered through silica, eluting with dichloromethane. Removal of solvent *in vacuo* gave the amine borane complex **3** as a white solid (0.107 g, 86% yield). **^{1}H NMR** (400 MHz, $CDCl_3$) δ = 3.03-2.99 (m, 6H), 2.00 (septet, $^1J_{H\text{-}H}$ 3.2 Hz, 1H), 1.77-1.72 (m, 6H see below), 1.81-1.11 (br, q, 3H see below); **^{13}C{^{1}H} NMR** (125 MHz, $CDCl_3$) δ = 53.6 (s), 25.3 (s), 20.4 (s); **^{11}B{^{1}H} NMR** (128 MHz, $CDCl_3$) δ = −12.1 (s).

The two multiplets highlighted above in the ^{1}H NMR spectra (1.77-1.72 and 1.81-1.11 ppm) overlap, the total area (1.77-1.11 ppm) integrates to 9H. The broad quartet at 1.81-1.11 ppm is attributed to the BH_3, and consequently assumed to correspond to 3H.

Data are in accordance with that previously reported.[2]

Tris(*p*-chlorophenyl)phosphine borane complex, 4

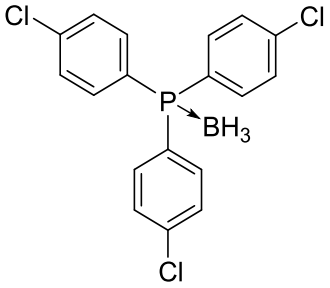

To a solution of tris(*p*-chlorophenyl)phosphine (0.344 g, 0.942 mmol) in dry dichloromethane (3 mL), borane dimethylsulfide complex (0.9 mL, 9.42 mmol) was added under an atmosphere of nitrogen. After stirring for 20 hours at room temperature, a saturated aqueous NH_4Cl solution (5 mL) was added and the reaction was stirred for a further 3 hours. A significant amount of effervescence was observed during this period, and consequently the vessel was opened to prevent an accumulation of pressure. The reaction mixture was poured onto water (50 mL) and then extracted into dichloromethane (3 x 50 mL). The combined organics were washed with a saturated aqueous $NaHCO_3$ solution (50 mL), dried over $MgSO_4$, filtered, and the solvent was removed *in vacuo* to afford a white solid. This was redissolved in

dichloromethane and filtered through silica, eluting with dichloromethane. Removal of solvent *in vacuo* gave phosphine borane complex **4** as a white solid (0.297 g, 83% yield). **m.p.** (sample recrystallized from toluene) 137-139 °C; **^{1}H NMR** (400 MHz, $CDCl_3$) δ = 7.51-7.43 (m, 12H), 1.54-0.83 (br, q (*unresolved*), 3H); **^{13}C{^{1}H} NMR** (125 MHz, $CDCl_3$) δ = 138.6 (d, $J_{C\text{-}P}$ 2.9 Hz), 134.5 (d, $J_{C\text{-}P}$ 10.7 Hz), 129.5 (d, $J_{C\text{-}P}$ 10.8 Hz), 127.0 (d, $J_{C\text{-}P}$ 58.6 Hz); **^{11}B{^{1}H} NMR** (128 MHz, $CDCl_3$) δ = −38.1 (br, app. s); **^{31}P{^{1}H} NMR** (162 MHz, $CDCl_3$) δ = 20.3 (br, app. d); **IR** (solid, intense peaks only, cm^{-1}) ν =, 2399, 2371, 1574, 1562, 1479, 1388, 1084, 1068, 1012, 818, 761, 744, 641, 616, 556; **MS** (ESI): m/z (%) 781 (M_2Na^+), 403 (MNa^+); **HRMS** (ESI) calculated: $C_{18}H_{15}{}^{11}B_1{}^{35}Cl_3{}^{23}Na_1P_1$ 400.9962, found: 400.9969.

Tris(*p*-trifluoromethylphenyl)phosphine borane complex, 5

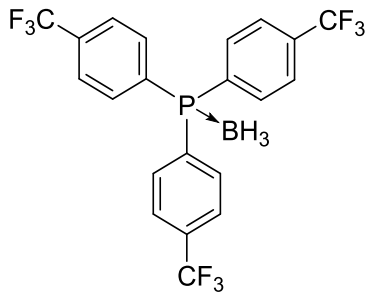

To a solution of tris(*p*-trifluoromethylphenyl)phosphine (0.43 g, 0.92 mmol) in dry dichloromethane (6 mL), borane dimethylsulfide complex (1 mL, 11 mmol) was added under an atmosphere of nitrogen. After stirring for 14 hours at room temperature, water (10 mL) was added and the reaction was stirred at ambient temperature for a further 2 hours. A significant amount of effervescence was observed during this period, and consequently the vessel was opened to prevent an accumulation of pressure. The reaction mixture was poured onto water (10 mL) and then extracted into dichloromethane (3 x 20 mL). The combined organics were washed with a saturated aqueous $NaHCO_3$ solution (20 mL), dried over $MgSO_4$, filtered, and the solvent was removed *in vacuo* to afford a white solid. This was redissolved in dichloromethane and filtered through silica, eluting with dichloromethane. Removal of solvent *in vacuo* gave phosphine borane complex **5** as a white solid (0.34 g, 78% yield). **m.p.** (sample crystallized *via* vapour diffusion dichloromethane/hexane) 163-164 °C; **^{1}H NMR** (400 MHz, $CDCl_3$) δ = 7.78-7.70 (m, 12H), 1.67-0.86 (br, q (*unresolved*), 3H); **^{13}C{^{1}H} NMR** (100 MHz, $CDCl_3$) δ = 134.1 (dd, $J_{C\text{-}F}$ 33.0 Hz, $J_{C\text{-}P}$ 2.4 Hz), 133.8 (d, J 10.2 Hz), 132.3 (d, $J_{C\text{-}P}$ 52.5 Hz), 126.2 (dd, J 10.5 Hz, J 3.7 Hz), 123.5 (qd, $J_{C\text{-}F}$ 272.8 Hz, $J_{C\text{-}P}$ 1 Hz); **^{11}B{^{1}H} NMR** (128 MHz, $CDCl_3$) δ = −39.2 (br, app. s); **^{31}P{^{1}H} NMR** (162 MHz, $CDCl_3$) δ = 23.3 (br, app. d); **^{19}F NMR** (376 MHz, $CDCl_3$) δ = −63.0 (s); **IR** (solid, intense peaks only, cm^{-1}) ν = 2381, 1399, 1318, 1261, 1166, 122, 1106, 1059, 1015, 961, 834, 791, 748, 724, 713, 700, 641, 613, 597, 561, 521; **MS**

(ESI): m/z (%) 503 (MNa^+); **HRMS** (ESI) calculated: $C_{21}H_{15}{}^{11}B_1F_9{}^{23}Na_1P_1$ 503.07529, found: 503.07750.

Tris(*p*-methoxyphenyl)phosphine borane complex, 6

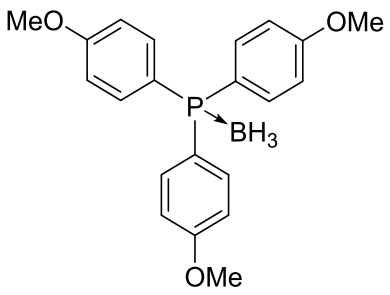

To a solution of tris(*p*-methoyphenyl)phosphine (0.31 g, 0.87 mmol) in dry dichloromethane (2 mL), borane dimethylsulfide complex (0.8 mL, 8.4 mmol) was added under an atmosphere of nitrogen. After stirring for 20 hours at room temperature, a saturated aqueous NH_4Cl (5 mL) solution was added and the reaction was stirred at ambient temperature for a further 2 hours. A significant amount of effervescence was observed during this period, and consequently the vessel was opened to prevent an accumulation of pressure. The reaction mixture was poured onto water (20 mL) and then extracted into dichloromethane (3 x 20 mL). The combined organics were washed with a saturated aqueous $NaHCO_3$ solution (20 mL), dried over $MgSO_4$, filtered, and the solvent was removed *in vacuo* to afford a white solid. This was redissolved in dichloromethane and filtered through silica, eluting with dichloromethane. Removal of solvent *in vacuo* gave phosphine borane complex **6** as a white solid (0.25 g, 80% yield). **m.p.** (sample crystallized *via* vapour diffusion dichloromethane/hexane) 146-147 °C; **^{1}H NMR** (400 MHz, $CDCl_3$) δ = 7.48 (dd, $J_{H\text{-}P}$ 10.4 Hz, $J_{H\text{-}H}$ 8.8 Hz, 6H), 6.94 (dd, $J_{H\text{-}H}$ 8.8 Hz, $J_{H\text{-}P}$ 1.7 Hz, 6H), 3.83 (s, 9H), 1.54-0.86 (br, q (*unresolved*), 3H); **^{13}C{^{1}H} NMR** (100 MHz, $CDCl_3$) δ = 162.0 (d, $J_{C\text{-}P}$ 2.4 Hz), 134.8 (d, $J_{C\text{-}P}$ 10.8 Hz), 120.9 (d, $J_{C\text{-}P}$ 63.4 Hz), 114.5 (d, $J_{C\text{-}P}$ 11.0 Hz), 55.5 (s); **^{11}B{^{1}H} NMR** (96 MHz, $CDCl_3$) δ = −38.7 (br, app. s); **^{31}P{^{1}H} NMR** (121 MHz, $CDCl_3$) δ = 17.0 (br, app. d); **IR** (solid, intense peaks only, cm^{-1}) ν = 2960, 2835, 2365, 2359, 2337, 1595, 1569, 1498, 1455, 1437, 1406, 1308, 1290, 1250, 1178, 1136, 1107, 1060, 1024, 827, 799, 748, 717, 657, 643, 625, 584; **MS** (ESI): m/z (%) 747 (M_2Na^+), 389 (MNa^+); **HRMS** (ESI) calculated: $C_{21}H_{24}O_3{}^{11}B_1{}^{23}Na_1P_1$ 389.14483, found: 38914550.

Tris(*p*-tolyl)phosphine borane complex, 7

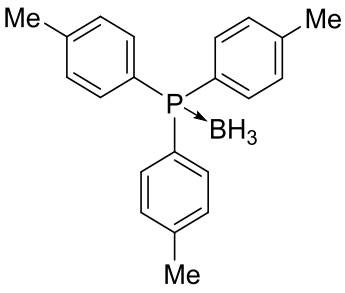

To a solution of tris(*p*-tolyl)phosphine (0.42 g, 1.4 mmol) in dry dichloromethane (3 mL), borane dimethylsulfide complex (1.1 mL, 11.6 mmol) was added under an atmosphere of nitrogen. After stirring for 24 hours at room temperature, a saturated aqueous NH_4Cl (10 mL) solution

was added and the reaction was stirred at ambient temperature for a further 2 hours. A significant amount of effervescence was observed during this period, and consequently the vessel was opened to prevent an accumulation of pressure. The reaction mixture was poured onto water (20 mL) and then extracted into dichloromethane (3 x 20 mL). The combined organics were washed with a saturated aqueous $NaHCO_3$ solution (20 mL), dried over $MgSO_4$, filtered, and the solvent was removed *in vacuo* to afford a white solid. This was redissolved in dichloromethane and filtered through silica, eluting with dichloromethane. Removal of solvent *in vacuo* gave phosphine borane complex **7** as a white solid (0.30 g, 83% yield). **m.p.** (sample crystallized *via* vapour diffusion dichloromethane/hexane) 217-218 °C; **^{1}H NMR** (400 MHz, $CDCl_3$) δ = 7.45 (dd, $J_{H\text{-}P}$ 10.7 Hz, $J_{H\text{-}H}$ 8.1 Hz, 6H), 7.23 (d, $J_{H\text{-}H}$ 8.1 Hz, 6H), 2.38 (s, 3H), 1.55-0.87 (br, q (*unresolved*), 3H); **^{13}C{^{1}H} NMR** (100 MHz, $CDCl_3$) δ = 141.6 (d, $J_{C\text{-}P}$ 2.6 Hz), 133.2 (d, $J_{C\text{-}P}$ 9.9 Hz), 129.6 (d, $J_{C\text{-}P}$ 10.6 Hz), 126.3 (d, $J_{C\text{-}P}$ 59.9 Hz), 21.6 (d, $J_{C\text{-}P}$ 1.0 Hz); **^{11}B{^{1}H} NMR** (96 MHz, $CDCl_3$) δ = −38.7 (br, d, $J_{B\text{-}P}$ 45 Hz); **^{31}P{^{1}H} NMR** (121 MHz, $CDCl_3$) δ = 19.0 (br, app. d); **IR** (solid, intense peaks only, cm^{-1}) ν = 2373, 2340, 1598, 1497, 1444, 1396, 1310, 1188, 1135, 1105, 1064, 1020, 848, 810, 753, 707, 662, 642, 630, 575; **MS** (ESI): m/z (%) 659 (M_2Na^+), 341 (MNa^+), 317 ($[M\text{-}H]^+$); **HRMS** (ESI) calculated: $C_{21}H_{24}{}^{11}B_1{}^{23}Na_1P_1$ 341.16009, found: 341.16070.

Tris(*m*-tolyl)phosphine borane complex, 8

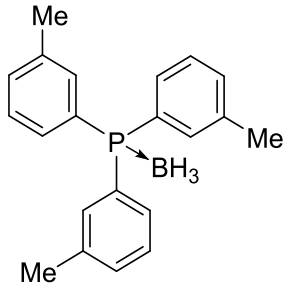

To a solution of tris(*m*-tolyl)phosphine (0.69 g, 2.3 mmol) in dry dichloromethane (5 mL), borane dimethylsulfide complex (2 mL, 21 mmol) was added under an atmosphere of nitrogen. After stirring for 16 hours at room temperature, water (10 mL) was added and the reaction was stirred at ambient temperature for a further 2 hours. A significant amount of effervescence was observed during this period, and consequently the vessel was opened to prevent an accumulation of pressure. The reaction mixture was poured onto water (5 mL) and then extracted into dichloromethane (3 x 10 mL). The combined organics were washed with a saturated aqueous $NaHCO_3$ solution (20 mL), dried over $MgSO_4$, filtered, and the solvent was removed *in vacuo* to afford a white solid. This was redissolved in dichloromethane and filtered through silica, eluting with dichloromethane. Removal of solvent *in vacuo* gave phosphine borane complex **8** as a white solid (0.62 g, 86% yield). **m.p.** (sample crystallized *via* slow evaporation of dichloromethane) 108-109 °C; **^{1}H NMR** (400 MHz, $CDCl_3$) δ = 7.43 (d, 11.8 Hz, 3H), 7.33-7.25 (m, 9H), 2.35 (s, 9H), 1.53-0.90 (br, q (*unresolved*), 3H);

$^{13}C\{^{1}H\}$ NMR (100 MHz, $CDCl_3$) δ = 138.7 (d, $J_{C\text{-}P}$ 10.5 Hz), 133.7 (d, $J_{C\text{-}P}$ 10.7 Hz), 132.1 (d, $J_{C\text{-}P}$ 2.5 Hz), 130.3 (d, $J_{C\text{-}P}$ 8.5 Hz), 129.2 (d, $J_{C\text{-}P}$ 57.9 Hz), 128.6 (d, $J_{C\text{-}P}$ 10.4 Hz), 21.6 (s); **$^{11}B\{^{1}H\}$ NMR** (96 MHz, $CDCl_3$) δ = −38.8 (br, d $J_{B\text{-}P}$ 45 Hz); **$^{31}P\{^{1}H\}$ NMR** (121 MHz, $CDCl_3$) δ = 20.6 (br, app. d); **IR** (solid, intense peaks only, cm^{-1}) ν = 2408, 1477, 1105, 1072, 1061, 997, 888, 858, 787, 745, 695, 618, 540; **MS** (ESI): m/z (%) 635 (M_2-H^+), 341 (MNa^+), 317 ($M-H^+$); **HRMS** (ESI) calculated: $C_{18}H_{24}{}^{11}B_1{}^{23}Na_1P_1$ 341.16009, found: 341.16060.

Tris(*p*-fluorophenyl)phosphine borane complex, 9

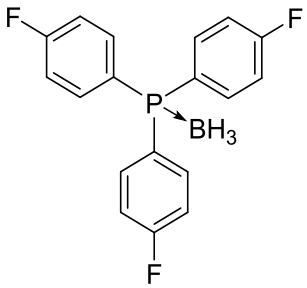

To a solution of tris(*p*-fluorophenyl)phosphine (0.19 g, 0.60 mmol) in dry dichloromethane (2 mL), borane dimethylsulfide complex (0.5 mL, 5.2 mmol) was added under an atmosphere of nitrogen. After stirring for 16 hours at room temperature, water (5 mL) was added and the reaction was stirred at ambient temperature for a further hour. A significant amount of effervescence was observed during this period, and consequently the vessel was opened to prevent an accumulation of pressure. The reaction mixture was poured onto water (5 mL) and then extracted into dichloromethane (3 x 10 mL). The combined organics were washed with a saturated aqueous $NaHCO_3$ solution (10 mL), dried over $MgSO_4$, filtered, and the solvent was removed *in vacuo* to afford a white solid. This was redissolved in dichloromethane and filtered through silica, eluting with dichloromethane. Removal of solvent *in vacuo* gave phosphine borane complex **9** as a white solid (0.12 g, 61% yield). **m.p.** (sample crystallized *via* vapour diffusion dichloromethane/hexane) 159-160 °C; **^{1}H NMR** (400 MHz, $CDCl_3$) δ = 7.56 (m, 6H), 7.16 (m, 6H), 1.56-0.88 (br, q (*unresolved*), 3H); **$^{13}C\{^{1}H\}$ NMR** (100 MHz, $CDCl_3$) δ = 165.0 (d, $J_{C\text{-}F}$ 254.7 Hz), 135.5 (dd, *J* 9.0 Hz, *J* 10.8 Hz), 124.7 (d, $J_{C\text{-}P}$ 59.9 Hz), 116.6 (dd, *J* 11.8 Hz, *J* 22.0 Hz); **$^{11}B\{^{1}H\}$ NMR** (128 MHz, $CDCl_3$) δ = −38.6 (br, d $J_{B\text{-}P}$ 44 Hz); **$^{31}P\{^{1}H\}$ NMR** (162 MHz, $CDCl_3$) δ = 19.7 (br, app. d); **^{19}F NMR** (376 MHz, $CDCl_3$) δ = −107.0 (m); **IR** (solid, intense peaks only, cm^{-1}) ν = 2390, 2353, 1587, 1495, 1397, 1226, 1159, 1132, 1106, 1069, 1059, 1013, 844, 825, 750, 712, 705, 664, 574; **MS** (ESI): m/z (%) 683 (M_2Na^+), 353 (MNa^+); **HRMS** (ESI) calculated: $C_{21}H_{15}{}^{11}B_1F_3{}^{23}Na_1P_1$ 353.08488, found: 353.08480.

Tris(*o*-tolyl)phosphine borane complex, 10

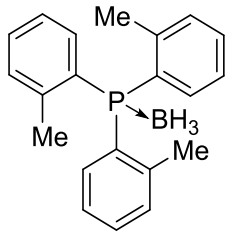

To a solution of tris(*o*-tolyl)phosphine (0.61 g, 2.0 mmol) in dry dichloromethane (5 mL), borane dimethylsulfide complex (1.9 mL, 20 mmol) was added under an atmosphere of nitrogen. After stirring for 19 hours at room temperature, a saturated aqueous NH_4Cl (10 mL) solution was added and the reaction was stirred at ambient temperature for a further 2 hours. A significant amount of effervescence was observed during this period, and consequently the vessel was opened to prevent an accumulation of pressure. The reaction mixture was poured onto water (20 mL) and then extracted into dichloromethane (3 x 25 mL). The combined organics were washed with a saturated aqueous $NaHCO_3$ solution (25 mL), dried over $MgSO_4$, filtered, and the solvent was removed *in vacuo* to afford a white solid. This was redissolved in dichloromethane and filtered through silica, eluting with dichloromethane. Removal of solvent *in vacuo* gave phosphine borane complex **10** as a white solid (0.47 g, 74% yield). **^{1}H NMR** (400 MHz, $CDCl_3$) δ = 7.43 (t, $J_{H\text{-}H}$ 7.5 Hz, 3H), 7.34 (m, 3H), 7.15 (t, $J_{H\text{-}H}$ 7.5 Hz, 3H), 7.00 (m, 3H), 2.43 (s, 9H), 2.011.10 (br, q (*unresolved*), 3H); **^{13}C{^{1}H} NMR** (100 MHz, $CDCl_3$) δ = 144.1 (d, $J_{C\text{-}P}$ 10.7 Hz), 133.6 (d, $J_{C\text{-}P}$ 6.7 Hz), 132.2 (d, $J_{C\text{-}P}$ 9.6 Hz), 131.4 (d, $J_{C\text{-}P}$ 2.26 Hz), 127.1 (d, $J_{C\text{-}P}$ 53.6 Hz), 126.1 (d, $J_{C\text{-}P}$ 9.10 Hz), 23.2 (d, $J_{C\text{-}P}$ 4.2 Hz); **^{11}B{^{1}H} NMR** (96 MHz, $CDCl_3$) δ = −32.0 (br, app. s); **^{31}P{^{1}H} NMR** (121 MHz, $CDCl_3$) δ = 23.4 (br, app. d).

Data are in accordance with that previously reported.[1]

Tris(*o*-methoxyphenyl)phosphine borane complex, 11

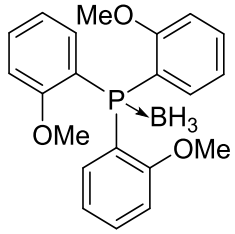

To a solution of tris(*o*-methoxyphenyl)phosphine (0.37 g, 1.0 mmol) in dry dichloromethane (5 mL), borane dimethylsulfide complex (1 mL, 10 mmol) was added under an atmosphere of nitrogen. After stirring for 19 hours at room temperature, a saturated aqueous NH_4Cl (10 mL) solution was added and the reaction was stirred at ambient temperature for a further 3 hours. A significant amount of effervescence was observed during this period, and consequently the vessel was opened to prevent an accumulation of pressure. The reaction mixture was poured onto water (10 mL) and then extracted into dichloromethane (3 x 20 mL). The combined organics were washed with a saturated aqueous $NaHCO_3$ solution (20 mL), dried over $MgSO_4$, filtered, and the solvent was removed *in vacuo* to afford a white solid. This was redissolved in dichloromethane and filtered through silica, eluting with

dichloromethane. Removal of solvent *in vacuo* gave phosphine borane complex **11** as a white solid (0.36 g, 94% yield). **m.p.** (sample recrystallized *via* vapour diffusion dichloromethane/hexane) 209-210 °C (decomposed); **^{1}H NMR** (400 MHz, $CDCl_3$) δ = 7.48-7.41 (m, 6H), 6.96 (m, 3H), 6.89 (m, 3H), 3.47 (s, 9H), 1.53-0.88 (br, q (*unresolved*), 3H); **^{13}C{^{1}H} NMR** (100 MHz, $CDCl_3$) δ = 164.6 (d, $J_{C\text{-}P}$ 2.9 Hz), 135.2 (d $J_{C\text{-}P}$ 8.3 Hz), 132.5 (d, $J_{C\text{-}P}$ 2.2 Hz), 120.6 (d, $J_{C\text{-}P}$ 10.2 Hz), 117.8 (d, $J_{C\text{-}P}$ 60.0 Hz), 111.8 (d, $J_{C\text{-}P}$ 5.0 Hz), 55.6 (s); **^{11}B{^{1}H} NMR** (96 MHz, $CDCl_3$) δ = −36.9 (br, app. s); **^{31}P{^{1}H} NMR** (121 MHz, $CDCl_3$) δ = 14.3 (br, app. d); **IR** (solid, intense peaks only, cm^{-1}) ν = 2437, 2413, 2331, 1589, 1574, 1477, 1458, 1430, 1277, 1251, 1161, 1135, 1077, 1046, 1022, 803, 751, 677, 604; **MS** (ESI): m/z (%) 781 (M_2Na^+), 403 (MNa^+), 365 ($[M\text{-}H]^+$); **HRMS** (ESI) calculated: $C_{21}H_{24}O_3{}^{11}B_1{}^{23}Na_1P_1$ 389.14483, found: 389.14520.

Tris(*o*-fluorophenyl)phosphine borane complex, 12

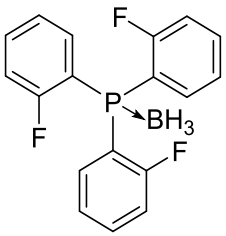

A solution of fluorobenzene (1 mL, 11 mmol) in degassed THF (30 mL) was cooled to −78 °C under an atmosphere of nitrogen. A solution of *sec*-BuLi (1.4 M in cyclohexane, 7.5 mL, 11 mmol) was added dropwise over 30 minutes. The solution was left stirring at −78 °C for 2 hours. A solution of phosphorus trichloride (0.3 mL, 3.4 mmol, in 5 mL degassed THF) was added dropwise over 10 minutes. The reaction mixture was left to stir for 2 hours before being allowed to warm to room temperature. Degassed water (15 mL) was added and the reaction mixture stirred for a further 30 minutes. The reaction mixture was then extracted into diethyl ether (3 x 30 mL), and the combined organics dried over $MgSO_4$, filtered and solvent removed *in vacuo* to reveal a white solid. Dry dichloromethane (18 mL) and then borane dimethylsulfide complex (5 mL, 52 mmol) were added. The resulting solution was stirred for 16 hours at ambient temperature. Water (15 mL) was added and the reaction was stirred at ambient temperature for a hour. A significant amount of effervescence was observed during this period, and consequently the vessel was opened to prevent an accumulation of pressure. The reaction mixture was poured onto water (10 mL) and then extracted into dichloromethane (3 x 20 mL). The combined organics were washed with a saturated aqueous $NaHCO_3$ solution (20 mL), dried over $MgSO_4$, filtered, and the solvent was removed *in vacuo* to afford a white solid. This was redissolved in dichloromethane and filtered through silica, eluting with dichloromethane. Removal of solvent *in vacuo* gave phosphine borane complex **12** as a white solid (0.78 g, 69% yield). **m.p.** (sample crystallized *via* slow evaporation of dichloromethane) 145-146 °C; **^{1}H NMR** (400 MHz, $CDCl_3$) δ =

7.71-7.63 (m, 3H), 7.58-7.52 (m, 3H), 7.25 (m, 3H), 7.14-7.09 (m, 3H), 1.65-0.89 (br, q (*unresolved*), 3H); **^{13}C{^{1}H} NMR** (125 MHz, $CDCl_3$) δ = 164.0 (d, $J_{C\text{-}F}$ 253.7 Hz), 134.7 (app. d, J 10.2 Hz), 134.45-134.37 (m), 124.9 (d, J 10.7 Hz), 116.55-116.33 (m), 115.4 (dd, $^{1}J_{C\text{-}P}$ 57.8 Hz, $^{2}J_{C\text{-}F}$ 18.0 Hz); **^{11}B{^{1}H} NMR** (96 MHz, $CDCl_3$) δ = −36.7 (br, app. s); **^{31}P{^{1}H} NMR** (121 MHz, $CDCl_3$) δ = 8.7 (br, app. d); **^{19}F NMR** (376 MHz, $CDCl_3$) δ = −98.9 (s); **IR** (solid, intense peaks only, cm^{-1}) ν = 2398, 1599, 1569, 1471, 1442, 1262, 1222, 1123, 1078, 1062, 827, 752, 717, 675, 550, 526; **MS** (ESI): m/z (%) 353 (MNa^+); **HRMS** (ESI) calculated: $C_{18}H_{15}{}^{11}B_1F_3{}^{23}Na_1P_1$ 353.08488, found: 353.08550.

Diphenylcyclohexylphosphine borane complex, 13

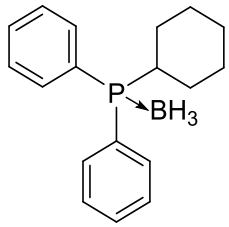

To a solution of diphenylcyclohexylphosphine (0.064 g, 0.237 mmol) in dry dichloromethane (1 mL), borane dimethylsulfide complex (0.2 mL, 2.11 mmol) was added under an atmosphere of nitrogen. After stirring for 20 hours at room temperature, a saturated aqueous NH_4Cl solution (10 mL) was added and the reaction was stirred for a further 2 hours. A significant amount of effervescence was observed during this period, and consequently the vessel was opened to prevent an accumulation of pressure. The reaction mixture was poured onto water (10 mL) and then extracted into dichloromethane (3 x 20 mL). The combined organics were washed with a saturated aqueous $NaHCO_3$ solution (30 mL), dried over $MgSO_4$, filtered, and the solvent was removed *in vacuo* to afford a white solid. This was redissolved in dichloromethane and filtered through silica, eluting with dichloromethane. Removal of solvent *in vacuo* gave phosphine borane complex **13** as a white solid (0.060 g, 90% yield). **^{1}H NMR** (400 MHz, $CDCl_3$) δ = 7.77-7.71 (m, 4H), 7.50-7.41 (m, 6H), 2.46-2.35 (m, 1H), 1.83-1.63 (m, 5H), 1.53-1.40 (m, 2H), 1.34-1.17 (m, 3H see below), 1.30-0.60 (br, q (*unresolved*), 3H see below); **^{13}C{^{1}H} NMR** (76 MHz, $CDCl_3$) δ = 132.7 (d, $J_{C\text{-}P}$ 8.5 Hz), 131.5 (d, $J_{C\text{-}P}$ 2.5 Hz), 128.8 (d, $J_{C\text{-}P}$ 9.5 Hz), 128.5 (d, $J_{C\text{-}P}$ 53.5 Hz), 33.8 (d, $J_{C\text{-}P}$ 36.1 Hz), 26.8 (d, $J_{C\text{-}P}$ 12.4 Hz), 26.6 (d, $J_{C\text{-}P}$ 0.9 Hz), 25.9 (d, $J_{C\text{-}P}$ 1.7 Hz);**^{11}B{^{1}H} NMR** (128 MHz, $CDCl_3$) δ = −42.8 (br d, $^{1}J_{B\text{-}P}$ 56 Hz); **^{31}P{^{1}H} NMR** (121 MHz, $CDCl_3$) δ = 21.7 (br, app. d).

The two multiplets highlighted above in the ^{1}H NMR spectrum (1.34-1.17 and 1.30-0.60 ppm) overlap, the total area (1.34-0.60 ppm) integrates to 6H. The broad quartet at 1.30-0.60 ppm is attributed to the BH_3, and consequently, it is assumed that each multiplet corresponds to 3H.

Data are in accordance with that previously reported.[3]

Dicyclohexylphenylphosphine borane complex, 14

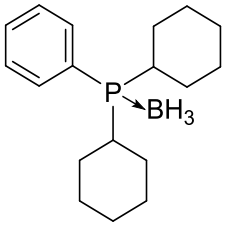

To a solution of dicyclohexylphenylphosphine (0.058 g, 0.212 mmol) in dry degassed dichloromethane (2 mL), borane dimethylsulfide complex (0.2 mL, 2.11 mmol) was added under an atmosphere of nitrogen. After stirring for 17 hours at room temperature, a saturated aqueous NH_4Cl solution (2 mL) was added and the reaction was stirred for a further 2 hours. A significant amount of effervescence was observed during this period and consequently the vessel was opened to prevent an accumulation of pressure. The reaction mixture was poured onto water (5 mL) and then extracted into dichloromethane (3 x 10 mL). The combined organics were washed with a saturated aqueous $NaHCO_3$ solution (25 mL), dried over $MgSO_4$, filtered, and the solvent was removed *in vacuo* to afford a white solid. This was redissolved in dichloromethane and filtered through silica, eluting with dichloromethane. Removal of solvent *in vacuo* gave phosphine borane complex **14** as a white solid (0.049 g, 79% yield). **^{1}H NMR** (400 MHz, $CDCl_3$) δ = 7.71-7.66 (m, 2H), 7.52-7.42 (m, 3H), 2.13-1.92 (m, 4H), 1.82-1.58 (m, 8H), 1.35-1.07 (m, 10H), 0.94-0.27 (br, q (*unresolved*), 3H); **^{13}C{^{1}H} NMR** (100 MHz, $CDCl_3$) δ = 133.6 (d, $J_{C\text{-}P}$ 7.5 Hz), 131.5 (d, $J_{C\text{-}P}$ 2.5 Hz), 128.5 (d, $J_{C\text{-}P}$ 9.1 Hz), 125.7 (d, $J_{C\text{-}P}$ 48.3 Hz), 31.3 (d, $J_{C\text{-}P}$ 34.0 Hz), 26.9 (d, $J_{C\text{-}P}$ 3.0 Hz), 26.8 (d, $J_{C\text{-}P}$ 1.2 Hz), 26.7 (s), 26.3 (d, $J_{C\text{-}P}$ 2.7 Hz), 26.0 (d, $J_{C\text{-}P}$ 1.4 Hz); **^{11}B{^{1}H} NMR** (128 MHz, $CDCl_3$) δ = −43.6 (br d, $^1J_{B\text{-}P}$ 61 Hz); **^{31}P{^{1}H} NMR** (162 MHz, $CDCl_3$) δ = 26.2 (br, app. d).

Data are in accordance with that previously reported.[3]

Tricyclohexylphosphine borane complex, 15

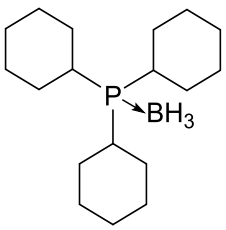

To a solution of tricyclohexylphosphine (0.138 g, 0.492 mmol) in dry degassed dichloromethane (2 mL), borane dimethylsulfide complex (4 mL, 4.2 mmol) was added under an atmosphere of nitrogen. After stirring for 20 hours at room temperature, a saturated NH_4Cl solution (2 mL) was added and the reaction was stirred for a further 2 hours. A significant amount of effervescence was observed during this period and consequently the vessel was opened to prevent an accumulation of pressure. The reaction mixture was poured

onto water (10 mL) and extracted into dichloromethane (3 x 15 mL). The combined organics were washed with a saturated aqueous $NaHCO_3$ solution (20 mL), dried over $MgSO_4$, filtered, and the solvent was removed *in vacuo* to afford a white solid. This was redissolved in dichloromethane and filtered through silica, eluting with dichloromethane. Removal of solvent *in vacuo* gave the phosphine borane complex **15** as a white solid (0.089 g, 62% yield). **^{1}H NMR** (300 MHz, $CDCl_3$) δ = 1.93-1.71 (m, 18H), 1.44-1.23 (m, 15H), 0.72-−0.18 (*minus 0.18*) (br, q (*unresolved*), 3H); **^{13}C{^{1}H} NMR** (125 MHz, $CDCl_3$) δ = 31.1 (d, $J_{C\text{-}P}$ 30.5 Hz), 28.0 (d, $J_{C\text{-}P}$ 1.6 Hz), 27.4 (d, $J_{C\text{-}P}$ 10.3 Hz), 26.3 (s); **^{11}B{^{1}H} NMR** (96 MHz, $CDCl_3$) δ = −44.5 (br, d, $^1J_{B\text{-}P}$ 65 Hz); **^{31}P{^{1}H} NMR** (121 MHz, $CDCl_3$) δ = 28.1 (br, unresolved multiplet).

Data are in accordance with that previously reported.[1]

Diphenylmethylphosphine borane complex, 16

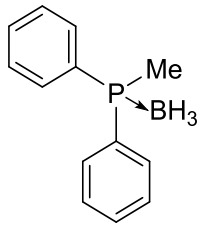

To a solution of diphenylmethylphosphine (0.4 mL, 2.1 mmol) in dry degassed dichloromethane (4 mL), borane dimethylsulfide complex (1.4 mL, 14.8 mmol) was added under an atmosphere of nitrogen. After stirring for 16 hours at room temperature, water (5 mL) was added and the reaction was stirred for a further 2 hours. A significant amount of effervescence was observed during this period and consequently the vessel was opened to prevent an accumulation of pressure. The reaction mixture was poured onto water (5 mL) and extracted into dichloromethane (3 x 10 mL). The combined organics were washed with a saturated aqueous $NaHCO_3$ solution (20 mL), dried over $MgSO_4$, filtered, and the solvent was removed *in vacuo* to afford a white solid. This was redissolved in dichloromethane and filtered through silica, eluting with dichloromethane. Removal of solvent *in vacuo* gave the phosphine borane complex **16** as a white solid (0.33 g, 72% yield). **^{1}H NMR** (300 MHz, $CDCl_3$) δ = 7.70-7.63 (m, 4H), 7.52-7.41 (m, 6H), 1.87 (d, $^2J_{H\text{-}P}$ 10.2 Hz, 3H), 1.49-0.54 (br, q (*unresolved*), 3H); **^{13}C{^{1}H} NMR** (125 MHz, $CDCl_3$) δ = 131.9 (d, $J_{C\text{-}P}$ 9.5 Hz), 131.3 (d, $J_{C\text{-}P}$ 2.5 Hz), 130.6 (d, $J_{C\text{-}P}$ 56.3 Hz), 129.0 (d, $J_{C\text{-}P}$ 10.0 Hz), 12.0 (d, $J_{C\text{-}P}$ 40.2 Hz); **^{11}B{^{1}H} NMR** (96 MHz, $CDCl_3$) δ = −39.0 (br, d, $^1J_{B\text{-}P}$ 59 Hz); **^{31}P{^{1}H} NMR** (121 MHz, $CDCl_3$) δ = 10.7 (br, unresolved multiplet).

Data are in accordance with that previously reported.[3]

Dimethylphenylphosphine borane complex, 17

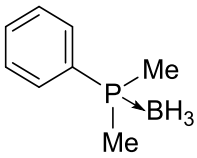

To a solution of dimethylphenylphosphine (0.4 mL, 2.8 mmol) in dry degassed dichloromethane (5 mL), borane dimethylsulfide complex (2 mL, 21.1 mmol) was added under an atmosphere of nitrogen. After stirring for 15 hours at room temperature, water (5 mL) was added and the reaction was stirred for a further 2 hours. A significant amount of effervescence was observed during this period and consequently the vessel was opened to prevent an accumulation of pressure. The reaction mixture was poured onto water (5 mL) and extracted into dichloromethane (3 x 15 mL). The combined organics were washed with a saturated aqueous $NaHCO_3$ solution (20 mL), dried over $MgSO_4$, filtered, and the solvent was removed *in vacuo* to afford a colourless liquid. This was redissolved in dichloromethane and filtered through silica, eluting with dichloromethane. Removal of solvent *in vacuo* gave the phosphine borane complex **17** as a colourless liquid (0.39 g, 91% yield). **^{1}H NMR** (300 MHz, $CDCl_3$) δ = 7.76-7.69 (m, 2H), 7.54-7.43 (m, 3H), 1.57 (d, $^{2}J^{H\text{-}P}$ 10.4 Hz, 6H), 0.75 (br, qd, $^{1}J_{H\text{-}B}$ 95.3 Hz, $^{2}J_{H\text{-}P}$ 15.6 Hz, 3H); **^{13}C{^{1}H} NMR** (125 MHz, $CDCl_3$) δ = 131.4 (d, $J_{C\text{-}P}$ 2.4 Hz), 131.0 (d, $J_{C\text{-}P}$ 9.6 Hz), 130.1 (s, see below), 129.0 (d, $J_{C\text{-}P}$ 9.9 Hz), 13.2 (d, $J_{C\text{-}P}$ 39.0 Hz); **^{11}B{^{1}H} NMR** (96 MHz, $CDCl_3$) δ = −39.1 (br, d, $^{1}J_{B\text{-}P}$ 61 Hz); **^{31}P{^{1}H} NMR** (162 MHz, $CDCl_3$) δ = 2.8 (br, q, unresolved).

Data are in accordance with that previously reported.[3]

Trimethylphosphine borane complex, 18

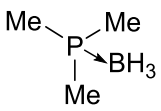

To a solution of trimethylphosphine (0.4 mL, 3.9 mmol) in dry degassed toluene (6 mL), borane dimethylsulfide complex (1.2 mL, 12.7 mmol) was added under an atmosphere of nitrogen. After stirring for 15 hours at room temperature, water (5 mL) was added and the reaction was stirred for a further 2 hours. A significant amount of effervescence was observed during this period, and consequently the vessel was opened to prevent an accumulation of pressure. The reaction mixture was poured onto water (10 mL) and then extracted into toluene (3 x 10 mL). The combined organics were washed with a saturated aqueous $NaHCO_3$ solution (20 mL), dried over $MgSO_4$, filtered, and the solvent was removed *in vacuo* (at pressures no less than 38 torr, 40 °C, rotary evaporator) to afford phosphine borane complex **18** as a colourless crystalline solid (0.32 g, 93% yield). **^{1}H NMR** (400 MHz, $CDCl_3$) δ = 1.27 (d, $^{2}J_{H\text{-}P}$ 10.7 Hz, 9H), 0.42 (br, qd $^{1}J_{H\text{-}B}$ 94.6 Hz, $^{2}J_{H\text{-}P}$ 16.2 Hz, 3H); **^{13}C{^{1}H} NMR** (100 MHz, $CDCl_3$) δ = 13.1 (d, $J_{C\text{-}P}$ 38.0

Hz); **^{11}B{^{1}H} NMR** (128 MHz, $CDCl_3$) δ = −38.2 (d, $^{1}J_{B\text{-}P}$ 64 Hz); **^{31}P{^{1}H} NMR** (162 MHz, $CDCl_3$) δ = −1.3 (br, app. q, unresolved).

Data are in accordance with that previously reported.[3]

Diphenyl-*t*-butylphosphine borane complex, 19

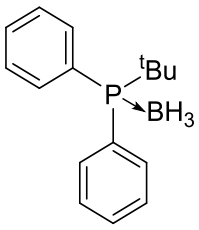

To a solution of diphenyl-*t*-butylphosphine (0.47 g, 1.9 mmol) in dry degassed dichloromethane (3 mL), borane dimethylsulfide complex (3 mL, 20.0 mmol) was added under an atmosphere of nitrogen. After stirring for 19 hours at room temperature, water (3 mL) was added and the reaction was stirred for a further 2 hours. A significant amount of effervescence was observed during this period and consequently the vessel was opened to prevent an accumulation of pressure. The reaction mixture was poured onto water (5 mL) and extracted into dichloromethane (3 x 15 mL). The combined organics were washed with a saturated aqueous $NaHCO_3$ solution (20 mL), dried over $MgSO_4$, filtered, and the solvent was removed *in vacuo* to afford a white solid. This was redissolved in dichloromethane and filtered through silica, eluting with dichloromethane. Removal of solvent *in vacuo* gave the phosphine borane complex **19** as a white solid (0.19 g, 40% yield). **m.p.** (sample crystallized *via* slow evaporation of dichloromethane) 53-54 °C; **^{1}H NMR** (300 MHz, $CDCl_3$) δ = 7.91-7.83 (m, 4H), 7.52-7.41 (m, 6H), 1.30 (d, $^{2}J_{H\text{-}P}$ 14.1 Hz, 9H see below), 1.52-0.61 (br, q (*unresolved*), 3H see below); **^{13}C{^{1}H} NMR** (100 MHz, $CDCl_3$) δ = 134.1 (d, $J_{C\text{-}P}$ 8.1 Hz), 131.1 (d, $J_{C\text{-}P}$ 2.4 Hz), 128.5 (d, $J_{C\text{--}P}$ 9.5 Hz), 128.2 (d, $J_{C\text{-}P}$ 51.2 Hz), 31.2 (d, $J_{C\text{-}P}$ 31.6 Hz), 27.1 (d, $J_{C\text{-}P}$ 2.7 Hz); **^{11}B{^{1}H} NMR** (96 MHz, $CDCl_3$) δ = −40.5 (br, d, $^{1}J_{B\text{-}P}$ 58 Hz); **^{31}P{^{1}H} NMR** (121 MHz, $CDCl_3$) δ = 34.0 (br, app. d, unresolved); **IR** (solid, intense peaks only, cm^{-1}) ν = 2961, 2902, 2382, 2281, 1473, 1435, 1394, 1366, 1184, 1145, 1102, 1069, 10001, 811, 736, 689, 637, 575; **MS** (ESI): m/z (%) 279 (MNa^+); **HRMS** (ESI) calculated: $C_{16}H_{22}{}^{11}B_1{}^{23}Na_1P_1$ 279.14444, found: 279.14570.

The doublet and broad quartet highlighted above in the ^{1}H spectrum (1.30 and 1.52-0.61 ppm) overlap, with the total area integrating to 12H. The broad quartet at 1.52-0.61 ppm is attributed to the BH_3, and consequently, assigned to 3H.

Di-*t*-butylphenylphosphine borane complex, 20

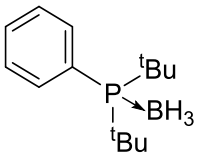

To a solution of di-*t*-butylphenylphosphine (0.6 mL, 2.5 mmol) in dry degassed dichloromethane (5 mL), borane dimethylsulfide complex (2 mL, 21.1 mmol) was added under an atmosphere of nitrogen. After stirring for 20 hours at room temperature, water (5 mL) was added and the reaction was stirred for a further 2 hours. A significant amount of effervescence was observed during this period and consequently the vessel was opened to prevent an accumulation of pressure. The reaction mixture was poured onto water (10 mL) and extracted into dichloromethane (3 x 20 mL). The combined organics were washed with a saturated aqueous $NaHCO_3$ solution (25 mL), dried over $MgSO_4$, filtered, and the solvent was removed *in vacuo* to afford a white solid. This was redissolved in dichloromethane and filtered through silica, eluting with dichloromethane. Removal of solvent *in vacuo* gave the phosphine borane complex **20** as a white solid (0.089 g, 60% yield). **m.p.** (sample crystallized *via* slow evaporation of dichloromethane) 122-123 °C; **^{1}H NMR** (300 MHz, $CDCl_3$) δ = 7.97 (t, $J_{H\text{-}H}$ 8.3 Hz, 2H), 7.5-7.37 (m, 3H), 1.30 (d, $^{3}J_{H\text{-}P}$ 13.1 Hz, 8H), 1.20-0.29 (br, q (*unresolved*), 3H); **^{13}C{^{1}H} NMR** (100 MHz, 45 °C, $CDCl_3$) δ = 135.3 (br d, $J_{C\text{-}P}$ 5.0 Hz), 131.0 (d, $J_{C\text{-}P}$ 2.4 Hz), 128.1 (d, $J_{C\text{-}P}$ 9.0 Hz), 127.6 (d, $J_{C\text{-}P}$ 44.5 Hz), 33.3 (d, $J_{C\text{-}P}$ 26.5 Hz), 29.1 (d, $J_{C\text{-}P}$ 1.8 Hz); **^{11}B{^{1}H} NMR** (96 MHz, $CDCl_3$) δ = −42.4 (br, d, $^{1}J_{B\text{-}P}$ 63 Hz); **^{31}P{^{1}H} NMR** (121 MHz, $CDCl_3$) δ = 45.1 (br, app. q, unresolved); **IR** (solid, intense peaks only, cm^{-1}) ν = 2945, 2870, 2383, 1476, 1461, 1435, 1393, 1367, 1183, 1024, 1074, 1024, 814, 743, 699, 640, 610, 558; **MS** (ESI): m/z (%) 495 (M_2Na^+), 259 (MNa^+); **HRMS** (ESI) calculated: $C_{18}H_{26}{}^{11}B_1{}^{23}Na_1P_1$ 259.17574, found: 259.17340.

The broadness of the aromatic peaks $^{13}C\{^{1}H\}$ spectrum display a temperature dependence, with sharper peaks observed at increased temperature (in the range 10-45 °C). This was particularly true of the doublet reported at 135.3 ppm, the doublet nature was not resolved at 27 °C. This is attributed to restricted rotation about the P-C(aromatic) bond.

Tri-*t*-butylphosphine borane complex, 21

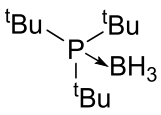

To a solution of tri-*t*-butylphosphine (0.18 g, 0.87 mmol) in dry, degassed dichloromethane (2 mL), borane dimethylsulfide complex (0.8 mL, 8.4 mmol) was added under an atmosphere of nitrogen. After stirring for 18 hours at room temperature, degassed water (5 mL) was added and the reaction was stirred for a further 3 hours. A significant amount of effervescence was observed during this period,

and consequently the vessel was opened to prevent an accumulation of pressure. The reaction mixture was poured onto water (5 mL) and then extracted into dichloromethane (3 x 10 mL). The combined organics were washed with a saturated aqueous $NaHCO_3$ solution (25 mL), dried over $MgSO_4$, filtered, and the solvent was removed *in vacuo* to afford a white solid. This was redissolved in dichloromethane and filtered through silica, eluting with dichloromethane. Removal of solvent *in vacuo* gave phosphine borane complex **21** as a white solid (0.13 g, 60% yield). **^{1}H NMR** (400 MHz, $CDCl_3$) δ = 1.42 (d, $^3J_{H\text{-}P}$ 11.6 Hz, 27H), 0.42 (br, q (1:1:1:1), $^1J_{H\text{-}B}$ 95.0 Hz, 3H); **^{11}B{^{1}H} NMR** (96 MHz, $CDCl_3$) δ = −42.0 (br, d, $^1J_{B\text{-}P}$ 62 Hz); **^{31}P{^{1}H} NMR** (162 MHz, $CDCl_3$) δ = 58.3 (br, app. q, unresolved).

Data are in accordance with that previously reported.[1]

Tri-*n*-butylphosphine borane complex, 22

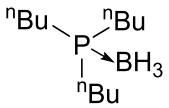

To a solution of tri-*n*-butylphosphine (0.5 mL, 2.0 mmol) in dry, degassed dichloromethane (4 mL), borane dimethylsulfide complex (1.5 mL, 15.8 mmol) was added under an atmosphere of nitrogen. After stirring for 17 hours at room temperature, degassed water (5 mL) was added and the reaction was stirred for a further 3 hours. A significant amount of effervescence was observed during this period, and consequently the vessel was opened to prevent an accumulation of pressure. The reaction mixture was poured onto water (10 mL) and then extracted into dichloromethane (3 x 10 mL). The combined organics were washed with a saturated aqueous $NaHCO_3$ solution (20 mL), dried over $MgSO_4$, filtered, and the solvent was removed *in vacuo* to afford a colourless oil. This was redissolved in dichloromethane and filtered through silica, eluting with dichloromethane. Removal of solvent *in vacuo* gave phosphine borane complex **22** as a colourless oil (0.43 g, 98% yield). **^{1}H NMR** (500 MHz, $CDCl_3$) δ = 1.58-1.36 (m, 18H), 0.93 (t, $J_{H\text{-}H}$ 7.2 Hz, 9H), 0.65-0.10 (br, q (*unresolved*), 3H); **^{13}C{^{1}H} NMR** (125 MHz, $CDCl_3$) δ = 24.9 (d, $J_{C\text{-}P}$ 2.1 Hz), 24.5 (d, $J_{C\text{-}P}$ 12.6 Hz), 23.0 (d, $J_{C\text{-}P}$ 34.7 Hz), 13.7 (s); **^{11}B{^{1}H} NMR** (128 MHz, $CDCl_3$) δ = −41.0 (br, m); **^{31}P{^{1}H} NMR** (162 MHz, $CDCl_3$) δ = 14.4 (br, app. q, unresolved).

Data are in accordance with that previously reported.[3]

Diphenyl-*i*-propylphosphine borane complex, 23

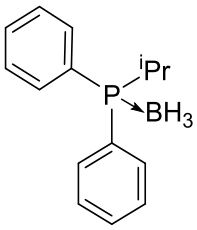

To a solution of isopropyldiphenylphosphine (0.42 g, 1.82 mmol) in dry degassed dichloromethane (5 mL), borane dimethylsulfide complex (0.5 mL, 6.58 mmol) was added under an atmosphere of nitrogen. After stirring for 16 hours at room temperature, water (10 mL) was added and the reaction was stirred for a further 2 hours. A significant amount of effervescence was observed during this period and consequently the vessel was opened to prevent an accumulation of pressure. The reaction mixture was poured onto water (10 mL) and then extracted into dichloromethane (3 x 20 mL). The combined organics were washed with a saturated aqueous $NaHCO_3$ solution (25 mL), dried over $MgSO_4$, filtered, and the solvent was removed *in vacuo* to afford a white solid. This was redissolved in dichloromethane and filtered through silica, eluting with dichloromethane. Removal of solvent *in vacuo* gave phosphine borane complex **23** as a colourless oil (0.42 g, 95% yield). Crystallisation was observed after storage of **23** (one week under an atmosphere of nitrogen) to give colourless needle-like crystals. **^{1}H NMR** (400 MHz, $CDCl_3$) δ = 7.77-7.73 (m, 4H), 7.49-7.41 (m, 6H), 2.71 (dhept, $^2J_{H\text{-}P}$ 14.0 $^3J_{H\text{-}H}$ 7.0 Hz, 1H), 1.17 (dd, $^3J_{H\text{-}P}$ 16.0 $^3J_{H\text{-}H}$ 7.0 Hz, 6H, see below), 1.26-0.57 (br, q (*unresolved*), 3H, see below); **^{13}C{^{1}H} NMR** (100 MHz, $CDCl_3$) δ = 132.7 (d, $J_{C\text{-}P}$ 8.4 Hz), 131.2 (d, $J_{C\text{-}P}$ 2.4 Hz), 128.9 (d, $J_{C\text{-}P}$ 55.4 Hz), 128.8 (d, $J_{C\text{-}P}$ 9.6 Hz), 23.9 (d, $J_{C\text{-}P}$ 36.7 Hz), 17.0 (d, $J_{C\text{-}P}$ 2.2 Hz); **^{11}B{^{1}H} NMR** (128 MHz, $CDCl_3$) δ = −42.5 (br d, $^1J_{B\text{-}P}$ 58 Hz); **^{31}P{^{1}H} NMR** (162 MHz, $CDCl_3$) δ = 25.2 (br, app. q); **IR** (solid, intense peaks only, cm^{-1}) ν = 2378, 1436, 1137, 1106, 1065, 735, 691, 577.

The two multiplets highlighted above in the ^{1}H NMR spectrum (1.26-0.57 and 1.17 ppm) overlap, the total area (126-0.57 ppm) integrates to 9H. The broad quartet at 1.26-0.57 ppm is attributed to the BH_3, and consequently, it is assumed to correspond to 3H.

Data are in accordance with that previously reported.[4]

Tri-*i*-propylphosphine borane complex, 24

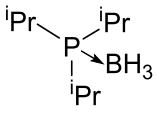

To a solution of tri-*i*-propylphosphine (0.15 g, 0.92 mmol) in dry degassed dichloromethane (4 mL), borane dimethylsulfide complex (0.4 mL, 0.42 mmol) was added under an atmosphere of nitrogen. After stirring for 15 hours at room temperature, water (5 mL) was added and the reaction was stirred for a further 2 hours. A significant amount of effervescence was observed during this period and consequently the vessel was opened to prevent an accumulation of pressure. The reaction

mixture was poured onto water (10 mL) and extracted into dichloromethane (3 x 15 mL). The combined organics were washed with a saturated aqueous $NaHCO_3$ solution (25 mL), dried over $MgSO_4$, filtered, and the solvent was removed *in vacuo* to afford a white solid. This was redissolved in dichloromethane and filtered through silica, eluting with dichloromethane. Removal of solvent *in vacuo* gave the phosphine borane complex **24** as a white solid (0.13 g, 82% yield). **m.p.** (sample crystallized *via* slow evaporation of dichloromethane) 39-40 °C; **^{1}H NMR** (400 MHz, $CDCl_3$) δ = 2.11 (dhept, $^{2}J_{H\text{-}P}$ 10.6 $^{3}J_{H\text{-}H}$ 7.2 Hz, 3H), 1.23 (dd, $^{3}J_{H\text{-}P}$ 13.3 $^{3}J_{H\text{-}H}$ 7.2 Hz, 18H), 0.69-−0.06 (*minus 0.06*) (br, qd (*unresolved*), 3H); **^{13}C{^{1}H} NMR** (100 MHz, $CDCl_3$) δ = 21.1 (d, $J_{C\text{-}P}$ 30.8 Hz), 18.1 (s); **^{11}B{^{1}H} NMR** (128 MHz, $CDCl_3$) δ = −44.0 (br, d, $^{1}J_{B\text{-}P}$ 63 Hz); **^{31}P{^{1}H} NMR** (162 MHz, $CDCl_3$) δ = 38.7 (br, unresolved multiplet); **IR** (solid, intense peaks only, cm^{-1}) ν = 2382, 1400, 1333, 1219, 1089, 1051, 1009, 853, 846, 733, 689, 612, 565; **MS** (ESI): m/z (%) 197 (MNa^{+}); **HRMS** (ESI) calculated: $C_9H_{24}O_2{}^{11}B_1{}^{23}Na_1P_1$ 197.1601, found: 197.1591.

Diphenyl-(*o*-tolyl)phosphine borane complex, 25

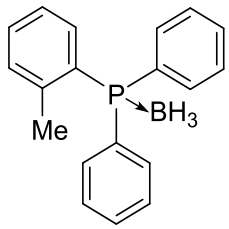

To a solution of diphenyl(*o*-tolyl)phosphine (0.10 g, 0.37 mmol) in dry dichloromethane (2 mL), borane dimethylsulfide complex (0.3 mL, 3.2 mmol) was added under an atmosphere of nitrogen. After stirring for 21 hours at room temperature, a saturated aqueous NH_4Cl solution (5 mL) was added and the reaction was stirred for a further hour. A significant amount of effervescence was observed during this period, and consequently the vessel was opened to prevent an accumulation of pressure. The reaction mixture was poured onto water (10 mL) and then extracted into dichloromethane (3 x 10 mL). The combined organics were washed with a saturated aqueous $NaHCO_3$ solution (20 mL), dried over $MgSO_4$, filtered, and the solvent was removed *in vacuo* to afford a white solid. This was redissolved in dichloromethane and filtered through silica, eluting with dichloromethane. Removal of solvent *in vacuo* gave phosphine borane complex **25** as a white solid (0.09 g, 92% yield). **^{1}H NMR** (400 MHz, $CDCl_3$) δ = 7.67-7.59 (m, 4H), 7.55-7.36 (m, 7H), 7.27-7.24 (m, 1H), 7.14 (t, $J_{H\text{-}H}$ 7.7 Hz, 1H), 7.02 (dd, J 12.0 Hz, $J_{H\text{-}H}$ 7.7 Hz, 1H), 2.27 (s, 3H), 1.79-0.90 (br, q (*unresolved*), 3H); **^{13}C{^{1}H} NMR** (76 MHz, $CDCl_3$) δ = 143.1 (d, $J_{C\text{-}P}$ 10.6 Hz), 134.3 (d, $J_{C\text{-}P}$ 8.5 Hz), 133.4 (d, $J_{C\text{-}P}$ 9.4 Hz), 132.0 (d, $J_{C\text{-}P}$ 8.8 Hz), 131.5 (d, $J_{C\text{-}P}$ 2.4 Hz), 131.3 (d, $J_{C\text{-}P}$ 2.4 Hz), 129.2 (d, $J_{C\text{-}P}$ 57.5 Hz), 129.0 (d, $J_{C\text{-}P}$ 10.0 Hz), 127.8 (d, $J_{C\text{-}P}$ 55.4 Hz), 126.0 (d, $J_{C\text{-}P}$ 9.4 Hz), 22.6 (d, $J_{C\text{-}P}$ 5.0 Hz); **^{11}B{^{1}H} NMR** (128 MHz, $CDCl_3$) δ = −36.7 (br, app. s); **^{31}P{^{1}H} NMR** (162 MHz, $CDCl_3$) δ = 20.8 (br, app. d).

Data are in accordance with that previously reported.[5]

Di(*o*-tolyl)phenylphosphine borane complex, 26

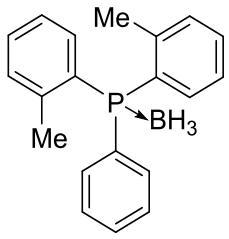

To a stirred suspension of magnesium (0.49 g, 20 mmol) in dry, degassed THF (3.8 mL) *o*-bromotoluene (0.7 mL, 6 mmol) was added under an atmosphere of nitrogen. Upon addition, the reaction mixture turned black and a slight exotherm was observed. A solution of *o*-bromotoulene (1.3 mL, 11 mmol, in 18 mL dry, degassed THF) was added dropwise over 30 minutes. The reaction mixture was heated at reflux for 1 hour, before being cooled to −78 °C. A solution of dichlorophenylphosphine (1.1 mL, 8.1 mmol, in 2 mL dry, degassed THF) was added dropwise over 10 minutes. The cloudy reaction mixture was left stirring at −78 °C for 30 minutes, before being allowed to warm to room temperature. 20 g of ice was added, and this was stirred for 2 hours. The reaction mixture was extracted into diethyl ether (3 x 30 mL), the combined organics were dried over $MgSO_4$, filtered and solvent removed *in vacuo* to reveal a white solid. Dry dichloromethane (6 mL) was added to give a homogenous colourless solution. Borane dimethylsulfide complex (1 mL, 11 mmol) was added and the reaction stirred at room temperature for 20 hours. Water (10 mL) was added and the reaction stirred for a further hour. A significant amount of effervescence was observed during this period, and consequently the vessel was opened to prevent an accumulation of pressure. The reaction mixture was poured onto water (5 mL) and then extracted into dichloromethane (3 x 20 mL). The combined organics were washed with a saturated aqueous $NaHCO_3$ solution (20 mL), dried over $MgSO_4$, filtered, and the solvent was removed *in vacuo* to afford a white solid. This was redissolved in dichloromethane and filtered through silica, eluting with dichloromethane. Removal of solvent *in vacuo* gave phosphine borane complex **26** as a white solid (0.50 g, 40% yield). **^{1}H NMR** (300 MHz, $CDCl_3$) δ = 7.65-7.38 (m, 7H), 7.32-7.28 (m, 2H), 7.22-7.12 (m, 4H), 2.37 (s, 6H), 1.74-1.12 (br, q (*unresolved*), 3H); **^{13}C{^{1}H} NMR** (76 MHz, $CDCl_3$) δ = 143.1 (d, $J_{C\text{-}P}$ 10.7 Hz), 133.8 (d, $J_{C\text{-}P}$ 9.0 Hz), 133.6 (d, $J_{C\text{-}P}$ 8.4 Hz), 132.0 (d, $J_{C\text{-}P}$ 8.7 Hz), 131.4 (d, $J_{C\text{-}P}$ 2.4 Hz), 131.2 (d, $J_{C\text{-}P}$ 2.5 Hz), 128.9 (d, $J_{C\text{-}P}$ 10.0 Hz), 128.6 (d, $J_{C\text{-}P}$ 57.0 Hz), 127.6 (d, $J_{C\text{-}P}$ 54.2 Hz), 126.1 (d, $J_{C\text{-}P}$ 9.4 Hz), 22.7 (d, $J_{C\text{-}P}$ 4.7 Hz); **^{11}B{^{1}H} NMR** (96 MHz, $CDCl_3$) δ = −38.8 (br, app. s); **^{31}P{^{1}H} NMR** (121 MHz, $CDCl_3$) δ = 21.3 (br, app. d).

Data are in accordance with that previously reported.[5]

Diphenyl-(*o*-methoxyphenyl)phosphine borane complex, 27

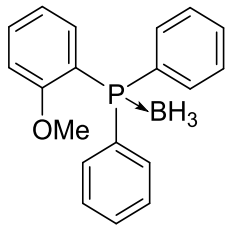

To a solution of diphenyl(*o*-methoxyphenyl)phosphine (0.51 g, 1.7 mmol) in dry dichloromethane (5 mL), borane dimethylsulfide complex (1.7 mL, 17.9 mmol) was added under an atmosphere of nitrogen. After stirring for 16 hours at room temperature, water (5 mL) was added and the reaction was stirred for a further 2 hours. A significant amount of effervescence was observed during this period, and consequently the vessel was opened to prevent an accumulation of pressure. The reaction mixture was poured onto water (5 mL) and then extracted into dichloromethane (3 x 10 mL). The combined organics were washed with a saturated aqueous $NaHCO_3$ solution (20 mL), dried over $MgSO_4$, filtered, and the solvent was removed *in vacuo* to afford a white solid. This was redissolved in dichloromethane and filtered through silica, eluting with dichloromethane. Removal of solvent *in vacuo* gave phosphine borane complex **27** as a white solid (0.48 g, 90% yield). **m.p.** (sample crystallized *via* slow evaporation of dichloromethane) 121-122 °C; **^{1}H NMR** (300 MHz, $CDCl_3$) δ = 7.69-7.30 (m, 5H), 7.55-7.37 (m, 7H), 7.05 (t, $J_{H\text{-}H}$ 7.5 Hz, 1H), 6.94-6.90 (m, 1H), 3.53 (s, 3H), 1.72-0.83 (br, q (*unresolved*), 3H); **^{13}C{^{1}H} NMR** (100 MHz, $CDCl_3$) δ = 161.4 (s), 136.1 (d, $J_{C\text{-}P}$ 12.3 Hz), 134.0 (s), 132.9 (d, $J_{C\text{-}P}$ 10.0 Hz), 130.7 (d, $J_{C\text{-}P}$ 2.6 Hz), 129.6 (d, $J_{C\text{-}P}$ 60.3 Hz), 128.3 (d, $J_{C\text{-}P}$ 10.6 Hz), 121.2 (d, $J_{C\text{-}P}$ 11.7 Hz), 116.6 (d, $J_{C\text{-}P}$ 56.6 Hz), 111.8 (d, $J_{C\text{-}P}$ 4.4 Hz), 55.3 (s); **^{11}B{^{1}H} NMR** (96 MHz, $CDCl_3$) δ = −37.8 (br, app. s); **^{31}P{^{1}H} NMR** (162 MHz, $CDCl_3$) δ = 19.1 (br, app. d); **IR** (solid, intense peaks only, cm^{-1}) ν = 2839, 2386, 2252, 1588, 1574, 1478, 1463, 1432, 1280, 1253, 1180, 1166, 1134, 1058, 1020, 802, 762, 739, 605, 544; **MS** (ESI): m/z (%) 329 (MNa^+); **HRMS** (ESI) calculated: $C_{19}H_{20}O_1{}^{11}B_1{}^{23}Na_1P_1$ 329.12371, found: 329.12540.

Di(*o*-methoxyphenyl)phenylphosphine borane complex, 28

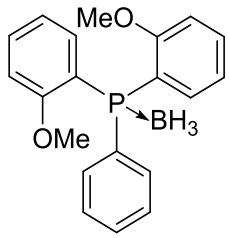

To a solution of bis(*o*-methoxyphenyl)phenylphosphine (0.34 g, 1.05 mmol) in dry dichloromethane (8 mL), borane dimethylsulfide complex (1.0 mL, 10.5 mmol) was added under an atmosphere of nitrogen. After stirring for 17 hours at room temperature, water (5 mL) was added and the reaction was stirred for a further 2 hours. A significant amount of effervescence was observed during this period, and consequently the vessel was opened to prevent an accumulation of pressure. The reaction mixture was poured onto water (10 mL) and then extracted into dichloromethane (3 x 10 mL). The combined organics were washed with a saturated aqueous $NaHCO_3$ solution (20 mL), dried over $MgSO_4$, filtered, and the

solvent was removed *in vacuo* to afford a white solid. This was redissolved in dichloromethane and filtered through silica, eluting with dichloromethane. Removal of solvent *in vacuo* gave phosphine borane complex **28** as a white solid (0.26 g, 74% yield). **m.p.** (sample crystallized *via* vapour diffusion dichloromethane/hexane) 139-140 °C; **^{1}H NMR** (400 MHz, $CDCl_3$) δ = 7.74-7.69 (m, 2H), 7.51-7.34 (m, 7H), 7.01-6.97, (m, 2H), 6.97-6.88 (m, 2H), 3.54 (s, 6H), 1.53-0.87 (br, q (*unresolved*), 3H); **^{13}C{^{1}H} NMR** (125 MHz, $CDCl_3$) δ = 161.5 (d, $J_{C\text{-}P}$ 1.7 Hz), 135.0 (d, $J_{C\text{-}P}$ 10.2 Hz), 133.3 (d, $J_{C\text{-}P}$ 10.0 Hz), 133.0 (d, $J_{C\text{-}P}$ 2.0 Hz), 130.4 (d, $J_{C\text{-}P}$ 2.5 Hz), 129.8 (d, $J_{C\text{-}P}$ 60.5 Hz), 128.0 (d, $J_{C\text{-}P}$ 10.8 Hz), 121.0 (d, $J_{C\text{-}P}$ 11.0 Hz), 117.7 (d, $J_{C\text{-}P}$ 59.4 Hz), 111.6 (d, $J_{C\text{-}P}$ 4.8 Hz), 55.5 (s); **^{11}B{^{1}H} NMR** (128 MHz, $CDCl_3$) δ = −36.6 (br, app. s); **^{31}P{^{1}H} NMR** (162 MHz, $CDCl_3$) δ = 15.9 (br, app. d); **IR** (solid, intense peaks only, cm^{-1}) ν = 2410, 2398, 2381, 2349, 1588, 1572, 1500, 1478, 1431, 1276, 1249, 1182, 1158, 1103, 1056, 1017, 950, 918, 819, 802, 739, 694, 682, 605; **MS** (ESI): m/z (%) 695 (M_2Na^+), 359 (MNa^+), 335 (M^+-H); **HRMS** (ESI) calculated: $C_{20}H_{22}O_2{}^{11}B_1{}^{23}Na_1P_1$ 359.13427, found: 359.13300.

Diphenyl(*p*-methoxyphenyl)phosphine borane complex, 29

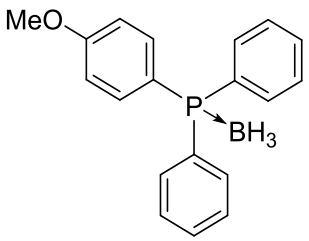

To a stirred suspension of magnesium (0.21 g, 8.6 mmol) in dry, degassed THF (6 mL) *p*-bromoanisole (0.3 mL, 2.4 mmol) was added under an atmosphere of nitrogen. The solution was heated to initiate the reaction, where upon the reaction mixture turned a pale brown colour. A solution of *p*-bromoansiole (0.7 mL, 5.6 mmol) was added dropwise over 30 minutes. The reaction mixture was heated at reflux for 2 hour, before being cooled to ambient temperature. The reaction mixture was then added to a solution of chlorodiphenylphosphine (1.4 mL, 7.6 mmol, in 2 mL dry, degassed THF) at −78 °C. After stirring for half an hour the cloudy reaction mixture was allowed to warm to room temperature and stirred for a further 2 hours. Following the addition of degassed water (10 mL), the reaction mixture was extracted into diethyl ether (2 x 25 mL), and the combined organics were dried over $MgSO_4$, filtered and solvent removed *in vacuo* to reveal a pale yellow oil. Dry dichloromethane (14 mL) was added followed by borane dimethylsulfide complex (3.5 mL, 37 mmol). The reaction was stirred at room temperature for 14 hours before water (15 mL) was added and the reaction stirred for a further hour. A significant amount of effervescence was observed during this period, and consequently the vessel was opened to prevent an accumulation of pressure. The reaction mixture was extracted into dichloromethane (3 x 15 mL) and the combined organics

were washed with a saturated aqueous $NaHCO_3$ solution (20 mL), dried over $MgSO_4$, filtered, and the solvent was removed *in vacuo* to afford a white solid. Recrystallisation from ethylacetate gave phosphine borane complex **29** as a white solid (0.51 g, 22% yield). **m.p.** (sample crystallized *via* slow evaporation of dichloromethane) 125-126 °C; **^{1}H NMR** (400 MHz, $CDCl_3$) δ = 7.61-7.40 (m, 12H), 6.99-6.95 (m, 2H), 3.83 (s, 3H), 1.59-0.95 (br, q (*unresolved*), 3H); **^{13}C{^{1}H} NMR** (125 MHz, $CDCl_3$) δ = 162.2 (d, $J_{C\text{-}P}$ 2.3 Hz), 135.1 (d, $J_{C\text{-}P}$ 10.9 Hz), 133.1 (d, $J_{C\text{-}P}$ 9.9 Hz), 131.2 (d, $J_{C\text{-}P}$ 2.3 Hz), 129.9 (d, $J_{C\text{-}P}$ 58.3 Hz), 128.8 (d, $J_{C\text{-}P}$ 10.4 Hz), 119.6 (d, $J_{C\text{-}P}$ 62.9 Hz), 114.6 (d, $J_{C\text{-}P}$ 11.3 Hz), 55.4 (s); **^{11}B{^{1}H} NMR** (128 MHz, $CDCl_3$) δ = −37.8 (br, app. s); **^{31}P{^{1}H} NMR** (162 MHz, $CDCl_3$) δ = 19.2 (br, app. d); **IR** (solid, intense peaks only, cm^{-1}) ν = 2377, 2345, 1594, 1568, 1500, 1456, 1433, 1407,1300, 1259, 1180, 1133, 1104, 1059, 1026, 998, 830, 803, 761, 738, 701, 692, 649, 599, 528, 507; **MS** (ESI): m/z (%) 3299 (MNa^+); **HRMS** (ESI) calculated: $C_{19}H_{20}O_1{}^{11}B_1{}^{23}Na_1P_1$ 329.12371, found: 329.12440.

Di(*p*-methoxyphenyl)phenylphosphine borane complex, 30

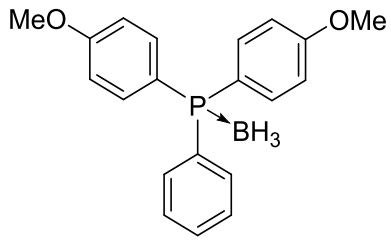

To a stirred suspension of magnesium (0.09 g, 3.7 mmol) in dry, degassed THF (4 mL) *p*-bromoanisole (0.4 mL, 3.2 mmol) was added dropwise over 15 minutes under an atmosphere of nitrogen. The reaction mixture was heated at reflux for 2 hour, before being cooled to ambient temperature. The reaction mixture was then added to a solution of chlorodiphenylphosphine (0.2 mL, 1.5 mmol, in 2 mL dry, degassed THF) at −78 °C. After stirring for half an hour the cloudy reaction mixture was allowed to warm to room temperature and stirred for a further hour. Following the addition of degassed water (8 mL), the reaction mixture was extracted into diethyl ether (3 x 10 mL), and the combined organics were dried over $MgSO_4$, filtered and solvent removed *in vacuo* to reveal a pale yellow oil. Dry dichloromethane (6 mL) was added followed by borane dimethylsulfide complex (0.7 mL, 7.4 mmol). The reaction was stirred at room temperature for 15 hours before water (10 mL) was added and the reaction stirred for a further 2 hours. A significant amount of effervescence was observed during this period, and consequently the vessel was opened to prevent an accumulation of pressure. The reaction mixture was extracted into dichloromethane (3 x 15 mL) and the combined organics were washed with a saturated aqueous $NaHCO_3$ solution (20 mL), dried over $MgSO_4$, filtered, and the solvent was removed *in vacuo* to afford a white solid. Column chromatography, eluiting with tolene, gave phosphine borane complex **30** as a white solid

(0.10 g, 21% yield). **m.p.** (sample crystallized *via* vapour diffusion dichloromethane/hexane) 120-121 °C; **^{1}H NMR** (400 MHz, $CDCl_3$) δ = 7.56-7.39 (m, 9H), 6.97-6.93 (m, 4H), 3.83 (s, 6H), 1.55-0.89 (br, q (*unresolved*), 3H); **^{13}C{^{1}H} NMR** (125 MHz, $CDCl_3$) δ = 162.1 (d, $J_{C\text{-}P}$ 2.3 Hz), 135.0 (d, $J_{C\text{-}P}$ 10.8 Hz), 133.1 (d, $J_{C\text{-}P}$ 9.8 Hz), 131.1 (d, $J_{C\text{-}P}$ 2.3 Hz), 130.6 (d, $J_{C\text{-}P}$ 58.4 Hz), 128.8 (d, $J_{C\text{-}P}$ 10.1 Hz), 120.4 (d, $J_{C\text{-}P}$ 63.3 Hz), 114.6 (d, $J_{C\text{-}P}$ 11.0 Hz), 55.5 (s); **^{11}B{^{1}H} NMR** (128 MHz, $CDCl_3$) δ = −37.7 (br, app. s); **^{31}P{^{1}H} NMR** (162 MHz, $CDCl_3$) δ = 17.8 (br, app. s); **IR** (solid, intense peaks only, cm^{-1}) ν = 2368, 2335, 1594, 1568, 1499, 1456, 1438, 1405, 1296, 1253, 1176, 1107, 1055, 1026, 830 ,817, 801, 759, 739, 696, 655, 628, 591, 527, 510; **MS** (ESI): m/z (%) 359 (MNa^+); **HRMS** (ESI) calculated: $C_{20}H_{22}O_2{}^{11}B_1{}^{23}Na_1P_1$ 359.13427, found: 359.13160.

Phenyldiphenylphosphinite borane complex, 31

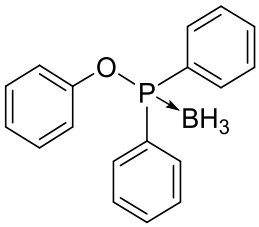

To a solution of phenyldiphenylphosphinite (1.16 g, 4.1 mmol) in dry degassed dichloromethane (4 mL), borane dimethylsulfide complex (1.5 mL, 15.8 mmol) was added under an atmosphere of nitrogen. After stirring for 16 hours at room temperature, the solvent was removed *in vacuo* (the volatiles collected were later quenched *via* addition of water) to reveal a white solid. Recrystallisation from dry hexane, washing with cold dry hexane gave the phosphinite borane complex **31** as a white solid (0.92 g, 76% yield). **m.p.** (sample crystallized *via* slow evaporation of dichloromethane) 102-103 °C; **^{1}H NMR** (400 MHz, d_6-benzene) δ = 7.88-7.83 (m, 4H), 7.10-7.08 (m, 2H), 7.04-6.96 (m, 6H), 6.93-6.89 (m, 2H), 6.80-6.76 (m, 1H), 2.31-1.57 (br, q (*unresolved*), 3H); **^{13}C{^{1}H} NMR** (100 MHz, d_6-benzene) δ = 155.9 (d, $J_{C\text{-}P}$ 4.7 Hz), 132.6 (d, $J_{C\text{-}P}$ 61.9 Hz), 132.1 (d, $J_{C\text{-}P}$ 2.4 Hz), 131.0 (d, $J_{C\text{-}P}$ 11.5 Hz), 129.7 (s), 128.9 (d, $J_{C\text{-}P}$ 10.5 Hz), 125.0 (s), 121.2 (d, $J_{C\text{-}P}$ 4.2 Hz); **^{11}B{^{1}H} NMR** (128 MHz, d_6-benzene) δ = −38.6 (br, d, $^{1}J_{B\text{-}P}$ 52 Hz); **^{31}P{^{1}H} NMR** (162 MHz, d_6-benzene) δ = 110.8 (br, unresolved multiplet); **IR** (solid, intense peaks only, cm^{-1}) ν = 2340, 1587, 1487, 1437, 1183, 1112, 1061, 997, 909, 774, 755, 731, 687, 623, 609, 554, 503; **MS** (ESI): m/z (%) 607 (M_2Na^+), 315 (MNa^+); **HRMS** (ESI) calculated: $C_{18}H_{18}O_1{}^{11}B_1{}^{23}Na_1P_1$ 315.10806, found: 315.10830.

Unstable in $CDCl_3$.

Diphenylphenylphosphonite borane complex, 32

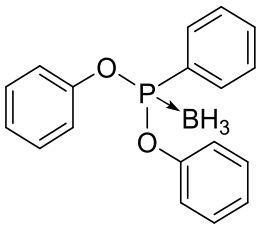

To a solution of phenol (0.19 g, 2.0 mmol) and 4-dimethylaminopyridine (0.05 g, 0.4 mmol) in dry, degassed THF (10 mL) was added trimethylamine (0.6 mL, 4.3 mmol) under an atmosphere of nitrogen. The resultant solution was cooled to 0 °C before dichlorophenylphosphine (0.13 mL, 0.96 mmol) was added whereupon the rapid formation of a white precipitate was observed. After 10 minutes, the reaction mixture was allowed to warm to room temperature and left stirring for 16.5 hours. Volatiles were removed *in vacuo* to reveal a pale yellow solid that was redissolved in hexane:ethyl acetate (9:1, 10 mL) and filtered through a plug of Celite and basic alumina. Solvent was removed *in vacuo* and the remaining solid dissolved in dry, degassed dichloromethane (5 mL) before addition of borane dimethylsulfide complex (0.5 mL, 5.3 mmol) under an atmosphere of nitrogen. The reaction mixture was left stirring for a further 16 hours at room temperature, at which point the solvent was removed *in vauco* (the volatiles collected were later quenched *via* addition of water) to reveal a colourless viscous liquid. This was redissolved in 9:1 hexane:ethyl acetate and filtered through silica, eluting with the same solvent mixture. Removal of solvent *in vacuo* gave the phosphonite borane complex **32** as a colourless oil (0.17 g, 59% yield). Colourless crystalline solid was observed after storage of **32** for several weeks under an atmosphere of nitrogen. **^{1}H NMR** (400 MHz, d_6-benzene) δ = 7.99-7.94 (m, 2H), 7.12-7.08 (m, 4H), 7.05-6.96 (m, 3H), 6.93-6.89 (m, 4H), 2.07-1.31 (br, q (*unresolved*), 3H); **^{13}C{^{1}H} NMR** (126 MHz, d_6-benzene) δ = 152.1 (d, $J_{C\text{-}P}$ 7.4 Hz), 133.0 (d, $J_{C\text{-}P}$ 2.0 Hz), 131.4 (d, $J_{C\text{-}P}$ 13.8 Hz), 131.4 (d, $J_{C\text{-}P}$ 75.0 Hz), 129.9 (s), 128.8 (d, $J_{C\text{-}P}$ 11.2 Hz), 125.5 (s), 121.6 (d, $J_{C\text{-}P}$ 4.0 Hz); **^{11}B{^{1}H} NMR** (128 MHz, d_6-benzene) δ = −39.9 (br, d, $^{1}J_{B\text{-}P}$ 65 Hz); **^{31}P{^{1}H} NMR** (162 MHz, d_6-benzene) δ = 135.1 (br, unresolved multiplet); **IR** (liquid, intense peaks only, cm^{-1}) ν = 2395, 1590, 1487, 1438, 1205, 1182, 1160, 1122, 913, 895, 780, 750, 735, 686, 629, 610; **MS** (ESI): m/z (%) 331 (MNa^+); **HRMS** (ESI) calculated: $C_{18}H_{18}O_2{}^{11}B_1{}^{23}Na_1P_1$ 331.10297, found: 331.10330.

Triphenylphosphite borane complex, 33

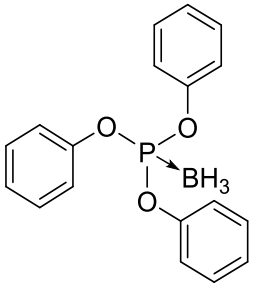

To a solution of triphenylphosphite (0.6 mL, 2.3 mmol) in dry degassed dichloromethane (8 mL), borane dimethylsulfide complex (0.8 mL, 8.4 mmol) was added under an atmosphere of nitrogen. After stirring for 16 hours at room temperature, water (10 mL) was added and the reaction was stirred for a further 2 hours. A significant

amount of effervescence was observed during this period and consequently the vessel was opened to prevent an accumulation of pressure. The reaction mixture was poured onto water (5 mL) and extracted into dichloromethane (3 x 15 mL). The combined organics were washed with a saturated aqueous $NaHCO_3$ solution (20 mL), dried over $MgSO_4$, filtered, and the solvent was removed *in vacuo* to afford a white solid. This was redissolved in dichloromethane and filtered through silica, eluting with dichloromethane. Removal of solvent *in vacuo* gave the phosphite borane complex **33** as a white solid (0.42 g, 57% yield). **^{1}H NMR** (300 MHz, $CDCl_3$) δ = 7.41-7.37 (m, 6H), 7.29-7.20 (m, 9H), 0.97-0.27 (br, q (*unresolved*), 3H); **^{13}C{^{1}H} NMR** (125 MHz, $CDCl_3$) δ = 150.4 (d, $J_{C\text{-}P}$ 6.9 Hz), 130.0 (s), 125.9 (s), 121.1 (d, $J_{C\text{-}P}$ 3.9 Hz); **^{11}B{^{1}H} NMR** (128 MHz, $CDCl_3$) δ = −42.4 (br, d, $^1J_{B\text{-}P}$ 80 Hz); **^{31}P{^{1}H} NMR** (162 MHz, $CDCl_3$) δ = 107.0 (br, app. q (*unresolved*)).

Data are in accordance with that previously reported.[6]

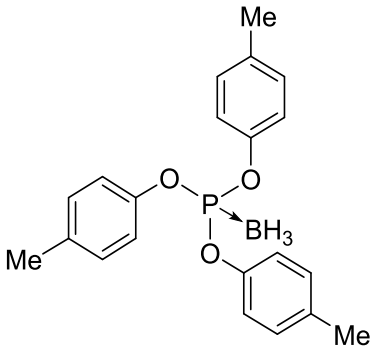

Tris(*p*-tolyl)phosphite borane complex, 34

To a solution of tri(*p*-tolyl)phosphite (0.3 mL, 0.9 mmol) in dry degassed dichloromethane (2.5 mL), borane dimethylsulfide complex (0.4 mL, 4.2 mmol) was added under an atmosphere of nitrogen. After stirring for 16 hours at room temperature, the reaction mixture was concentrated *in vacuo* (the volatiles collected were later quenched *via* addition of water), and triturated from hexane. Filtration and removal of remaining solvent *in vacuo* gave the phosphite borane complex **34** as a white solid (0.089 g, 62% yield). **m.p.** (sample crystallized *via* slow evaporation of dichloromethane) 98-99 °C; **^{1}H NMR** (400 MHz, $CDCl_3$) δ = 7.13 (d, $J_{H\text{-}H}$ 8.4 Hz, 6H), 7.06 (d, $J_{H\text{-}H}$ 8.4 Hz, 6H), 2.33 (s, 9H), 0.88-0.21 (br, q (*unresolved*), 3H); **^{13}C{^{1}H} NMR** (100 MHz, $CDCl_3$) δ = 148.2 (d, $J_{C\text{-}P}$ 6.7 Hz), 135.5 (s), 130.4 (s), 120.8 (d, $J_{C\text{-}P}$ 3.9 Hz), 21.0 (s); **^{11}B{^{1}H} NMR** (128 MHz, $CDCl_3$) δ = −42.6 (br, d, $^1J_{B\text{-}P}$ 75 Hz); **^{31}P{^{1}H} NMR** (162 MHz, $CDCl_3$) δ = 107.1 (br, unresolved multiplet); **IR** (solid, intense peaks only, cm^{-1}) ν = 2412, 2369, 1500, 1221, 1182, 1158, 1125, 1102, 1064, 949. 917, 824, 736, 719, 699, 640, 596, 530, 519; **MS** (ESI): m/z (%) 755 (M_2Na^+), 359 (MNa^+); **HRMS** (ESI) calculated: $C_{21}H_{24}O_3{}^{11}B_1{}^{35}Cl_3{}^{23}Na_1P_1$ 389.14483, found: 389.14450.

Di-*t*-butylcyclohexylphosphine borane complex, 35

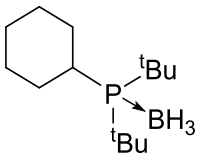

To a solution of di-t-butylcyclohexylphosphine (0.5 mL, 1.9 mmol) in dry degassed dichloromethane (5 mL), borane dimethylsulfide complex (1.8 mL, 19.0 mmol) was added under an atmosphere of nitrogen. After stirring for 17 hours at room temperature, water (5 mL) was added and the reaction was stirred for a further 2 hours. A significant amount of effervescence was observed during this period and consequently the vessel was opened to prevent an accumulation of pressure. The reaction mixture was poured onto water (5 mL) and extracted into dichloromethane (3 x 15 mL). The combined organics were washed with a saturated aqueous $NaHCO_3$ solution (20 mL), dried over $MgSO_4$, filtered, and the solvent was removed *in vacuo* to afford a white solid. This was redissolved in dichloromethane and filtered through silica, eluting with dichloromethane. Removal of solvent *in vacuo* gave the phosphine borane complex **35** as a white solid (0.38 g, 80% yield). **m.p.** (sample crystallized *via* slow evaporation of dichloromethane) 95-96 °C; **^{1}H NMR** (300 MHz, $CDCl_3$) δ = 2.35-2.29 (m, 2H), 1.84-1.69 (m, 4H), 1.56-1.46 (m, 2H), 1.32-1.18 (m, 21H), 0.80-−0.13 (*minus* 0.13) (br q, (*unresolved*), 3H); **^{13}C{^{1}H} NMR** (100 MHz, $CDCl_3$) δ = 33.3 (d, $J_{C\text{-}P}$ 24.4 Hz), 33.8 (d, $J_{C\text{-}P}$ 24.6 Hz), 30.3 (d, $J_{C\text{-}P}$ 3.1 Hz), 29.1 (s), 28.2 (d, $J_{C\text{-}P}$ 9.6 Hz), 23.4 (s; **^{11}B{^{1}H} NMR** (96 MHz, $CDCl_3$) δ = −42.3 (br, d, $^{1}J_{B\text{-}P}$ 64 Hz); **^{31}P{^{1}H} NMR** (121 MHz, $CDCl_3$) δ = 48.3 (br, app. q); **IR** (solid, intense peaks only, cm^{-1}) ν = 2926, 2868, 2377, 1480, 1463, 1447, 1366, 1142, 1070, 1024, 852, 815, 767, 639, 563; **MS** (ESI): m/z (%) 507 (M_2Na^+), 265 (MNa^+); **HRMS** (ESI) calculated: $C_{14}H_{32}{}^{11}B_1{}^{35}Cl_3{}^{23}Na_1P_1$ 265.22269, found: 265.22160.

Dicyclohexyl-*t*-butylphosphine borane complex, 36

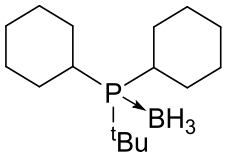

To a solution of dicyclohexyl-t-butylphosphine (0.5 mL, 1.8 mmol) in dry degassed dichloromethane (5 mL), borane dimethylsulfide complex (1.7 mL, 18.0 mmol) was added under an atmosphere of nitrogen. After stirring for 16 hours at room temperature, water (5 mL) was added and the reaction was stirred for a further 2 hours. A significant amount of effervescence was observed during this period and consequently the vessel was opened to prevent an accumulation of pressure. The reaction mixture was poured onto water (10 mL) and extracted into dichloromethane (3 x 15 mL). The combined organics were washed with a saturated aqueous $NaHCO_3$ solution (20 mL), dried over $MgSO_4$, filtered, and the solvent was removed *in vacuo* to afford a white solid. This was redissolved in dichloromethane and

filtered through silica, eluting with dichloromethane. Removal of solvent *in vacuo* gave the phosphine borane complex **36** as a white solid (0.48 g, 98% yield). **m.p.** (sample crystallized *via* slow evaporation of dichloromethane) 115-117 °C; **^{1}H NMR** (300 MHz, $CDCl_3$) δ = 2.01-1.43 (m, 16H), 1.31-1.19 (m, 15H, 0.75-−0.14 (*minus* 0.14) (br q (*unresolved*), 3H); **^{13}C{^{1}H} NMR** (100 MHz, $CDCl_3$) δ = 32.7 (d, $J_{C\text{-}P}$ 27.8 Hz), 31.0 (d, $J_{C\text{-}P}$ 27.8 Hz), 28.9 (d, $J_{C\text{-}P}$ 1.9 Hz), 28.7 (d, $J_{C\text{-}P}$ 1.0 Hz), 28.4 (d, $J_{C\text{-}P}$ 1.9 Hz), 27.7 (d, $J_{C\text{-}P}$ 3.4 Hz), 27.6 (d, $J_{C\text{-}P}$ 3.4 Hz), 26.2 (d $J_{C\text{-}P}$ 1.1 Hz); **^{11}B{^{1}H} NMR** (96 MHz, $CDCl_3$) δ = −44.4 (br, d, $^{1}J_{B\text{-}P}$ 63 Hz); **^{31}P{^{1}H} NMR** (121 MHz, $CDCl_3$) δ = 38.8 (br, app. q); **IR** (solid, intense peaks only, cm^{-1}) ν = 2929, 2850, 2378, 2355, 1443, 1438, 1064, 1006, 853, 803, 745, 621, 573; **MS** (ESI): m/z (%) 535 (M_2−H^+), 291 (MNa^+), 267 (M−H^+); **HRMS** (ESI) calculated: $C_{16}H_{34}{}^{11}B_1{}^{23}Na_1P_1$ 291.23834, found: 291.23880.

Methyl-*t*-butyl(*p*-methoxyphenyl)phosphine borane complex, 37

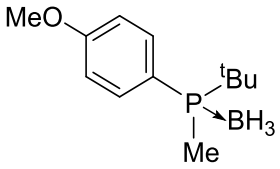

To a suspension of magnesium (0.057 g, 2.35 mmol) in dry, degassed THF (5 mL) was added *p*-bromoanisole (0.05 mL) under an atmosphere of nitrogen. The reaction mixture was heated to initiate and an additional 0.15 mL of *p*-bromoanisole (total = 0.2 mL, 1.60 mmol) were added dropwise over the course of 1 hour. The reaction mixture was refluxed under an atmosphere of nitrogen for 3 hours, before being cooled to room temperature and diluted with dry, degassed THF (6 mL). The reaction mixture was added dropwise to a solution of chloro-*t*-butylmethylphosphine (90% excluding diethyl ether, used as purchased from Sigma Aldrich, 0.1 mL, maximum 0.61 mmol) at −78 °C in THF (2 mL) over 30 mins, under an atmosphere of nitrogen. After 1 hour stirring at −78 °C, the reaction mixture was warmed to warm to ambient temperature and stir for a further hour. Degassed water (10 mL) was added and extracted with degassed diethyl ether (2 x 20 mL) and solvent removed *in vacuo* to reveal a yellow oil. Dry, degassed dichloromethane (1.5 mL) and borane dimethylsulfide complex (0.5 mL, 5.3 mmol) were added under an atmosphere of nitrogen, and the resulting solution left to stir for 18 hours at ambient temperature. Water (10 mL) was added and the mixture left to stir for a further two hours, a significant amount of effervescence was observed during this period and consequently the vessel was opened to prevent an accumulation of pressure. The reaction mixture was poured onto water (10 mL) and extracted into dichloromethane (3 x 20 mL). The combined organics were washed with a saturated aqueous $NaHCO_3$ solution (25 mL), dried over $MgSO_4$, filtered, and the solvent was removed *in vacuo* to afford a white solid. This was redissolved in dichloromethane and

filtered through silica, eluting with dichloromethane. Removal of solvent *in vacuo* gave a white solid, that was purified by column chromatography (eluting with 15% ethylacetate:hexane) to phosphine borane **37** as a white solid (0.008 g, 7%). **m.p.** (bulk sample) 63-64 °C; **^{1}H NMR** (400 MHz, $CDCl_3$) δ = 7.66-7.60 (m, 2H), 6.99-6.95 (m, 2H), 3.84 (s, 3H), 1.54 (d, $J_{H\text{-}P}$ 9.7 Hz, 3H), 1.09 (d, $J_{H\text{-}P}$ 13.9 Hz, 9H), 1.04-0.35 (br, q (*unresolved*), 3H); **^{13}C{^{1}H} NMR** (125 MHz, $CDCl_3$) δ = 162.1 (d, $J_{C\text{-}P}$ 2.4 Hz), 134.7 (d, $J_{C\text{-}P}$ 9.3 Hz), 118.4 (d, $J_{C\text{-}P}$ 54.9 Hz), 114.1 (d, J 10.3 Hz), 55.5 (s), 28.8 (d, $J_{C\text{-}P}$ 11.3 Hz), 25.3 (d, $J_{C\text{-}P}$ 2.8 Hz), 5.3 (d, $J_{C\text{-}P}$ 38.2 Hz); **^{11}B{^{1}H} NMR** (128 MHz, $CDCl_3$) δ = −40.4 (br, m); **^{31}P{^{1}H} NMR** (162 MHz, $CDCl_3$) δ = 23.2 (br, app. q (*unresolved*)); **IR** (solid, intense peaks only, cm^{-1}) ν = 2383, 2354, 1597, 1503, 1459, 1363, 1292, 1252, 1182, 1141, 1111, 1070, 1019, 905, 896, 885, 834, 814, 803, 781, 743, 648, 630, 622, 558, 522; **MS** (ESI): m/z (%) 471 (M_2Na^+), 247 (MNa^+); **HRMS** (ESI) calculated: $C_{12}H_{22}O_1{}^{11}B_1{}^{23}Na_1P_1$ 247.13936, found: 247.14110.

Dicyclohexyl(*o*-tolyl)phosphine borane complex, 38

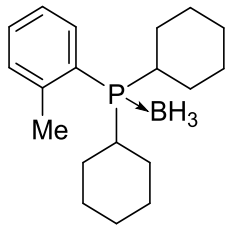

To a solution of dicyclohexyl(*o*-tolyl)phosphine (0.51 g, 1.8 mmol) in dry degassed dichloromethane (5 mL), borane dimethylsulfide complex (1.5 mL, 15.8 mmol) was added under an atmosphere of nitrogen. After stirring for 16 hours at room temperature, water (5 mL) was added and the reaction was stirred for a further 2 hours. A significant amount of effervescence was observed during this period and consequently the vessel was opened to prevent an accumulation of pressure. The reaction mixture was poured onto water (10 mL) and extracted into dichloromethane (3 x 15 mL). The combined organics were washed with a saturated aqueous $NaHCO_3$ solution (20 mL), dried over $MgSO_4$, filtered, and the solvent was removed *in vacuo* to afford a white solid. This was redissolved in dichloromethane and filtered through silica, eluting with dichloromethane. Removal of solvent *in vacuo* gave the phosphine borane complex **38** as a white solid (0.50 g, 94% yield). **m.p.** (sample crystallized *via* slow evaporation of toluene) 117-118 °C; **^{1}H NMR** (400 MHz, $CDCl_3$) δ = 7.83-7.79 (m, 1H), 7.38-7.33 (m, 1H), 7.26-7.20 (m, 2H), 2.56 (s, 3H), 2.28-2.18 (m, 2H), 1.99-1.94 (m, 2H), 1.85-1.80 (m, 2H), 1.74-1.65 (m, 4H), 1.58-1.47 (m, 2H), 1.42-0.26 (m, 13H, (inc. q (*unresolved*), BH_3); **^{13}C{^{1}H} NMR** (100 MHz, $CDCl_3$) δ = 143.0 (d, $J_{C\text{-}P}$ 4.8 Hz), 135.7 (d, $J_{C\text{-}P}$ 11.2 Hz), 131.8 (d, $J_{C\text{-}P}$ 7.6 Hz), 131.0 (d, $J_{C\text{-}P}$ 2.4 Hz), 125.8 (d, $J_{C\text{-}P}$ 10.4 Hz), 124.9 (d, $J_{C\text{-}P}$ 45.4 Hz), 33.8 (d, $J_{C\text{-}P}$ 32.9 Hz), 28.1 (s), 27.3 (d, $J_{C\text{-}P}$ 1.1 Hz), 27.2 (d, $J_{C\text{-}P}$ 10.6 Hz), 27.1 (d, $J_{C\text{-}P}$ 11.6 Hz), 26.0 (d, 1.3 $J_{C\text{-}P}$ Hz), 23.0 (d, $J_{C\text{-}P}$ 2.4 Hz); **^{11}B{^{1}H} NMR** (96 MHz,

$CDCl_3$) δ = −42.6 (br, d, $^1J_{B\text{-}P}$ 54 Hz); **$^{31}P\{^1H\}$ NMR** (121 MHz, $CDCl_3$) δ = 30.9 (br, app. d); **IR** (solid, intense peaks only, cm^{-1}) ν = 2926, 2853, 2383, 1448, 1135, 1064, 1004, 893, 853, 747, 717, 671, 596, 518; **MS** (ESI): m/z (%) 929 (M_3Na^+), 627 (M_2Na^+), 325 (MNa^+); **HRMS** (ESI) calculated: $C_{19}H_{32}{}^{11}B_1{}^{23}Na_1P_1$ 325.2226, found: 325.22240.

Thirteen peaks are observed in the $^{13}C\{^1H\}$ NMR spectrum (instead of eleven, which might be expected based on the structure). This is attributed to restricted rotation of the cyclohexyl rings around the P-C bond. A HSQC spectrum was used to assist identifying peaks observed in the $^{13}C\{^1H\}$ spectrum.

4-dimethylaminopyridine borane complex, 39

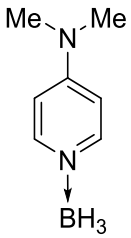

To a solution of 4-dimethylaminopyridine (0.24 g, 2.2 mmol) in dry dichloromethane (8 mL), borane dimethylsulfide complex (0.75 mL, 7.9 mmol) was added under an atmosphere of nitrogen. After stirring for 15 hours at room temperature, water (10 mL) was added and the reaction was stirred for a further 2 hours. A significant amount of effervescence was observed during this period and consequently the vessel was opened to prevent an accumulation of pressure. The reaction mixture was poured onto water (5 mL) and extracted into dichloromethane (3 x 15 mL). The combined organics were washed with a saturated aqueous $NaHCO_3$ solution (20 mL), dried over $MgSO_4$, filtered, and the solvent was removed *in vacuo* to afford a white solid. This was redissolved in dichloromethane and filtered through silica, eluting with dichloromethane. Removal of solvent *in vacuo* gave the amine borane complex **39** as a white solid (0.21 g, 72% yield). **^1H NMR** (400 MHz, $CDCl_3$) δ = 8.08 (d, $J_{H\text{-}H}$ 7.3 Hz, 2H), 6.49 (d, $J_{H\text{-}H}$ 7.3 Hz, 2H), 3.09 (s, 3H), 2.75-2.10 (br, q (*unresolved*), 3H); **$^{13}C\{^1H\}$ NMR** (125 MHz, $CDCl_3$) δ = 157.8 (s), 147.1 (s), 106.5 (s), 39.6 (s); **$^{11}B\{^1H\}$ NMR** (128 MHz, $CDCl_3$) δ = −13.9 (s).

Data are in accordance with that previously reported.[7]

4-methoxypyridine borane complex, 40

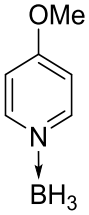

To a solution of 4-methoxypyridine (0.2 mL, 2.0 mmol) in dry dichloromethane (8 mL), borane dimethylsulfide complex (0.75 mL, 7.9 mmol) was added under an atmosphere of nitrogen. After stirring for 22 hours at room temperature, water (10 mL) was added and the reaction was stirred for a further 2 hours. A significant

amount of effervescence was observed during this period and consequently the vessel was opened to prevent an accumulation of pressure. The reaction mixture was poured onto water (5 mL) and extracted into dichloromethane (3 x 15 mL). The combined organics were washed with a saturated aqueous $NaHCO_3$ solution (20 mL), dried over $MgSO_4$, filtered, and the solvent was removed *in vacuo* to afford a white solid. This was redissolved in dichloromethane and filtered through silica, eluting with dichloromethane. Removal of solvent *in vacuo* gave the amine borane complex **40** as a white solid (0.23 g, 89% yield). **m.p.** (sample crystallized *via* slow evaporation of toluene) 93-94 °C; **^{1}H NMR** (500 MHz, $CDCl_3$) δ = 8.40 (d, $J_{H\text{-}H}$ 7.3 Hz, 2H), 6.92 (d, $J_{H\text{-}H}$ 7.3 Hz, 2H), 3.95 (s, 3H), 2.79-2.25 (br, q (*unresolved*), 3H); **^{13}C{^{1}H} NMR** (125 MHz, $CDCl_3$) δ = 167.4 (s), 149.2 (s), 111.0 (s), 56.3 (s); **^{11}B{^{1}H} NMR** (128 MHz, $CDCl_3$) δ = −12.8 (s); **IR** (solid, intense peaks only, cm^{-1}) ν =2363, 2312, 2287, 1625, 1569, 1510, 1434, 1311, 1299, 1162, 1096, 1060, 1045, 1010, 930, 834, 709, 598, 525, 515; **MS** (ESI): m/z (%) 269 (M_2Na^+), 146 (MNa^+), 122 ($[M\text{-}H]^+$); **HRMS** (ESI) calculated: $C_7H_{10}O_1N_1{}^{11}B_1{}^{23}Na_1$ 146.07477, found: 146.07440.

Data are in accordance with that previously reported.[8]

4-methylpyridine borane complex, 41

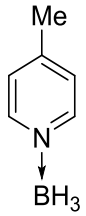

To a solution of 4-methylpyridine (0.5 mL, 5.1 mmol) in dry dichloromethane (8 mL), borane dimethylsulfide complex (2 mL, 21 mmol) was added under an atmosphere of nitrogen. After stirring for 16 hours at room temperature, water (10 mL) was added and the reaction was stirred for a further 2 hours. A significant amount of effervescence was observed during this period and consequently the vessel was opened to prevent an accumulation of pressure. The reaction mixture was poured onto water (5 mL) and extracted into dichloromethane (3 x 15 mL). Removal of solvent *in vacuo* gave a white solid, which after recrystallization from 1:1 diethyl ether:hexane gave amine borane **41** as a white solid (0.5 g, 91% yield). **^{1}H NMR** (400 MHz, $CDCl_3$) δ = 8.44 (d, $J_{H\text{-}H}$ 6.2 Hz, 2H), 7.29 (d, $J_{H\text{-}H}$ 6.2 Hz, 2H), 2.48 (s, 3H see below), 2.91-2.22 (br, q (*unresolved*), 3H see below); **^{13}C{^{1}H} NMR** (100 MHz, $CDCl_3$) δ = 151.4 (s), 147.0 (s), 126.0 (s), 21.3 (s); **^{11}B{^{1}H} NMR** (128 MHz, $CDCl_3$) δ = −12.7 (s).

The two multiplets highlighted above in the ^{1}H NMR spectra (2.48 and 2.91-2.22 ppm) overlap, the total area (2.91-2.22 ppm) integrates to 6H. The broad quartet at 2.91-2.22 ppm is attributed to the BH_3, and consequently assumed to correspond to 3H.

Data are in accordance with that previously reported.[9]

3-methylpyridine borane complex, 42

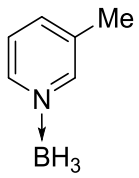

To a solution of 3-methylpyridine (0.52 mL, 5.1 mmol) in dry dichloromethane (6 mL), borane dimethylsulfide complex (1.5 mL, 15.8 mmol) was added under an atmosphere of nitrogen. After stirring for 2.5 hours at room temperature, water (10 mL) was added and the reaction was stirred for a further 2 hours. A significant amount of effervescence was observed during this period and consequently the vessel was opened to prevent an accumulation of pressure. The reaction mixture was poured onto water (5 mL) and extracted into dichloromethane (3 x 15 mL). The combined organics were washed with a saturated aqueous $NaHCO_3$ solution (25 mL), dried over $MgSO_4$, filtered, and the solvent was removed *in vacuo* to afford a colourless oil. This was redissolved in dichloromethane and filtered through silica, eluting with dichloromethane. Removal of solvent *in vacuo* gave the amine borane complex **42** as a colourless oil (0.52 g, 95% yield). **^{1}H NMR** (400 MHz, $CDCl_3$) δ = 8.45-8.41 (m, 2H), 7.72 (d, $J_{H\text{-}H}$ 7.8 Hz, 1H), 7.39 (dd, $J_{H\text{-}H}$ 7.7, 5.7 Hz, 1H), 2.42 (s, 3H see below), 2.94-2.22 (br, q (*unresolved*), 3H see below); **^{13}C{^{1}H} NMR** (100 MHz, $CDCl_3$) δ = 147.8 (s), 144.9 (s), 139.7 (s), 135.9 (s), 124.9 (s), 18.6 (s); **^{11}B{^{1}H} NMR** (128 MHz, $CDCl_3$) δ = −12.3 (s); **IR** (liquid, intense peaks only, cm^{-1}) ν = 2360, 2308, 2271, 1587, 1161, 1126, 1104, 1088, 792, 686; **MS** (ESI): m/z (%) 237 (M_2Na^+), 130 (MNa^+); **HRMS** (ESI) calculated: $C_6H_{10}N_1{}^{11}B_1{}^{23}Na_1$ 130.07985, found: 130.08110.

The two multiplets highlighted above in the ^{1}H NMR spectra (2.42 and 2.94-2.22 ppm) overlap, the total area (2.94-2.22 ppm) integrates to 6H. The broad quartet at 2.94-2.22 ppm is attributed to the BH_3, and consequently assumed to correspond to 3H.

Data are in accordance with that previously reported.[10]

Pyridine borane complex, 43

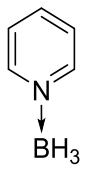

To a solution of pyridine (0.1 mL, 1.2 mmol) in dry dichloromethane (5 mL), borane dimethylsulfide complex (0.5 mL, 5.3 mmol) was added under an atmosphere of nitrogen. After stirring for 16 hours at room temperature, water (10 mL) was added and the reaction was stirred for a further 2 hours. A significant amount of effervescence was observed during this period and consequently the vessel was opened to prevent an accumulation of pressure. The reaction mixture was poured onto water (5 mL) and extracted into dichloromethane (3 x 15 mL). The combined organics were washed with a saturated aqueous $NaHCO_3$ solution (20 mL), dried over $MgSO_4$, filtered, and the solvent was removed *in vacuo* to afford a white solid. This was redissolved in

dichloromethane and filtered through silica, eluting with dichloromethane. Removal of solvent *in vacuo* gave the amine borane complex **43** as a colourless liquid (0.95 g, 82% yield). **^{1}H NMR** (400 MHz, $CDCl_3$) δ = 8.63 (d, $J_{H\text{-}H}$ 5.6 Hz, 2H), 7.93 (m, 1H), 7.52 (m, 2H), 3.01-2.29 (br, q (*unresolved*), 3H); **^{13}C{^{1}H} NMR** (100 MHz, $CDCl_3$) δ = 147.7 (s), 139.4 (s), 125.4 (s); **^{11}B{^{1}H} NMR** (128 MHz, $CDCl_3$) δ = −12.2 (s).

Commerically available, data are in accordance with that previously reported.[11]

4-trifluoromethylpyridine borane complex, 44

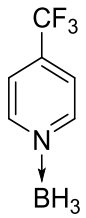

To a solution of 4-trifluoromethylpyridine (0.2 mL, 1.7 mmol) in dry dichloromethane (6 mL), borane dimethylsulfide complex (0.6 mL, 6.3 mmol) was added under an atmosphere of nitrogen. After stirring for 16 hours at room temperature, water (5 mL) was added and the reaction was stirred for a further 2 hours. A significant amount of effervescence was observed during this period and consequently the vessel was opened to prevent an accumulation of pressure. The reaction mixture was poured onto water (5 mL) and extracted into dichloromethane (3 x 10 mL). The combined organics were washed with a saturated aqueous $NaHCO_3$ solution (20 mL), dried over $MgSO_4$, filtered, and the solvent was removed *in vacuo* to afford a white solid. This was redissolved in dichloromethane and filtered through silica, eluting with dichloromethane. Removal of solvent *in vacuo* gave the amine borane complex **44** as a white solid (0.26 g, 95% yield). **m.p.** (sample crystallized *via* slow evaporation of toluene) 78-79 °C; **^{1}H NMR** (400 MHz, $CDCl_3$) δ = 8.85 (d, $J_{H\text{-}H}$ 6.2 Hz, 2H), 7.77 (d, $J_{H\text{-}H}$ 6.2 Hz, 2H), 3.01-2.34 (br, q (*unresolved*), 3H); **^{13}C{^{1}H} NMR** (125 MHz, $CDCl_3$) δ = 148.9 (s), 141.1 (q, $J_{C\text{-}F}$ 35.5 Hz), 121.9 (q, $J_{C\text{-}F}$ 3.4 Hz), 121.8 (q, $J_{C\text{-}F}$ 274.1 Hz); **^{11}B{^{1}H} NMR** (128 MHz, $CDCl_3$) δ = −11.5 (s); **IR** (solid, intense peaks only, cm^{-1}) ν = 2372, 2286, 1432, 1318, 1130, 1112, 1089, 1058, 930, 835, 800, 736, 709, 598, 548; **MS** (ESI): m/z (%) 345 (M_2Na^+), 184 (MNa^+); **HRMS** (ESI) calculated: $C_6H_7N_1{}^{11}B_1F_3{}^{23}Na_1$ 184.05159, found: 184.05130.

Data are in accordance with that previously reported.[8]

2-methylpyridine borane complex, 45

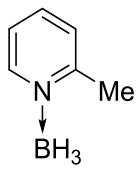

To a solution of 2-methylpyridine (0.5 mL, 5.1 mmol) in dry dichloromethane (6 mL), borane dimethylsulfide complex (1.5 mL, 15.8 mmol) was added under an atmosphere of nitrogen. After stirring for 15 hours at room temperature, the reaction mixture was subject to vacuum, (waste collected in a

trap at −78 °C, and quenched later) to afford a white solid. This was dissolved in dichloromethane and filtered through silica, eluting with dichloromethane. Removal of solvent *in vacuo* gave the amine borane complex **45** as a white solid (0.53 g, 98% yield). **m.p.** (sample crystallized *via* slow evaporation of dichloromethane) 45-46 °C; **^{1}H NMR** (400 MHz, $CDCl_3$) δ = 8.76 (d, $J_{H\text{-}H}$ 5.7 Hz, 1H), 7.81 (t, $J_{H\text{-}H}$ 7.8 Hz, 1H), 7.37 (d, $J_{H\text{-}H}$ 7.8 Hz, 1H), 7.31-7.27 (m, 1H), 2.77 (s, 3H see below), 2.84-2.12 (br, q (*unresolved*), 3H see below); **^{13}C{^{1}H} NMR** (100 MHz, $CDCl_3$) δ = 158.1 (s), 149.0 (s), 139.7 (s), 126.9 (s), 122.6 (s), 22.8 (s); **^{11}B{^{1}H} NMR** (128 MHz, $CDCl_3$) δ = −13.8 (s); **IR** (solid, intense peaks only, cm^{-1}) ν = 2398, 2367, 2330, 2261, 1618, 1571, 1493, 1481, 1459, 1422, 1380, 1297, 1246, 1182, 1120, 1088, 1042, 938, 764, 755, 712; **MS** (ESI): m/z (%) 237 (M_2Na^+), 130 (MNa^+); **HRMS** (ESI) calculated: $C_6H_{10}N_1{}^{11}B_1{}^{23}Na_1$ 130.07985, found: 130.08140.

The two multiplets highlighted above in the ^{1}H NMR spectra (2.77 and 2.84-2.12 ppm) overlap, the total area (2.77-2.12 ppm) integrates to 6H. The broad quartet at 2.84-2.12 ppm is attributed to the BH_3, and consequently assumed to correspond to 3H.

Data are in accordance with that previously reported.[10,12]

2-methoxypyridine borane complex, 46

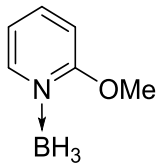

To a solution of 2-methoxypyridine (0.3 mL, 2.8 mmol) in dry dichloromethane (5 mL), borane dimethylsulfide complex (0.8 mL, 8.4 mmol) was added under an atmosphere of nitrogen. After stirring for 16 hours at room temperature, water (10 mL) was added and the reaction stirred for a further 2 hours. A significant amount of effervescence was observed during this period and consequently the vessel was opened to prevent an accumulation of pressure. The reaction mixture was poured onto water (10 mL) and extracted into dichloromethane (3 x 15 mL). The combined organics were washed with a saturated aqueous $NaHCO_3$ solution (25 mL), dried over $MgSO_4$, filtered, and the solvent was removed *in vacuo* to afford a white solid. This was redissolved in dichloromethane and filtered through silica, eluting with dichloromethane. Removal of solvent *in vacuo* gave the amine borane complex **46** as a white solid (0.3 g, 94% yield). **m.p.** (sample crystallized *via* slow evaporation of dichloromethane) 68-69 °C; **^{1}H NMR** (400 MHz, $CDCl_3$) δ = 8.51 (d, $J_{H\text{-}H}$ 5.6 Hz, 1H), 7.95-7.91 (m, 1H), 7.06-7.02 (m, 1H), 6.96 (d, $J_{H\text{-}H}$ 8.4 Hz, 1H), 4.10 (s, 3H), 2.76-2.07 (br, q (*unresolved*), 3H); **^{13}C{^{1}H} NMR** (100 MHz, $CDCl_3$) δ = 163.1 (s), 148.6 (s), 142.8 (s), 117.0 (s), 107.7 (s), 57.1 (s); **^{11}B{^{1}H} NMR** (128 MHz, $CDCl_3$) δ = −15.1 (s); **IR** (solid, intense peaks only,

cm^{-1}) ν = 2361, 2316, 2272, 1622, 1574, 1494, 1432, 1307, 1179, 1155, 1128, 1083, 1050, 1017, 929, 805, 764, 733, 703, 594, 525; **MS** (ESI): m/z (%) 146 (MNa^+), 122 ($[M-H]^+$); **HRMS** (ESI) calculated: $C_6H_{10}O_1N_1{}^{11}B_1{}^{23}Na_1$ 146.07477, found: 146.07550.

Data are in accordance with that previously reported.[12]

2-*i*-propylpyridine borane complex, 47

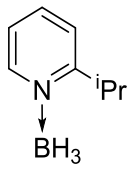

To a solution of 2-isopropylpyridine (0.3 mL, 3.6 mmol) in dry dichloromethane (6 mL), borane dimethylsulfide complex (1.0 mL, 10.5 mmol) was added under an atmosphere of nitrogen. After stirring for 16 hours at room temperature, the reaction mixture was subject to vacuum, (waste collected in a trap at −78 °C, and quenched later) to afford a colourless oil. This was cooled to −78 °C, to give a white solid, which was washed with cold dry hexane. Warming to room temperature and removal of any remaining solvent *in vauco* gave the amine borane complex **47** as a colourless oil (0.4 g, 85% yield). **^{1}H NMR** (400 MHz, $CDCl_3$) δ = 8.74 (d, $J_{H\text{-}H}$ 5.8 Hz, 1H), 7.88 (t, $J_{H\text{-}H}$ 7.8 Hz, 1H), 7.46 (app. d, $J_{H\text{-}H}$ 7.8 Hz, 1H), 7.25 (ddd, $J_{H\text{-}H}$ 7.3, 5.8, 1.4 Hz, 1H), 4.20 (septet, $J_{H\text{-}H}$ 6.9 Hz, 1H), 2.94-2.23 (br, q (*unresolved*), 3H), 1.31 (d, $J_{H\text{-}H}$ 6.9 Hz, 6H); **^{13}C{^{1}H} NMR** (100 MHz, $CDCl_3$) δ = 167.4 (s), 149.1 (s), 140.0 (s), 122.8 (s), 122.2 (s), 31.4 (s), 22.2 (s); **^{11}B{^{1}H} NMR** (128 MHz, $CDCl_3$) δ = −13.8 (s); **IR** (solid, intense peaks only, cm^{-1}) ν = 2372, 2336, 1617, 1572, 1486, 1145, 1186, 1153, 1071, 930, 774, 750, 543; **MS** (ESI): m/z (%) 239 (M_2Na^+), 158 (MNa^+); **HRMS** (ESI) calculated: $C_8H_{14}N_1{}^{11}B_1{}^{23}Na_1$ 158.11115, found: 158.11100.

2,6-dimethylpyridine borane complex, 48

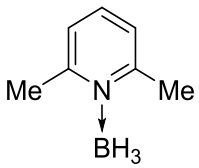

To a solution of 2,6-dimethylpyridine (0.5 mL, 4.3 mmol) in dry dichloromethane (6 mL), borane dimethylsulfide complex (1.2 mL, 12.7 mmol) was added under an atmosphere of nitrogen. After stirring for 16 hours at room temperature, water (10 mL) was added and the reaction was stirred for a further 2 hours. A significant amount of effervescence was observed during this period and consequently the vessel was opened to prevent an accumulation of pressure. The reaction mixture was poured onto water (10 mL) and extracted into dichloromethane (3 x 15 mL). The combined organics were washed with a saturated aqueous $NaHCO_3$ solution (25 mL), dried over $MgSO_4$, filtered, and the solvent was removed *in vacuo* to afford the amine borane complex **48** as a white solid (0.45 g, 88% yield). **^{1}H NMR** (400 MHz, $CDCl_3$)

δ = 8.63 (t, $J_{H\text{-}H}$ 7.7 Hz, 1H), 7.22 (d, $J_{H\text{-}H}$ 7.7 Hz, 2H), 2.80 (s, 6H), 2.65-1.94 (br, q (*unresolved*), 3H); **^{13}C{^{1}H} NMR** (100 MHz, $CDCl_3$) δ = 158.6 (s), 138.2 (s), 124.8 (s), 25.4 (s); **^{11}B{^{1}H} NMR** (128 MHz, $CDCl_3$) δ = −18.3 (s).

Data are in accordance with that previously reported.[13]

3-bromo-5-methylpyridine borane complex, 49

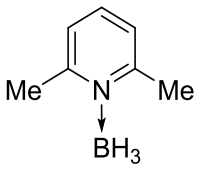

To a solution of 3-bromo-5-methylpyridine (0.35 mL, 3.0 mmol) in dry dichloromethane (6 mL), borane dimethylsulfide complex (0.8 mL, 8.4 mmol) was added under an atmosphere of nitrogen. After stirring for 14 hours at room temperature, water (10 mL) was added and the reaction was stirred for a further 2 hours. A significant amount of effervescence was observed during this period and consequently the vessel was opened to prevent an accumulation of pressure. The reaction mixture was poured onto water (10 mL) and extracted into dichloromethane (3 x 15 mL). The combined organics were washed with a saturated aqueous $NaHCO_3$ solution (25 mL), dried over $MgSO_4$, filtered, and the solvent was removed *in vacuo* to afford the amine borane complex **49** as a white solid (0.54 g, 98% yield). **m.p.** (sample crystallized *via* slow evaporation of dichloromethane) 106-108 °C; **^{1}H NMR** (400 MHz, $CDCl_3$) δ = 8.57 (s, 1H), 8.40 (s, 1H), 7.88 (s, 1H), 2.42 (s, 3H see below), 2.91-2.22 (br, q (*unresolved*), 3H see below); **^{13}C{^{1}H} NMR** (100 MHz, $CDCl_3$) δ = 146.4 (s), 146.3 (s), 142.4 (s), 137.2 (s), 120.6 (s), 18.4 (s); **^{11}B{^{1}H} NMR** (128 MHz, $CDCl_3$) δ = −11.9 (s); **IR** (solid, intense peaks only, cm^{-1}) ν = 2369, 1569, 1463, 1180, 1159, 1136, 1118, 871, 734, 674, 532; **MS** (EI): m/z (%) 146 (M^+); **HRMS** (EI) calculated: $C_6H_9N_1{}^{11}B_1{}^{79}Br_1$ 185.00059, found: 184.99900.

The singlet and broad quartet highlighted above in the ^{1}H spectrum (2.42 and 2.91-2.22 ppm) overlap, with the total area integrating to 6H. The broad quartet at 2.92-2.22 ppm is attributed to the BH_3, and consequently, assigned to 3H.

Tris(*o*-methyl-3,4,5,6-d_4-phenyl)phosphine, S1

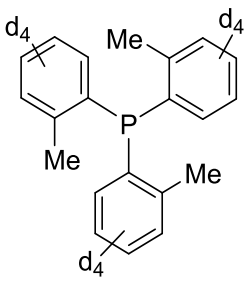

To a solution of magnesium (0.067 g, 2.7 mmol) in dry, degassed THF (12 mL) was added 3,4,5,6-d_4-*o*-bromotoluene (0.42g , 2.4 mmol) dropwise. After the addition was complete, the reaction was heated to reflux for 2 hours, before being left to cool to ambient temperature. A freshly made trichlorophosphine THF solution (0.8 M

trichlorophosphine in dry, degassed THF; made in a 5 mL volumetric flask fitted with a J. Youngs valve – 1 mL transferred to reaction vessel) was added dropwise over 30 minutes at ambient temperature. The resulting solution was stirred for 1.25 hours before the addition of 10 mL degassed water. The resulting solution was extracted with degassed diethyl ether (3 x 20 mL), dried over $MgSO_4$, filtered and the solvent was removed *in vacuo* to afford a pale yellow oil. Recrystallization from degassed ethanol gave the phosphine **S1** as a white solid. (0.044 g, 6% yield). **m.p.** (sample recrystallized from ethanol) 125-126 °C; **^{1}H NMR** (400 MHz, $CDCl_3$) δ = 2.39 (d, $^{4}J_{H\text{-}P}$ 1.42 Hz, 9H); **^{2}H NMR** (400 MHz, $CHCl_3$) δ = 7.28 (app. s, estimated as 2H, *overlap with residual $CDCl_3$*), 7.11 (app. s, 1H), 6.76 (app. s, 1H); **^{13}C{^{1}H,^{2}H} NMR** (100 MHz, $CDCl_3$) δ = 142.8 (d, $J_{C\text{-}P}$ 26.4 Hz), 134.5 (d, $J_{C\text{-}P}$ 10.9 Hz), 132.8 (s), 129.8 (d, $J_{C\text{-}P}$ 4.9 Hz), 128.3 (s), 125.8 (s), 21.3 (d, $J_{C\text{-}P}$ 21.4 Hz); **^{31}P{^{1}H} NMR** (162 MHz, $CDCl_3$) δ = −30. (s); **IR** (solid, intense peaks only, cm^{-1}) ν = 1558, 1537, 1439, 1380, 1328, 836, 754, 720, 590, 540.

Di-*t*-butyl-(*o*-biphenyl)phosphine borane complex, S2

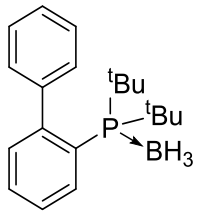

To a solution of di-*t*-butyl(*o*-biphenyl)phosphine (0.060 g, 0.20 mmol) in dry, degassed dichloromethane (2 mL), borane dimethylsulfide complex (0.10 mL, 1.0 mmol) was added under an atmosphere of nitrogen. After stirring for 16 hours at room temperature, water (4 mL) was added and the reaction was stirred for a further 2 hours. A significant amount of effervescence was observed during this period, and consequently the vessel was opened to prevent an accumulation of pressure. The reaction mixture was poured onto water (5 mL) and then extracted into dichloromethane (3 x 10 mL). The combined organics were washed with a saturated aqueous $NaHCO_3$ solution (20 mL), dried over $MgSO_4$, filtered, and the solvent was removed *in vacuo* to afford a white solid. This was redissolved in dichloromethane and filtered through silica, eluting with dichloromethane. Removal of solvent *in vacuo* gave phosphine borane complex **S2** as a white solid (0.052 g, 84% yield). **m.p.** (sample crystallized *via* slow evaporation of dichloromethane) 119-120 °C; **^{1}H NMR** (500 MHz, $CDCl_3$) δ = 7.98 (t, *J* 7.6 Hz, 1H), 7.47-7.28 (m, 5H), 7.24-7.21 (m, 1H), 7.17-7.15 (m, 2H), 1.32 (d, $^{3}J_{H\text{-}P}$ 12.9 Hz, 18H), 0.27-−0.27 (*minus 0.27*) (br, q (*unresolved*), 3H); **^{13}C{^{1}H} NMR** (125 MHz, $CDCl_3$) δ = 150.9, 150.8, 142.3, 142.2, 135.5, 133.6, 133.5, 130.4, 129.86, 129.85, 127.4, 126.9, 125.6, 125.5, 125.4, 125.3, 34.9 (d, $J_{C\text{-}P}$ 24.6 Hz), 29.5 (d, $J_{C\text{-}P}$ 1.7 Hz), (*due to the complexity arising from coupling with ^{31}P assignments have not been made for aromatic carbons*); **^{11}B{^{1}H} NMR** (128 MHz, $CDCl_3$) δ = −39.3 (br, app. s);

$^{31}P\{^{1}H\}$ NMR (162 MHz, $CDCl_3$) δ = 49.6 (br, app. d); **IR** (solid, intense peaks only, cm^{-1}) ν = 2444.3, 2353.7, 1475, 1465, 1443, 1365, 1071, 1023, 759, 741, 697, 625, 602, 551, 543; **MS** (ESI): m/z (%) 647 (M_2Na^+), 335 (MNa^+); **HRMS** (ESI) calculated: $C_{20}H_{30}{}^{11}B_1{}^{23}Na_1P_1$ 335.20704, found: 325.20980.

Diphenylbenzylphosphine borane complex, S3

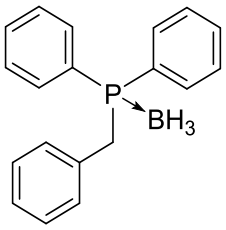

To a solution of benzyldiphenylphosphine (0.28 g, 1.01 mmol) in dry degassed dichloromethane (5 mL), borane dimethylsulfide complex (0.3 mL, 3.16 mmol) was added under an atmosphere of nitrogen. After stirring for 16 hours at room temperature, water (10 mL) was added and the reaction was stirred for a further 2 hours. A significant amount of effervescence was observed during this period and consequently the vessel was opened to prevent an accumulation of pressure. The reaction mixture was poured onto water (10 mL) and then extracted into dichloromethane (3 x 20 mL). The combined organics were washed with a saturated aqueous $NaHCO_3$ solution (25 mL), dried over $MgSO_4$, filtered, and the solvent was removed *in vacuo* to afford a white solid. This was redissolved in dichloromethane and filtered through silica, eluting with dichloromethane. Removal of solvent *in vacuo* gave phosphine borane complex **S3** as a white solid (0.27 g, 93% yield). **^{1}H NMR** (400 MHz, $CDCl_3$) δ = 7.65-7.59 (m, 4H), 7.52-7.47 (m, 2H), 7.44-7.40 (m, 4H), 7.18-7.12 (m, 3H), 6.96-6.93 (m, 2H), 3.60 (d, $^{2}J_{H\text{-}P}$ 12.0 Hz, 1H), 1.25-0.58 (br, q (*unresolved*), 3H); **$^{13}C\{^{1}H\}$ NMR** (125 MHz, $CDCl_3$) δ = 132.8 (d, $J_{C\text{-}P}$ 8.8 Hz), 132.0 (d, $J_{C\text{-}P}$ 4.2 Hz), 131.4 (d, $J_{C\text{-}P}$ 2.5 Hz), 130.4 (d, $J_{C\text{-}P}$ 4.7 Hz), 128.9 (d, $J_{C\text{-}P}$ 53.7 Hz), 128.8 (d, $J_{C\text{-}P}$ 9.9 Hz), 128.2 (d, $J_{C\text{-}P}$ 2.5 Hz), 127.1 (d, $J_{C\text{-}P}$ 3.1 Hz), 34.3 (d, $J_{C\text{-}P}$ 32.2 Hz); **$^{11}B\{^{1}H\}$ NMR** (128 MHz, $CDCl_3$) δ = −39.2 (br d, $^{1}J_{B\text{-}P}$ 48 Hz); **$^{31}P\{^{1}H\}$ NMR** (162 MHz, $CDCl_3$) δ = 18.2 (br, app. q); **IR** (solid, intense peaks only, cm^{-1}) ν = 2376, 1434, 1105, 1056, 790, 733, 694, 593, 570, 503.

Data are in accordance with that previously reported.[4]

Tri(2-furyl)phosphine borane complex, S4

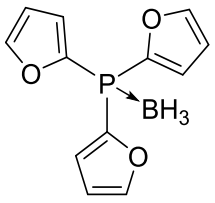

To a solution of tri(2-furyl)phosphine (0.56 g, 2.4 mmol) in dry, degassed dichloromethane (10 mL), borane dimethylsulfide complex (1.0 mL, 10.5 mmol) was added under an atmosphere of nitrogen. The reaction mixture was left stirring for 20 hours at room temperature, at

which point the solvent was removed *in vauco* (the volatiles collected were later quenched *via* addition of water) to reveal a pale yellow solid. This was redissolved in dichloromethane and filtered through silica, eluting with dichloromethane. Removal of solvent *in vacuo* gave the phosphine borane complex **S4** as a white solid (0.38 g, 64% yield). **m.p.** (sample crystallized *via* slow evaporation of dichloromethane) 59-60 °C; **^{1}H NMR** (400 MHz, d_8-toluene) δ = 7.05-7.04 (m, 1H), 7.02-7.01 (m, 1H, *overlapping with residual solvent peak*), 5.86 (dt, $^{4}J_{H\text{-}P}$ 3.5, $^{3}J_{H\text{-}H}$ 1.8 Hz, 1H), 2.27-1.55 (br, q (*unresolved*), 3H); (500 MHz, $CDCl_3$) δ = 7.76-7.75 (m, 1H), 7.17-7.16 (m, 1H), 6.51 (dt, $^{4}J_{H\text{-}P}$ 3.5, $^{3}J_{H\text{-}H}$ 1.8, Hz, 1H), 1.49-0.90 (br, q (*unresolved*), 3H); **^{13}C{^{1}H} NMR** (100 MHz, d_8-toluene) δ = 149.4 (d, $J_{C\text{-}P}$ 5.5 Hz), 143.7 (d, $J_{C\text{-}P}$ 83.2 Hz), 124.1 (d, $J_{C\text{-}P}$ 22.5 Hz), 111.6 (d, $J_{C\text{-}P}$ 8.4 Hz); (125 MHz, $CDCl_3$) δ = 149.5 (d, $J_{C\text{-}P}$ 5.5 Hz), 142.4 (d, $J_{C\text{-}P}$ 85.6 Hz), 123.8 (d, $J_{C\text{-}P}$ 22.2 Hz), 111.4 (d, $J_{C\text{-}P}$ 8.4 Hz); **^{11}B{^{1}H} NMR** (128 MHz, d_8-toluene) δ = −39.6 (app. s); **^{31}P{^{1}H} NMR** (162 MHz, d_8-toluene) δ = −24.2 (br, unresolved multiplet); **IR** (solid, intense peaks only, cm^{-1}) ν = 2396, 2351, 1550, 1460, 1369, 1214, 1132, 1069, 1056, 1008, 906, 883, 756, 652, 642, 617, 594, 502; **MS** (ESI): m/z (%) 296 (MNa^+); **HRMS** (ESI) calculated: $C_{12}H_{12}O_3{}^{11}B_1{}^{23}Na_1P_1$ 269.05096, found: 269.05190.

Tri(2-thienyl)phosphine borane complex, S5

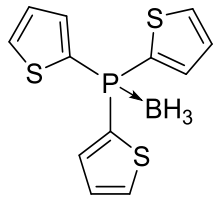

To a solution of tri(2-thienyl)phosphine (0.17 g, 0.61 mmol) in dry, degassed dichloromethane (5 mL), borane dimethylsulfide complex (0.2 mL, 2.1 mmol) was added under an atmosphere of nitrogen. The reaction mixture was left stirring for 15 hours at room temperature, at which point the solvent was removed *in vauco* (the volatiles collected were later quenched *via* addition of water) to reveal a white solid. This was redissolved in dichloromethane and filtered through silica, eluting with dichloromethane. Removal of solvent *in vacuo* gave the phosphine borane complex **S5** as a white solid (0.16 g, 87% yield). **m.p.** (sample crystallized *via* slow evaporation of dichloromethane) 113-114 °C; **^{1}H NMR** (400 MHz, $CDCl_3$) δ = 7.74 (ddd, $^{3}J_{H\text{-}H}$ 4.9, $^{4}J_{H\text{-}P}$ 3.1, $^{4}J_{H\text{-}H}$ 1.1 Hz, 3H), 7.61 (ddd, $^{3}J_{H\text{-}P}$ 7.3, $^{3}J_{H\text{-}H}$ 3.6, $^{4}J_{H\text{-}H}$ 1.1 Hz, 3H), 7.19 (ddd, $^{3}J_{H\text{-}H}$ 4.9, 3.6, $^{4}J_{H\text{-}P}$ 1.6, Hz, 3H), 1.76-1.05 (br, q (*unresolved*), 3H); **^{13}C{^{1}H} NMR** (125 MHz, $CDCl_3$) δ = 137.4 (d, $J_{C\text{-}P}$ 11.2 Hz), 134.4 (d, $J_{C\text{-}P}$ 3.5 Hz), 130.8 (d, $J_{C\text{-}P}$ 65.5 Hz), 128.6 (d, $J_{C\text{-}P}$ 12.2 Hz); **^{11}B{^{1}H} NMR** (128 MHz, $CDCl_3$) δ = −36.0 (br, d, $^{1}J_{B\text{-}P}$ 45 Hz); **^{31}P{^{1}H} NMR** (162 MHz, $CDCl_3$) δ = −3.43 (br, unresolved multiplet); **IR** (solid, intense peaks only, cm^{-1}) ν = 2383, 1400, 1332, 1218,

1088, 1050, 1008, 846, 716, 603, 566; **MS** (ESI): m/z (%) 316 (MNa^+); **HRMS** (ESI) calculated: $C_{12}H_{12}{}^{11}B_1{}^{23}Na_1P_1{}^{32}S_3$ 316.98241, found: 316.98100.

5.3 General kinetic procedures

General procedure A

Dry solvent was added to Lewis base borane adduct in an oven-dried Schlenk under at atmosphere of nitrogen. The suspension was stirred and heated (not above the desired temperature of the kinetic experiment) in an oil until all fully dissolved. Nucleophile was added to the resulting solution (t = 0) and after dissolution (typically occurring within a matter of seconds), a sample was transferred via pipette to an NMR tube. This was placed in a pre-heated NMR spectrometer and NMR experiments were run at set time intervals.

General procedure B

To an NMR tube containing Lewis base borane adduct was added a stock solution of nucloephile in dry, degassed toluene, (t = 0) to give a total volume of 0.6 mL. The NMR tube was either placed into a preheated NMR spectrometer (for *in situ* analysis), or into a water bath (tube taken to NMR spectrometer perdioically before being returned to water bath).

General procedure C – comptetition experiments

To a 10 mL volutmetic flask was added a range of Lewis bases and a reference amine borane adduct ($Me_3N{\cdot}BH_3$ or $Me_2NH{\cdot}BH_3$), the mass was recorded before and after every addition to determine the actual amounts present. Dry toluene (arrpox. 5 mL) was added, followed by borane dimethylsulfide complex, again, the mass taken before and afterwards. The volumetic flask was then filled to the graduation with dry toluene. 0.6 mL of this stock solution was then added to an NMR tube containing a large excess of quinuclidine (t = 0) which was placed in a pre-heated NMR spectrometer and NMR experiments were run at set time intervals.

5.4 Correlations with existing parameters

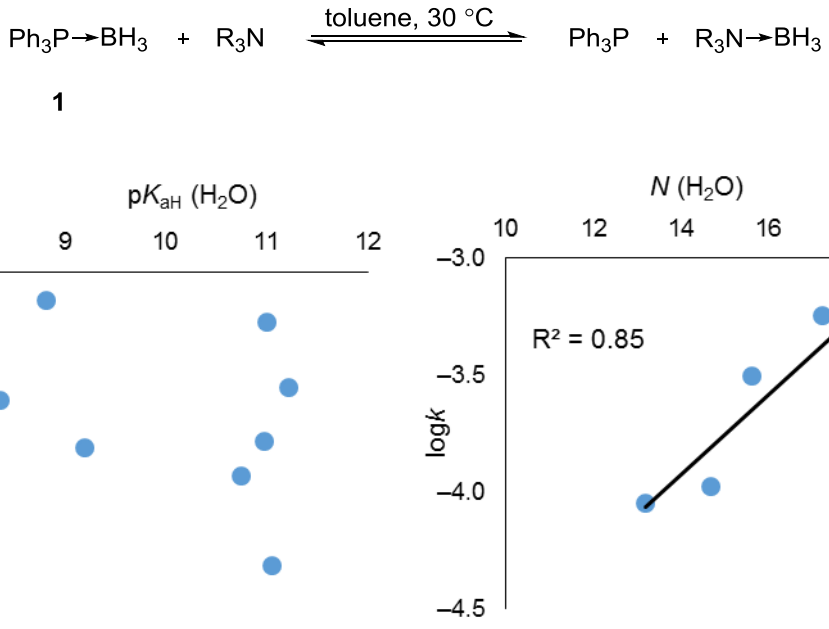

Figure 5.1 Correlation between a) aqueous pK_a[14] or b) Mayr's nucleophilicity parameter[15–20] (N) and the second order rate constant for the of displacement of Ph_3P from its borane adduct by various amines in toluene at 30 °C.

5.5 Computational details

Computational geometry optimisations were carried out in Gaussian 09 with the B3LYP density functional and a 6-31G(d) basis set.[21] Grimme's dispersion correction and a PCM solvent correction (toluene) were applied. The transition state calculation was carried out using the synchronous transit-guided quasi-Newton (STQN) method (QST2) at the same level of theory, including dispersion correction, but excluding any solvation effects. QST2 input structures include reactants **1** and **2** with a 180° P-B-N angle and a 4 Å B-N distance. The input for the products contained **3** and Ph_3P aligned in a similar manner. The transition state was confirmed by a frequency calculation to check for the presence of a single imaginary frequency and the corresponding eigenvector was found to display the expected reaction coordinate. The transition state was then subjected to a single point energy calculation using the same parameters as the geometry optimisation (i.e. including a solvation model), relative energies obtained are displayed in Figure 2.6. Detailed atomic coordinates are included in Appendix, Section 6.4.

5.5 Crystallographic structural data

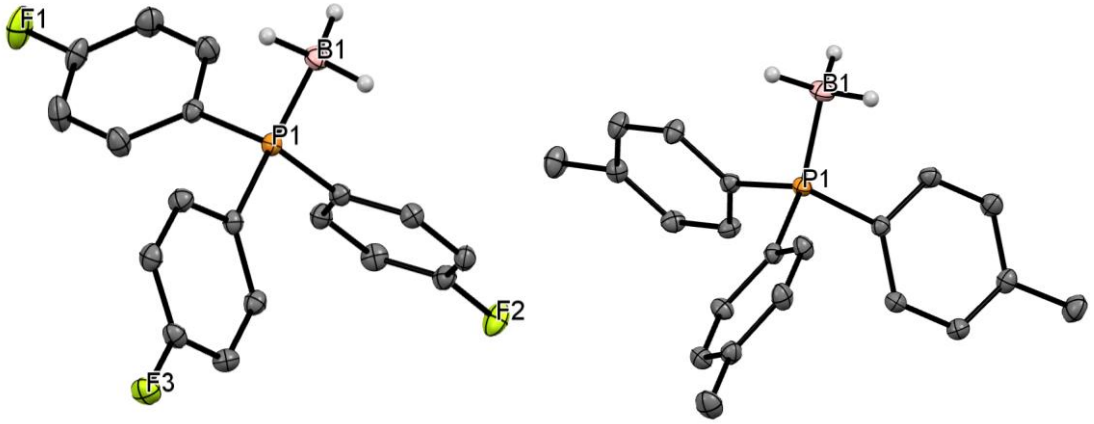

Figure 5.2 Structures of (*p*-fluorophenyl)$_3$P·BH$_3$ **9** and (*p*-tolyl)$_3$P·BH$_3$ **10**, with all non B-H hydrogens removed for clarity. Thermal ellipsoids are calculated at 50% probability. Selected bond length and angle data are presented in Table 5.1.

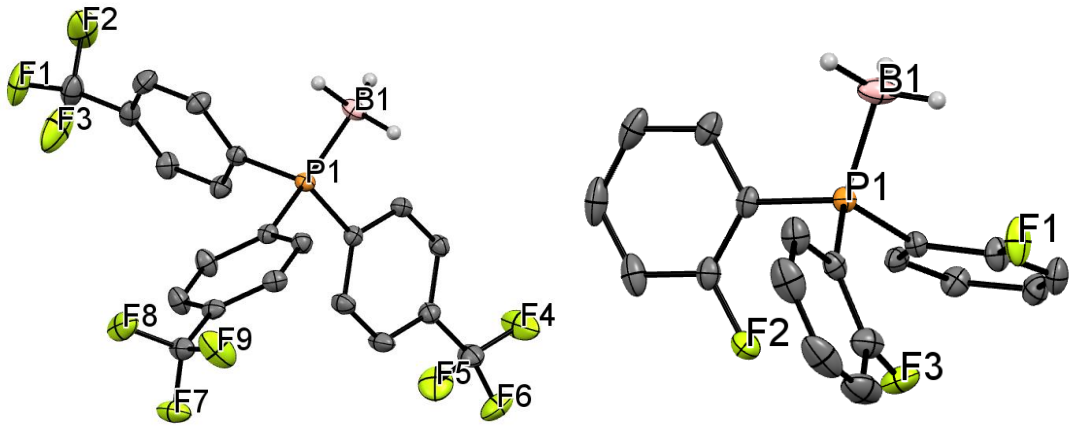

Figure 5.3 Structures of (*p*-trifluoromethylphenyl)$_3$P·BH$_3$ **5** and (*o*-fluorophenyl)$_3$P·BH$_3$ **12**, with all non B-H hydrogens removed for clarity. Thermal ellipsoids are calculated at 50% probability. Selected bond length and angle data are presented in Table 5.1.

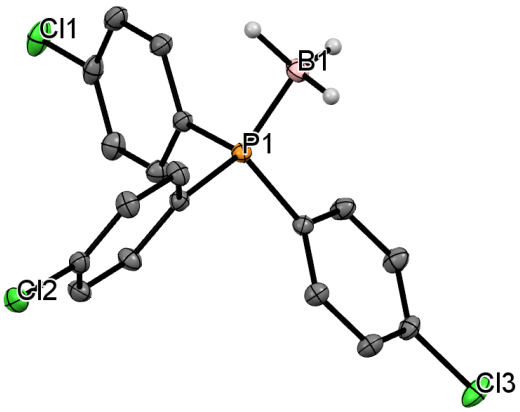

Figure 5.4 Structure of (*p*-chlorophenyl)$_3$P·BH$_3$ **4**, with all non B-H hydrogens removed for clarity Thermal ellipsoids are calculated at 50% probability. Selected bond length and angle data are presented in Table 5.1.

Table 5.1 Selected bond lengths and angles for structures in Figures 2.8, 5.2, 5.3 and 5.4.

Entry	Compound	P-B / Å	Av. C-P-C / °	Av. B-P-C / °	Av. P-C / Å
1	(*p*-tolyl)$_3$P·BH$_3$	1.9238(17)	106.45	112.33	1.807
2	(*p*-fluorophenyl)$_3$P·BH$_3$	1.9233(16)	106.10	112.66	1.814
3	(*p*-trifluoromethylphenyl)$_3$P·BH$_3$	1.9284(15)	108.19	113.32	1.815
4	(*o*-fluorophenyl)$_3$P·BH$_3$	1.919(2)	106.97	111.84	1.812
5	(*o*-methoxyphenyl)$_3$P·BH$_3$	1.949(5)	106.19	112.58	1.812
6	(*p*-chlorophenyl)$_3$P·BH$_3$	1.9243(12)	105.99	112.72	1.823
7	(*o*-tolyl)$_3$P·BH$_3$	1.9542(10)	105.60	113.11	1.824

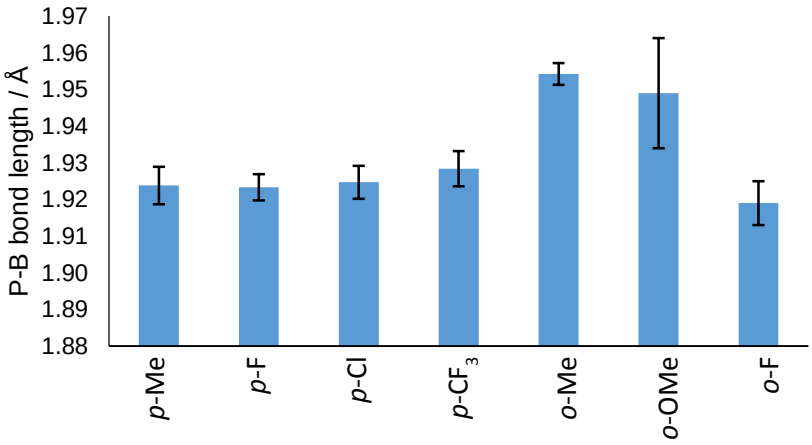

Figure 5.5 P-B bond length data for a range of substituted triarylphosphine borane complexes. Error bars shown are calculated as ± 3σ. Trends in R factor are known to influence the observed bond lengths, as such, this data should not be taken as definitive.[22]

5.6 References

[1] M. Van Overschelde, E. Vervecken, S. G. Modha, S. Cogen, E. Van der Eycken, J. Van der Eycken, *Tetrahedron* **2009**, *65*, 6410–6415.

[2] Y. Kawano, K. Yamaguchi, S. Miyake, T. Kakizawa, M. Shimoi, *Chem. Eur. J.* **2007**, *13*, 6920–6931.

[3] C. A. Busacca, R. Raju, N. Grinberg, N. Haddad, P. James-Jones, H. Lee, J. C. Lorenz, A. Saha, C. H. Senanayake, *J. Org. Chem.* **2008**, *73*, 1524–1531.

[4] H. Lebel, S. Morin, V. Paquet, *Org. Lett.* **2003**, *5*, 2347–2349.

[5] D. B. G. Williams, P. D. R. Kotze, A. C. Ferreira, C. W. Holzapfel, *J. Iran. Chem. Soc.* **2011**, *8*, 240–246.

[6] E. Rivard, A. J. Lough, I. Manners, *J. Chem. Soc. Dalt. Trans.* **2002**, 2966–2972.

[7] M. J. G. Lesley, A. Woodward, N. J. Taylor, T. B. Marder, I. Cazenobe, I. Ledoux, J. Zyss, A. Thornton, D. W. Bruce, A. K. Kakkar, *Chem. Matter.* **1998**, *10*, 1355–1365.

[8] M. A. Weiner, M. Lattman, *Inorg. Nucl. Chem. Lett.* **1975**, *11*, 723–728.

[9] K. Yamada, M. Takeda, T. Iwakuma, *J. Chem. Soc. Perkin Trans. 1* **1983**, 265–270.

[10] E. F. Mooney, M. A. Qaseem, *J. Inorg. Nucl. Chem.* **1968**, *30*, 1439–1446.

[11] N. Farfán, R. Contreras, *J. Chem. Soc., Perkin Trans. 2* **1987**, 771–773.

[12] K. C. Nainan, G. E. Ryschkewitsch, *Inorg. Chem.* **1969**, *8*, 2671–2674.

[13] P. V. Ramachandran, B. C. Raju, P. D. Gagare, *Org. Lett.* **2012**, *14*, 6119–6121.

[14] pK_a data taken from tables compiled by R. Williams, accessed online (December 2014) at: http://research.chem.psu.edu/brgroup/pKa_compilation.pdf

[15] M. Baidya, S. Kobayashi, F. Brotzel, U. Schmidhammer, E. Riedle, H. Mayr, *Angew. Chem. Int. Ed.* **2007**, *46*, 6176–9.

[16] F. Brotzel, Y. C. Chu, H. Mayr, *J. Org. Chem.* **2007**, *72*, 3679–3688.

[17] T. Kanzian, T. a. Nigst, A. Maier, S. Pichl, H. Mayr, *Eur. J. Org. Chem.* **2009**, *2009*, 6379–6385.

[18] J. Ammer, M. Baidya, S. Kobayashi, H. Mayr, *J. Phys. Org. Chem.* **2010**, *23*, 1029–1035.

[19] T. Nigst, J. Ammer, H. Mayr, *J. Phys. Chem. A* **2012**, *116*, 8494–8499.

[20] F. Brotzel, B. Kempf, T. Singer, H. Zipse, H. Mayr, *Chem. Eur. J.* **2007**, *13*, 336–345.

[21] M. J. Frisch, G. W. Trucks, H. B. Schlegel, G. E. Scuseria, M. A. Robb, J. R. Cheeseman, G. Scalmani, V. Barone, B. Mennucci, G. A. Petersson, H. Nakatsuji, M. Caricato, X. Li, H. P. Hratchian, A. F. Izmaylov, J. Bloino, G. Zheng, J. L. Sonnenberg, M. Hada, M. Ehara, K. Toyota, R. Fukuda, J. Hasegawa, M. Ishida, T. Nakajima, Y. Honda, O. Kitao, H. Nakai, T. Vreven, J. A. Montgomery, Jr., J. E. Peralta, F. Ogliaro, M. Bearpark, J. J. Heyd, E. Brothers, K. N. Kudin, V. N. Staroverov, R. Kobayashi, J. Normand, K. Raghavachari, A. Rendell, J. C. Burant, S. S. Iyengar, J. Tomasi, M. Cossi, N. Rega, J. M. Millam, M. Klene, J. E. Knox, J. B. Cross, V. Bakken, C. Adamo, J. Jaramillo, R. Gomperts, R. E. Stratmann, O. Yazyev, A. J. Austin, R. Cammi, C. Pomelli, J. W. Ochterski, R. L. Martin, K. Morokuma, V. G. Zakrzewski, G. A. Voth, P. Salvador, J. J. Dannenberg, S. Dapprich, A. D. Daniels, Ö. Farkas, J. B. Foresman, J. V. Ortiz, J. Cioslowski, and D. J. Fox, Gaussian, Inc., Wallingford CT, 2009.

[22] D. G. Gilheany, *Chem. Rev.* **1994**, *94*, 1339–1374.

6 Appendix

6.1 Temporal concentration data

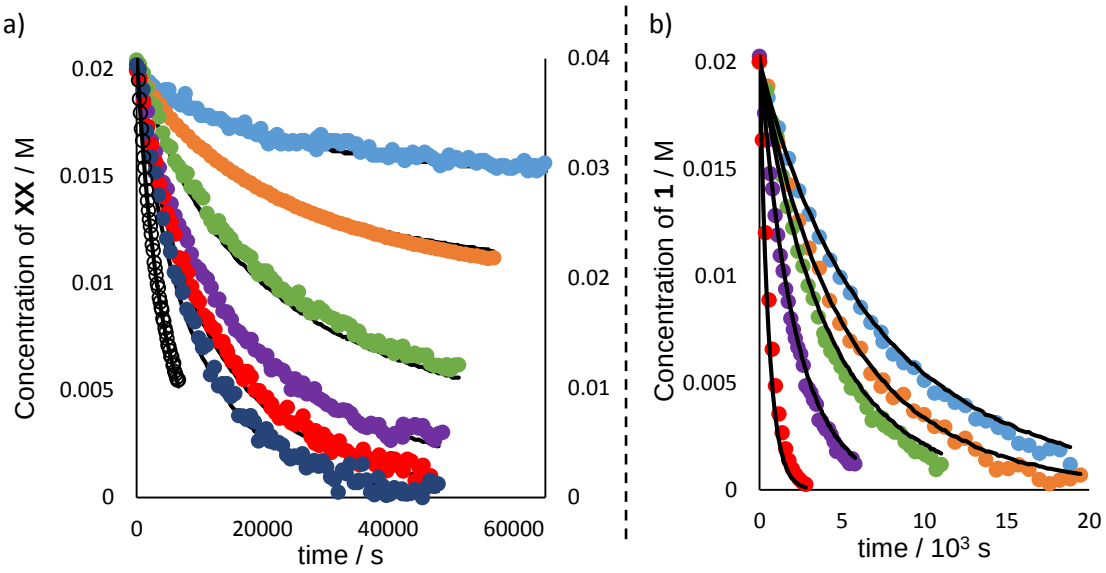

Figure 6.1 Temporal concentration data for reaction of **1** ([**1**]$_0$ = 0.02 M) with various initial concentrations of quinuclidine, **2**. Circles are experimental data. Lines are simulation according to $-d[\mathbf{1}]/dt = k([\mathbf{1}][\mathbf{2}]-[\mathbf{3}][Ph_3P]/K)$; k = 2.6 × 10^{-3} M^{-1} s^{-1}, K = 7.4 × 10^3. a) blue: [**2**]$_0$ = 0.005 M, orange: [**2**]$_0$ = 0.01 M, green: [**2**]$_0$ = 0.02 M, purple: [**2**]$_0$ = 0.03 M, red: [**2**]$_0$ = 0.04 M and dark blue: [**2**]$_0$ = 0.05 M. Hollow circles correspond secondary axis (rhs) with [**1**]$_0$ = 0.04 M and [**2**]$_0$ = 0.10 M. b) blue: [**2**]$_0$ = 0.06 M, orange: [**2**]$_0$ = 0.08 M, green: [**2**]$_0$ = 0.10 M, purple: [**2**]$_0$ = 0.19 M and red: [**2**]$_0$ = 0.73 M.

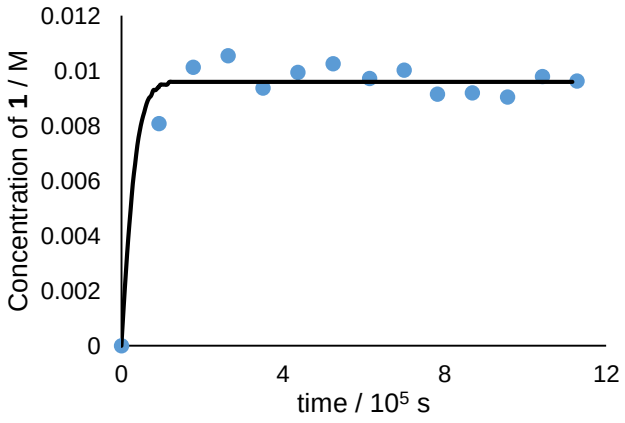

Figure 6.2 Temporal concentration data for reaction of **3** ([**3**]$_0$ = 0.72 M) with Ph_3P, [Ph_3P]$_0$ = 1.00 M. Circles are experimental data. Lines are simulation according to $d[\mathbf{1}]/dt = k([\mathbf{1}][\mathbf{2}]-[\mathbf{3}][Ph_3P]/K)$; k = 2.6 × 10^{-3} M^{-1} s^{-1}, K = 7.4 × 10^3.

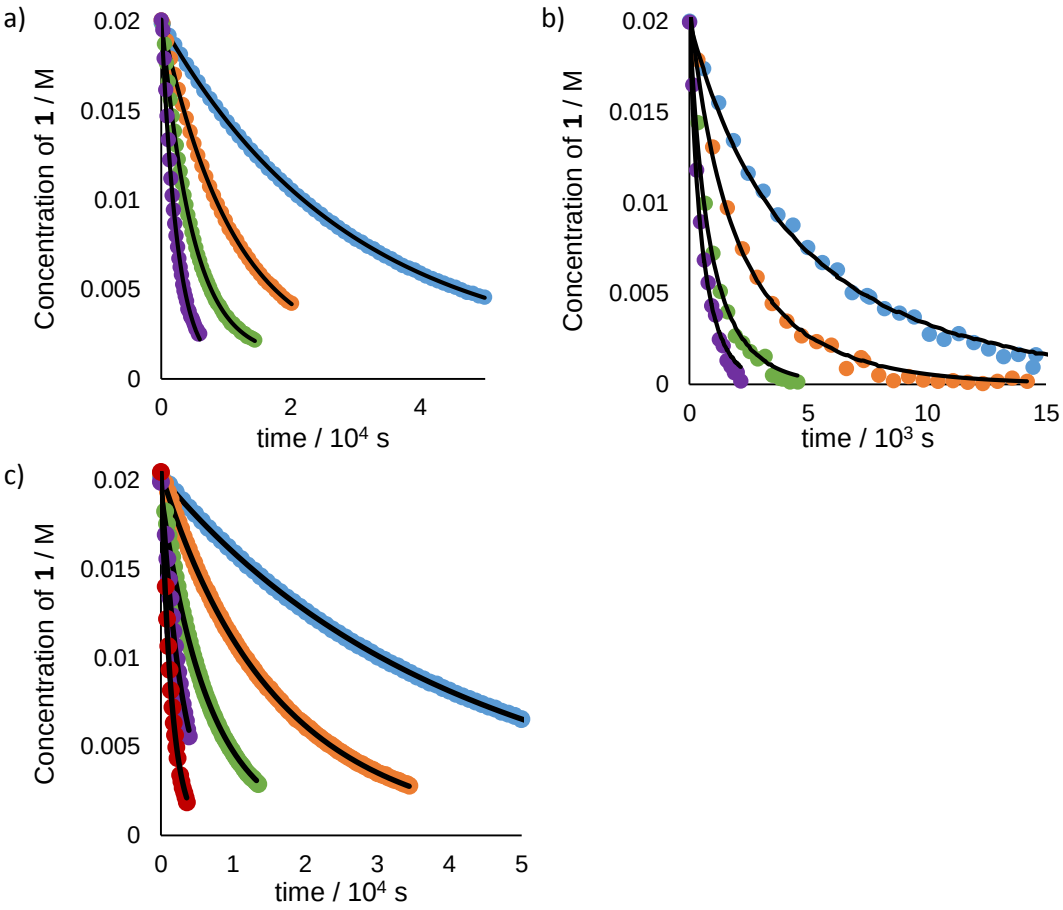

Figure 6.3 Temporal concentration data for reaction of **1** ($[\mathbf{1}]_0$ = 0.02 M) with a) triethylamine, $[Et_3N]_0$ = 0.40 M, blue (40 °C), orange (50 °C), green (60 °C) and purple (70 °C). b) quinuclidine, $[\mathbf{2}]_0$ = 0.04 M, blue (40 °C), orange (50 °C), green (60 °C) and purple (70 °C). c) morpholine, $[morpholine]_0$ = 0.12 M, blue (30 °C), orange (40 °C), green (50 °C), purple (60 °C) and red (70 °C). Circles are experimental data (*in situ* $^{11}B\{^1H\}$ NMR). Lines are simulation according to $-d[\mathbf{1}]/dt = k([\mathbf{1}][amine]-[amine{\cdot}BH_3][Ph_3P]/K)$; *k* and *K* values are displayed in Table 6.1.

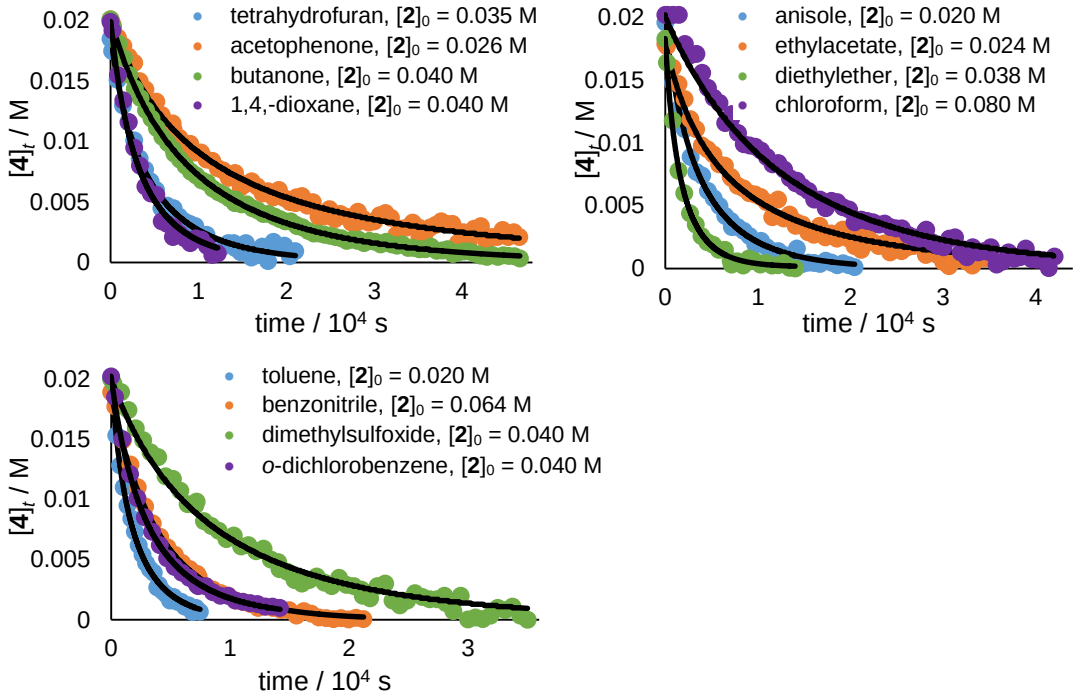

Figure 6.4 Temporal concentration data for reaction of **4** ([**4**]$_0$ = 0.02 M) with quinuclidine, **2**, in a variety of solvents at 30 °C. Circles are experimental data (*in situ* $^{11}B\{^1H\}$ NMR). Lines are simulation according to $-d[\mathbf{4}]/dt = k([\mathbf{4}][\mathbf{2}]-[\mathbf{3}][Ar_3P]/K)$; *k* values are displayed in Table 6.3, in all cases data was not sufficient to accurately determine values for *K*.

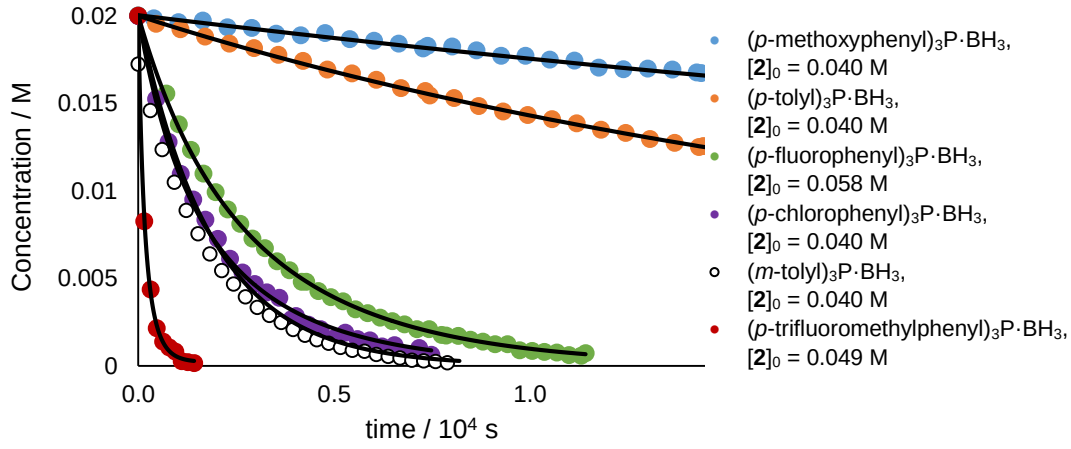

Figure 6.5 Temporal concentration data for reaction of a range of triarylphosphine borane complexes with quinuclidine, **2**, in toluene at 30 °C. Circles are experimental data (*in situ* $^{11}B\{^1H\}$ NMR). Lines are simulation according to $-d[Ar_3P{\cdot}BH_3]/dt = k([Ar_3P{\cdot}BH_3][\mathbf{2}]-[\mathbf{3}][Ar_3P]/K)$; *k* values are displayed in Table 6.4, in all cases data was not sufficient to accurately determine values for *K*. Data shown is truncated for **6** and **7**, reactions were monitored to 49% and 75% conversion of $R_3P{\cdot}BH_3$ respectively.

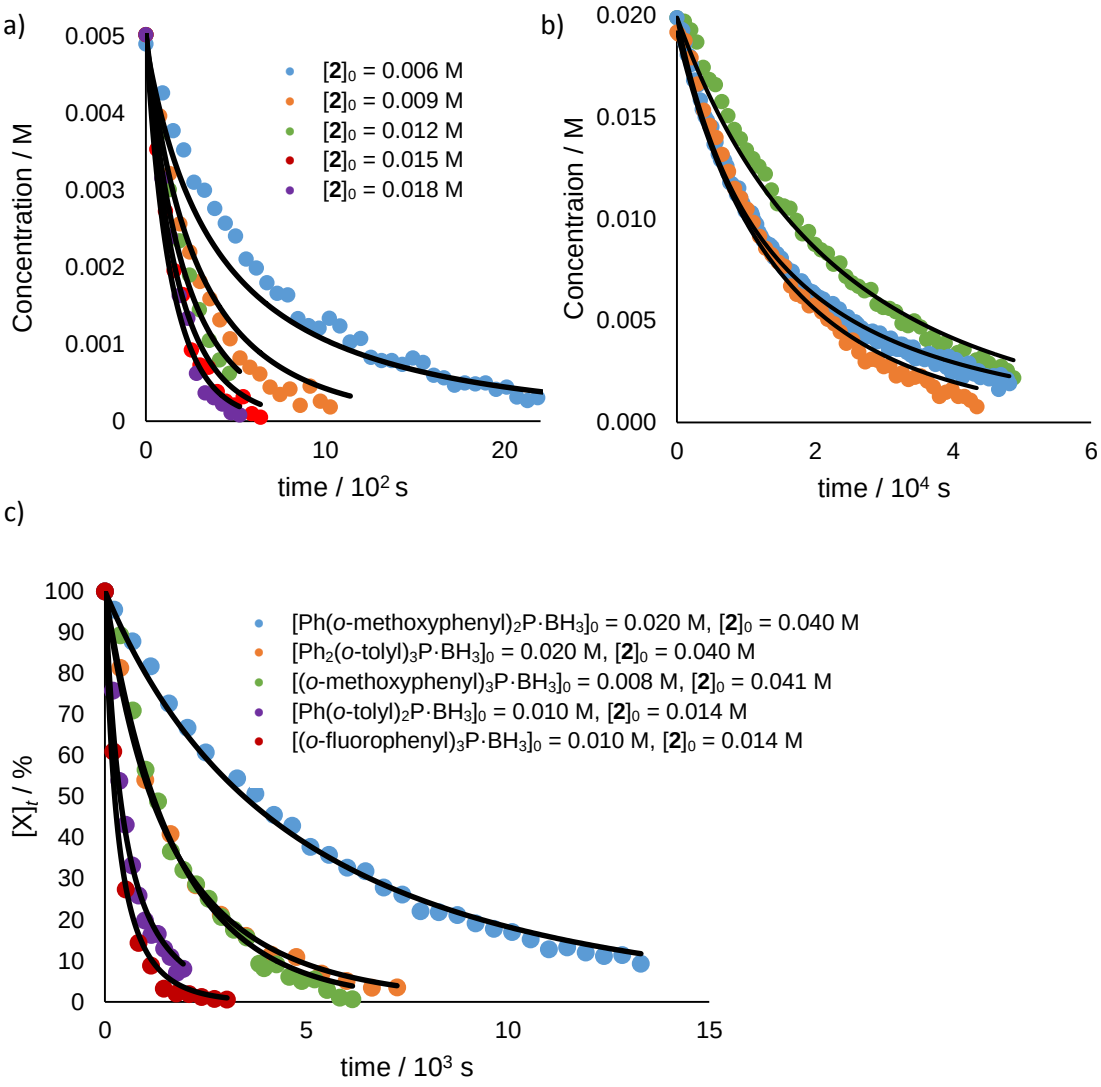

Figure 6.6 Temporal concentration data for reaction of a range of triarylphosphine borane complexes with quinuclidine, **2**, in toluene at 30 °C. Circles are experimental data (*in situ* $^{11}B\{^1H\}$ NMR). Lines are simulation according to $-d[Ar_3P{\cdot}BH_3]/dt = k([Ar_3P{\cdot}BH_3][\mathbf{2}]-[\mathbf{3}][Ar_3P]/K)$; *k* values are displayed in Table 6.4, in all cases data was not sufficient to accurately determine values for *K*. a) (*o*-tolyl)$_3$P·BH$_3$ with a range of [**2**]$_0$. b) green: Ph(*p*-methoxyphenyl)$_2$P·BH$_3$, [**2**]$_0$ = 0.060 M, blue: Ph$_2$(*o*-methoxyphenyl)P·BH$_3$, [**2**]$_0$ = 0.060 M, orange: Ph$_2$(*p*-methoxyphenyl)P·BH$_3$, [**2**]$_0$ = 0.050 M.

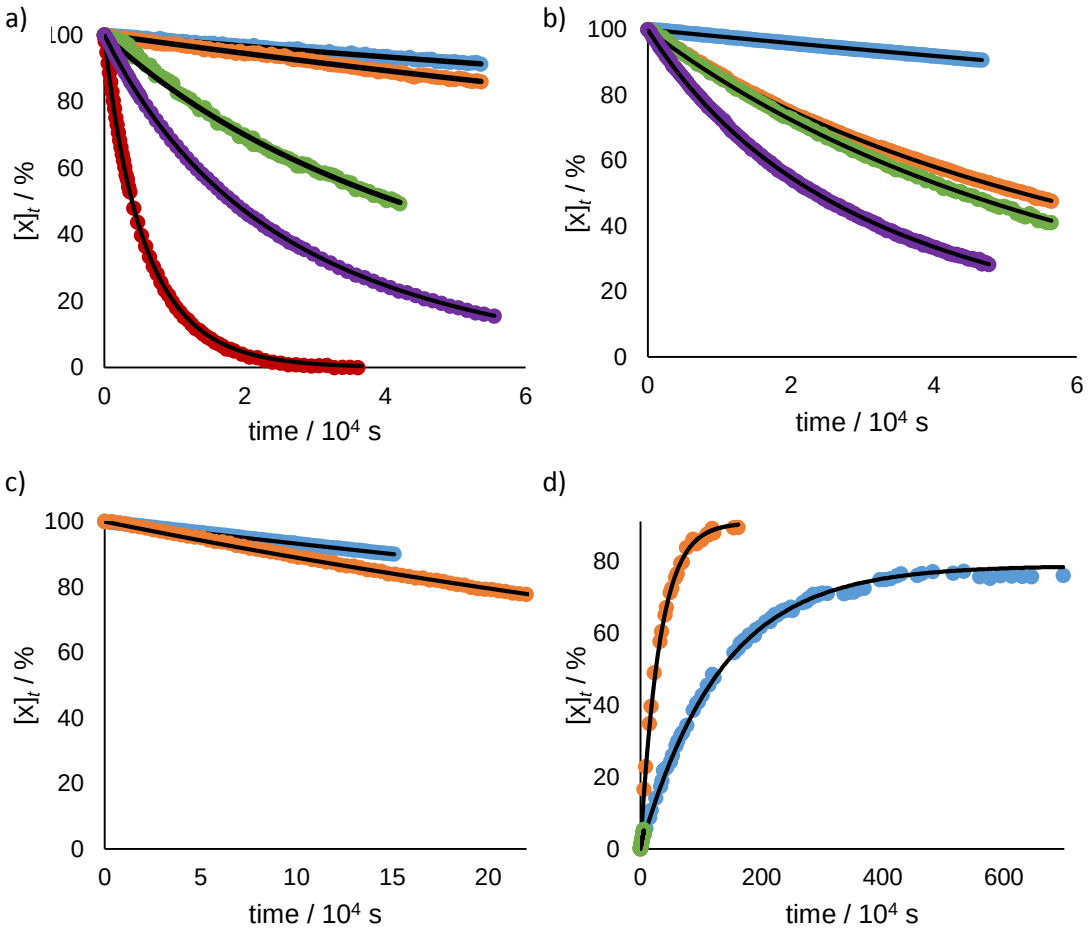

Figure 6.7 Temporal concentration data for reaction of a variety of phosphine borane adducts with quinuclidine, **2**, in toluene at 30 °C. Circles are experimental data (*in situ* $^{11}B\{^1H\}$ NMR). Lines are simulation according to $-d[R_3P{\cdot}BH_3]/dt = k([R_3P{\cdot}BH_3][\mathbf{2}]-[\mathbf{3}][R_3P]/K)$; k and K values are displayed in Table 6.5. a) blue: $[^tBu_3P{\cdot}BH_3]_0$ = 0.154 M, $[\mathbf{2}]_0$ = 0.863 M; orange: $[^tBu_2PhP{\cdot}BH_3]_0$ = 0.050 M, $[\mathbf{2}]_0$ = 0.102 M; green: $[^tBuPh_2P{\cdot}BH_3]_0$ = 0.020 M, $[\mathbf{2}]_0$ = 0.039 M; purple: $[benzylPh_2P{\cdot}BH_3]_0$ = 0.019 M, $[\mathbf{2}]_0$ = 0.050 M; red: $[(o\text{-biphenyl})^tBu_2P{\cdot}BH_3]_0$ = 0.020 M, $[\mathbf{2}]_0$ = 0.078 M. b) blue: $[Me_3P{\cdot}BH_3]_0$ = 0.286 M, $[\mathbf{2}]_0$ = 0.600 M; orange: $[Me_2PhP{\cdot}BH_3]_0$ = 0.180 M, $[\mathbf{2}]_0$ = 0.436 M; green: $[^iPrPh_2P{\cdot}BH_3]_0$ = 0.016 M, $[\mathbf{2}]_0$ = 0.092 M; purple: $[MePh_2P{\cdot}BH_3]_0$ = 0.051 M, $[\mathbf{2}]_0$ = 0.100 M. c) blue: $[^iPr_3P{\cdot}BH_3]_0$ = 0.021 M, $[\mathbf{2}]_0$ = 0.511 M; orange: $[^nBu_3P{\cdot}BH_3]_0$ = 0.197 M, $[\mathbf{2}]_0$ = 0.462 M. d) Reverse reaction, between R_3P and **3**, blue: $[^tBu_3P]_0$ = 0.432 M, $[\mathbf{3}]_0$ = 0.085 M; orange: $[Me_3P]_0$ = 1.396 M, $[\mathbf{3}]_0$ = 0.085 M; green: $[^nBu_3P]_0$ = 1.00 M, $[\mathbf{3}]_0$ = 0.300 M.

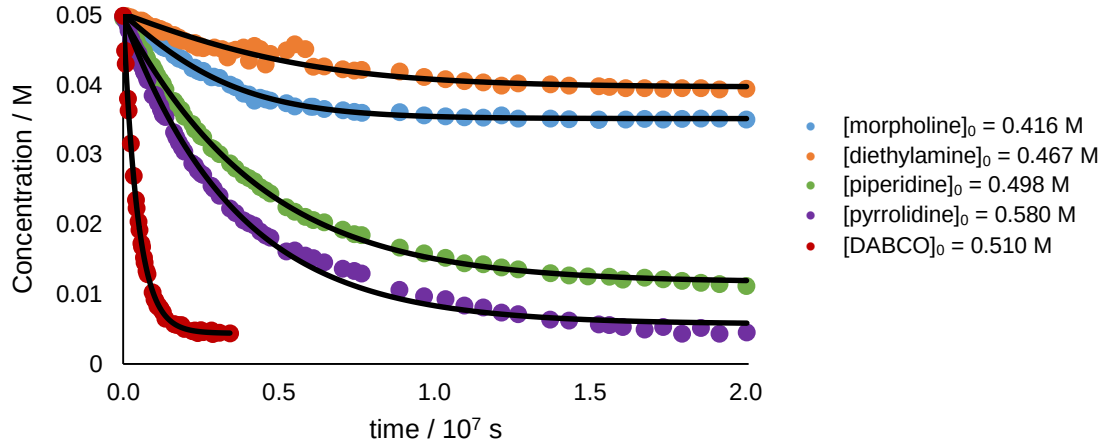

Figure 6.8 Temporal concentration data for reaction of $^{t}Bu_3P{\cdot}BH_3$, **21**, with a variety of amines in toluene at 30 °C. Circles are experimental data (*in situ* $^{11}B\{^1H\}$ NMR). Lines are simulation according to $-d[\mathbf{21}]/dt = k([\mathbf{21}][R_3N]-[R_3N{\cdot}BH_3][^tBu_3P]/K)$; *k* and *K* values are in a) le 6.6.

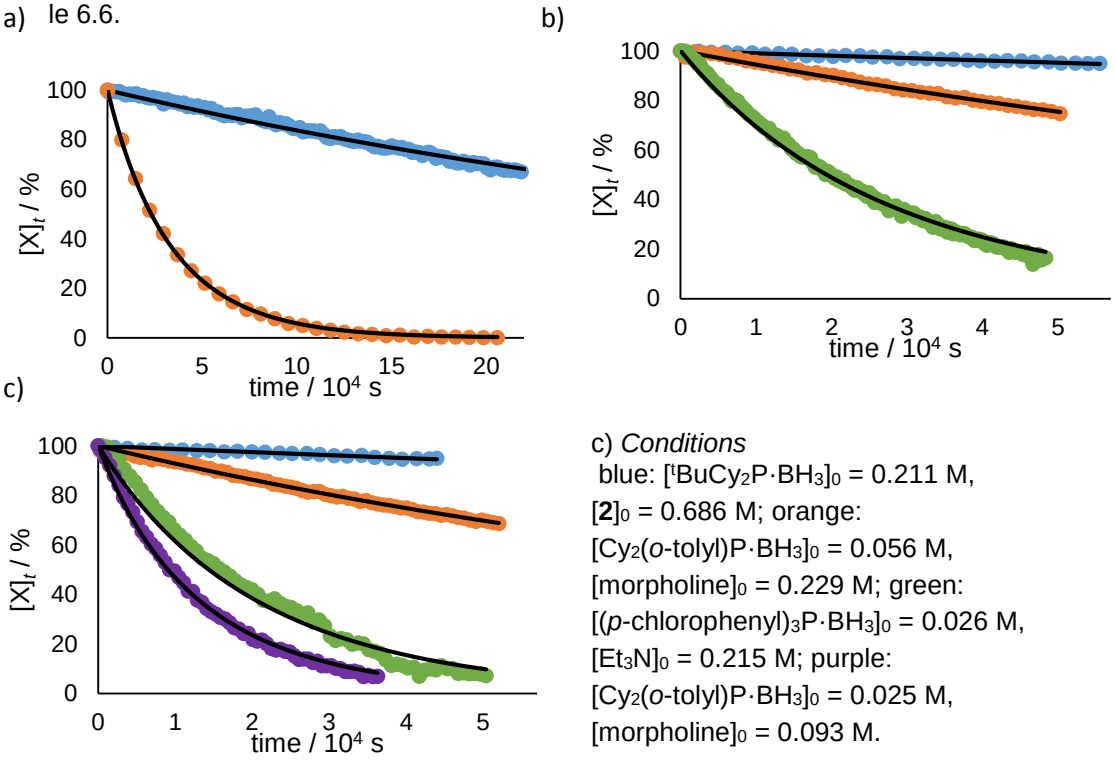

c) *Conditions*
blue: $[^tBuCy_2P{\cdot}BH_3]_0$ = 0.211 M, $[\mathbf{2}]_0$ = 0.686 M; orange: $[Cy_2(o\text{-tolyl})P{\cdot}BH_3]_0$ = 0.056 M, $[morpholine]_0$ = 0.229 M; green: $[(p\text{-chlorophenyl})_3P{\cdot}BH_3]_0$ = 0.026 M, $[Et_3N]_0$ = 0.215 M; purple: $[Cy_2(o\text{-tolyl})P{\cdot}BH_3]_0$ = 0.025 M, $[morpholine]_0$ = 0.093 M.

Figure 6.9 Temporal concentration data for reactions described (toluene, 30 °C). Circles are experimental data (*in situ* $^{11}B\{^1H\}$ NMR). Lines are simulation according to $-d[R_3P{\cdot}BH_3]/dt = k[R_3P{\cdot}BH_3][\mathbf{2}]$; *k* values are displayed in Table 6.7. a) blue: $[^tBuMe(p\text{-methoxyphenyl})P{\cdot}BH_3]_0$ = 0.021 M, $[\mathbf{2}]_0$ = 0.105 M; orange: $[^tBu_2PhP{\cdot}BH_3]_0$ = 0.101 M, $[DABCO]_0$ = 0.726 M. b) blue: $[^tBu_2CyP{\cdot}BH_3]_0$ = 0.206 M, $[\mathbf{2}]_0$ = 0.373 M; orange: $[MePh_2P{\cdot}BH_3]_0$ = 0.055 M, $[Et_2NH]_0$ = 0.387 M; green: $[Cy_2(o\text{-tolyl})P{\cdot}BH_3]_0$ = 0.021 M, $[\mathbf{2}]_0$ = 0.197 M.

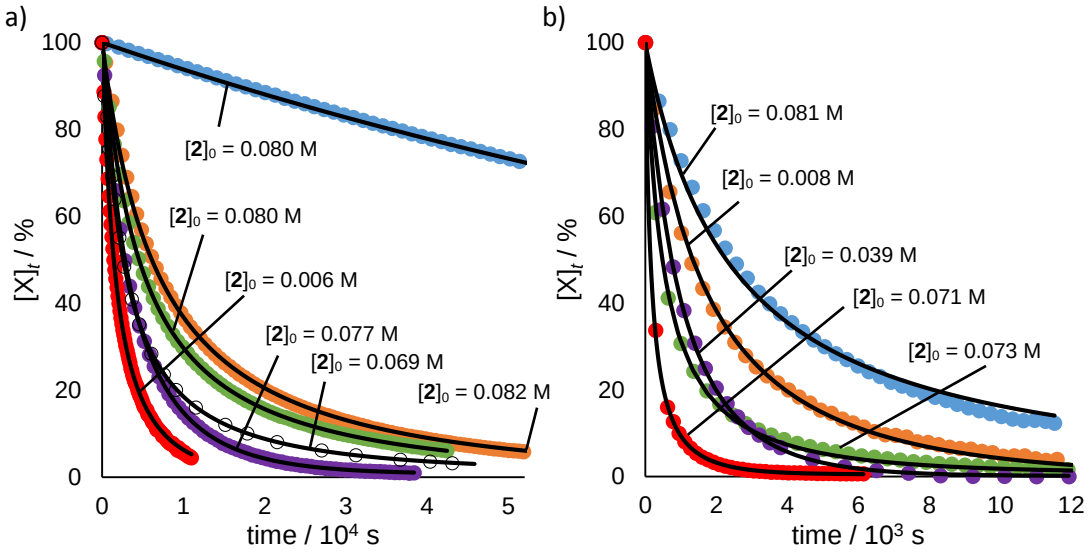

Figure 6.10 Temporal concentration data for reactions of pyridine borane adducts with quinuclidine (toluene, 30 °C). Circles are experimental data (*in situ* ^{1}H NMR). Lines are simulation according to $-d[\text{pyridine}\cdot BH_3]/dt = k[\text{pyridine}\cdot BH_3][\mathbf{2}]-[\mathbf{3}][\text{pyridine}]/K)$; k and K values are displayed in Table 6.8. a) blue: [4-dimethylaminopyridine·BH_3]$_0$ = 0.020 M; orange: [4-methoxypyridine·BH_3]$_0$ = 0.069 M; green: [4-methylpyridine·BH_3]$_0$ = 0.071 M; purple: [3-methylpyridine·BH_3] = 0.047 M; red: [4-trifluoromethylpyridine·BH_3] = 0.005 M; hollow circles: [2-methylpyridine·BH_3] = 0.062 M. b) blue: [pyridine·BH_3]$_0$ = 0.074 M; orange: [3-bromo-5-methylpyridine·BH_3]$_0$ = 0.006 M; green: [2,6-dimethylpyridine·BH_3]$_0$ = 0.064 M; purple: [2-isopropylpyridine·BH_3] = 0.018 M; red: [2-methoxypyridine·BH_3] = 0.061 M.

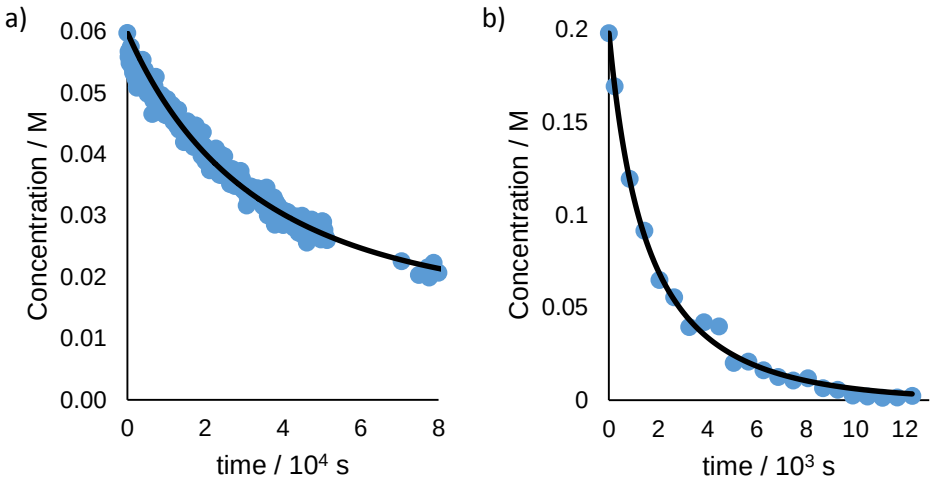

Figure 6.11 Temporal concentration data for reactions of reference amine borane adducts a) $Me_2NH\cdot BH_3$ **50** and b) $Me_3N\cdot BH_3$ **54** with quinuclidine ([**2**]$_0$ = 0.070 and 0.301 M, respectively) in toluene at 30 °C. Circles are experimental data (*in situ* $^{13}C\{^{1}H\}$ NMR). Lines are simulation according to $-d[\text{amine}\cdot BH_3]/dt = k[\text{amine}\cdot BH_3][\mathbf{2}]$; k values are displayed in Table 6.9.

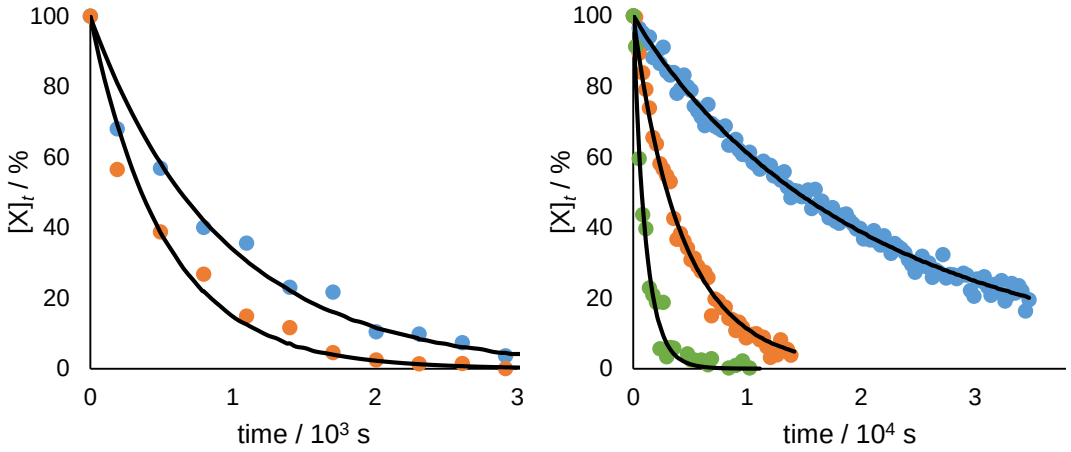

Figure 6.12 Examples of temporal concentration data for reactions of *in situ* generated amine borane adducts with quinuclidine in toluene at 30 °C. Circles are experimental data (*in situ* $^{13}C\{^1H\}$ NMR). Lines are simulation according to $-d[amine{\cdot}BH_3]/dt = k[amine{\cdot}BH_3][\mathbf{2}]$; *k* values are displayed in Table 6.9. a) $[\mathbf{2}]_0 = 0.523$ M; blue: $[Me_3N{\cdot}BH_3] = 0.031$ M, orange: $[Cy_2NH{\cdot}BH_3]_0 = 0.022$ M. b) $[\mathbf{2}]_0 = 0.493$ M; blue: $[Me_2NH{\cdot}BH_3] = 0.042$ M, orange: $[^nPr_2NH{\cdot}BH_3]_0 = 0.056$ M, green: [*N*-ethylpiperidine·BH_3]$_0$ = 0.031 M.

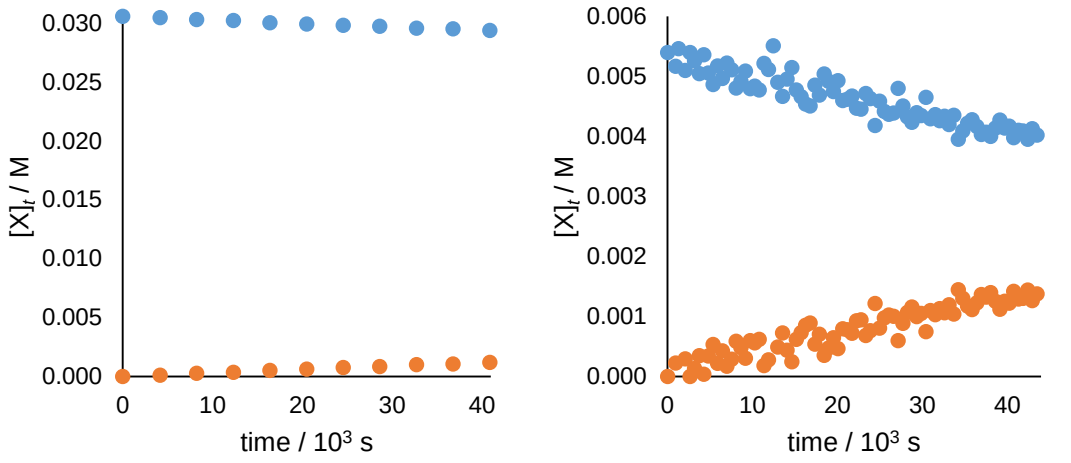

Figure 6.13 Temporal concentration data for the direct displacement reactions between a phosphine borane adduct and the corresponding deuterated phosphine in toluene at 30 °C (*in situ* $^{31}P\{^1H\}$ NMR analysis). a) Starting conditions: $[\mathbf{1}]_0 = 0.031$ M, $[d_{15}\text{-}Ph_3P]_0 = 0.030$ M; blue circles = **1**, orange circles = Ph_3P. b) Starting conditions: $[\mathbf{10}]_0 = 0.054$ M, $[d_{12}\text{-}(o\text{-tolyl})_3P]_0 = 0.069$ M; blue circles = **10**, orange circles = $(o\text{-tolyl})_3P$.

6.2 Rate and equilibrium constants

The rate constants displayed below were obtained through fitting temporal concentration data to model data using Dynochem 2011 v4 in. The residuals quoted alongside the values in the tables below were generated from Dynochem using a 95% confidence integral (assuming residuals are normally distributed). However, given the robustness of the reactions examined, the residuals quotes are likely only poor estimator of the error in the values. Errors arising from variation in the temperature between the many different NMR spectrometers used are likely to be more significant, in addition to errors occurring in the weighing/measuring of reagents and solvents. With that said, the wide variation in rate constants observed (spanning more than five orders of magnitude) should put any estimated errors in context even if all values were out by up to 5%.

Table 6.1 Rate constants for the deprotection of $Ph_3P{\cdot}BH_3$, **1**, by a variety of amines in toluene at the temperatures specified. For quinuclidine and morpholine, where *K* is large and reactions, no significant information on *K* is available. The values of *K* optimised by Dynochem for triethylamine, as can be seen from the residuals, should be taken as approximate.

Entry	**Amine**	***k* / M^{-1} s^{-1} or *K***			
		40 °C	**50 °C**	**60 °C**	**70 °C**
1	quinuclidine (*k*)	$6.42 \pm 0.3 \times 10^{-3}$	$1.49 \pm 0.1 \times 10^{-2}$	$3.53 \pm 0.3 \times 10^{-2}$	$6.24 \pm 0.6 \times 10^{-3}$
2	Et_3N (*k*)	$8.11 \pm 0.1 \times 10^{-5}$	$2.09 \pm 0.1 \times 10^{-4}$	$4.82 \pm 0.1 \times 10^{-4}$	$9.87 \pm 0.4 \times 10^{-4}$
3	Et_3N (*K*)	$7.7 \pm 0.6 \times 10^{-1}$	$9.0 \pm 2 \times 10^{-1}$	$7.8 \pm 0.9 \times 10^{-1}$	-
4	morpholine (*k*)	$5.26 \pm 0.1 \times 10^{-4}$	$1.24 \pm 0.1 \times 10^{-3}$	$2.77 \pm 0.2 \times 10^{-3}$	$5.81 \pm 0.3 \times 10^{-3}$

Table 6.2 Rate and equilibrium constants for the deprotection of $Ph_3P{\cdot}BH_3$, **1**, by a variety of amines in toluene at 30 °C.

Entry	Amine	k / M^{-1} s^{-1}	K
1	diisopropylamine	$3.7 \pm 0.04 \times 10^{-6}$	$2.3 \pm 0.03 \times 10^{-2}$
2	triethylamine	$4.1 \pm 0.07 \times 10^{-5}$	$10 \pm 0.2 \times 10^{-1}$
3	DMAP	$8.8 \pm 0.08 \times 10^{-5}$	$1.1 \pm 0.2 \times 10^{2}$
4	diethylamine	$1.0 \pm 0.06 \times 10^{-4}$	$1.3 \pm 0.14 \times 10^{1}$
5	morpholine	$3.1 \pm 0.05 \times 10^{-4}$	$3.1 \pm 0.2 \times 10^{1}$
6	piperidine	$4.5 \pm 0.08 \times 10^{-4}$	≥ 660
7	pyrrolidine	$5.6 \pm 0.09 \times 10^{-4}$	≥ 990
8	*N*-methylpyrrolidine	$6.9 \pm 0.10 \times 10^{-4}$	$4.7 \pm 0.08 \times 10^{1}$
9	quinuclidine	$2.6 \pm 0.01 \times 10^{-3}$	$7.4 \pm 0.5 \times 10^{3}$
10	DABCO	$k_1 = 4.6 \pm 0.01 \times 10^{-3}$, $k_2 = 8.6 \pm 0.9 \times 10^{-4}$	$K_1 \geq 400$, $K_2 = 7 \pm 1$

Table 6.3 Rate constants for the deprotection of $(p\text{-chlorophenyl})_3P{\cdot}BH_3$, **4**, by quinuclidine, **2**, in various solvents at 30 °C.

Entry	Solvent	$k \times 10^3$ / M^{-1} s^{-1}
1	diethylether	17 ± 0.7
2	toluene	17 ± 0.4
3	*o*-dichlorobenzene	9.1 ± 0.2
4	1,4-dioxane	9.0 ± 0.5
5	anisole	8.1 ± 0.2
6	tetrahydrofuran	8.0 ± 0.4
7	ethylacetate	7.4 ± 0.2
8	benzonitrile	4.3 ± 0.08
9	acetophenone	4.1 ± 0.1
10	dimethylsulfoxide	3.4 ± 0.1
11	butanone	3.2 ± 0.03
12	chloroform	1.0 ± 0.03

Table 6.4 Rate constants for the deprotection of $R_3P{\cdot}BH_3$ (R = aryl) by quinuclidine, **2**, in toluene at 30 °C.

Entry	R_3P	k / M^{-1} s^{-1}
1	(*p*-methoxyphenyl)$_3$P	$3.4 \pm 0.02 \times 10^{-4}$
2	(*p*-tolyl)$_3$P	$9.0 \pm 0.06 \times 10^{-4}$
3	(*m*-tolyl)$_3$P	$9.9 \pm 0.06 \times 10^{-4}$
4	(*p*-fluorophenyl)$_3$P	$6.8 \pm 0.05 \times 10^{-3}$
5	(*p*-chlorophenyl)$_3$P	$1.7 \pm 0.03 \times 10^{-2}$
6	(*p*-trifluoromethylphenyl)$_3$P	$1.7 \pm 0.07 \times 10^{-1}$
7	Ph(*p*-methoxyphenyl)$_2$P	$7.9 \pm 0.2 \times 10^{-4}$
8	Ph$_2$(*p*-methoxyphenyl) P	$1.5 \pm 0.05 \times 10^{-3}$
9	(*o*-tolyl)$_3$P	$4.4 \pm 0.2 \times 10^{-1}$
10	Ph(*o*-tolyl)$_2$P	$1.6 \pm 0.2 \times 10^{-1}$
11	Ph$_2$(*o*-tolyl)P	$1.8 \pm 0.1 \times 10^{-2}$
12	(*o*-methoxyphenyl)$_3$P	$1.5 \pm 0.1 \times 10^{-2}$
13	Ph(*o*-methoxyphenyl)$_2$P	$5.8 \pm 0.1 \times 10^{-3}$
14	Ph$_2$(*o*-methoxyphenyl)P	$3.0 \pm 0.05 \times 10^{-3}$
15	(*o*-fluorophenyl)$_3$P	$2.5 \pm 0.3 \times 10^{-1}$

Table 6.5 Rate and equilibrium constants for the deprotection of $R_nPh_{3-n}P{\cdot}BH_3$ by quinuclidine, **2**, in toluene at 30 °C.

Entry	R		k / M^{-1} s^{-1} or K		
			***n* = 1**	***n* = 2**	***n* = 3**
1	Cy	k	$2.1 \pm 0.02 \times 10^{-4}$	$1.9 \pm 0.06 \times 10^{-5}$	$2.5 \pm 0.04 \times 10^{-6}$
		K	$5.2 \pm 0.4 \times 10^{2}$	$2.4 \pm 0.4 \times 10^{1}$	$1.4 \pm 0.1 \times 10^{0}$
2	Me	k	$3.5 \pm 0.01 \times 10^{-4}$	$3.5 \pm 0.01 \times 10^{-5}$	$3.6 \pm 0.01 \times 10^{-6}$
		K	-	-	$1.8 \pm 0.1 \times 10^{0}$
3	^{t}Bu	k	$4.9 \pm 0.01 \times 10^{-4}$	$2.9 \pm 0.01 \times 10^{-5}$	$2.0 \pm 0.02 \times 10^{-6}$
		K	-	-	$1.5 \pm 0.08 \times 10^{0}$
4	^{n}Bu	k	-	-	$2.6 \pm 0.03 \times 10^{-6}$
		K	-	-	$2.6 \pm 0.05 \times 10^{0}$
5	^{i}Pr	k	$1.8 \pm 0.01 \times 10^{-4}$	-	$1.4 \pm 0.008 \times 10^{-6}$
6	benzyl	k	$8.3 \pm 0.01 \times 10^{-4}$	-	-
7	*o*-biphenyl[a]	k^{a}	$2.4 \pm 0.02 \times 10^{-3}$	-	-

[a]second order rate constant for (*o*-biphenyl)$^{t}Bu_2P{\cdot}BH_3$.

Table 6.6 Rate and equilibrium constants for the deprotection of $^{t}Bu_3P{\cdot}BH_3$, **21**, by a variety of amines in toluene at 30 °C.

Entry	Amine	k / M^{-1} s^{-1}	K
1	diethylamine	$7.1 \pm 0.5 \times 10^{-8}$	$6.1 \pm 0.6 \times 10^{-3}$
2	morpholine	$1.9 \pm 0.03 \times 10^{-7}$	$1.6 \pm 0.03 \times 10^{-2}$
3	piperidine	$3.4 \pm 0.03 \times 10^{-7}$	$2.7 \pm 0.09 \times 10^{-1}$
4	pyrrolidine	$4.2 \pm 0.08 \times 10^{-7}$	$6.4 \pm 0.8 \times 10^{-1}$
5	DABCO	$3.8 \pm 0.04 \times 10^{-6}$	$1.0 \pm 0.04 \times 10^{0}$

Table 6.7 Rate constants for the deprotection of $R_3P{\cdot}BH_3$, by a variety of amines in toluene at 30 °C.

Entry	R_3P	amine	k / M^{-1} s^{-1}
1	$^tBu_2CyP$	quinuclidine	$2.6 \pm 0.1 \times 10^{-6}$
2	$^tBuCy_2P$	quinuclidine	$1.9 \pm 0.2 \times 10^{-6}$
3	^{t}BuMe(*p*-methoxyphenyl)P	quinuclidine	$1.7 \pm 0.05 \times 10^{-5}$
4	Cy_2(*o*-tolyl)P	quinuclidine	$2.7 \pm 0.1 \times 10^{-4}$
5	Cy_2(*o*-tolyl)P	morpholine	$3.3 \pm 0.1 \times 10^{-5}$
6	$^tBu_2$PhP	DABCO	$4.3 \pm 0.1 \times 10^{-5}$
7	(*p*-chlorophenyl)$_3$P	triethylamine	$2.3 \pm 0.08 \times 10^{-4}$
8	Ph(*o*-methoxyphenyl)$_2$P	morpholine	$8.9 \pm 0.1 \times 10^{-4}$
5	Ph_2MeP	diethylamine	$1.5 \pm 0.07 \times 10^{-5}$

Table 6.8 Rate constants for the borane transfer from substituted pyridine borane adducts to quinuclidine, **2**, in toluene at 30 °C.

Entry	pyridine	k / M^{-1} s^{-1} (and K)
1	4-dimethylaminopyridine	$k = 8.0 \pm 0.08 \times 10^{-5}$
2	4-methoxypyridine	$k = 1.9 \pm 0.02 \times 10^{-3}$
3	4-methylpyridine	$k = 2.6 \pm 0.05 \times 10^{-3}$, $K = 3.4 \pm 0.04 \times 10^{3}$
4	3-methylpyridine	$k = 3.9 \pm 0.04 \times 10^{-3}$, $K = 2.9 \pm 0.3 \times 10^{2}$
5	pyridine	$k = 5.1 \pm 0.1 \times 10^{-3}$
6	2-methylpyridine	$k = 5.4 \pm 0.06 \times 10^{-3}$, $K = 5.9 \pm 0.9 \times 10^{2}$
7	2,6-dimethylpyridine	$k = 2.6 \pm 0.06 \times 10^{-2}$
8	2-isopropylpyridine	$k = 2.8 \pm 0.06 \times 10^{-2}$
9	2-methoxypyridine	$k = 8.7 \pm 0.1 \times 10^{-2}$
10	4-trifluoromethylpyridine	$k = 1.0 \pm 0.02 \times 10^{-1}$
11	3-bromo-5-methylpyridine	$k = 7.6 \pm 0.2 \times 10^{-2}$

Table 6.9 Rate constants for the borane transfer from amine borane adducts to quinuclidine, **2**, in toluene at 30 °C.

Entry	amine	k / M^{-1} s^{-1}
1	Me_2NH	$3.4 \pm 0.1 \times 10^{-4}$
2	Me_3N	$2.4 \pm 0.2 \times 10^{-3}$
3	$^{i}PrNH_2$	$7.4 \pm 1 \times 10^{-5}$
4	pyrrolidine	$1.1 \pm 0.07 \times 10^{-4}$
5	piperidine	$1.1 \pm 0.07 \times 10^{-4}$
6	$^{t}BuNH_2$	$5.5 \pm 1.6 \times 10^{-4}$
7	morpholine	$5.6 \pm 0.6 \times 10^{-4}$
8	$^{n}BuMeNH$	$6.6 \pm 0.4 \times 10^{-4}$
9	Et_2NH	$7.7 \pm 1 \times 10^{-4}$
10	CyEtNH	$1.1 \pm 0.2 \times 10^{-3}$
11	$^{n}Pr_2NH$	$1.5 \pm 0.1 \times 10^{-3}$
12	$^{t}BuMeNH$	$1.9 \pm 0.3 \times 10^{-3}$
13	$^{i}Pr_2NH$	$2.2 \pm 0.5 \times 10^{-3}$
14	*N*-methylpyrrolidine	$2.3 \pm 0.5 \times 10^{-3}$
15	Me_2EtN	$2.5 \pm 0.6 \times 10^{-3}$
16	$MeEt_2N$	$2.7 \pm 0.5 \times 10^{-3}$
17	Et_3N	$2.9 \pm 0.4 \times 10^{-3}$
18	Cy_2NH	$4.2 \pm 0.9 \times 10^{-3}$
19	$^{n}Pr_3N$	$4.4 \pm 0.7 \times 10^{-3}$
20	*N*-ethylpiperidine	$5.8 \pm 0.4 \times 10^{-3}$
21	*N*-methylpiperidine	$6.9 \pm 0.4 \times 10^{-3}$
22	$^{n}Bu_3N$	$7.1 \pm 1.3 \times 10^{-3}$

6.3 Crystallographic data

Table 6.10 Crystal data and structural refinement for (*p*-tolyl)$_3$P·BH$_3$, **7**, and (*p*-fluorophenyl)$_3$P·BH$_3$, **9**.

Compound name	Tris(*p*-tolyl)phosphine borane	Tris(*p*-fluorophenyl)phosphine borane
Empirical formula	$C_{21}H_{24}BP$	$C_{18}H_{15}BF_3P$
Formula weight	318.18	330.08
Temperature / K	100.0	100.00
Wavelength	0.71073 Å	0.71073 Å
Crystal system	Trigonal	Monoclinic
Space group	R -3	P 1 21/n 1
Unit cell dimensions	a = 12.0465(17) Å α = 90°	a = 10.5831(2) Å α = 90°
	b = 12.0465(17) Å β = 90°	b = 11.1836(2) Å β = 94.0490(10)°
	c = 22.023(4) Å γ = 120°	c = 13.6279(3) Å γ = 90°
Volume	2767.8(10) Å^3	1608.93(5) Å^3
Z	6	4
Density (calculated)	1.145 Mg/m^3	1.363 Mg/m^3
Absorption coefficient	0.146 mm^{-1}	0.196 mm^{-1}
F(000)	1020	680
Crystal size	0.32 x 0.15 x 0.14 mm^3	0.21 x 0.13 x 0.12 mm^3
θ range for data collection	2.160 to 32.283°	2.358 to 27.603°
Index ranges	$-17 \le h \le 16$, $-16 \le k \le 17$, $-31 \le l \le 30$	$-13 \le h \le 13$, $-13 \le k \le 14$, $-17 \le l \le 17$
Reflections collected	9267	14313
Independent reflections	1936 [R_{int} = 0.0129]	3729 [R_{int} = 0.0313]
Completeness to θ = 25.242°	99.9 %	100.0 %
Absorption correction	Semi-empirical from equivalents	Semi-empirical from equivalents
Max. and min. transmission	0.7464 and 0.6769	0.7456 and 0.6401
Refinement method	Full-matrix least-squares on F^2	Full-matrix least-squares on F^2
Data/restraints/parameters	1936 / 0 / 75	3729 / 0 / 220
Goodness-of-fit on F^2	1.076	1.018
Final R indices [I>2 σ (I)]	R_1 = 0.0316, wR_2 = 0.0915	R_1 = 0.0325, wR_2 = 0.0758
R indices (all data)	R_1 = 0.0333, wR_2 = 0.0927	R_1 = 0.0423, wR_2 = 0.0810
Largest diff. peak and hole	0.461 and −0.274 eÅ^{-3}	0.335 and −0.338 eÅ^{-3}

Table 6.11 Crystal data details for (*p*-trifluoromethylphenyl)$_3$P·BH$_3$, **5**, and (*o*-fluorophenyl)$_3$P·BH$_3$, **12**.

Compound name	Tris(*p*-trifluoromethylphenyl)phosphine borane	Tris(*o*-fluorophenyl)phosphine borane
Empirical formula	$C_{21}H_{15}BF_9P$	$C_{18}H_{15}BF_3P$
Formula weight	480.11	330.08
Temperature / K	100.0	100.00
Wavelength	0.71073 Å	0.71073 Å
Crystal system	Monoclinic	Monoclinic
Space group	P 1 21/c 1	P 1 21/n 1
Unit cell dimensions	a = 10.6519(5) Å α = 90°	a = 11.6138(5) Å α = 90°
	b = 15.4516(7) Å β = 104.801(2)°	b = 11.8516(5) Å β = 113.820(2)°
	c = 13.3955(6) Å γ = 90°	c = 12.6878(4) Å γ = 90°
Volume	2131.59(17) Å^3	1597.61(11) Å^3
Z	4	4
Density (calculated)	1.496 Mg/m^3	1.372 Mg/m^3
Absorption coefficient	0.212 mm^{-1}	0.197 mm^{-1}
F(000)	968	680
Crystal size	0.21 x 0.13 x 0.12 mm^3	0.2 x 0.14 x 0.1 mm^3
θ range for data collection	1.977 to 27.566°	2.575 to 27.583°
Index ranges	$-13 \le h \le 13, -20 \le k \le 20, -17 \le l \le 17$	$-13 \le h \le 15, -9 \le k \le 15, -16 \le l \le 16$
Reflections collected	54029	14215
Independent reflections	4919 [R_{int} = 0.0252]	3682 [R_{int} = 0.0437]
Completeness to θ = 25.242°	100.0 %	99.9 %
Absorption correction	Semi-empirical from equivalents	Semi-empirical from equivalents
Max. and min. transmission	0.7456 and 0.7104	0.4305 and 0.3832
Refinement method	Full-matrix least-squares on F^2	Full-matrix least-squares on F^2
Data/restraints/parameters	4919 / 163 / 386	3682 / 6 / 230
Goodness-of-fit on F^2	1.026	1.020
Final R indices [I>2 σ (I)]	R_1 = 0.0331, wR_2 = 0.0853	R_1 = 0.0383, wR_2 = 0.0830
R indices (all data)	R_1 = 0.0392, wR_2 = 0.0902	R_1 = 0.0579, wR_2 = 0.0914
Largest diff. peak and hole	0.520 and −0.369 eÅ^{-3}	0.296 and −0.382 eÅ^{-3}

Table 6.12 Crystal data details for (*o*-methoxyphenyl)$_3$P·BH$_3$, **11**, and (*o*-chlorophenyl)$_3$P·BH$_3$, **4**.

Compound name	Tris(*o*-methoxyphenyl)phosphine borane	Tris(*p*-chlorophenyl)phosphine borane
Empirical formula	$C_{21}H_{24}BO_3P$	$C_{18}H_{15}BCl_3P$
Formula weight	366.18	379.43
Temperature / K	100.0	100.00
Wavelength	1.54178 Å	0.71073 Å
Crystal system	Monoclinic	Monoclinic
Space group	P 1 21/n 1	P 1 21/c 1
Unit cell dimensions	a = 8.4187 (10) Å α = 90°	a = 8.9386(2) Å α = 90°
	b = 27.584(4) Å β = 98.484(11)°	b = 12.3148(3) Å β = 96.960(2)°
	c = 8.5478(10) Å γ = 90°	c = 32.8241(8) Å γ = 90°
Volume	1963.2(4) Å^3	3586.56(15) Å^3
Z	4	8
Density (calculated)	1.239 Mg/m^3	1.405 Mg/m^3
Absorption coefficient	1.373 mm^{-1}	0.595 mm^{-1}
F(000)	776	1552
Crystal size	0.26 x 0.16 x 0.15 mm^3	0.24 x 0.16 x 0.15 mm^3
θ range for data collection	3.204 to 66.425°.	1.768 to 40.249°
Index ranges	$-9 \le h \le 9, -32 \le k \le 23, -9 \le l \le 10$	$-16 \le h \le 12, -20 \le k \le 22, -59 \le l \le 58$
Reflections collected	13753	94643
Independent reflections	3305 [R_{int} = 0.0741]	22569 [R_{int} = 0.0534]
Completeness to θ = 25.242°	95.9 %	99.9 %
Absorption correction	Semi-empirical from equivalents	Semi-empirical from equivalents
Max. and min. transmission	0.7528 and 0.6339	0.7458 and 0.6766
Refinement method	Full-matrix least-squares on F^2	Full-matrix least-squares on F^2
Data/restraints/parameters	3305 / 36 / 250	22569 / 0 / 443
Goodness-of-fit on F^2	1.090	1.032
Final R indices [I>2 σ (I)]	R_1 = 0.0779, wR_2 = 0.2139	R_1 = 0.0442, wR_2 = 0.0925
R indices (all data)	R_1 = 0.0883, wR_2 = 0.2228	R1 = 0.0795, wR_2 = 0.1053
Largest diff. peak and hole	0.563 and −0.433 eÅ^{-3}	0.672 and −0.637 e.Å^{-3}

Table 6.13 Crystal data details for (*o*-tolyl)$_3$P·BH$_3$, **10**.

Compound name	Tris(*o*-tolyl)phosphine borane
Empirical formula	$C_{21}H_{25.98}BCl_{11.98}P$
Formula weight	402.26
Temperature / K	100.00
Wavelength	0.71073 Å
Crystal system	Monoclinic
Space group	P 1 21/c 1
Unit cell dimensions	a = 9.2259(2) Å α = 90°
	b = 9.2259(2) Å β = 104.9530(10)°
	c = 17.3617(4) Å γ = 90°
Volume	2138.12(8) Å^3
Z	4
Density (calculated)	1.250 Mg/m^3
Absorption coefficient	0.379 mm^{-1}
F(000)	846
Crystal size	0.21 x 0.12 x 0.11 mm^3
θ range for data collection	1.910 to 40.249°
Index ranges	$-16 \leq h \leq 16$, $-25 \leq k \leq 25$, $-31 \leq l \leq 31$
Reflections collected	101737
Independent reflections	13436 [R_{int} = 0.0461]
Completeness to θ = 25.242°	99.7 %
Absorption correction	Semi-empirical from equivalents
Max. and min. transmission	0.7482 and 0.6697
Refinement method	Full-matrix least-squares on F^2
Data/restraints/parameters	13436 / 10 / 289
Goodness-of-fit on F^2	1.027
Final R indices [I>2 σ (I)]	R_1 = 0.0545, wR_2 = 0.1561
R indices (all data)	R1 = 0.0738, wR_2 = 0.1739
Largest diff. peak and hole	0.838 and −1.043 e.Å^{-3}

6.4 Computational coordinates

Table 6.14 Atomic coordinates for optimised geometry of $Ph_3P{\cdot}BH_3$, **1**.

Atom Type	x-coordinate / Å	y-coordinate / Å	z-coordinate / Å
P	0.00389	–0.00220	0.96493
C	3.51065	–2.42629	–0.82853
C	1.40441	–0.92211	0.23878
C	0.09778	1.67337	0.24431
C	–0.35179	3.26605	–1.52826
C	1.95334	–0.58195	–1.00670
H	1.56887	0.27489	–1.55222
C	–0.47631	1.98040	–0.99823
H	–1.02766	1.21885	–1.54204
C	0.78471	2.66754	0.95751
H	1.21108	2.43244	1.92811
C	3.00183	–1.33509	–1.53853
H	3.42466	–1.06602	–2.50269
C	0.90530	3.95203	0.42429
H	1.43555	4.71936	0.98158
C	1.92380	–2.01315	0.95232
H	1.51047	–2.26250	1.92494
C	–2.70238	–0.64105	0.95499
H	–2.70992	–0.14888	1.92287
C	0.34018	4.25153	–0.81858
C	–1.47958	–1.41230	–0.99345
H	–0.54467	–1.52065	–1.53546
C	–1.49731	–0.75343	0.24486
C	2.97273	–2.76259	0.41691
H	3.37290	–3.60478	0.97466
B	0.00894	–0.00534	2.90481
C	–3.87880	–1.17105	0.42251
H	–4.80886	–1.08347	0.97735
C	–3.85899	–1.81837	–0.81618
C	–2.65892	–1.94068	–1.52220
H	–2.63890	–2.45195	–2.48084
H	–0.79964	3.49902	–2.49051
H	–0.97379	0.62479	3.23904
H	1.04805	0.53014	3.23332
H	–0.04452	–1.17330	3.23340
H	4.32942	–3.00891	–1.24217
H	0.43287	5.25288	–1.23049
H	–4.77548	–2.23288	–1.22748

Table 6.15 Atomic coordinates for optimised geometry of Ph_3P.

Atom Type	x-coordinate / Å	y-coordinate / Å	z-coordinate / Å
C	–3.28241	–0.06461	1.28966
C	–2.05506	0.27466	0.71404
C	–1.61703	–0.36217	–0.45765
C	–2.43782	–1.34170	–1.04152
C	–3.65931	–1.68788	–0.46122
C	–4.08559	–1.04772	0.70606
H	–3.60950	0.43889	2.19599

H	–1.43596	1.03744	1.17667
H	–2.11865	–1.83555	–1.95684
H	–4.28087	–2.45020	–0.92386
H	–5.03999	–1.31029	1.15496
C	0.49065	1.58213	–0.46195
C	1.22294	1.63747	0.73426
C	0.09615	2.78533	–1.07002
C	1.54821	2.86799	1.31048
H	1.53826	0.71555	1.21363
C	0.41307	4.01509	–0.48988
H	–0.46130	2.75873	–2.00382
C	1.14214	4.05869	0.70186
H	2.11775	2.89607	2.23609
H	0.09824	4.93734	–0.97136
H	1.39664	5.01523	1.15087
C	1.12006	–1.21363	–0.46837
C	2.37126	–1.44336	–1.06445
C	0.79550	–1.90562	0.70882
C	3.28251	–2.33198	–0.49097
H	2.63296	–0.92413	–1.98396
C	1.70345	–2.80251	1.27787
H	–0.16884	–1.74188	1.18037
C	2.94905	–3.01586	0.68168
H	4.24771	–2.49629	–0.96309
H	1.43749	–3.33287	2.18887
H	3.65399	–3.71410	1.12535
P	–0.00529	0.00409	–1.29180

Table 6.16 Atomic coordinates for optimised geometry of quinuclidine, **2**.

Atom Type	x-coordinate / Å	y-coordinate / Å	z-coordinate / Å
C	–0.80244	–0.92125	–1.03400
C	1.29694	–0.00477	0.00094
C	0.76131	–0.96787	–1.07700
H	–1.21670	–1.91308	–0.81704
H	–1.21015	–0.59362	–1.99783
H	1.12707	–1.98412	–0.88215
H	1.13433	–0.66612	–2.06405
C	–0.80217	–0.43030	1.31621
H	–1.21113	0.25470	2.06853
H	–1.21487	–1.42688	1.51365
C	0.76146	–0.45345	1.37498
H	1.13298	0.22094	2.15707
H	1.12869	–1.46152	1.60609
H	2.39281	–0.00892	0.00178
C	0.76997	1.41279	–0.29652
H	1.14342	2.11450	0.46015
H	1.14181	1.75085	–1.27218
C	–0.79393	1.36033	–0.28389
H	–1.20093	2.03235	0.48107
H	–1.20290	1.67184	–1.25244
N	–1.29875	0.00517	–0.00100

Table 6.17 Atomic coordinates for optimised geometry of quinuclidine·BH_3, **3**.

Atom Type	x-coordinate / Å	y-coordinate / Å	z-coordinate / Å
C	–0.43895	–0.58392	1.28294
C	1.64292	–0.00055	–0.00003
C	1.10958	–0.68324	1.27197
H	–0.80941	0.06566	2.07893
H	–0.92114	–1.55776	1.38966
H	1.52436	–0.19719	2.16207
H	1.42526	–1.73280	1.28958
C	–0.43791	1.40321	–0.13572
H	–0.80884	1.76788	–1.09608
H	–0.91934	1.98291	0.65450
C	1.11055	1.44278	–0.04435
H	1.52530	1.97090	–0.91018
H	1.42616	1.98244	0.85605
H	2.73762	–0.00112	–0.00003
C	1.10967	–0.75972	–1.22767
H	1.42470	–0.24891	–2.14488
H	1.52478	–1.77344	–1.25293
C	–0.43881	–0.81953	–1.14695
H	–0.92111	–0.42613	–2.04412
H	–0.80874	–1.83363	–0.98116
N	–0.95395	0.00027	0.00000
B	–2.58445	0.00069	–0.00028
H	–2.91466	0.64663	0.97692
H	–2.91353	0.52380	–1.04871
H	–2.91386	–1.16877	0.07066